CHEMICAL STRESS RELAXATION

OF

POLYURETHANE ELASTOMERS

Bryan David Ludbrook

Thesis submitted for the degree of

Ph.D at the University of London

ABSTRACT

The chemical stress relaxation behaviour of a polyester urethane rubber, Genthane S, and a polyether urethane rubber, Adiprene CM, has been studied in air and nitrogen and under conditions of high humidity. To facilitate the interpretation of these results the materials were thoroughly characterised to determine their chemical compositions, crosslink densities etc.

The chemical stress relaxation measurements showed that both Adiprene CM and Genthane S underwent scission and crosslinking reactions. Adiprene CM in air degraded with an activation energy of 130.5 kJ $mole^{-1}$ due to the oxidation of the crosslinks. Adiprene CM in nitrogen and Genthane S in air or nitrogen underwent second order scission and crosslinking reactions that were attributed to the thermal dissociation of the urethane link. The activation energies for scission and crosslinking were respectively 110.6 and 95.7 kJ $mole^{-1}$ for Adiprene CM and 94.6 and 107.9 kJ $mole^{-1}$ for Genthane S. The rate of scission was unaffected by high humidity conditions.

A mechanism consistent with the experimental evidence was proposed to explain the various degradation processes; this involved the participation of a hydrogen bonded intermediate. This is reasonable since hydrogen bonding was shown to exist in Adiprene CM and Genthane S.

The characterisation work included the study of the infra-red and n.m.r. spectra of the polymers, the determination of molecular weights by osmometry and gel permeation chromatography

and the investigation of the stress-strain properties and the swelling behaviour of the elastomers.

This thesis includes descriptions of the apparatus used and reviews of the elastic properties of networks, the theory of chemical stress relaxation, the application of chemical stress relaxation to the study of elastomers and the relevant physics and chemistry of urethane rubbers.

+ + + + + +

ACKNOWLEDGEMENT

I would like to thank:

Dr. J.A. Barrie, my supervisor, for giving me the opportunity to conduct this work and for his help and encouragement during the past three years.

Dr. D.K. Thomas of the Royal Aircraft Establishment (Farnborough) for help and encouragement and for allowing me the use of his facilities and apparatus during a very enjoyable visit to Farnborough.

Mr. W. Edwards and the Ministry of Defence for providing financial support.

The Staff of the Chemistry Department Workshop at Imperial College for constructing the apparatus.

The Staff and Students of the Chemistry Department, Imperial College, who made my stay there both profitable and enjoyable, and in particular Dr. G. Scott, Mr. B. Coulsdon, Mr. R. Sheppard, Mr. R. Dawson, Mr. J. Sexton, Dr. D.W. Bassett and Mr. D. Tice.

Last but not least I would like to thank my wife, Jayne, my daughter, Michaela and my son, Steven, for tolerance and encouragement; my Mother who has spent many hours typing this manuscript and my Father and brother for their duties as chauffeurs.

+ + + + + + +

CONTENTS

Abstract 2

Acknowledgement 4

Chapter 1. Introduction 11

(1.1) Introduction 11

(1.2) The Structure and Properties of Elastomers 11

(1.2.1) The Elastic and Viscoelastic Properties of Elastomers 12
(1.2.2) The Elastic Properties of Elastomers 12
(1.2.3) The Interaction of Elastomers with Solvents 13
(1.2.4) The Elastic Properties of Swollen Elastomers 14
(1.2.5) Cohesive Energy Densities of Elastomers 14

(1.3) The Chemical Stress Relaxation of Elastomers 15

(1.3.1) Continuous Stress Relaxation 16
(1.3.2) Intermittent Stress Relaxation 16
(1.3.3) The Advantages of Chemical Stress Relaxation over Other Methods 17

(1.4) The Degradation of Elastomers 18

(1.5) Degradation Reactions in Urethane Elastomers 19

(1.6) The Objectives of the Present Investigation 20

Chapter 2. The Elastic Properties of Networks 22

(2.1) Introduction 22

(2.2) The Thermodynamics of Rubber Elasticity 22

(2.3) Statistical Mechanics of Single Chains 25

(2.4) Rubber Elastic Theory: Networks of Gaussian Chains 26

(2.4.1) The Kinetic or Statistical Theory 26
(2.4.2) The Elasticity and Swelling of Gaussian Networks 32
(2.4.3) The Swelling of Elastomers: Cohesive Energy Densities of Polymers 34

(2.5) Rubber Elastic Theory: Deviations from Kinetic Theory 36

(2.5.1) The Phenomenological Theory of Mooney and Rivlin 36

(2.5) (2.5.2) Deviations from Kinetic Theory 39

(2.5.2.1) Non-Gaussian Single Chain Statistics 39
(2.5.2.2) The Presence of Cross-links and Network Connectivity 40
(2.5.2.3) Non-Ideal Network Elements 41
(2.5.2.4) Volume Effects 44
(2.5.2.5) Deviations Due to the Deformation Process 45
(2.5.2.6) Molecular Interactions 46

(2.5.3) The Molecular Basis of the Second Mooney-Rivlin Constant 48

Chapter 3. Chemical Stress Relaxation: Theoretical Consideration 50

(3.1) Introduction 50

(3.2) Continuous and Intermittent Stress Relaxation: The Two Network Theory 50

(3.3) Cleavage Reactions in Elastomer Networks 54

(3.3.1) Cleavage in or at the Crosslinks 54
(3.3.2) Cleavage Within Network Chains 55

(3.4) Crosslinking Reactions in Elastomer Networks 61

(3.4.1) Crosslink Breakdown and Reformation: Reformed Crosslinks being Immune from Further Breakdown 61
(3.4.2) Crosslink Breakdown and Reformation: Reformed Crosslinks being Chemically Identical to those Initially Present 65
(3.4.3) Generalised Crosslink Formation Accompanying Scission 69

(3.5) The Kinetics of Network Reactions 71

(3.5.1) A Resume of Basic Kinetic Laws 72
(3.5.2) The Kinetic Interpretation of Chemical Stress Relaxation Data: Cleavage Reactions 73
(3.5.3) The Kinetic Interpretation of Chemical Stress Relaxation Data: Crosslinking Reactions 76
(3.5.4) The Kinetic Interpretation of Chemical Stress Relaxation Data: The Time-Temperature Superposition Method 77

Chapter 4. A Review of the Chemical Stress Relaxation of Elastomer Systems 80

(4.1) Introduction 80

(4.2) Chemical Stress Relaxation in Hydrocarbon Elastomers 80

(4.2.1) The Oxidation of Hydrocarbon Elastomers 83

(4.2.1.1) Chemical Stress Relaxation of Peroxide or Radiation Vulcanizates 83

(4.2.1.2) Chemical Stress Relaxation of Sulphur Donor Vulcanizates 91

(4.2.1.3) Chemical Stress Relaxation of Sulphur Vulcanizates 92

(4.2.2) The Effect of Non-Hydrocarbon Elements on the Oxidation of Hydrocarbon Elastomers 96

(4.2.2.1) The Presence of Sulphur 96

(4.2.2.2) The Presence of Oxygen 98

(4.2.2.3) Miscellaneous Substituents 100

(4.2.3) The Thermal Degradation of Hydrocarbon Elastomers 101

(4.2.4) The Radiolytic Stability of Hydrocarbon Elastomers 103

(4.2.5) The Mechanical Degradation of Hydrocarbon Elastomers 103

(4.3) The Chemical Stress Relaxation of Elastomers Containing Labile Links 103

(4.3.1) Polysulphide Rubbers 104

(4.3.2) Chemical Stress Relaxation of Wool and Allied Fibres 108

(4.3.3) Rubbers Containing Salt Links 110

(4.4) The Chemical Stress Relaxation of High Temperature Elastomers 112

(4.4.1) The Chemical Stress Relaxation of Silicone Rubbers 112

(4.4.1.1) The Chemical Stress Relaxation of Poly-dimethyl Siloxane 112

(4.4.1.2) The Chemical Stress Relaxation of Modified Silicone Rubbers 115

(4.4.2) The Chemical Stress Relaxation of Fluoro-Elastomers 119

(4.4.3) The Chemical Stress Relaxation of Nitroso Rubber 123

(4.5) The Chemical Stress Relaxation of Polyurethane Elastomers 124

Chapter 5. The Physical and Chemical Properties of Polyurethanes 130

(5.1) Introduction 130

(5.2) The Preparation and Cure of Urethane Elastomers 130

(5.3) Hydrogen Bonding in Polyurethane Elastomers 134

(5.4) The Environmental Stability of Polyurethane Elastomers 135

(5.4.1) The Thermal Stability of Polyurethane Elastomers 136

(5.4.1.1) The Urethane Link 136
(5.4.1.2) Other Nitrogen Containing Links 137
(5.4.1.3) Polyester and Polyether Segments 138

(5.4.2) The Thermooxidative Stability of Polyurethane Elastomers 136

(5.4.2.1) The Urethane Link 138
(5.4.2.2) Other Nitrogen Containing Links 139
(5.4.2.3) Polyether and Polyester Segments 139

(5.4.3) The Hydrolytic Stability of Polyurethane Elastomers 140

(5.4.3.1) The Urethane Link 140
(5.4.3.2) Other Nitrogen Containing Links 140
(5.4.3.3) Polyester and Polyether Segments 141

Chapter 6. The Characterisation of Adiprene CM and Genthane S 143

(6.1) Introduction 143

(6.2) The Materials Used 143

(6.3) Characterisation of the Uncured Polymer 144

(6.3.1) The Chemical Composition 144

(6.3.1.1) Nuclear Magnetic Resonance Spectra 144
(6.3.1.2) Infra Red Spectra 147

(6.3) (6.3.2) Physical Characterisation 151

(6.3.2.1) Number Average Molecular Weight 151
(6.3.2.2) Molecular Weight Distribution 152
(6.3.2.3) Glass Transition Temperatures and Densities 160
(6.3.2.4) Solubility 160

(6.4) Characterisation of the Cured Elastomer 166

(6.4.1) The Swelling of the Elastomers in Solvents 166
(6.4.2) The Stress-Strain Properties of the Elastomers in Simple Elongation 170

(6.4.1.2) An Apparatus for Measuring the Tensile Properties of Dry and Swollen Elastomers 170
(6.4.2.2) The Tensile Properties of Adiprene CM and Genthane S 176

(6.4.3) The Stress-Strain Properties of the Elastomers in Uniaxial Compression 186

(6.4.3.1) Apparatus and Experimental Method 186
(6.4.3.2) Compression of Adiprene CM and Genthane S 189

(6.5) Discussion of Results 197

(6.5.1) The Composition and Structure of the Polymers 197
(6.5.2) The Stress-Strain Properties of the Elastomers 197

Chapter 7. Chemical Stress Relaxation in Adiprene CM and Genthane S. 202

(7.1) Apparatus 202

(7.1.1) The Relaxometer 202
(7.1.2) The Furnace 207
(7.1.3) The Vacuum System 210
(7.1.4) The Control and Measuring System 210

(7.2) Chemical Stress Relaxation of Adiprene CM and Genthane S 221

(7.2.1) Continuous and Intermittent Stress Relaxation of Genthane S in Air 221
(7.2.2) Further Experiments on Genthane S and the Effect of Additives 239
(7.2.3) Continuous and Intermittent Relaxation of Adiprene CM in Air and Nitrogen 257
(7.2.4) Further Experiments on Adiprene CM and the Effect of Additives 248

(7.3) Discussion of Results 268

(7.3.1) Network Reactions in Genthane S 268
(7.3.2) Network Reactions in Adiprene CM 277
(7.3.3) The Mechanism of Urethane Degradation 278
(7.3.4) Conclusions and Suggestions for Further Work 284

+ + + + + +

References 286

Appendix A: Stress-Strain Data 294

Appendix B: Chemical Stress Relaxation Results 308

(I) Chemical Stress Relaxation of Genthane S 308
(II) Chemical Stress Relaxation of Adiprene CM 316

Appendix C: 325

(C1) A Computer Programme to Analyse the Results 325
(C2) A Computer Programme to Calculate the Best Arrhenius Plot and Calculate Activation Energies and Pre-exponential Factors 338

+ + + + + +

CHAPTER 1

INTRODUCTION

(1.1) INTRODUCTION

Polyurethane elastomers are often used where high abrasion resistance, resilience, tensile strength, hardness and shock absorbing properties are required.[1-8] Appropriate compounding and chemistry allow the physical properties to be varied over a wide range, permitting the tailoring of properties to meet particular specifications.[1,2] This leads, at one extreme, to enhanced properties relative to other elastomers. However, in common with other elastomers their range of applications is often limited by factors such as chemical and environmental instability, in particular, the polyurethanes are susceptible to thermal, oxidative and hydrolytic attack.[2,3]

The main object of this study is to assess the relative importance of these degradative processes in selected pure gum vulcanizates without fillers, additives or other compounding ingredients, and to study the kinetics and mechanisms of the associated chemical reactions.

(1.2) THE STRUCTURE AND PROPERTIES OF ELASTOMERS

The term "elastomer" is reserved for a polymeric network above its glass transition temperature, T_g. For example, vulcanised natural rubber has a T_g of about $-70^{\circ}C$ and the terms "rubber" and "elastomer" are used interchangeably.

A polymeric network is built up when a small number of interchain chemical bonds are introduced into an assemblage of very long polymer molecules. The bonds or "crosslinks" join the bulk of the initially distinct polymer molecules into one giant molecule. The number of crosslinks required per

primary polymer molecule must be greater than one, so that each of the primary molecules is subdivided into several shorter chains, termed "network chains".

(1.2.1) The Elastic and Viscoelastic Properties of Elastomers

When a sample of uncrosslinked polymer gum is subjected to an applied stress there are two contributions to the deformation. These are an elastic component which is reversible and is associated with the uncoiling or stretching of individual polymer molecules, and a viscous component, which is non-recoverable and arises from the viscous flow of molecules past each other.

When crosslinks are introduced the viscous component is removed and the resultant network can be deformed reversibly.

(1.2.2) The Elastic Properties of Elastomers

The long range and non-Hookean elastic behaviour of rubbers has attracted a great deal of theoretical and experimental attention.[10,11,12] Hookes law[9] states that for uniaxial elongation or compression at constant volume

$$\sigma = M(1 - \lambda) \qquad (1.1)$$

where σ is the applied stress with reference to the undeformed cross-sectional area, λ is the deformed length of the sample divided by its undeformed length and M is the elastic modulus. This equation is not obeyed by elastomers since M is not a constant but a function of λ. In technological usage the elastic behaviour of rubbers is characterised by their moduli, but in recognition of its dependence on λ, the percentage elongation at which the modulus was obtained is also quoted.

The equilibrium elastic behaviour of rubbers is more accurately described by the kinetic or statistical theory[10,11]

expression,

$$\sigma = G(\lambda - \lambda^{-2}) \qquad (1.2)$$

G is a constant, related to molecular parameters by

$$G = A \nu kT/V \qquad (1.3)$$

where ν is the number of network chains in the sample, k is the Boltzmann constant, T is the absolute temperature, V is the volume of the sample and A is a constant.

Equation (1.2) is a much better fit than equation (1.1) to the stress-strain properties of rubbers in the range of λ values close to unity, an even better fit is given by the Mooney-Rivlin equation[10,11] which is derived from phenomenological considerations and for uniaxial elongation or compression at constant volume takes the form,

$$\sigma = 2(C_1 + C_2/\lambda)(\lambda - \lambda^{-2}) \qquad (1.4)$$

where C_1 and C_2 are constant. A comparison of the coefficients of equations (1.2) and (1.4) has led to the identification of C_1 with $\frac{1}{2}G$; attempts to describe C_2 in molecular terms have not proved to be so successful.[10,11]

(1.2.3) The Interaction of Elastomers with Solvents

The polymer network is prevented from dissolving in a solvent by the presence of crosslinks. However, the network may swell to a greater or lesser extent depending on the number of crosslinks and the affinity of the solvent for the polymer.[12,13]

Swelling is equivalent to a bulk elastic deformation of the network[11,12] and the degree of swelling is determined by the free energy required to elastically deform the network and the free energy of mixing of network chains and solvent. Equilibrium swelling is attained when these two free energies are equal.

Using the kinetic theory[11] and the Flory-Huggins[12] equation respectively for the free energies of deformation and mixing, the following equation results for the equilibrium degree of swelling.[11,12]

$$\frac{A\nu}{LV}\phi_2^{-1/3} = -\ln(1-\phi_2) - \chi_1\phi_2^2 - \phi_2 \qquad (1.5)$$

where L is Avogadro's constant, ϕ_2 is the volume fraction of rubber in the swollen sample (often denoted V_r) and χ_1 is the Flory-Huggins constant[12] that describes the polymer-solvent interaction and depends on the affinity of the solvent for the polymer.

(1.2.4) The Elastic Properties of Swollen Elastomers

For uniaxial compression or elongation of a swollen sample at constant volume, kinetic theory yields[11]

$$\sigma = \frac{A\nu kT}{V}\phi_2^{-1/3}(\lambda - \lambda^{-2}) \qquad (1.6)$$

where σ is measured relative to the unswollen cross-sectional area of the sample but λ is measured relative to the swollen dimensions of the sample.

This equation has been shown experimentally to be a very good fit for swollen networks in many cases.[11]

(1.2.5) Cohesive Energy Densities of Elastomers

The interaction between liquids and rubbers is often characterised by the cohesive energy densities of liquid and rubber.[13,14] The cohesive energy density of a solvent is defined in terms of the molar cohesive energy of the solvent.[14]

$$\delta_1 = (E_1/V_1)^{\frac{1}{2}} \qquad (1.7)$$

where δ_1 is the cohesive energy density, E_1 is the molar cohesive energy and V_1 is the molar volume of the solvent. The molar cohesive energy is given by

$$E_1 = \Delta H_1 - RT \qquad (1.8)$$

where ΔH_1 is the molar heat of evaporation and R is the gas constant; ΔH_1 may be evaluated experimentally or evaluated from the boiling point so that[14]

$$\delta_1^2 = (23.7T_b + 0.020T_b^2 - 3542)/V_1 \qquad (1.9)$$

where T_b is the boiling point of the solvent.

The cohesive energy density of the polymer is more difficult to evaluate; the generally accepted method is to swell the rubber in a variety of different solvents. The maximum degree of swelling should be observed when the cohesive energy densities of the polymer and solvent are equal. It is important, for reasons to be discussed, that solvents should be chemically similar to each other and to the polymer.

(1.3) THE CHEMICAL STRESS RELAXATION OF ELASTOMERS

From equations (1.2) and (1.3) one obtains at constant volume and temperature

$$\sigma \alpha \nu \qquad (1.10)$$

When chemical reactions take place, changes in ν arising from scission of network chains or crosslinks and the introduction of new crosslinks may occur, accordingly the stress supported by the sample will change.[15]

$$\sigma_t \alpha f_t \alpha \nu_t \qquad (1.11)$$

where the subscript t refers to conditions as they exist at time t, and f is the force exerted by the sample.

So

$$f_t/f_o = \nu_t/\nu_o \qquad (1.12)$$

where the sample initially contains ν_o network chains and exerts a force f_o.

Suppose the network is subject to both a scission and a crosslinking reaction so, that of the original $\nu_1(o)$ network chains only $\nu_1(t)$ remain at time t. In addition a further $\nu_2(t)$ network chains are formed as a result of the crosslinking reaction. The total number of network chains present at time t is

$$\nu_t = \nu_1(t) + \nu_2(t) \tag{1.13}$$

and since

$$\nu_o = \nu_1(o) \tag{1.14}$$

$$f_t/f_o = [\nu_1(t) + \nu_2(t)]/\nu_1(o) \tag{1.15}$$

By performing two different experiments independent estimates of $\nu_1(t)$ and $\nu_2(t)$ may be obtained.

(1.3.1) Continuous Stress Relaxation

The sample is stretched to some elongation λ at which it is maintained for the duration of the experiment. Under these conditions it is postulated[15] that the force will only be supported by the fraction of the original crosslinks that have not been removed by scission; new crosslinks formed will support zero stress. It follows that

$$\left(\frac{f_t}{f_o}\right)_c = \frac{\nu_1(t)}{\nu_1(o)} \tag{1.16}$$

where the subscript, c, refers to the continuous experiment. The validity of this assumption has been questioned and will be discussed later.

(1.3.2) Intermittent Stress Relaxation

The sample is maintained in the unstretched state; at certain time intervals it is stretched to some extension λ and the force measured as quickly as possible. The sample

is then returned to the unstretched state. Ideally the length of time the sample is stretched is negligible compared with the time spent in the unstretched state.

In this case the force is supported by all the crosslinks[15] and

$$\left(\frac{f_t}{f_o}\right)_i = \frac{\nu_1(t) + \nu_2(t)}{\nu_1(o)} \qquad (1.17)$$

where the subscript, i, refers to the intermittent experiment. Combining equations (1.16) and (1.17)

$$\Delta = \left(\frac{f_t}{f_o}\right)_i - \left(\frac{f_t}{f_o}\right)_c = \frac{\nu_2(t)}{\nu_1(o)} \qquad (1.18)$$

so that both $\nu_1(t)$ and $\nu_2(t)$ may be obtained.

(1.3.3) The Advantages of Chemical Stress Relaxation over Other Methods

The principle advantages of chemical stress relaxation over other methods are:

(i) The method is extremely sensitive

(ii) It allows both scission and crosslinking reactions to be studied under the same conditions.

(iii) It allows the study of chemical reactions in crosslinked solid elastomers.

(iv) Interpretation of the results in terms of molecular parameters is comparatively straightforward.

The sensitivity of the method is such that when 10% of the network chains have been cut, the relative stress supported by the sample will have fallen by 10%. Network chains have fairly high molecular weights and may contain ten, one hundred

or more reactive groups; scission will occur when one of these has reacted, so that when 10% of the chains are cut, the change in reactive group concentration need only be 1% or less. Few chemical methods can match this sensitivity.

In sections (1.3.1) and (1.3.2) it was shown that both $\nu_1(t)$ and $\nu_2(t)$ may be estimated. Although the theoretical treatment in its simplest form is open to criticism this does not, in general, detract from the utility of the method.

Few other methods allow of the direct investigation of crosslinked elastomers and this is particularly important since the crosslinks may affect the stability of the backbone polymer or it may be the stability of the crosslinks that determine the overall stability of the network.

Lastly the measured quantities can be easily related to molecular parameters; this is not always as straightforward as it appears from sections (1.3), (1.3.1) and (1.3.2) as will be discussed further in Chapter 3.

The chief disadvantage of chemical stress relaxation is that although it can distinguish between scission and crosslinkin processes, it does not yield, directly, to information on the chemical reaction responsible.

(1.4) THE DEGRADATION OF ELASTOMERS

In section (1.3.3) it was shown that the modulus of an elastomer is reduced by 50% when 50% of the network chains are cut. Although this loss can be partially offset by simultaneous crosslinking reactions, nevertheless, the properties of the material will have substantially altered. As the new crosslinks formed in the deformed sample are not under stress until the deformation is changed, they will tend

to make the sample retain its deformed dimensions. If scission is also taking place the forces favouring the elastic recovery of the sample will be reduced. These two opposing effects lead to the phenomenon of chemical permanent set[15] which is often just as unwelcome as cleavage reactions alone, particularly in sealing applications.

Since very little chemical reaction need take place for the properties of the rubber to be substantially altered very sensitive methods for studying degradation reactions are needed.

(1.5) DEGRADATION REACTIONS IN URETHANE ELASTOMERS

Methods of studying degradation in polyurethane elastomers, other than chemical stress relaxation, normally involve a much larger amount of reaction at relatively higher temperatures.[1,2,3] The application of these results to the interpretation of chemical stress relaxation data, which involves a very much smaller degree of reaction usually at lower temperatures, must be treated with caution and is rarely justified. The type of non-chemical stress relaxation methods that have been used are weight loss, the examination of pyrolysis products etc.

Several investigations, using chemical stress relaxation, have been made on polyurethane elastomers.[16-20] The earliest of these were made using poorly characterised samples that contained a variety of cleavable links such as amide, disubstituted urea, biuret and allophanate linkages as well as urethane and ester or ether links.[16,17] Assuming that scission took place at the nitrogen containing links it was concluded that the order of thermal stability was[15]

ester or ether > urethane > disubstituted urea > biuret.

No conclusions were drawn regarding the stability of amide or allophanate links.

In more recent studies attempts were made to identify, more rigorously, the site of scission [18,19,20] which would seem to be associated with the urethane group. The role of weak linkages, other than the urethane group, is not fully understood and the kinetic model used to interpret the results is open to criticism.

(1.6) THE OBJECTIVES OF THE PRESENT INVESTIGATION

To interpret chemical stress relaxation data in a meaningful way it is important to know as much as possible about the chemical and physical structure and properties of the elastomer. In the past many studies [15,16,17] have failed to recognise this, with the result that it has been impossible to evaluate where in the system degradation occurs, because the precise chemical structure of the material was unknown. In this investigation efforts were made to ascertain the chemical compositions of the elastomers, the crosslink density of the elastomers, and several other physical characteristics that give insight into the nature of the materials.

The elastomers were cured with dicumyl peroxide, a curing system that gives crosslinks that are simple carbon-carbon bonds.

Since the base polymer contained only urethane and ester or ether groups, the weak links introduced as a consequence of the curing systems used by earlier workers [15,16,17] should be absent here. This simplifies the system a great deal, since it is always difficult to determine which weak

links are present and in what concentrations; interpretation of the data for this simplified system is thus facilitated.

The main objective of this investigation is to identify the sites at which cleavage and crosslinking take place, to investigate the kinetics of these processes and to suggest ways in which they may be inhibited. In this respect the degradation is expected to be thermal, oxidative and hydrolytic and it is important to assess the relative importance of these types of degradation processes. Most of the previous work was concerned with the thermal decomposition,[16-20] which may be important in determing the overall stability of the materials under the appropriate conditions.

The study of oxidation has received little attention although it may be important, and there is some evidence that oxidative attack of the urethane group does occur.[2] The role of hydrolytic processes has been the subject of a considerable amount of controversy[1,2,3] which will be discussed further in Chapter 5.

+ + + + + +

CHAPTER 2

THE ELASTIC PROPERTIES OF NETWORKS

(2.1) INTRODUCTION

The interpretation of chemical stress relaxation measurements necessitates the description of the elastic properties of polymeric networks in terms of the crosslink or network chain density of the samples.

The kinetic or statistical theory[10,11] gives the required type of equation although this does not generally fit experimental data very well, a better fit being given by the Mooney-Rivlin equation.[10,11] When the Mooney-Rivlin equation is used, the interpretation of the stress-strain properties in terms of molecular parameters is more difficult;[11] especially the second constant, C_2.

The theoretical description of the elastic properties of networks, their swelling in fluids and their deformation when swollen will be considered in this chapter.

(2.2) THE THERMODYNAMICS OF RUBBER ELASTICITY

When a sample of rubber is deformed by the application of a force f such that the length of the sample, measured in the direction of the force, is changed by dl, the first and second laws of thermodynamics give:[10]

$$dU = TdS + fdl - PdV \qquad (2.1)$$

where dU and dS are respectively the internal energy and entropy of deformation, T is the absolute temperature, P is the applied hydrostatic pressure and dV is the volume change.

To a good approximation a rubber network is incompressible and dV = 0.

$$\therefore \quad dU = TdS + fdl \qquad (2.2)$$

$$\therefore f = \left(\frac{dU}{dl}\right)_{T,V} - T\left(\frac{dS}{dl}\right)_{T,V} \qquad (2.3)$$

The Helmholz free energy of deformation is:[10]

$$dF = fdl - Sdt \qquad (2.4)$$

$$\therefore \left(\frac{dF}{dl}\right)_{T,V} = f \qquad (2.5)$$

$$\therefore \left(\frac{dF}{dT}\right)_{l,V} = - S \qquad (2.6)$$

$$\text{Since } \frac{d}{dl}\left(\frac{dF}{dT}\right)_{l,V} = \frac{d}{dT}\left(\frac{dF}{dl}\right)_{T,V} \qquad (2.7)$$

$$\therefore \left(\frac{dS}{dl}\right)_{T,V} = -\left(\frac{df}{dT}\right)_{l,V} \qquad (2.8)$$

Substitution into equation (2.3) gives:

$$f = \left(\frac{dU}{dl}\right)_{T,V} + T\left(\frac{df}{dT}\right)_{l,V} \qquad (2.9)$$

Hence $\left(\frac{dU}{dl}\right)_{T,V}$ and $\left(\frac{dS}{dl}\right)_{T,V}$ can be evaluated by studying the temperature dependence of f at constant l. It is clear from figure 2.1 that the entropy term makes the major contribution to f.

By analogy to gases an ideal rubber may be defined as one for which $\left(\frac{dU}{dl}\right)_{T,V} = 0$ and:

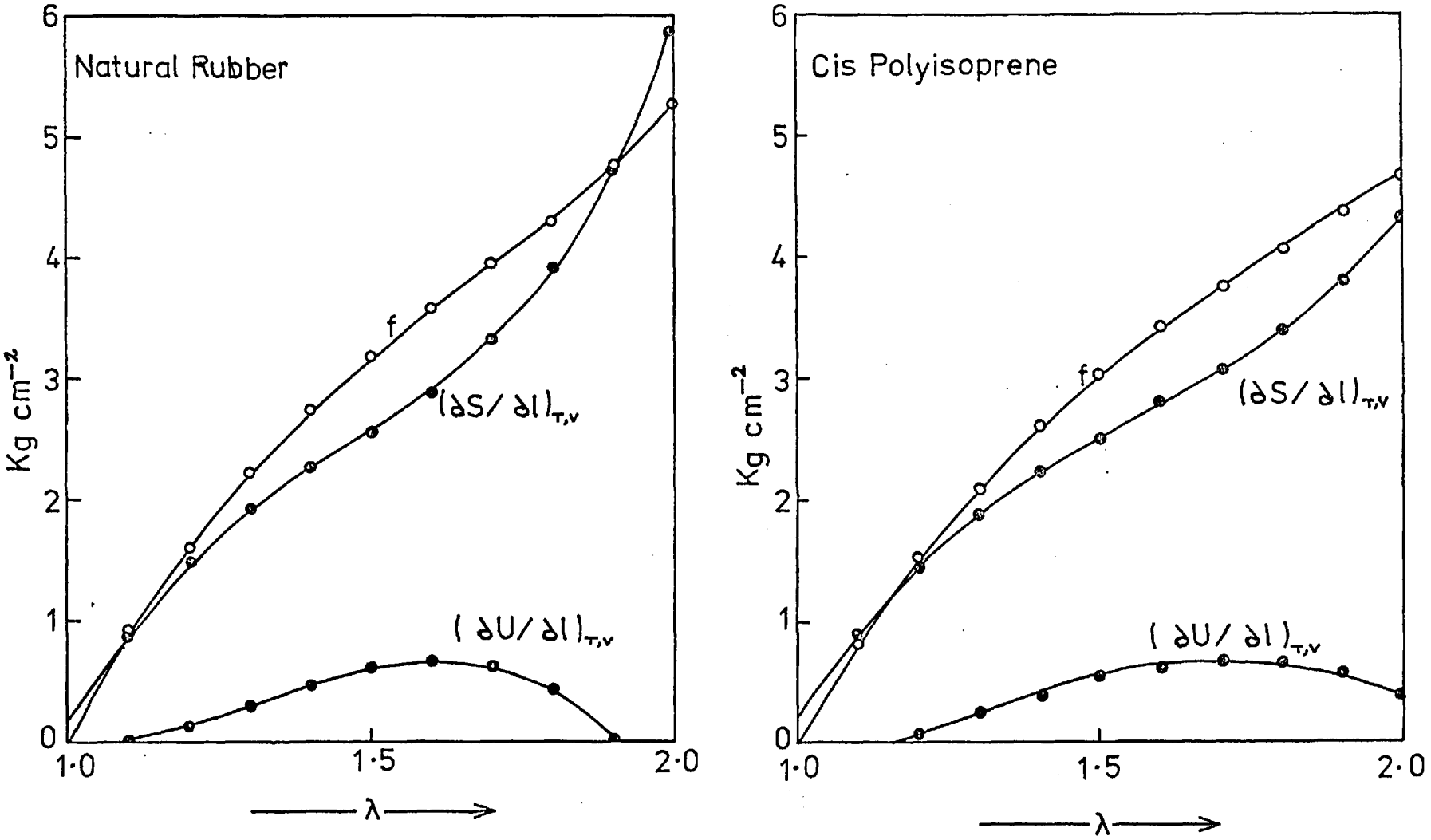
$$f = - T\left(\frac{dS}{dl}\right)_{T,V} = \left(\frac{dF}{dl}\right)_{T,V} \qquad (2.10)$$

It is convenient to characterise the deformation by a principal extension ratio λ defined as:

$$\lambda = l/l_o \qquad (2.11)$$

where l and l_o are respectively the final and initial lengths of the sample in the direction of f.

figure 2·1 : Thermoelastic Properties of Elastomers (data from Standen, ref. 21)



$$\text{Since } d\lambda = dl/l_o \tag{2.12}$$

equation (2.10) becomes:

$$f = -T/l_o(dS/d\lambda)_{T,V} = (1/l_o)(dF/d\lambda)_{T,V} \tag{2.13}$$

Most theories of rubber elasticity seek to evaluate either $(dS/d\lambda)_{T,V}$ or $(dF/d\lambda)_{T,V}$ by applying the methods of statistical mechanics.

(2.3) STATISTICAL MECHANICS OF SINGLE CHAINS

As a general rule, the starting point for a theory of rubber elasticity is the statistical mechanical description of a single polymer chain. Once the characteristics of the single chain have been established it is possible to consider the elastic properties of a network formed from such chains.

The statistical properties of single chains can be characterised by the probability distribution of the vectors joining the ends of the chains. The evaluation of this for a real chain is a complex problem [22-24] and does not lead to a simple analytical expression except in the limit of chains of infinite length when the distribution has the Gaussian form [10,11,22,23,24]:

$$p(\vec{r}) = \left[\frac{3}{2\pi\langle r^2\rangle_o}\right]^{3/2} \exp\left[-3r^2/2\langle r^2\rangle_o\right] \tag{2.14}$$

where $\vec{r}$ is the end-to-end vector and $\langle r^2\rangle_o$ is the mean square unperturbed end-to-end vector for the chain.

Although the Gaussian expression is valid only for infinite chains, it has been shown to be a good approximation for chains that are long but finite, provided $r \ll nl$ where n is the number of links of length l that comprise the chain. This requirement is specified because the Gaussian equation predicts that there is a finite probability that r can be

larger than the contour length of the chain nl.

The inverse Langevin distribution function is more realistic when $r \leqslant nl$ as it vanishes when $r > nl$, although it has been shown that it is a worse approximation when $r \ll nl$.[22] The inverse Langevin distribution has the form:

$$p(\vec{r}) = \left[\frac{A'L(r/nl)}{rl^2}\right]\left[L(r/nl)\sinh\left\{L^{-1}(r/nl)\right\}\right]^n \exp\left[-L^{-1}(r/nl).r/l\right] \qquad (2.15)$$

where $y = \coth x - 1/x = L(x)$, $L^{-1}(y) = x$ and A' is a normalising constant.

(2.4) RUBBER ELASTIC THEORY: NETWORKS OF GAUSSIAN CHAINS

(2.4.1) The Kinetic or Statistical Theory

The theory predicts that when a piece of rubber is deformed such that a point with coordinates (x_o, y_o, z_o) before the deformation has coordinates $(\lambda_x x_o, \lambda_y y_o, \lambda_z z_o)$ after the deformation:[11,25]

$$\Delta F_{net}/kT = (A\nu/2)(\lambda_x^2 + \lambda_y^2 + \lambda_z^2 - 3) - B\nu \ln\lambda_x\lambda_y\lambda_z \qquad (2.16)$$

ΔF_{net} is the free energy of deformation, k is the Boltzmann constant, ν is the number of network chains and A and B are constants. Several derivations of equation (2.16) have been made;[26-29] these fall into one of two groups depending on the initial assumptions made. The most rigorous method is that of James and Guth[26,27] in which the elastic network[30,31] is treated as an assemblage of Gaussian chains terminated by crosslinks (or junction points) at which these network chains are bonded to one another. The number of chains that met at a junction point was not specified and could assume values $\geqslant 2$; this meant that any link junction could be considered as a junction point.

The junction points were divided into "fixed points", at which the network was immobilised by external constraints and exerted forces on the external system, and other junction points, which exhibit Brownian motion compatible with the constraints in the network. If $r_\alpha r_\beta$ ..... describe the positions of fixed points α, β ...; r_i, r_j .... describe the positions of free junction points i,j ....; and r_τ, r_ν .... describe the positions of junction points τ, ν .... whether they be fixed or free: the total number of configurations available to the network consistent with the given positions of the fixed points is:[27,31]

$$Q(r_\alpha r_\beta \ldots) = \int dV_i \int dV_j \ldots \prod_{\tau>\nu} \prod p(|\vec{r}_{\tau\nu}|) \qquad (2.17)$$

where $\vec{r}_{\tau\nu}$ is the vector joining junction points τ and ν. The most probable position of a given free junction point can be evaluated by choosing the coordinates that maximise equation (2.17):

$$\begin{aligned} x_{oj} &= \sum_\alpha C_{j\alpha} x_\alpha \\ y_{oj} &= \sum_\alpha C_{j\alpha} y_\alpha \\ z_{oj} &= \sum_\alpha C_{j\alpha} z_\alpha \end{aligned} \qquad (2.18)$$

where $C_{j\alpha}$ is a constant depending on the number of links comprising the chains, $n_{\tau\nu}$, that make up the network: the mean position of the junction j depends only on the known positions of the fixed points.

When the sample is deformed the coordinates of the fixed points will be changed by the same extension ratios as the external dimensions of the sample; if these are $\lambda_x, \lambda_y, \lambda_z$ equation (2.18) gives the new mean position of junction j:

$$x'_{oj} = \lambda_x \sum_{\alpha} C_{j\alpha} x_{\alpha} = \lambda_x x_{oj} \qquad (2.19)$$

with similar equations for y and z components.

This proves that the mean position of the network junctions undergo an affine deformation when the network as a whole is deformed; thus the mean positions of the junctions are displaced according to the same principal extension ratios that define the change in the initial macroscopic shape of the sample.

Integration of equation (2.17) gives:[27,31]

$$Q(r_\alpha, r_\beta \ldots) = K_1 \exp\left[-(3/21^2)\sum_{\tau>\nu}\sum (x_{o\tau} - x_{o\nu})^2 + (y_{o\tau} - y_{o\nu})^2 + (z_{o\tau} - z_{o\nu})^2\right] \qquad (2.20)$$

when the network is deformed:

$$Q(r_\alpha, r_\beta \ldots) = K_1 \exp\left[-(K_x\lambda_x^2 + K_y\lambda_y^2 + K_z\lambda_z^2)\right] \qquad (2.21)$$

where $K_x = (3/21^2)\sum_{\tau>\nu}\sum (x_{o\tau} - x_{o\nu})^2$ with similar equations for K_y and K_z. Assuming the material to be isotropic $K_2 = K_x = K_y = K_z$ where

$$K_2 = (1/21^2)\sum_{\tau>\nu}\sum (1/n_{\tau\nu})\left[(x_{o\tau} - x_{o\nu})^2 + (y_{o\tau} - y_{o\nu})^2 + (z_{o\tau} - z_{o\nu})^2\right] \qquad (2.22)$$

$$\therefore Q(\lambda_x, \lambda_y, \lambda_z) = K_1 \exp\left[-K_2(\lambda_x^2 + \lambda_y^2 + \lambda_z^2)\right] \qquad (2.23)$$

K_1 can be equated with $\left[3/(2\pi\langle r^2\rangle_o)\right]^{3/2}$ of equation (2.14) although James and Guth, unconvinced of the equivalence of these two quantities, preferred to leave it unspecified.

$$\Delta F_{net}/kT = -\ln\left[Q(\lambda_x, \lambda_y, \lambda_z)/Q(1,1,1)\right] \qquad (2.24)$$

$$= K_2(\lambda_x^2 + \lambda_y^2 + \lambda_z^2 - 3) \qquad (2.25)$$

James and Guth showed that if crosslinking could be considered as the instantaneous freezing of a system of unconstrained molecules,[26,32] the distribution of end to end vectors of the network chains would be that of the unconstrained molecules and K_2 would be $\nu/2$; so that A = 1 and B = 0. James and Guth[32] regarded this as an unreasonable model of the curing process and Guth[26] suggested that as an alternative assumption all $n_{\gamma\nu}$ were equal:

$$K_2 = (\nu/2)\langle r_o^2\rangle / \langle r^2\rangle_o \qquad (2.26)$$

where $\langle r_o^2\rangle$ is the mean square end to end distance of the network chains in the undeformed state and $\langle r^2\rangle_o$ is the mean square end to end distance in a system of unconstrained, unperturbed, Gaussian chains. In this case $A = \langle r_o^2\rangle / \langle r^2\rangle_o$ and B = 0.

The most realistic model of the curing process[26,32] regarded it as comprising the gradual growth and reinforcement of the network and led to the approximate result that $A = \frac{1}{2}$ and B = 0.

The second approach proferred by Flory, Wall and Hermans[28,29,34,36,37] was much simpler: the total number of configurations available to the network under a deformation $\lambda_x,\lambda_y,\lambda_z$, at constant temperature was:[11]

$$Q(\lambda_x,\lambda_y,\lambda_z) = \sum_{\nu}\left[\nu!/\pi_i \nu_i!\right] \prod_i q(\vec{r}_i)^{\nu_i} \qquad (2.27)$$

where $q(\vec{r}_i)$ was the probability that a chain had an end-to-end vector $\vec{r}_i$ and ν_i was the number of such network chains. The summation extended over all possible sets of ν_i values, provided $\sum \nu_i = \nu$ the total number of chains, and the permutation term resulted from their indistinguishability.

The maximum term $Q_{max}(\lambda_x\lambda_y\lambda_z)$ was evaluated and assumed to be the dominant term in the summation so that:

$$\Delta F_{el}/kT = \ln \left[Q_{max}(\lambda_x,\lambda_y,\lambda_z)/Q_{max}(1,1,1,)\right] \qquad (2.28)$$

In $Q_{max}(1,1,1,)$ the distribution $q(\vec{r}_i)$ is assumed to be Gaussian and the mean square components of the end-to-end vectors are assumed to be affinely deformed:

$$\therefore\ \Delta F_{el}/kT = (\nu/2)(\lambda_x^2 + \lambda_y^2 + \lambda_z^2 - 3) - \nu \ln\lambda_x\lambda_y\lambda_z \qquad (2.29)$$

This model derives the elastic free energy from the probability that the uncrosslinked polymer will occur in configurations consistent with the formation of a deformed or an undeformed network respectively and necessarily assumes that there is no difference between the free energies of crosslinking in the deformed and undeformed states respectively.

Flory[11,38,39] argues otherwise such that if V and V_o are the volumes of the deformed and the undeformed network respectively, then the difference between the respective free energies of crosslinking will be:

$$\Delta F_{cr}/kT = (\nu - 2\nu/f')\ \ln\lambda_x\lambda_y\lambda_z \qquad (2.30)$$

$$\Delta F_{net}/kT = (\Delta F_{el} + \Delta F_{cr})/kT = \nu/2(\lambda_x^2 + \lambda_y^2 + \lambda_x^2 - 3) - (2\nu/f')\ \ln\lambda_x\lambda_y\lambda_z \qquad (2.31)$$

where f' is the functionality of the crosslinks.

The two main differences between the James and Guth and the Hermans, Flory, Wall approaches are:

(i) The presence of a logarithmic term in the HFW treatment; this discrepancy is not very important as the elastic deformation of a piece of rubber is usually very close to being a constant volume process where $\lambda_x\lambda_y\lambda_z = 1$

and the logarithmic term vanishes. An exception to this is the case of the swelling of rubbers in fluids which will be considered later.

(ii) The coefficient of $kT(\lambda_x^2 + \lambda_y^2 + \lambda_z^2 - 3)$ is $\nu/2$ in the HFW treatment and undefined or equal to $\nu/4$ in the JG treatment. If the same assumptions about the curing process are made, the JG treatment gives the same result as the HFW method; the controversy is that James and Guth regard these assumptions as unrealistic.

Accepting the general form for the network free energy as:[11]

$$\Delta F_{net}/kT = (A\nu/2)(\lambda_x^2 + \lambda_y^2 + \lambda_z^2 - 3) - B\nu \ln\lambda_x\lambda_y\lambda_z \tag{2.32}$$

The case of uniaxial compression or tension where:

$$\lambda_x\lambda_y\lambda_z V_o = V, \quad \lambda_x = \lambda \text{ and } \lambda_y = \lambda_z$$

gives

$$\Delta F_{net}/kT = (A\nu/2)(\lambda^2 + 2V/V_o\lambda - 3) - B\nu \ln (V/V_o) \tag{2.33}$$

$$f = (1/l_o)(\partial \Delta F_{net}/\partial \lambda)_{T,V} = (A\nu kT/l_o)(\lambda - V/V_o\lambda^2) \tag{2.34}$$

If the deformation is a constant volume process

$$f = (A\nu kT/l_o)(\lambda - \lambda^{-2}) \tag{2.35}$$

$$\sigma = f/l_o^2 = (A\nu kT/V)(\lambda - \lambda^{-2}) \tag{2.36}$$

where σ is the stress exerted by the sample.

The principle extension ratios in equations (2.32) - (2.36) are defined with respect to a reference state in which the mean square end-to-end vector of the network chains is

identical with that of a system of equivalent unperturbed free chains.[11] As the crosslinking process may influence the chain dimensions, the reference state and the state of the undeformed network may be different.[40-44] If $\langle r^2 \rangle_{od}$ and $\langle r^2 \rangle_i$ are the mean square end-to-end vectors of the reference state and the state of the undeformed network respectively:

$$\Delta F_{net}/kT = (A\nu/2)\left[\langle r^2\rangle_i / \langle r^2\rangle_{od}\right](\lambda_x^2 + \lambda_y^2 + \lambda_z^2 - 3) - B\nu \ln\lambda_x\lambda_y\lambda_z \qquad (2.37)$$

$$\sigma = (A\nu kT/V)\left[\langle r^2\rangle_i / \langle r^2\rangle_{od}\right](\lambda - \lambda^{-2}) \qquad (2.38)$$

where the λ's are measured with respect to the dimensions of the undeformed network. This correction term was first proposed by Tobolsky[42-44] and James and Guth.[40,41]

(2.4.2) The Elasticity and Swelling of Gaussian Networks

Consideration of the properties of a network that has been swollen by a diluent is complicated: the reference state, when the extension ratios are unity, may depend on the degree of swelling, the nature of the diluent, etc.[11,12]

The free energy of swelling is given

$$\Delta F_{sw}/kT = (3A\nu/2)\left[\langle r^2\rangle_{is}/\langle r^2\rangle_{os} - \langle r^2\rangle_i/\langle r^2\rangle_{od}\right] - (3\nu/2)\ln\left[\left\{\langle r^2\rangle_{is}/\langle r^2\rangle_i\right\}\left\{\langle r^2\rangle_{od}/\langle r^2\rangle_{os}\right\}\right] \qquad (2.39)$$

where $\langle r^2\rangle_{is}$ and $\langle r^2\rangle_{os}$ are respectively the values of $\langle r^2\rangle_i$ and $\langle r^2\rangle_{od}$ that occur in swollen samples.

The HFW theory gives the free energy of crosslinking a swollen network as:

$$\Delta F_{cr}/kT = (\nu - B\nu)\ln \phi_2 \qquad (2.40)$$

where ϕ_2 is the volume fraction rubber in the swollen, undeformed network.

Finally the Gibbs free energy of mixing is obtained from the Flory-Huggins equation:[12]

$$\Delta G_{mix}/kT = N_1 \ln(1 - \phi_2) + \chi_1 N_1 \phi_2^2 \qquad (2.41)$$

where N_1 is the number of diluent molecules and χ_1 is a constant describing the polymer/solvent interaction.

The total free energy change on swelling a rubber network is[11]

$$\Delta G/kT = \Delta F_{sw}/kT + \Delta F_{cr}/kT + \Delta G_{mix}/kT \qquad (2.42)$$

$$= (3A\nu/2)\left[\langle r^2\rangle_i / \langle r^2\rangle_{os}\right]\left[\phi_2^{-2/3} - \langle r^2\rangle_{os} / \langle r^2\rangle_{od}\right]$$

$$+ \nu B \ln\phi_2 + \ln\left[\langle r^2\rangle_{os} / \langle r^2\rangle_{od}\right]^{3/2}$$

$$+ N_1 \ln(1 - \phi_2) + \chi_1 N_1 \phi_2 \qquad (2.43)$$

If the network is swollen in pure diluent the difference in the chemical potential of the solvent inside and outside of the network is:

$$\Delta\mu_1 = (\partial \Delta G / \partial N_1)_{T,V} \qquad (2.44)$$

At equilibrium $\Delta\mu_1 = 0$ and:

$$A\nu^*\bar{V}_1 q_o^{-2/3}\ \phi_2^{-1/3} = -\left[\ln(1 - \phi_2) + (1 - B\nu^*\bar{V}_1)\phi_2 + \chi_1\phi_2^2\right] \qquad (2.45)$$

where $q_o^{2/3} = \langle r^2\rangle_{os} / \langle r^2\rangle_i$, $\bar{V}_1$ is the partial molar volume of the diluent and ν^* is the number of moles of network chains per unit volume of rubber.

If the freely swollen network is deformed, then for the case of uniaxial compression or tension:[11]

$$\sigma = (A\nu^* RT)\phi^{-1/2} q_o^{-2/3}(\lambda - \phi_d / \lambda^2\phi_2) \qquad (2.46)$$

where σ is defined with respect to the dimensions of the dry undeformed network, whilst λ is defined with respect to the swollen but undeformed network; ϕ_d is the volume fraction

of rubber in the swollen deformed network. For a constant volume deformation $\phi_d = \phi_2$ so:

$$\sigma = (A\nu^*RT)\phi_2^{-1/3} q^{-2/3}(\lambda - \lambda^{-2}) \qquad (2.47)$$

A swollen network is characterised by A, B, χ_1, ν^* and q_o; the possible values of A and B have been discussed. q_o is often assumed to be unity which implies that $\langle r^2_{11}\rangle_{od} = \langle r^2\rangle_{os}$ although this has not been theoretically justified. A may be obtained from stress-strain measurements, so if $B\nu^*\bar{V}_1$ is assumed to be much smaller than unity (B is assumed to be zero by James and Guth) then χ_1 may be obtained from equation (2.45). Introducing the assumptions that B is zero and q_o is unity gives:

$$A\nu^*\bar{V}_1\phi_2^{-1/2} = -\left[\ln(1-\phi_2) + \phi_2 + \chi_1\phi_2^2\right] \qquad (2.48)$$

and: $$\sigma = (A\nu^*RT)\phi_2^{-1/3}(\lambda - \lambda^{-2}) \qquad (2.49)$$

which are the more commonly encountered forms of these equations.

(2.4.3) The Swelling of Elastomers: Cohesive Energy Densities of Polymers

The Flory-Huggins constant[12], χ_1, is a free energy of mixing comprising an enthalpy of mixing and a non-combinational contribution to the entropy of the system:

$$\chi_1 = \chi_H + \chi_S \qquad (2.50)$$

$$\chi_H = \left[W_{12} - \tfrac{1}{2}(W_{11} + W_{22})\right]Z/kT \qquad (2.51)$$

where W_{12}, W_{11} and W_{22} are the energies associated with solvent/polymer, solvent/solvent and polymer/polymer contacts respectively and Z is the number of nearest neighbour contacts. If the system is free from specific interactions then to a good approximation:[45]

$$W_{12} \approx (W_{11}W_{22})^{\frac{1}{2}} \tag{2.52}$$

$$\therefore \chi_H = -Z(W_{11}^{\frac{1}{2}} - W_{22}^{\frac{1}{2}})/2kT \tag{2.53}$$

or[45,46] $$\chi_H = V_1/RT\left[(E_1/V_1)^{\frac{1}{2}} - (E_2/V_2)^{\frac{1}{2}}\right] \tag{2.54}$$

E_1 and E_2 are respectively the molar cohesive energies of solvent and polymer (i.e. $E_1 = -ZW_{11}/2$ and $E_2 = -ZMW_{22}/2$ where M is the number of polymer segments per chain) and V_1 and V_2 are respectively the molar volumes of solvent and polymer.

Equation (2.54) gives:

$$\chi_H = V_1/RT(\delta_1^2 - \delta_2^2) \tag{2.55}$$

where $\delta_1 = (E_1/V_1)^{\frac{1}{2}}$ and $\delta_2 = (E_2/V_2)^{\frac{1}{2}}$ are respectively the cohesive energy densities or solubility parameters of solvent and polymer.

It follows from the Flory-Huggins equation that a polymer will be soluble in a diluent over the entire range of composition, $1 > \phi_2 > 0$, if χ_1 is less than 0.5. Many workers have found empirically that χ_s has a value of 0.3-0.4 so for χ_1 to be less than 0.5, χ_H must be very small; as the smaller χ_1, the better the solvent, the best solvent will have a zero χ_H value and:

$$\delta_1 = \delta_2 \tag{2.56}$$

This relation provides the method for evaluating δ_2 by swelling the rubber in a series of solvents, plotting the degree of swelling against δ_1, values of which are tabulated, and interpolating to obtain the δ_2 value corresponding to the maximum swell.[47,48,49] As systems devoid of specific interactions are a rare occurence the solvents used to determine δ_2 should all be of the same chemical type (i.e. all esters, ketones, ethers, alcohols etc.), and preferably similar

to the rubber, so specific interactions would all have approximately the same magnitude and non-specific interactions would be dominant in determining degrees of swelling. In this case the method may be applied to systems with specific interactions although it is clearly not highly accurate and should only be regarded as of semi-quantitative or qualitative value.

The method may be improved by splitting the overall δ_1 value for a solvent into components describing the various types of interaction[14,50,51,52] including specific interactions such as hydrogen bonding etc.[14]

$$\delta^2 = \delta_H^2 + \delta_p^2 + \delta_D^2 \qquad (2.57)$$

where δ_H is the hydrogen bonding contribution and includes other similar types of weak intermolecular bonds; δ_p is the contribution from polarisation forces due to dipole interactions etc., and δ_D is the contribution from dispersion forces.

(2.5) RUBBER ELASTIC THEORY: DEVIATIONS FROM KINETIC THEORY

Many dry samples do not obey the kinetic theory; a better fit to the data is generally given by the two parameter Mooney-Rivlin equation,[10] proposed on purely phenomenological grounds (see figure 2.2).

A large number of attempts have been made to improve on the kinetic theory expression and to describe the second Mooney-Rivlin constant in molecular terms.

(2.5.1) The Phenomenological Theory of Mooney and Rivlin

Rivlin[53] showed that the free energy of deformation of a body, composed of a material that is isotropic in the undeformed state and in which any point (x_o, y_o, z_o) in the

undeformed state undergoes an affine deformation having coordinates $(\lambda_x x_o, \lambda_y y_o, \lambda_z z_o)$ in the deformed state was:

$$\Delta F_{def} = \sum_{i=o}^{\infty} \sum_{j=o}^{\infty} \sum_{k=o}^{\infty} C_{ijk}(I_1-3)^i(I_2-3)^j(I_3-3)^k \qquad (2.58)$$

where
$$I_1 = \lambda_x^2 + \lambda_y^2 + \lambda_z^2$$
$$I_2 = \lambda_x^2\lambda_y^2 + \lambda_y^2\lambda_z^2 + \lambda_x^2\lambda_z^2 \qquad (2.59)$$
$$I_3 = \lambda_x^2\lambda_y^2\lambda_z^2$$

Assuming that the material is imcompressible, when $I_3 = 1$:

$$\Delta F_{def} = \sum_{i=o}^{\infty} \sum_{j=o}^{\infty} C_{ij}(I_1-3)^i(I_2-3)^j \qquad (2.60)$$

The first non-zero term in this expansion is:

$$\Delta F_{def} = C_{10}(I_1-3) \qquad (2.61)$$

which has the same form as the kinetic theory equation. The sum of the first two terms is:

$$\Delta F_{def} = C_{10}(I_1-3) + C_{01}(I_2-3) \qquad (2.62)$$

which was first derived by Mooney[54]. For uniaxial tension or compression this gives:

$$\sigma = 2(C_1 + C_2/\lambda)(\lambda - \lambda^{-2}) \qquad (2.63)$$

where $C_1 = C_{10}/V$ and $C_2 = C_{01}/V$. Equation (2.63) has been shown to fit the stress-strain properties of dry elastomer networks over a fairly wide range of λ values.

Other phenomenological equations[21,55,56,57] have been proposed but none has been used as widely as the Mooney-Rivlin equation.

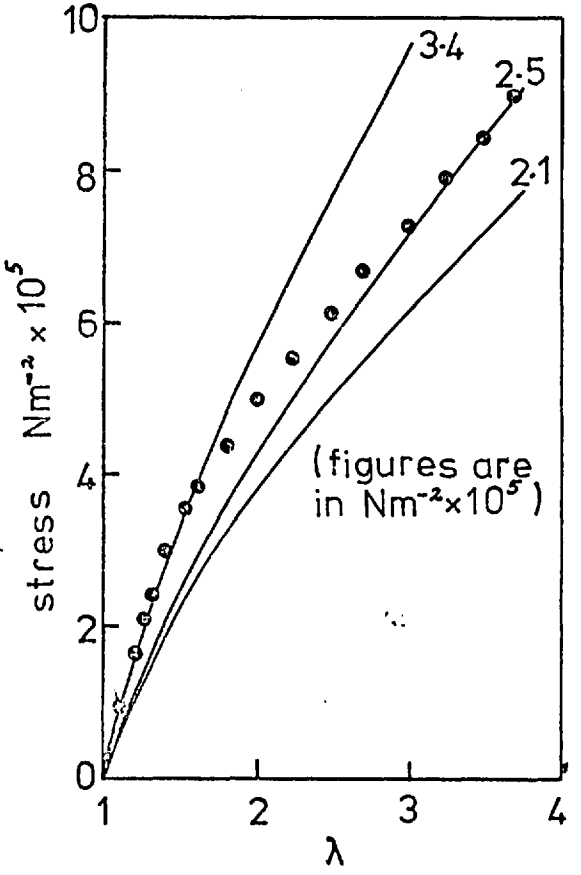
When applied to the case of swollen networks the Mooney-Rivlin equation takes the form:

$$\sigma = 2(C_1 + C_2/\lambda)\phi_2^{-1/3}(\lambda - \lambda^{-2}) \qquad (2.64)$$

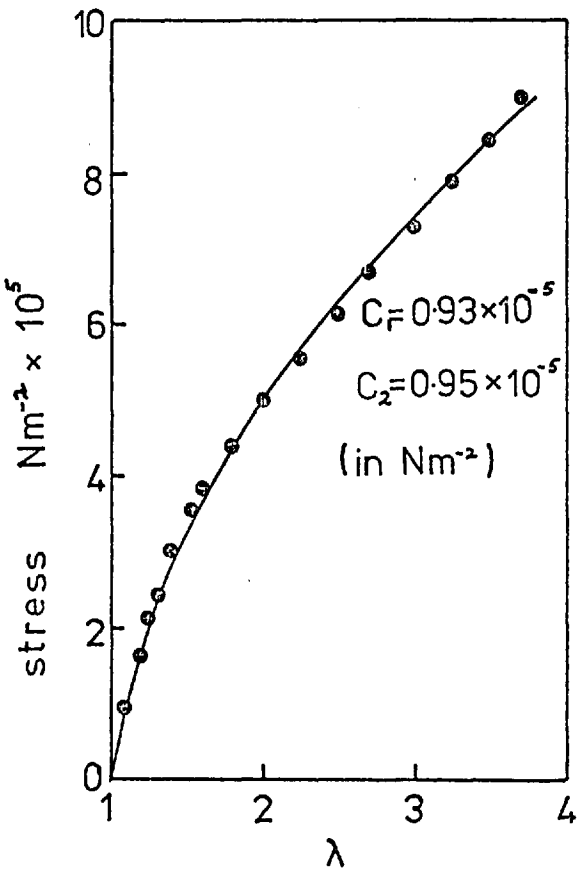
The two coefficients C_1 and C_2 cannot be interpreted in molecular terms from the Mooney-Rivlin theory but comparing coefficients with the kinetic theory gives[11]:

$$2C_1 = (A\nu kT/V)\langle r^2\rangle_i/\langle r^2\rangle_{od} \text{ for dry networks} \qquad (2.65)$$

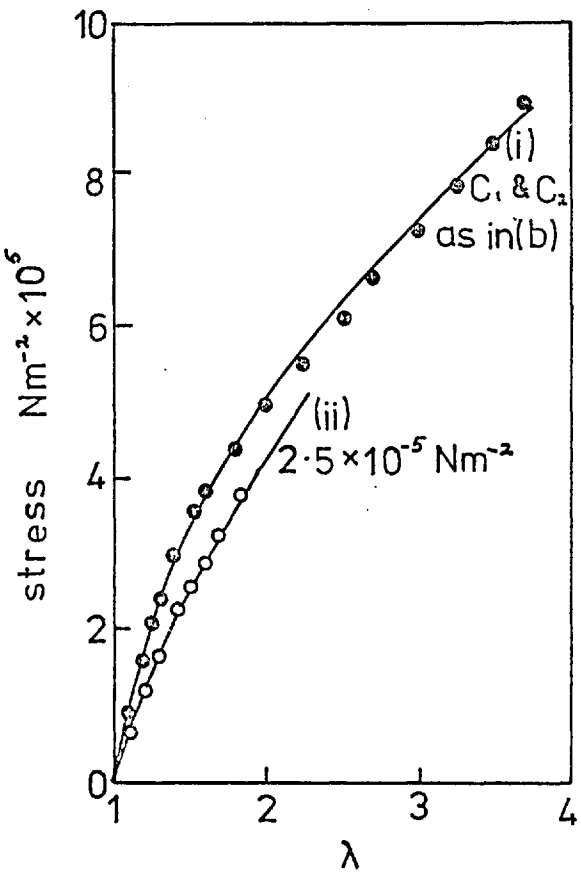
figure 2·2



(a) kinetic theory plots: lines are theoretical for different ($A\nu kT/V$) values – points are experimental for Genthane S cured with 1·5 % Dicumyl Peroxide



(b) Mooney-Rivlin plot: line is theoretical – points as in (a)



(c) plots of data for swollen and dry samples : ∘ sample as in (a); ∘ sample as in a but swollen in ethyl acetate – lines: (i) Mooney-Rivlin ; (ii) kinetic theory

and $2C_1 = (A\nu kT/V)q_o^{-2/3}$ for swollen networks (2.66)

If $\langle r^2\rangle_i/\langle r^2\rangle_{od}$ and q_o are assumed to be unity:

$2C_1 = (A\nu kT/V)$ for both dry and swollen networks (2.67)

C_2 cannot be interpreted in this way but is often small or zero for swollen samples indicating that these obey kinetic theory (see fig. 2.2c).

(2.5.2) Deviations From Kinetic Theory

(2.5.2.1) Non-Gaussian Single Chain Statistics

The Gaussian approximation is only valid when the end-to-end vector of a network chain is small compared with its contour length; when this is not so the inverse Langevin distribution is a better approximation. Guth[26] used a series expansion approximation of the inverse Langevin distribution and showed by the JG method that

$$\sigma = D_1(\lambda - \lambda^{-2}) + 2/3D_2^{11}(1 - \lambda^{-3}) + D_2^1(\lambda^3 - \lambda^{-3}) \quad (2.68)$$

where $D_1 = K_2kT$, $D_2^1 = \frac{1}{2}K_2^1kT$ and $D_2^{11} = D_2^1$; K_2^1 has the same characteristics as K_2. Smith, Ciferri and Hermans[58] used a similar series expansion but employed the HFW method to obtain an equation identical to equation (2.68) but with

$D_1 = (A\nu kT/V)(1 - n^{-1})$, $D_2^1 = (3AkT/5nV)$ and

$$D_2^{11} = (3AkT/10nV) \quad (2.69)$$

Equation (2.68) contains a term with the same form as the second term of the Mooney-Rivlin equation, in addition to a term in $(\lambda^3 - \lambda^{-3})$. However, Guth[26] suggests that when inter and intramolecular interaction effects are taken into account there may be a partial cancellation of this term, as will be shown later.

Treloar[10] has used the inverse Langevin distribution in conjunction with the regular cubic three chain and the regular tetrahedral four chain model, such as has been used by Flory and Rehner[34,35], which gives

$$\sigma = (\nu kT/3)m^{\frac{1}{2}} \left[L^{-1}(\lambda/m^{\frac{1}{2}}) - \lambda^{-3/2} \; L^{-1}(\lambda^{-\frac{1}{2}}m^{-\frac{1}{2}}) \right] \qquad (2.70)$$

for the three chain model and

$$\sigma = (\nu kT/3)(m^{\frac{1}{2}}/3)^{\frac{1}{2}}(\lambda - \lambda^{-2}) \left[\frac{L^{-1}\left\{ (\lambda^2 + 2/\lambda)^{\frac{1}{2}}(3/m^{\frac{1}{2}})^{\frac{1}{2}} \right\}}{(\lambda^2 + 2/\lambda)} \right] \qquad (2.71)$$

for the four chain model. In both cases ml is the contour length of the chains that contain m links each of length l.

Both these equations give good fits to the data after careful choice of ν and m but this, like that obtained using the Mooney-Rivlin equation; is simply a two parameter fit, although the molecular significance of the constants is more obvious.

Apart from the inverse Langevin distribution, Thomas[55] has used an empirical distribution by the inclusion of a term that corresponds to a small attractive force resisting extension of the chain. This gives the stress-strain equation:

$$\sigma = C \left[(\lambda - \lambda^{-2}) + m^* \left\{ \left[3/2(\lambda^3 - 1) \right] - \frac{(\lambda^2 + 2)\, \tan^{-1}(\lambda^3 - 1)^{\frac{1}{2}}}{(\lambda^3 - 1)^{3/2}} \right\} \right]$$

where $C = (A \nu kT/V) \left\langle r^2 \right\rangle_i / \left\langle r^2 \right\rangle_{od}$ and m^* is a constant.

This equation gives a σ vs λ curve that is very similar to that predicted by the Mooney-Rivlin equation.[59]

(2.5.2.2) The Presence of Crosslinks and Network Connectivity

Gordon[60] has proposed a stress-strain equation in which network connectivity was introduced via Dirac delta functions.

For uniaxial compression or tension at constant volume this takes the form

$$\left[\sigma^2/(I_1 - 3) - D_1\nu^2\right](I_1 - 3)^{-1} = D_2\nu^2(I_1 - 3) \qquad (2.73)$$

where D_1 and D_2 are constants related to molecular parameters and $I_1 = (\lambda^2 + 2/\lambda)$. Rearrangement of this equation shows σ to be proportional to ν as in all the other equations considered so far. This equation gives a good fit to the data as does the Mooney-Rivlin equation.[60]

In the derivation of the kinetic theory expression it was implicitly assumed that the crosslinks were randomly distributed throughout the network. A non-random distribution of crosslinks might result from the non-random distribution of crosslink sites throughout the base polymer and this could well result in deviations from kinetic theory. The effect of non-random distributions of crosslinks and inhomogeneous network formation has been considered in detail by Dusek and Prins.[11]

(2.5.2.3) Non-Ideal Network Elements

Several authors have considered the effect of non-ideal network elements such as are illustrated in figure 2.3.

Loose ends (figure 2.3a), which are usually the ends of the primary polymer molecules, will not support the stress.[12] This problem has been treated in some detail and will be discussed fully in section 3·3·2 (page 55).

Entanglements[12,61] (figure 2.3b) and loops (figure 2.3c) may also occur. Permanent entanglements cannot be unentangled without breaking network chains or crosslinks whilst temporary entanglements can be removed without network chain or crosslink cleavage. In general temporary entanglements will not affect

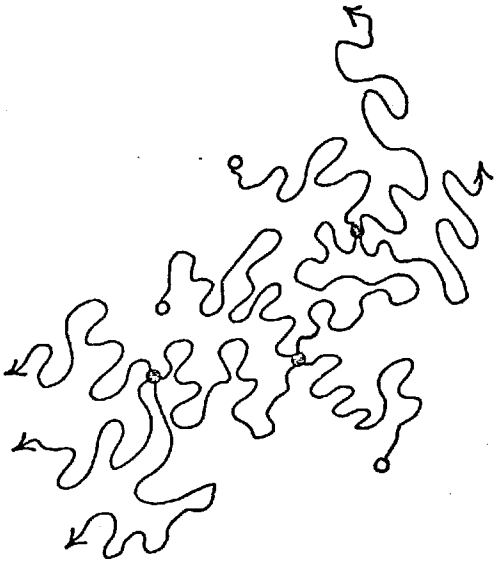
the equilbrium elastic properties of the network but may contribute to the approach to equilibrium as a viscoelastic effect[25]: on the other hand, permanent entanglements will act as additional partial crosslinks.[61]

Loops will affect the elastic properties of the network in the same way as loose ends unless they interpenetrate other loops (figure 2.3d) or are entangled (figure 2.3e) in these cases they will behave as permanent entanglements.[12]

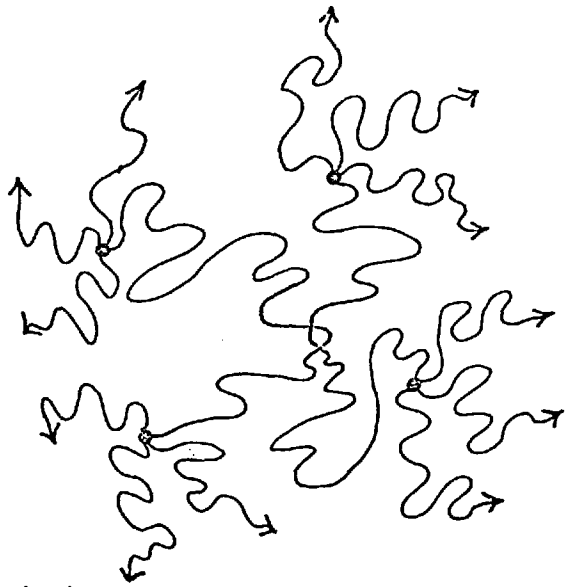
Other non-ideal elements arise in the form of structuring or pre-existing order within the network. In its most extreme form this exists as distinct microcrystalline regions, although it can also occur as local ordering such as correlated regions or bundles of molecules, chains or segments.[11] Since these regions will tend to become preferentially orientated when the network is deformed they will give rise to an additional entropy contribution. Volkenstein, Gotlib and Ptitsyn[62] have treated this case and obtained:

$$\sigma = (A\nu kT/V)\left[\langle r^2\rangle_i/\langle r^2\rangle_{od}\right](\lambda - \lambda^{-2}) + (0.72\nu_b kT/V)(1 - \lambda^{-3}) \qquad (2.74)$$

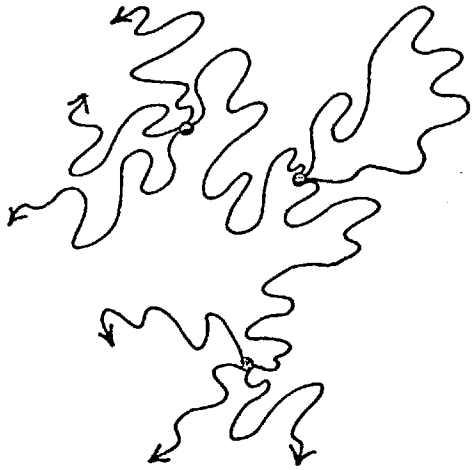
where ν_b is the number of bundles; this equation has the same form as the Mooney-Rivlin equation.[63] James and Guth[64] have also obtained a similar equation and Blockland has derived a more complicated equation that is theoretically less satisfactory. A recent equation to describe networks of partially crystalline chains has been proposed by Yamamoto and White[65] and will be discussed in section (2.5.2.5)



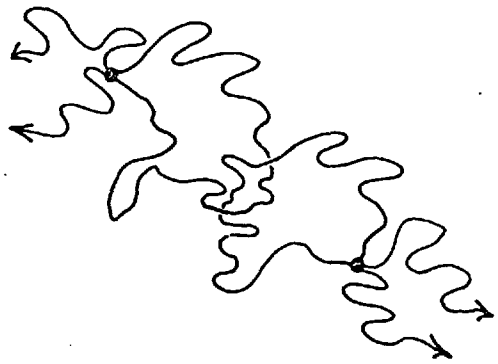
(a) loose ends



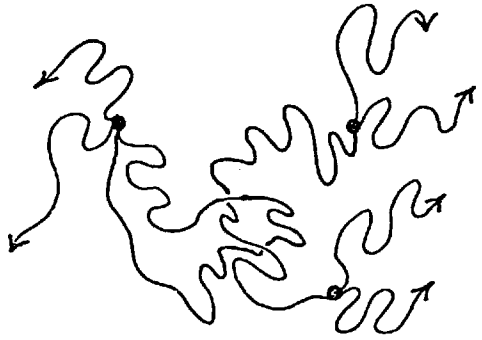
(b) entanglement



(c) loop



(d) interpenetrating loops



(e) an entangled loop

figure 2·3 : Network Defects
(• – a crosslink ; o – a loose end ; ← – point of connection to network)

(2.5.2.4) Volume Effects

Implicit in the kinetic theory is the assumption that the polymer segments, which comprise the network chains, have zero volume; in reality polymer segments have a small but finite volume so that a region of space that is occupied by a polymer segment cannot be occupied by another segment. Since polymer segments are excluded from the volume already occupied by other polymer segments, the number of configurations available to a network chain is less than that predicted by the Gaussian distribution. Several distribution functions that include excluded volume effects have been proposed.[67,68,69] These have been reviewed by Shen, Hall and De Wames[66] and give a stress-strain equation.

$$\sigma = A_1(\lambda - \lambda^{-2}) + A_2 \Phi(\lambda) \qquad (2.75)$$

where A_1 and A_2 are constants related to molecular parameters (both are proportional to νkT) and $\Phi(\lambda)$ is a complicated function of λ having roughly the same dependence on λ as $(1 - \lambda^{-3})$. Unfortunately $\Phi(\lambda)$ usually has the opposite sign to $(1 - \lambda^{-3})$ which makes it unlikely to be the only explanation for the deviations from kinetic theory.

Di Marzio[70] suggested that neighbouring network chains would compete for the available space, reducing the number of configurations of a chain below the number predicted by the Gaussian distribution. This results in the appearance of a "packing entropy" giving the equation

$$\sigma = (\nu kT/V)(\lambda - \lambda^{-2}) + (\nu kT/3V)\left[2\lambda(1 + 3\lambda^2/n)^{-\frac{1}{2}} + 1/\lambda^2(1 + 3/n\lambda)\right] \ln\left[\frac{2(1 - \alpha_z)}{1 + \alpha_z}\right] \qquad (2.76)$$

where n is the number of segments per chain and

$$\alpha_z = 1/3 + 2/9\left[(1 + 3\lambda^2/n)^{\frac{1}{2}} - (1 + 3/m\lambda)^{\frac{1}{2}}\right] \qquad (2.77)$$

This correction term does have the correct sign but is generally smaller than the second term in the Mooney-Rivlin equation.

(2.5.2.5) Deviations Due to the Deformation Process

Priss[71] suggested that whilst end-to-end vectors were transformed affinely, the number of configurations available to the deformed network was reduced due to the fact that chains may not pass through other network chains. This gave an equation:

$$\sigma = (A\nu kT/V)\left[\langle r^2\rangle_i/\langle r^2\rangle_{od}\right]\left[(\lambda - \lambda^{-2}) + m^* \Phi(\lambda)\right] \qquad (2.78)$$

where $$\Phi(\lambda) = \left[3\lambda^2/3(\lambda^3-1)\right] - \lambda^{-1} + \frac{\lambda(\lambda^3 - 4)\tan^{-1}(\lambda^3 - 1)^{\frac{1}{2}}}{2(\lambda^3 - 1)^{3/2}} \qquad (2.79)$$

and m^* is a constant.

Jackson, Shen and McQuarrie[72] have also treated the case of molecular obstruction and obtained

$$\sigma = (\nu kT/V)(\lambda - \lambda^{-2}) - (\nu kTq/3n(1-q)V)(2\lambda^3 - \lambda^{-3} - 1) \qquad (2.80)$$

where q is the fractional occupied space in the network. This equation was found to account for 20 - 60 % of the C_2 term for several different rubbers.

Dobson and Gordon[73] suggested that short chains and crosslinks (which are short chains) would follow the rotational part of the affine deformation but not the dilatational part giving an equation identical to equation (2.78) but with

$$\Phi(\lambda) = \left[3\lambda^{-1}/\ 2(\lambda^3-1)\right] - \lambda^{-1} + \frac{3\lambda^2\tan^{-1}(\lambda^3 - 1)^{\frac{1}{2}}}{2(\lambda^3 - 1)^{3/2}} \qquad (2.81)$$

Gordon, Love and Pugh[59] showed that this resulted from ignoring the Brownian motion of crosslinks and that a proper

derivation showed this effect to be negligible. Thirion and Chasset[74] combined an empirical equation expressing non-affine deformation with inverse Langevin statistics giving a complicated equation that simulated, fairly well, the general shape of the experimental data.

(2.5.2.6) Molecular Interactions

Guth[26] has considered the case of networks with molecular interactions that result in a change in the internal energy of the network on stretching; for interactions between neighbouring segments

$$\sigma = D_1(\lambda - \lambda^{-2}) + D_2(1 - \lambda^{-3}) - 2D_2(\lambda^3 - \lambda^{-3}) \qquad (2.82)$$

where $D_1 = MkT\langle w^2\rangle$, $D_2 = M\langle w^2\rangle kT/5\,[(5kT/Bz) + 1]$, M is the number of segments per unit volume, $\langle w^2\rangle$ is the mean-square fractional extension of the network chains, B is a constant describing the intersegmental interaction and z is the number of next-neighbour segments. The interaction is regarded as being analogous to the Van der Waals forces introduced into imperfect gas theory. Comparison of this equation with equation (2.68) shows that they have the same form; combination of the two equations gives

$$\sigma = D_1(\lambda - \lambda^{-2}) + (D_2 + 2/3D_2^{II})(1 - \lambda^{-3}) + (D_2^{I} - 2D_2)(\lambda^3 - \lambda^{-3}) \qquad (2.83)$$

and if, at some particular temperature, $D_2^{I} \approx 2D_2$ then the equation reduces to the Mooney-Rivlin equation. Although an exact cancellation is unlikely it is possible that there might be a partial cancellation.

An alternative approach has been proposed by Krigbaum and Kaneko[75] who considered a network of "cubic lattice chains". These are chains in which the angle between successive links is $\pi/2$ and in which any link is perpendicular to the

plane formed by the previous two. Thus every third link is in the same direction (e.g. the x direction) and the only difference between two links lying in this direction is their sign (i.e. + or -). Consequently the system of cubic chains is regarded as comprising three sets of one dimensional chains, interactions being introduced by assigning different energies to successive pairs of bonds with like and unlike signs. Use of the JG method gives

$$\sigma = (\nu kT/V)(V_s/V^2)^{1/3}(\lambda - \lambda^{-2})Q \qquad (2.84)$$

where

$$Q = 1 + 9N(V_s/V)^{2/3}(3e^{2k} - e^{-2k})(\lambda^2 + 4/3\lambda) \qquad (2.85)$$

V_s is the volume of the strained sample, $K = \Delta\epsilon/2kT$, $\Delta\epsilon = \epsilon_{unlike} - \epsilon_{like}$ and ϵ_{unlike} and ϵ_{like} are respectively the energies of pairs of bonds with unlike and like signs. Tobolsky, Carlson and Indictor[42] and Flory, Hoeve and Ciferri[76] have treated the problem in a similar manner using one dimensional chains and have obtained equations with the same strain dependence as kinetic theory, only the front factor was modified. The Krigbaum and Kaneko equation fits the experimental data giving negative K values that indicate that the stretching process is opposed by the internal energy effects in the sense that coiled configurations are energetically preferred over the more extended configurations.

A recent approach by Yamamoto and White[65] has used a lattice model for networks with internal energy contributions that depend on the relative configurations of sequences of bonds (assuming bonds may be in either gauche or trans configurations). This theory gives

$$\sigma = (A\nu kT/V)\left\{\left(\langle r^2\rangle_i/\langle r^2\rangle_{od}\right) - 2(3\Delta b/Mb)(M-1)(\lambda^2+\lambda^{-1})f(f-1)\right\}(\lambda - \lambda^{-2}) \qquad (2.86)$$

where M is the number of segments per polymer chain, Mb is the extended length of a chain, $\Delta b = b_T - b_G$, Mb_T and Mb_G are respectively the extended lengths of polymer chains with all bonds in the trans or gauche configuration, $f = \left[(z' - 2)X\right] / \left[1 + (z' - 2)X\right]$, $X = \exp\left[\left\{-(\epsilon_G - \epsilon_T) + (kT\Delta b/Mb)(\lambda^2 - \lambda^{-1})\right\}/kT\right]$, z' is the coordination number of the polymer chain sub-lattice and ϵ_G and ϵ_T are respectively the energies associated with gauche and trans bonds.

This theory has been extended to treat a network of partially crystalline chains giving

$$\sigma = (A\nu kT/V)(1/1-\chi^*)\left[(\lambda - \lambda^{-2}) - \left(\frac{Mb\Delta b}{\pi\langle r^2\rangle_i}\right)\chi^* g(\lambda)\right] \qquad (2.87)$$

where χ^* is the fraction of the M segments of a chain that are crystalline and $g(\lambda)$ is a complicated function of λ. Equations (2.86) and (2.87) have been successfully applied to the prediction of crystallinity induced as a consequence of the deformation process.

(2.5.3) The Molecular Basis of the Second Mooney-Rivlin Constant

The second Mooney-Rivlin constant, C_2, which expresses the magnitude of the deviations from kinetic theory, is difficult to interpret in molecular terms.

In section (2.5.2) the theoretical proposals that have been advanced to explain these deviations have been reviewed. Many of these treatments give equations that are either identical or give approximately the same dependence on λ to the Mooney-Rivlin equation and consequently these equations fit the experimental data quite well. It would thus appear

that equations do exist which give molecular credibility to C_2 although it is impossible, from stress-strain measurements alone, to decide which of these equations apply to a particular rubber.

To add further to this confusion, it has been suggested[25,77] that none of these equilibrium explanations is responsible for C_2 which results from the failure of the network to reach equilibrium. Flory and Ciferri[25,77] reported that the magnitude of C_2 was influenced by the time scale of the experiment such that smaller C_2 values were obtained when the time interval between successive loadings of the sample was increased. This implied that the observed C_2 values arose, in part, from the failure to achieve equilibrium conditions when evaluation was based on stress-strain measurements where sufficient time was not allowed for the completion of stress relaxation. It was suggested[25,77] that under ideal equilibrium conditions C_2 would become vanishingly small.

Whilst there is evidence that C_2 can be reduced there is also a considerable body of evidence that even under these conditions C_2 still remains finite . That part of C_2 that depends on non-equilibrium effects will depend on the nature of the sample and will be reduced by swelling the sample in a diluent, which may also reduce the equilibrium part of C_2, and by increasing the temperature. C_2 can sometimes be reduced to zero by swelling the samples in a diluent and making stress-strain measurements on the swollen samples.

A feature of C_2 apparent from the theoretical treatments of section (2.5.2) and the experimental evidence[78] is that C_2 is proportional to ν ; this is important to the interpretation of chemical stress relaxation measurements to be discussed in Chapter 3.

CHAPTER 3

CHEMICAL STRESS RELAXATION: THEORETICAL CONSIDERATIONS

(3.1) INTRODUCTION

Chemical stress relaxation [15,79,80] is a method for measuring the progress of chemical reactions that result in changes of the number of elastically effective network chains within a polymer network. Experimentally the technique comprises measuring the force exerted by a strip of rubber at constant strain and temperature. Under these conditions both C_1 and C_2 are proportional to ν, (see Chapter 2) so

$$f \alpha \nu \qquad (3.1)$$

If C_2 is primarily due to non-equilibrium effects there may be deviations from equation (3.1), although chemical stress relaxation is conducted at higher temperatures than stress-strain measurements where viscoelastic relaxation will be fast. Thus non-equilibrium effects are likely to be small; their magnitude may be determined by comparing stress-relaxation data with estimates of the changes in ν obtained from swelling measurements.

If f_o and f_t are respectively the forces exerted by the network initially and at time t and ν_o and ν_t are respectively the network chain densities initially and at time t

$$f_t/f_o = \nu_t/\nu_o \qquad (3.2)$$

(3.2) CONTINUOUS AND INTERMITTENT STRESS RELAXATION: THE TWO NETWORK THEORY

The chemical stress relaxation experiment may be done [15,80,81] in one of two ways:

(i) The sample is maintained continuously at constant strain and temperature and the force exerted by it measured with respect to time. This is a continuous stress relaxation experiment.

(ii) The sample is maintained in the undeformed or relaxed state at constant temperature and stretched intermittently to a fixed strain in order to measure the force exerted by it; once the force has been measured it is returned to the relaxed state. Ideally, conditions are such that the sample is in the relaxed state for a very long time compared with the time for which it is in the deformed state. This is an intermittent stress relaxation experiment.

Tobolsky, Andrews and Hanson [81] proposed that the continuous experiment gives a measure of the fraction of the original network chains that have not been removed by scission up to time t, new crosslinks formed supporting zero stress. The sample behaves as if it comprises two interpenetrating, but independent networks; the first, whose unstretched length is that of the undeformed sample, contains the remainder of the original crosslinks; the second, whose unstretched length is that of the deformed sample, contains the new crosslinks formed.

New crosslinks formed are assumed to support zero stress because they are formed between chain segments that are close neighbours prior to crosslinking (see figure 3.1)

The intermittent experiment gives a measure of the change in overall network chain density, whether this is due to cleavage or additional crosslinking.

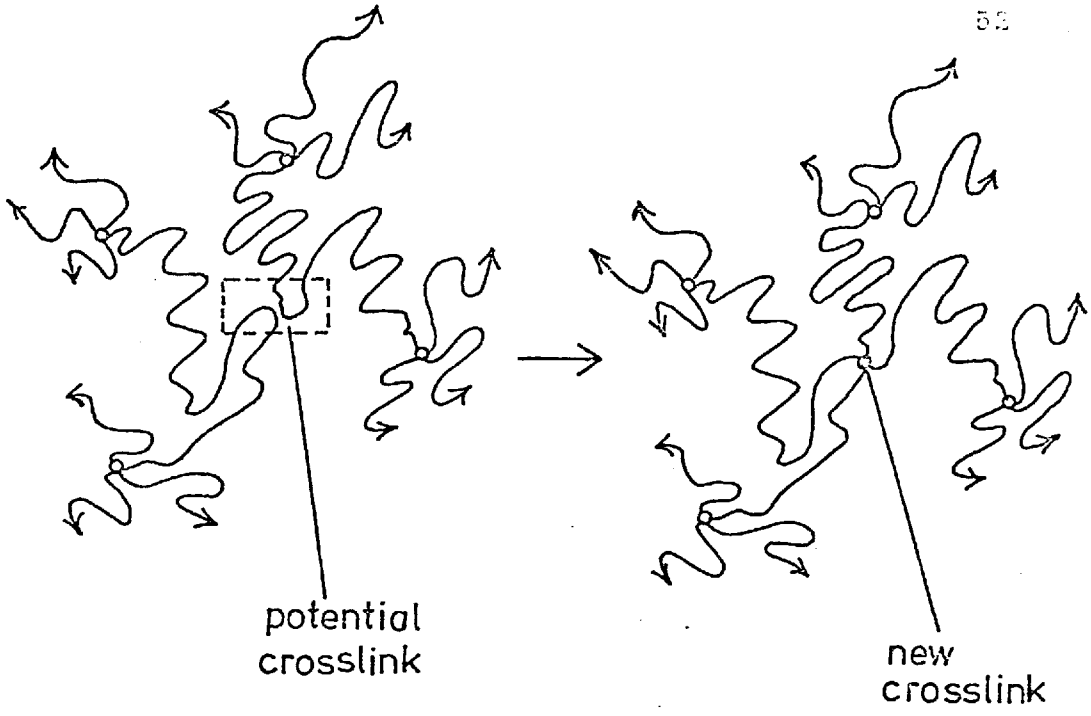


figure 3·1: Crosslink formation in a strained network (o original crosslink; ← point of connection to network)

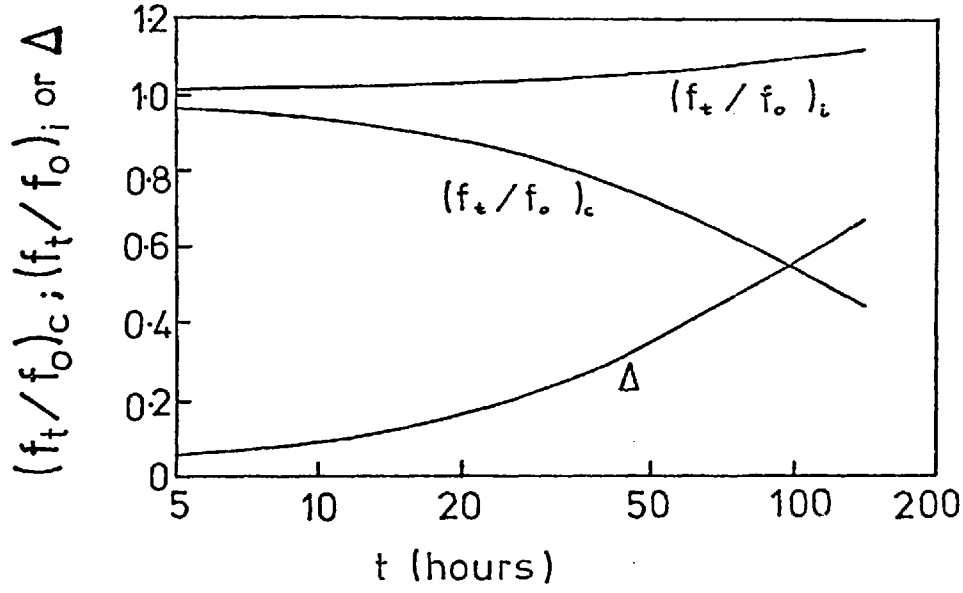


figure 3·2: Two network analysis of chemical stress relaxation data for relaxation of Adiprene CM in nitrogen at 120°C

If the network chains of the first network are ν_1 whilst those of the second network are ν_2

$$(f_t/f_o)_c = \nu_1(t)/\nu_1(o) \tag{3.3}$$

$$(f_t/f_o)_i = \frac{\nu_1(t) + \nu_2(t)}{\nu_1(o)} \tag{3.4}$$

so $$\Delta = (f_t/f_o)_i - (f_t/f_o)_c = \nu_2(t)/\nu_1(o) \tag{3.5}$$

where the subscripts c and i refer respectively to continuous and intermittant experiments (see figure 3.2).

Since the second network, formed in a deformed sample due to crosslink formation, is relaxed, it will tend to resist the return of the sample to its original length when the force is removed; relaxation of the first network will be accompanied by deformation of the second. This means that the sample will retract until the forces exerted by the two networks are equal. If l_o and l_x are respectively the original and the extended length of the sample and $l_s(t)$ is its final length; the percentage "chemical permanent set" is

$$PS(t) = \frac{l_s(t) - l_o}{l_x - l_o} \times 100 \tag{3.6}$$

so $$PS(t) = A_3\left[\left(\frac{A_1}{(\nu_1(t)/\nu_2(t))\,A_2} + 1\right)^{1/3} - 1\right] \tag{3.7}$$

where $A_1 = (l_x/l_o)^3 - 1$, $A_2 = (l_x/l_o)^2$, $A_3 = \dfrac{100}{(l_x/l_o - 1)}$

and $\nu_1(t)/\nu_2(t) = (f_t/f_o)_c\left[(f_t/f_o)_i - (f_t/f_o)_c\right]^{-1}$

Thus the percentage chemical permanent set can be obtained from continuous and intermittant stress relaxation measurements.

The "two network" hypothesis has been criticised by several authors [82,83,84,85] who argue that although new crosslinks are not under stress when formed they will take on a fractional stress as degradation of the first network proceeds. These criticisms will be discussed later.

(3.3) CLEAVAGE REACTIONS IN ELASTOMER NETWORKS [15,86]

(3.3.1) Cleavage in or at the Crosslinks

Suppose scission takes place in the crosslink (i.e. the bond joining two chains is cut). If there were $\nu(o)$ original network chains, that is $\nu(o)/2$ crosslinks, then after q cuts have been made, the number of crosslinks remaining is

$$\nu(q)/2 = \nu(o)/2 - q \qquad (3.8)$$

$$\therefore (f_t/f_o)_c = (\nu(t)/\nu(o)) = (\nu(q)/\nu(o)) = 1 - 2q(t)/\nu(o) \qquad (3.9)$$

Another case is that in which the presence of a crosslink introduces a cleavage site into the main chain adjacent to the crosslink. If one site is introduced per network chain then after q cuts have been made

$$\nu(q) = \nu(o) - q \qquad (3.10)$$

$$\therefore (f_t/f_o)_c = (\nu(q)/\nu(o)) = (\nu(t)/\nu(o)) = 1 - q(t)/\nu(o) \qquad (3.11)$$

If two sites are introduced per network chain then the probability that a site has undergone scission in $q/2\nu(o)$, the probability that a chain has not been cut is thus $\left[1 - q/2\nu(o)\right]^2$ and

$$(f_t/f_o)_c = (\nu(t)/\nu(o)) = (\nu(q)/\nu(o)) = \left[1 - (q(t)/2\nu(o))\right]^2 \qquad (3.12)$$

at short times when $q(t)/2\nu(o)$ is small

$$(f_t/f_o)_c \approx 1 - q(t)/\nu(o) \qquad (3.13)$$

A comparison of equations (3.9), (3.11) and (3.12) is shown in figure 3.3.

In equations (3.9), (3.11) and (3.12) $q_{(t)}$ will be proportional to $\nu(o)$, this means that $(f_t/f_o)_c$ will be independent of $\nu(o)$.

(3.3.2) Cleavage Within Network Chains

The case of cleavage within network chains, which is not as straightforward as crosslink cleavage, has been considered by several authors.[15,86,87,90] Tobolsky[15] and Berry and Watson[86,87] considered scission of network chains that contained a large number of cleavage sites; Tobolsky assumed that all the network chains contained the same number of sites, whilst Berry and Watson assumed that cleavage sites were randomly distributed amongst the network chains. In either case the probability that one of the x sites of a chain has undergone cleavage when q cuts have been made in the network is $q/x\,\nu(o,x)$, where $\nu(o,x)$ is the number of original network chains that contained x sites. The probability that a site has not been cleaved is $(1 - q/x\,\nu(o,x))$ and hence the probability that the chain has not been cut is $(1 - q/x\,\nu(o,x))^x$.

Tobolsky[15] assumed that all the chains contained the same number of sites, m, so

$$\nu(q)/\nu(o) = (1 - q/m\,\nu(o))^m \qquad (3.14)$$

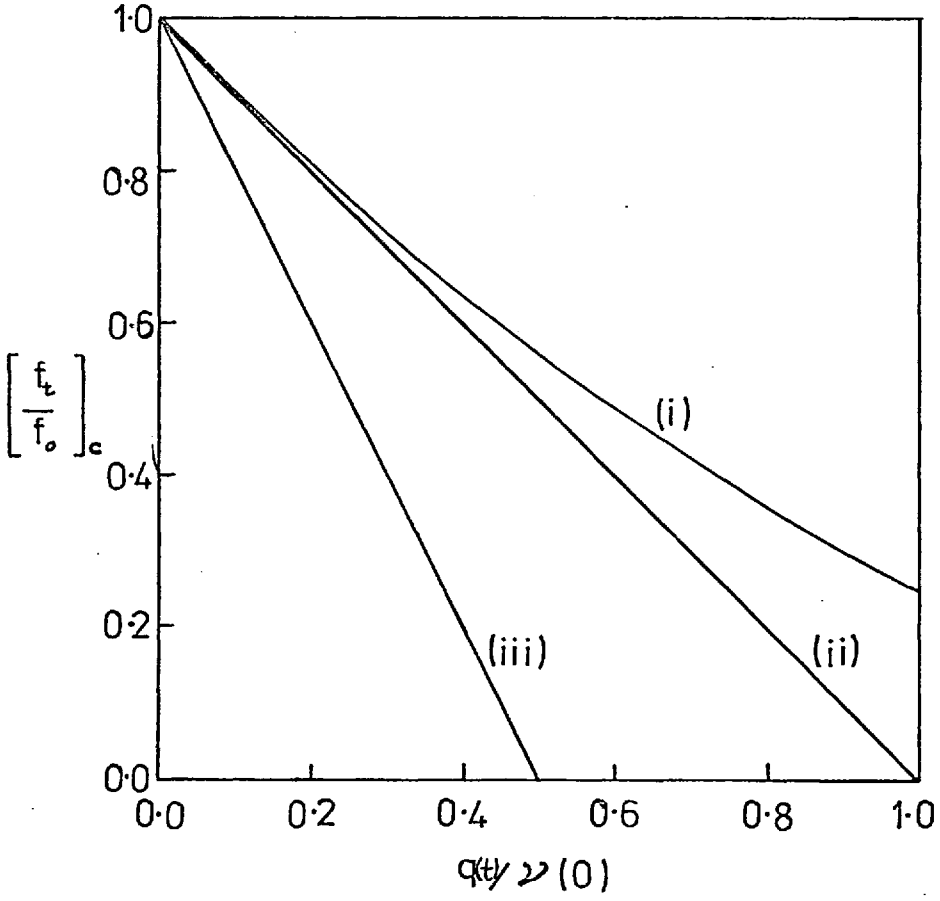


figure 3·3 : plots of $(f_t / f_o)_c$ vs $q/\nu(0)$ for cleavage in or at the crosslink – (i) cleavage at the crosslink - 2 cleavage sites per crosslink; (ii) cleavage at the crosslink - 1 cleavage site per crosslink; (iii) cleavage in the crosslink

$$\therefore \quad \ln\left[\nu(q)/\nu(o)\right] = m \ln\left[1 - q/m\nu(o)\right] \qquad (3.15)$$

q is usually much smaller than $m\nu(o)$ so to a good approximation

$$\ln\left[\nu(q)/\nu(o)\right] = -q/\nu(o) \qquad (3.16)$$

$$\therefore \quad \ln\left(f_t/f_o\right)_c = -q(t)/\nu(o) \qquad (3.17)$$

Berry and Watson[86,87] assumed that the number of chains containing $\nu(o,x)$ was given by the random distribution[12,86]

$$\nu(o,x) = \nu(o)p(1-p)^{x-1} \qquad (3.18)$$

where p is the reciprocal of the average chain length. This gives

$$\frac{\nu(q)}{\nu(o)} = \frac{\nu(o)p(1-q/\bar{x}\,\nu(o))}{p + (q/\bar{x}\,\nu(o))(1-p)} \qquad (3.19)$$

where $\bar{x}$ is the average number of cleavable units per chain.

When 1/p is large, i.e. the chains are long, equation (3.19) reduces to

$$\nu(q)/\nu(o) = \left[q/\nu(o) + 1\right]^{-1} \qquad (3.20)$$

$$\left(f_t/f_o\right)_c = \left[q(t)/\ (o) + 1\right]^{-1} \qquad (3.21)$$

Yu[89] has also considered the case of scission where scission sites are randomly distributed, although his derivation contains the implicit assumpton that cleaved bonds undergo regeneration[82]. Yu's equation reduces to equation (3.21) when 1/p is large.

These authors all treat the problem by introducing cuts into an initially perfect network (i.e. a network devoid of loose ends or other network defects); the network produced after n chains have been cut is the same as a network produced by the crosslinking of n primary molecules. This results

because n cut chains will give a network with 2n loose ends, and since each of the n primary molecules has 2 ends the network produced when these molecules are randomly crosslinked also contains 2n loose ends. The case of crosslinking n primary molecules has been considered by Flory,[12] Scanlan,[90] and others.[11,91,92,93]

Flory[12] suggested that the number of effective network chains (i.e. chains terminated at each end by a crosslink) was

$$\nu(q) = \nu(o) - 2n \qquad (3.22)$$

where q cuts result in the scission of n chains.

$$(f_t/f_o)_c = \nu(t)/\nu(o) = 1 - 2n/\nu(o) = 1 - 2q(t)/\nu(o) \qquad (3.23)$$

Scanlan[90] has corrected this result to include the effect of the presence of a sol fraction giving

$$(f_t/f_o)_c = (1 - s_1)^3(1 + s_1) \qquad (3.24)$$

for a random distribution where $s_1 = -\frac{1}{2}+\left[1/4 + (q(t)/\nu(o))\right]^{\frac{1}{2}}$. Scanlan,[90] Mullins and Thomas,[91] and Gordon and Dobson[92,93] have shown that Flory's treatment[12] does not take proper account of the effectiveness of three functional crosslinks generated when one of the chains attached to a four functional crosslink is cut. Gordon and Dobsons'[92,93] theory is the most general and gives the same result as the Mullins and Thomas[91] and Scanlan[90] treatments in this case, hence

$$(f_t/f_o)_c = (1 - s_1)^3(1 + 2s_1) \qquad (3.25)$$

A comparison of the four approaches is given in figure 3.4; equation (3.25) approaches the Tobolsky[15] and Berry and Watson[86,87] equations at small $q(t)/\nu(o)$ values and the Flory[12] equation at high $q(t)/\nu(o)$ values. Shaw[103] has considered mechanical

and electrical analogues and computer simulated networks which give a $(f_t/f_o)_c$ dependence intermediate between the Flory and Tobolsky equations provided no sol fraction effects are included.

These equations may also be used to correct the kinetic theory expression for network defects (see section 2.5.2.3) if $q(t)/\nu(o)$ is replaced by $\bar{M}n/\bar{M}c$, where $\bar{M}n$ is the number average molecular weight of the primary molecules and $\bar{M}c$ is the number average molecular weight between crosslinks. If the Scanlan[90] equation is used then $(A\nu kT/V)$ of equation (2.38) becomes $\left[A\nu(1 - s_1)^3(1 + 2s_1)kT/V\right]$ where

$$s_1 = -\tfrac{1}{2} + \left[1/4 + (\bar{M}c/\bar{M}n)\right]^{\frac{1}{2}} \qquad (3.26)$$

When applied to chemical stress relaxation measurements the theories predict

$$(f_t/f_o)_c = \Phi(q(t)/\nu(o)) \qquad (3.27)$$

where $\Phi(x)$ is some function, the nature of which depends on which theory is adopted. $q(t)$ will depend only on the number of cleavable bonds and will be independent of the crosslink density so that in networks identical in all respects except crosslink density, $q(t)$ will be at the same and

$$(f_t/f_o)_c = \Phi^{1}(\nu(o)^{-1}) \qquad (3.28)$$

so if $(f_t/f_o)_c$ is a function of $1/\nu(o)$ cleavage takes place randomly within the network chains whilst if $(f_t/f_o)_c$ is independent of $1/\nu(o)$ cleavage takes place in or at the crosslinks.

If network chains contain a small number of specific cleavage sites these equations may be modified but $(f_t/f_o)_c$ will still be a function of $1/\nu(o)$.

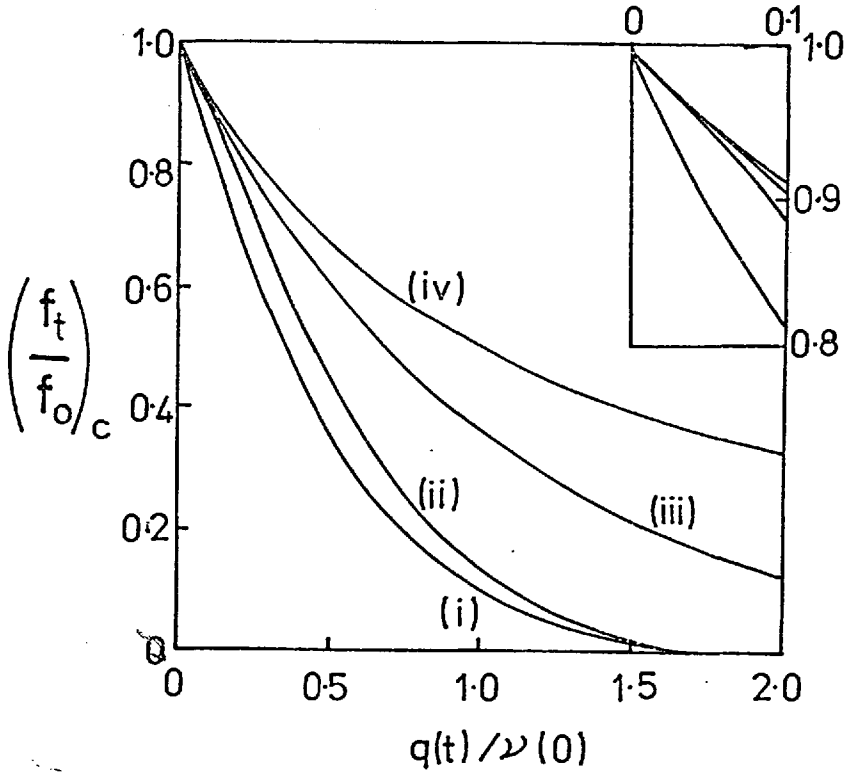


figure 3·4 : Comparison of equations relating $(f_t / f_o)_c$ to $q(t)/\nu(0)$ – (i) Flory; (ii) Scanlan; Dobson & Gordon; Mullins & Thomas; (iii) Tobolsky; (iv) Berry & Watson

(3.4) CROSSLINKING REACTIONS IN ELASTOMER NETWORKS

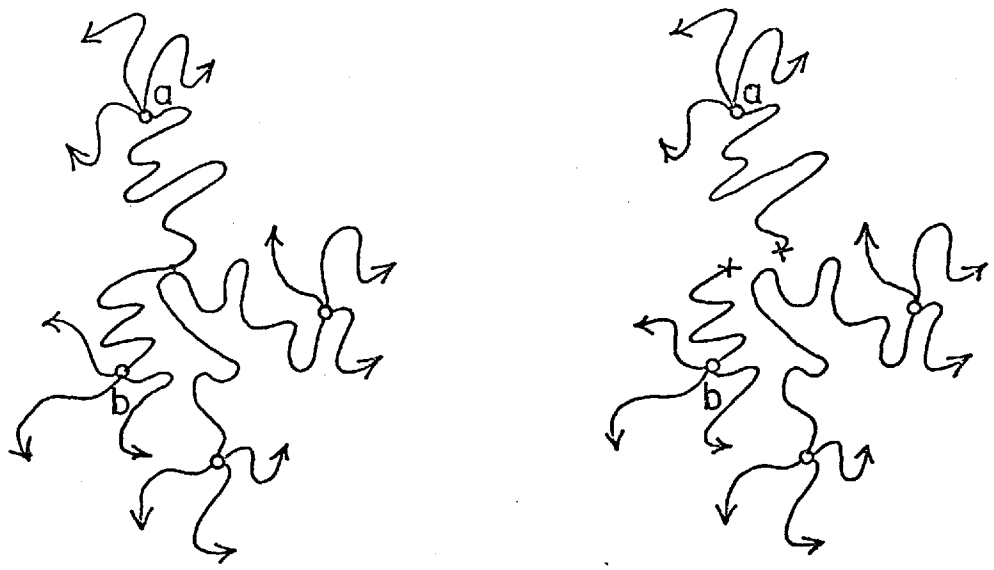
The use of the "two network theory" [15,81] to interpret the results of chemical stress relaxation experiments on networks undergoing simultaneous cleavage and crosslinking has been discussed in section 3.2. The central assumption of this theory was that new crosslinks formed in a strained sample supported zero stress. [82,83,84,85] This has been questioned: whilst it is probably valid at the instant of crosslink formation, the crosslinks may take on a fractional stress as neighbouring first stage crosslinks are removed.

The constraint imposed by a new crosslink is illustrated in figure 3.5: if there is no new crosslink, cleavage of chain ab frees crosslinks a and b so that they can take up new positions consistent only with the constraints afforded by the remaining three chains attached to each. If a new crosslink c has been formed, the freedom of b is restricted by its connection to c. Thus, on average, chains or crosslinks freed by cleavage of first stage chains or crosslinks will be partially constrained to the configurations or regions of space available to them prior to cleavage.

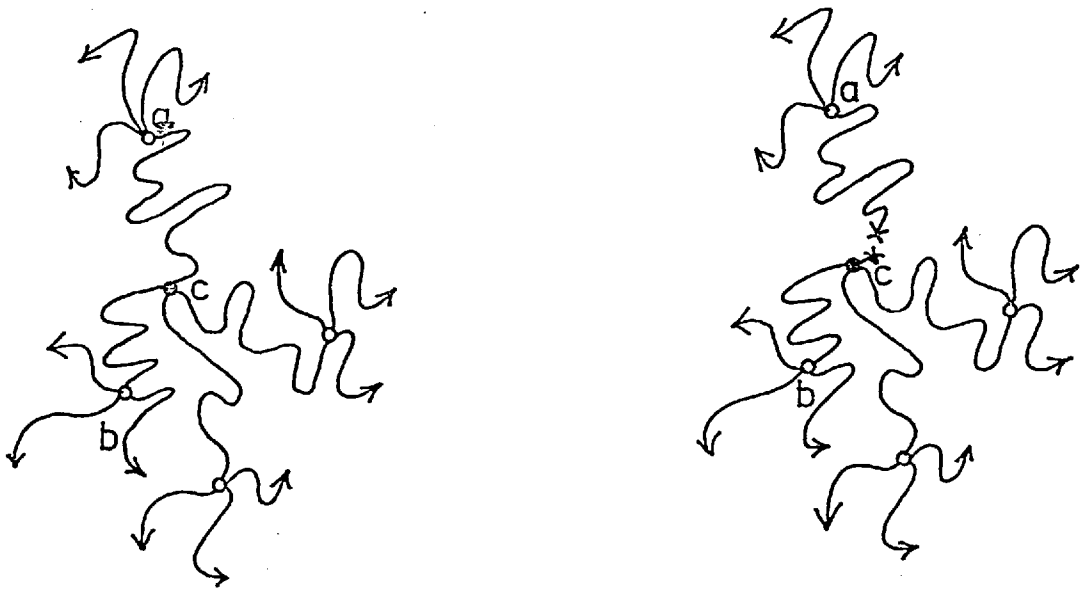
This problem is difficult to treat theoretically although several approaches have been made in specific cases.

(3.4.1) Crosslink Breakdown and Reformation: Reformed Crosslinks being Immune from Further Breakdown

This was treated by Scanlan [94] and Flory; [83] Scanlan's treatment is the more rigorous. The original crosslinks undergo cleavage, they then reform to produce stable crosslinks that do not undergo further rupture; Scanlan considers the effect of this occurence in a strained network.



(i) cleavage in a network devoid of new crosslinks



(ii) cleavage in a network with new crosslinks

figure 3·5

If the network, containing $\nu_1/2$ crosslinks, is deformed by $\lambda_{xo},\lambda_{yo},\lambda_{zo}$, $\nu_2/2$ further crosslinks introduced, followed by a further deformation to $\lambda_x,\lambda_y,\lambda_z$, the entropy change is

$$\Delta S = k/2 \left[\nu_1 I + \nu_2 I_2\right] \qquad (3.29)$$

where $I = \lambda_x^2 + \lambda_y^2 + \lambda_z^2 - 3$

and $I_2 = (\lambda_x/\lambda_{xo})^2 + (\lambda_y/\lambda_{yo})^2 + (\lambda_z/\lambda_{zo})^2 - 3$

These equations are derived in both theories except that Flory[85] generalises equation (3.29) by replacing I and I_2 by the traces of deformation gradient matrices so that the two deformations can be defined with different principal axes. Equation (3.29) can be extended to give the entropy of a network in which several sets of crosslinks have been introduced in different states of strain.

$$\Delta S = (k/2)\sum_\tau \nu_\tau I_\tau \qquad (3.30)$$

where $I_\tau = (\lambda_x/\lambda_{x\tau})^2 + (\lambda_y/\lambda_{y\tau})^2 + (\lambda_z/\lambda_{z\tau})^2 - 3$

$\lambda_x,\lambda_y,\lambda_z$ represent the final deformed state and $\lambda_{x\tau},\lambda_{y\tau},\lambda_{z\tau}$ the state in which the $\nu_\tau/2$ crosslinks were introduced. The result expressed in equation (3.29) and (3.30) for the case of crosslink formation without cleavage is identical with that obtained from the two network theory and may be regarded as a proof of the two network theory under these conditions (an equally valid proof in this case has also been given by Berry, Scanlan and Watson[82]).

Scanlan's theory considered the average entropy of freeing a monomer unit by removal of a crosslink. The distribution of end-to-end vectors for a chain between two unbroken first stage crosslinks under a deformation $\lambda_x,\lambda_y,\lambda_z$

was assumed to be given by the Wall distribution.[36] If one end of the chain under consideration is terminated by a crosslink that has broken and reformed its distribution of end-to-end vectors will not be given by the Wall distribution. Consider two neighbouring network chains derived from the same primary molecule which are joined by a reformed crosslink and the other ends of which are terminated by undisturbed crosslinks. The probability distribution for one of these chains will depend on the distribution for the second chain immediately prior to the scission, movement and reformation of the disturbed crosslink. If this second chain were terminated by a reformed crosslink its distribution function would depend on the distribution of the third chain derived from the same primary molecule immediately prior to disturbance of this second reformed crosslink. This argument can be continued such that the distribution of chain vectors, for a network chain, depends on the number of neighbouring crosslinks along the same primary molecule that have been broken and reformed sequentially starting with the most distant. Scanlan has shown that the distribution function for a chain that terminates a run of j sequentially broken and reformed crosslinks is

$$p_m(\vec{r}_i) = \frac{\beta_n^3}{\pi^{3/2} a_{xj}^{\frac{1}{2}} a_{yj}^{\frac{1}{2}} a_{zj}^{\frac{1}{2}}} \exp\left[-\beta_n^2\left(\frac{x_i^2}{a_{xj}} + \frac{y_i^2}{a_{yj}} + \frac{z_i^2}{a_{zj}}\right)\right] \qquad (3.31)$$

where $a_{xj} = 1/3\left\{(2 + \lambda_{xo}^2) + (2/4^j)(\lambda_{xo}^2 - 1)\right\}$ with similar equations for a_{yj} and a_{zj} and $\beta_n^2 = 3/2\langle r^2\rangle_o$.

The average entropy change for the freeing of one monomer unit that separates a chain terminating a run of j_i

sequentially broken and reformed crosslinks from a chain terminating a j_2 run can be obtained, and multiplied by the probability of a j_1 and a j_2 run occuring. Summing over all possible j_1 and j_2 values gives the average entropy change of freeing and refixing a monomer unit as

$$\Delta S_2 = k/2\left\{(3 - 2e^{b/4})(I + 3) + (2e^{b/4} - 2)(I_2 + 3)\right\} \tag{3.32}$$

where $b = q/\nu(o)$.

Combining equations (3.29) and (3.32) gives

$$\Delta S_{el} = (\nu(o)k/4)\left\{(7 + 3b - 8e^{b/4})I + (8e^{b/4} - 3b - 8)I_2\right\} \tag{3.33}$$

$$(f_t/f_o)_c = 7 + \left\{3q(t)/\nu(o)\right\} - 8\exp(q(t)/4\nu(o)) \tag{3.34}$$

Flory's[83] theory gives the approximate result

$$q(t)/\nu(o) = \gamma + \ln(f_t/f_o)_c - E_i\left[-(f_t/f_o)_c\right] \tag{3.35}$$

where $E_i(x)$ is the exponential integral and γ is Eulers constant (o.5772...). Expansion of this equation gives

$$q(t)/\nu(o) = \sum_{i=1}^{\infty}\left(\frac{(-1)^{i+1}}{i \times i!}\right)(f_t/f_o)_c^i \tag{3.36}$$

Figure 3.6 shows the close agreement between equations (3.34) and (3.36); this serves to increase the confidence in Flory's[83] more general theory.

(3.4.2) Crosslink Breakdown and Reformation: Reformed Crosslinks being Chemically Identical to those Initially Present

This case is also one of the ramifications of Flory's general theory[83].

The network was considered to have been prepared by the introduction of $\nu_1^*/2$ crosslinks in the unstrained state, the introduction of $\nu_2/2$ crosslinks in the state λ_1 and the removal

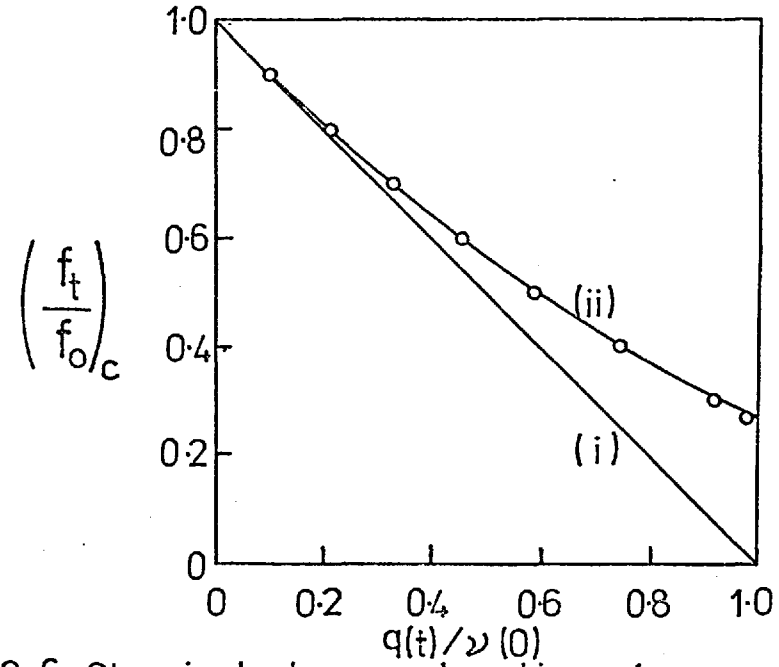


figure 3·6 : Chemical stress relaxation of a sample undergoing crosslink rupture and reformation – (i) two network theory; (ii) Scanlan's theory; (iii) points : Flory's theory

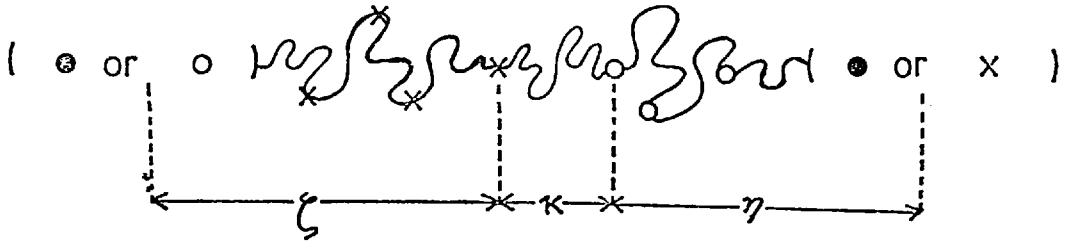


figure 3·7 : Definition of parameters ζ, κ and η. – ● residual first stage crosslink; o unit from which a first stage crosslink has been removed; x second stage crosslink.

ζ = number of chain links between x terminating a o~~x chain and the next o or ●; κ = number of links in a o~~x chain; η = number of links between o terminating a o~~x chain and the next ● or x.

of $\nu_1^o/2$ of the first stage crosslinks. Since the consequences of removing first stage crosslinks must be independent of the state of strain at which they were removed; they were removed at the final state of strain λ. After the introduction of $\nu_2/2$ crosslinks in the state λ_1, the network was deformed further to a final state λ, before removal of the first stage crosslinks. The λ's are in this case deformation gradient matrices such that:

$$\lambda = \lambda_1 \lambda_2 \tag{3.37}$$

where λ_1 and λ_2 are matrices with elements $\lambda_{ij;1}$ and $\lambda_{ij;2}$, i and j = x,y,z and

$$\lambda_{xx;1} = dx'/dx \qquad \lambda_{xy;1} = dx'/dy$$

$$\lambda_{xx;2} = dx''/dx' \qquad \lambda_{xy;2} = dx''/dy' \quad \text{etc}$$

where a point x,y,z in the unstrained state has coordinates x',y',z' in state λ_1 and coordinates x",y",z" in state λ.

At the end of the crosslinking and scission processes, when the network was in state λ, it contained network chains terminated by residual first stage crosslinks, second stage crosslinks, or units from which first stage crosslinks had been removed. Flory considered the possible combinations of such chain terminations and showed that they resulted in different contributions to the overall network elastic free energy; every first stage crosslink contributed $\frac{1}{2}\mathrm{Tr}(\tilde{\lambda}\lambda)$, every second stage crosslink, $\frac{1}{2}\mathrm{Tr}(\tilde{\lambda}_2\lambda_2)$, and every chain terminated by a second stage crosslink and a unit from which a first stage crosslink had been removed.

$\left[\xi\eta/(\eta+\kappa)(\xi+\kappa)\right]\mathrm{Tr}(\tilde{\lambda}\lambda - \tilde{\lambda}_2\lambda_2)$. ξ, η, κ are defined in figure 3.7, Tr(X) is the trace of matrix X and $\tilde{Y}$ is the transpose Matrix of Y.

The elastic free energy is given by

$$\Delta F_{el}/kT = \tfrac{1}{2}\left[(\nu_1 + \Phi\nu_2)I + (\nu_2 - \Phi\nu_2)I_2\right] \qquad (3.38)$$

where $I = \sum_{ij} \lambda_{ij}^2 - 3$ and $I_2 = \sum_{ij} \lambda_{ij;2}^2 - 3$ and

$$\Phi = \sum_{\xi}\sum_{\eta}\sum_{\kappa} H_{\xi\eta\kappa}\left[\xi\eta/(\xi+\kappa)(\eta+\kappa)\right] \qquad (3.39)$$

where $H_{\xi\eta\kappa}$ is the number of junction segments characterised by the subscripts. If all the network chains are the same length this summation can be evaluated as

$$\Phi = (2/\phi_2)\left[1 + (1-\phi_2)\phi_2^{-1}\ln(1-\phi_2)\right]\left[1 + (1-\phi_1^0)(\phi_1^0)^{-1}\ln(1-\phi_1^0)\right] \qquad (3.40)$$

where $\phi_1^0 = \nu_1^0/(\nu_1 + \nu_2)$ and $\phi_2 = \nu_2/(\nu_1 + \nu_2)$.

Flory generalised these results to treat the case of simultaneous formation and rupture of crosslinks. If the number of first stage crosslinks removed, $\nu_1^0/2$, is a vanishingly small number, it follows from equation (3.40) that

$$d\nu_{1e}/d\nu_1^0 = (1-\phi_2)\phi_2^{-1}\ln(1-\phi_2) \qquad (3.41)$$

$$d\nu_{2e}/d\nu_1^0 = -1 - (1-\phi_2)\phi_2^{-1}\ln(1-\phi_2) \qquad (3.42)$$

$$d\nu_{1e}/d\nu_2 = 0, \quad d\nu_{2e}/d\nu_2 = 1 \qquad (3.43)$$

where $\nu_{1e} = \nu_1 + \Phi\nu_2$ and $\nu_{2e} = \nu_2 - \Phi\nu_2$

If it is assumed that the effects of differential changes in the numbers of first and second stage crosslinks depend only on the effective numbers ν_{1e} and ν_{2e} of the two sets of chains then equations (3.41), (3.42) and (3.43) become

$$-(d\nu_{1e}/d\nu)_d = \nu_{1e}^2\,\nu^{-1}(\nu - \nu_{1e})^{-1}\ln(\nu_{1e}/\nu) \qquad (3.44)$$

$$-(d\nu_{2e}/d\nu)_d = -1 - \nu_{1e}^2\,\nu^{-1}(\nu-\nu_{1e})^{-1}\ln(\nu_{1e}/\nu) \qquad (3.45)$$

for changes in ν_{1e} and ν_{2e} with dissociation of the total number, $\nu/2$, of crosslinks and

$$(d\nu_{1e}/d\nu)_f = 0, \quad (d\nu_{2e}/d\nu)_f = 1 \qquad (3.46)$$

for changes due to formation of crosslinks.

These differential equations are quite general and the rates of change of ν_{1e} and ν_{2e} are obtained by feeding in the appropriate rate equations. The result discussed in section (3.4.1) was obtained from these equations.

In the case of crosslink interchange, new crosslinks are chemically identical to the initially present crosslinks and the overall number of crosslinks remains constant. The rates of dissociation and formation of crosslinks are equal and in the simplest case may be described by the rate law.

$$(d\nu/dt)_d = (d\nu/dt)_f = k'\nu \qquad (3.47)$$

where k' is a rate constant. Equations (3.44) and (3.45) give

$$d\nu_{1e}/dt = k'\nu_{1e}^2(\nu-\nu_{1e})^{-1}\ln(\nu_{1e}/\nu) \qquad (3.48)$$

which upon integration and application of the boundary conditions $\nu_{1e} = \nu$ at $t = o$ gives

$$k't = E_i\left[-\ln(\nu_{1e}/\nu)\right] - \ln\left[-\ln(\nu_{1e}/\nu)\right] - \gamma \qquad (3.49)$$

$$= w + w^2/2 \times 2! + w^3/3 \times 3! \ldots. \qquad (3.50)$$

where $w = -\ln(\nu_{1e}/\nu) = -\ln(f_t/f_o)_c$

A comparison of this result with that predicted by two network theory is shown in figure 3.8.

(3.4.3) Generalised Crosslink Formation Accompanying Scission

Apart from the results of sections (3.4.1) and (3.4.2),

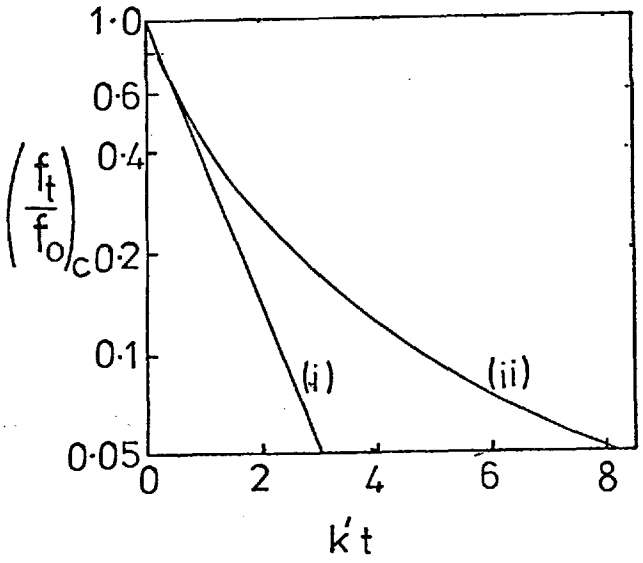


figure 3·8: Chemical stress relaxation of a sample undergoing crosslink interchange – (i) two network theory; (ii) Flory's theory.

theoretical treatments of generalised crosslinking and scission reactions are not available. In principle the case of crosslink formation and cleavage in the crosslinks may be treated using the appropriate rate laws in conjunction with equations (3.44), (3.45) and (3.46).

The case of main chain cleavage accompanying crosslink formation is more difficult to treat, particularly in view of the controversy over which equation should be used to describe the effect of main chain scission (see section 3.3.2).

In qualitative terms deviations from two network theory may be similar to those predicted in sections (3.4.1) and (3.4.2).

In all the cases considered the deviations from two network theory are much larger at small $(f_t/f_o)_c$ values than at values near to unity and the deviations may be sufficiently small when $(f_t/f_o)_c$ approaches unity for two network theory to be a reasonable approximation.

There is experimental evidence for deviations from the two network theory, particularly in the case discussed in section (3.4.1),[84] but in the main it is a good approximation.[13]

(3.5) THE KINETICS OF NETWORK REACTIONS

The possible reaction kinetics for the reactions taking place in polymeric networks are as varied as in non-polymeric materials. Once the kinetics responsible for the crosslinking or scission reactions in an elastomer are known they may be combined with the equations introduced in the first part of this chapter to give an equation that will account for the chemical stress relaxation behaviour of the network.

(3.5.1) A Resumé of Basic Kinetic Laws

The basic kinetic equations for simple cases are well known and their derivations given in elementary text books;[95] hence only the results will be summarised here.

(i) zero order kinetics: $c(o) - c(t) = kt$ (3.51)

(ii) first order kinetics: $c(t)/c(o) = \exp(-kt)$ (3.52)

(iii) second order kinetics (bimolecular combination):

$$c(o)/c(t) - 1 = c(o)kt \qquad (3.53)$$

The chemical reaction represented by these equations is

$$nc \xrightarrow{k'} \text{products}$$

where n is the order of reaction, c(o) and c(t) are respectively the reactant concentrations at time zero and time t. More complicated kinetic equations can be derived for particular reaction mechanisms; the methods of deriving these equations are described elsewhere.[95]

An important equation in chemical kinetics is the Arrhenius equation that describes the temperature dependence of the rate constant

$$k' = A\exp(-\Delta H/RT) \qquad (3.54)$$

where ΔH is the activation energy, A is a constant, T is the absolute temperature and R is the gas constant.

The theory of absolute reaction rates gives an analogous equation[95,96]

$$k' = RT/Lh \quad \exp(\Delta S^*/R)\exp(-\Delta H^*/RT) \qquad (3.55)$$

where L is Avogadro's number, h is Planks constant and ΔS^* and ΔH^* are respectively the entropy and enthalpy of activation.

For a liquid or solid phase reaction

$$\Delta H = \Delta H^{*} + RT \qquad (3.56)$$

and as RT is much smaller than ΔH^{*}

$$\Delta H \approx \Delta H^{*} \qquad (3,57)$$

The additional RT dependence of equation (3.55) over equation (3.54) will be small so that the two equations will be in close agreement with $A = RT/Lh \exp(\Delta S^{*}/R)$ allowing evaluation of the activation entropy.

(3.5.2) The Kinetic Interpretation of Chemical Stress Relaxation Data: Cleavage Reactions

The simplest case is that of cleavage in or at the crosslink.

Suppose the reaction is first order and cleavage of the crosslink occurs. Initially there were $\nu(o)/2$ crosslinks, when q(t) cuts have been made the number of crosslinks remaining is

$$\nu(t)/2 = \nu(o)/2 - q(t) \qquad (3.58)$$

and for a first order reaction

$$\nu(t)/2 = \nu(o)/2 \exp(-k_1 t) \qquad (3.59)$$

so $$q(t) = \nu(o)/2 \left[1 - \exp(-k_1 t)\right] \qquad (3.60)$$

Substitution into equation (3.9) gives

$$(f_t/f_o)_c = \exp(-k_1 t) \qquad (3.61)$$

$$\therefore \ln(f_t/f_o)_c = -k_1 t \qquad (3.62)$$

Similar reasoning for the cases of cleavage at the crosslink with one or two cleavage sites per chain gives

$$\ln(f_t/f_o)_c = -k_1 t \text{ for one site per chain and} \qquad (3.63)$$

$$\ln(f_t/f_o)_c = -2k_1 t \text{ for two sites per chain} \qquad (3.64)$$

Similar equations can be derived in the same way for other orders of reaction.

Treatment of random main chain cleavage is more difficult because of the numerous equations relating $(f_t/f_o)_c$ to $q(t)/\nu(o)$, (see section 3.3.2). For a first order reaction

$$m(t) = m(o)\exp(-k_1 t) \qquad (3.65)$$

where m(o) and m(t) are respectively the concentrations of reactive sites per unit volume at time zero and time t.

If $\bar{m}$ is the average number of reactive sites per network chain then use of Tobolsky's[15] equation (equation (3.17)) gives

$$(f_t/f_o)_c = (\nu(t)/\nu(o)) = \exp(-k_1\bar{m}t) \qquad (3.66)$$

$$\therefore \ln(f_t/f_o)_c = -k_1\bar{m}t \qquad (3.67)$$

Using Berry and Watson's[86,87] equation (equation (3.21)) gives

$$(f_o/f_t)_c - 1 = \bar{m}\left[1 - \exp(-k_1 t)\right] \qquad (3.68)$$

which for small $k_1 t$ reduces to

$$(f_o/f_t)_c - 1 = \bar{m}kt \qquad (3.69)$$

or

$$\ln(f_t/f_o)_c = -\bar{m}kt \qquad (3.70)$$

The Flory[12] equation (equation (3.23)) gives

$$(f_t/f_o)_c - 1 = 2\bar{m}\left[1 - \exp(-k_1 t)\right] \qquad (3.71)$$

which reduces for small $k_1 t$ to

$$(f_t/f_o)_c - 1 = 2\bar{m}kt \qquad (3.72)$$

These difficulties can be avoided by restricting measurements to small $(f_t/f_o)_c$ values where (see figure 3.4)[90] the Scanlan, Tobolsky[15] and Berry and Watson[86,87] equations converge to the same $(f_t/f_o)_c$ vs $q(t)/\nu(o)$ dependence when the Tobolsky or Berry and Watson equations may be used. The Flory equation

has been shown to be inaccurate at small $(f_t/f_o)_c$ values. The applicability of any of these equations can be tested by looking at the dependence of $(f_t/f_o)_c$ on $1/\nu(o)$.

Similar equations may be derived for other kinetic equations so that for second order kinetics Tobolsky gives

$$(f_o/f_t)_c = (1 + \bar{m}\,\nu(o)k_1 t)^{\bar{m}} \qquad (3.73)$$

which for small $\bar{m}\,\nu(o)k_1$ reduces to

$$(f_o/f_t)_c - 1 = \bar{m}^2\,\nu(o)k_1 t \qquad (3.74)$$

whilst Berry and Watson give

$$\left[(f_o/f_t)_c - 1\right]^{-1} = 1/\bar{m} + 1/\bar{m}^2 \quad (o)k_1(1/t) \qquad (3.75)$$

which for small $\nu(o)\bar{m}k_1 t$ reduces to

$$(f_o/f_t)_c - 1 = \bar{m}k_1 t \qquad (3.76)$$

Apart from this classical molecular approach the kinetics of removal of elastically effective chains could be considered. Assuming a pseudo chemical reaction causing scission as

$$n\nu \xrightarrow{k^*} \text{products}$$

the following equations may be derived:

$$(f_t/f_o)_c = 1 - k^* t/\nu(o) \quad \text{for a zero order reaction} \qquad (3.77)$$

$$\ln(f_t/f_o)_c = -k^* t \quad \text{for a first order reaction} \qquad (3.78)$$

$$(f_o/f_t)_c - 1 = \nu(o)k^* t \quad \text{for a second order reaction} \qquad (3.79)$$

These equations can give good fits to the data and have the same general form as the equations for molecular kinetics. Tobolsky and others [18,19,97-100] have found that good fits to the data can be obtained using an empirical equation

$$(f_t/f_o)_c = \sum_{j=i}^{n} A_j \exp(-k_j^* t) \qquad (3.80)$$

where $\sum_{j=i}^{n} A_j = 1$. This equation was first used to interpret the viscoelastic flow of uncrosslinked systems and has since been used to interpret chemical stress relaxation curves. It is usually applied to cases where the $\ln(f_t/f_o)_c$ vs t curve becomes approximately linear at long times, the slope of this linear portion is k_1^* and the intercept is A_1. A plot is then made of $\ln\left[(f_t/f_o)_c - A_1\exp(-k_1^* t)\right]$ vs t which will also have a linear region giving k_2^* and A_2. The process is repeated until the whole curve has been resolved although only two or, at most, three terms are usually required.

The equation has been given molecular significance for a system with $\bar{m}$ cleavable sites per chain of which, a small fraction, α are more readily cut than the others. This model gives:[100,101,102]

$$(f_t/f_o)_c = \sum_{i=o}^{\bar{m}} {}^{\bar{m}}C_i(1-\alpha)^{(\bar{m}-1)}\alpha^i \exp\left[-\left\{k(\bar{m}-i) + k_w i\right\} t\right] \qquad (3.81)$$

where ${}^{\bar{m}}C_i = \bar{m}!/(\bar{m}-i)!\,i!$ for $i \neq 1$ or $\bar{m}$ and

$${}^{\bar{m}}C_1 = {}^{\bar{m}}C_{\bar{m}} = 1$$

The various terms account for relaxation due to cleavage of chains with 0,1,2,3,,,$\bar{m}$ weak links; neglecting the few chains with more than one weak link:

$$(f_t/f_o)_c = (1-\alpha)^{\bar{m}}\exp(-k\bar{m}t) + \bar{m}(1-\alpha)^{\bar{m}-1}\alpha\exp\left[-\left\{k(\bar{m}-1) + k_w\right\} t\right] \qquad (3.82)$$

(3.5.3) The Kinetic Interpretation of Chemical Stress Relaxation Data: Crosslinking Reactions

The kinetics discussed in section 3.5.1 may also be applied to interpretation of the crosslinking process. Consider

a simple bimolecular combination reaction where the concentration of crosslinking sites is v(o) initially and the reaction is

$$2v \xrightarrow{k_2} \nu_2/2 \text{ (crosslinks)}$$

so that

$$[v(o)/v(t)] - 1 = v(o)k_2t \qquad (3.83)$$

the number of crosslinks formed is $\nu_2(t)/2 = \frac{1}{2}[v(o) - v(t)]$

so $$\nu_2(t)/\nu_1(o) = v(o)/\nu_1(o)\left[1 - (1 + v(o)kt)^{-1}\right] \qquad (3.84)$$

$$\therefore \nu_1(o)/\nu_2(t) = \left[\nu_1(o)/v(o)^2k\right](1/t) + \nu_1(o)/v(o) \qquad (3.85)$$

Since $$\Delta = (f_t/f_o)_i - (f_t/f_o)_c = \nu_2(t)/\nu_1(o) \qquad (3.86)$$

$$\therefore \quad t = \left[v(o)/\nu_1(o)\right](t/\Delta) - 1/v(o)k_2 \qquad (3.87)$$

so that a plot of t/Δ vs t should be linear

More complicated kinetics may be encountered and treated by the methods of chemical kinetics[95]; a case of particular interest is that of crosslink or bond interchange such as has been considered by Flory[83] (section 3.4.2)

(3.5.4) The Kinetic Interpretation of Chemical Stress Relaxation Data: The Time-Temperature Superposition Method

The time-temperature superposition principle[15] is commonly used to interpret the viscoelastic properties of polymers, although it may also be applied to the chemical stress relaxation properties of rubbers. The method may be applied to a relaxing system in which the relaxation behaviour may be described by a function of a series of relaxation times, τ_i,

$$(f_t/f_o) = \sum_{i=1}^{n} \Phi\,(t/\tau_i) \qquad (3.88)$$

for stress relaxation an appropriate form of this function is

$$\sum_{i=1}^{n} \Phi\,(t/\tau_i) = \sum_{i=1}^{n} A_i \exp(t/\tau_i) \qquad (3.89$$

where A_i is a constant. If, when the temperature is changed from T_1 to T_2, $\tau_i(T_1) = \alpha_{T_1 \rightarrow T_2} \tau_i(T_2)$ for all τ_i, where $\alpha_{T_1 \rightarrow T_2}$ is a constant, the relaxation curves at T_1 and T_2 may be superimposed by plotting (f_t/f_o) vs log t and sliding one of them along the log t axis as is illustrated in figure (3.9). The constant $\alpha_{T_1 \rightarrow T_2}$ is usually written at α_T and the temperature dependence of α_T will be characteristic of the relaxation process.

If relaxation results from a single chemical process the relaxation curve may be described by a single relaxation time, τ_{ch}, which is defined as the time taken for f_t/f_o to fall to 1/e of its initial value; for a first order reaction $\tau_{ch} = 1/k_1$.

It is not always convenient to use τ_{ch} to characterise chemical stress relaxation since its determination requires the experiment to be continued until gross degradation has occured, in fact $\tau_{(f_t/f_o)^*}$, the time taken for the stress to fall to some arbitrarily chosen value, $(f_t/f_o)^*$, or α_T measured with respect to an arbitrarily chosen temperature, may be used to characterise the relaxation behaviour. A plot of log α_T, $\log(1/\tau_{ch})$ or $\log(1/\tau_{(f_t/f_o)^*})$ vs 1/T will give a straight line with a slope of $\Delta H/R$ (see fig. 3.9). This is a simple means of representing the relative rates of relaxation of elastomeric materials and determining some kinetic parameters. Unfortunately it does not allow the evaluation of pre-exponential factors.

+ + + + + +

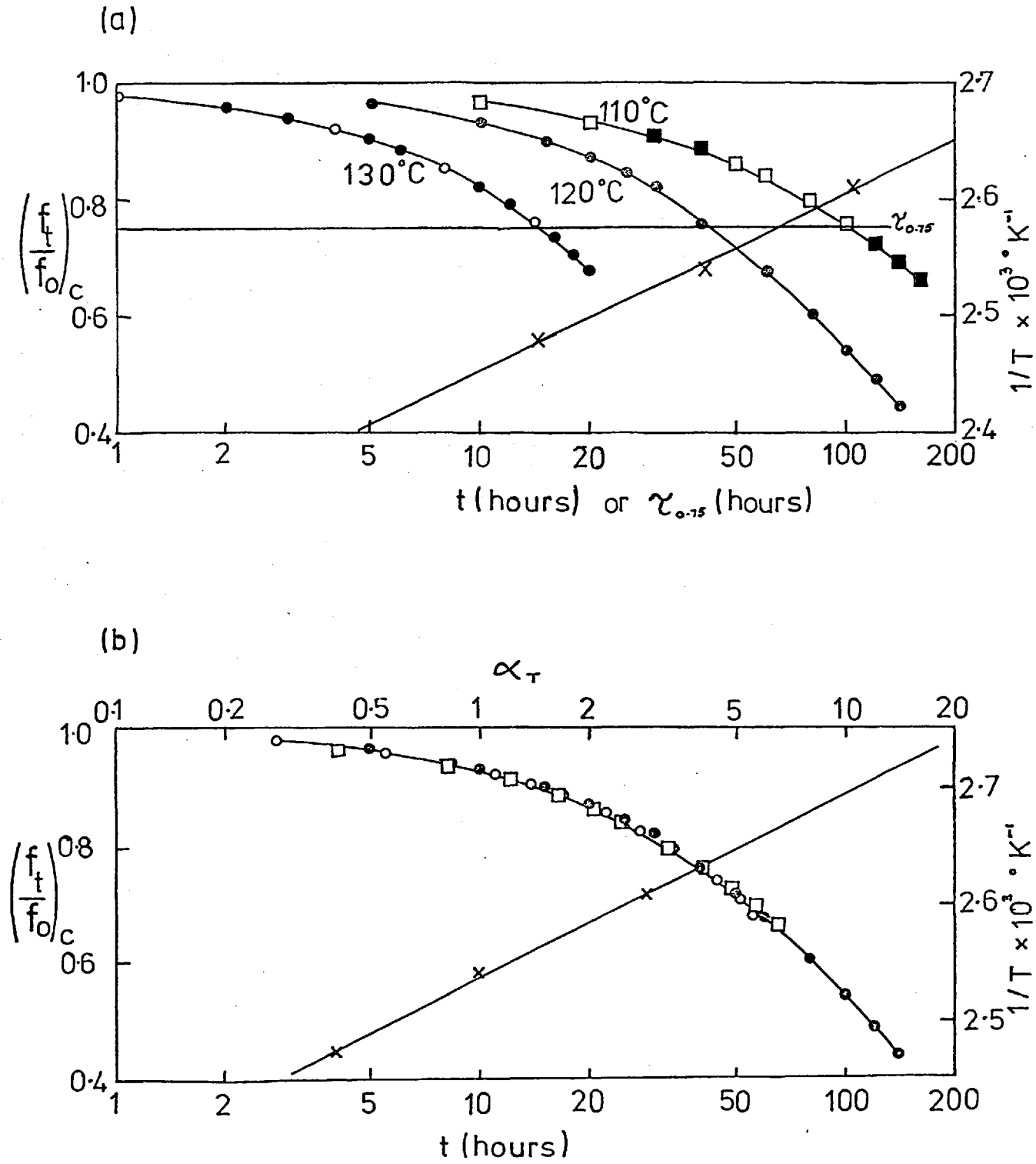


figure 3· 9: Application of the time - temperature superposition principle to the continuous stress relaxation of Adiprene CM in nitrogen - (a) relaxation curves and plot of $\gamma_{0.75}$ vs 1/T; (b) superposed relaxation curve and plot of α_T vs 1/T.

CHAPTER 4

A REVIEW OF THE CHEMICAL STRESS RELAXATION OF ELASTOMER SYSTEMS

(4.1) INTRODUCTION

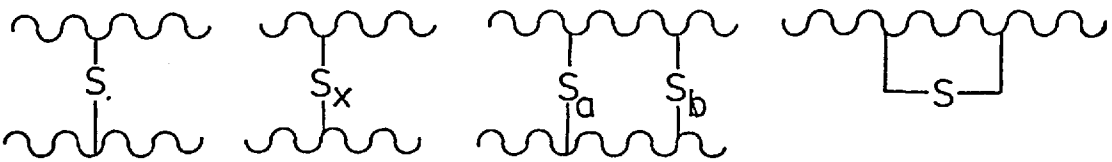
The method of chemical stress relaxation has been used to study the degradation of a wide range of elastomers under a variety of environmental conditions. In this chapter applications of this method will be briefly reviewed.

(4.2) CHEMICAL STRESS RELAXATION IN HYDROCARBON ELASTOMERS

The relaxation behaviour of an elastomer depends upon the constitution and structure of the backbone polymer and the crosslink. The effect of the crosslinks is particularly prominent in the relaxation of hydrocarbon elastomers which may be cured in several ways, giving crosslinks with different structures. The principle curing systems are:

(i) Those using free sulphur with or without catalysts, accelerators and other compounding ingredients.[104,106] This system resulted in vulcanizates containing the structures shown in figure 4.1 and also caused some main chain scission. Unaccelerated sulphur cures give a high proportion of polysulphide crosslinks and cyclic monosulphides whilst accelerators (MBT, CBS etc. see figure 4.2) increase the rate of crosslinking and decrease the numbers of vicinal polysulphide crosslinks, cyclic monosulphides, main chain scissions and the length of the sulphur chains in the polysulphide crosslinks.

(ii) Those using sulphur donors but without free sulphur.[104] The vulcanizates produced in this way contain mainly monosulphide crosslinks, with small numbers of disulphide and polysulphide links that can be almost eliminated if the cure time is



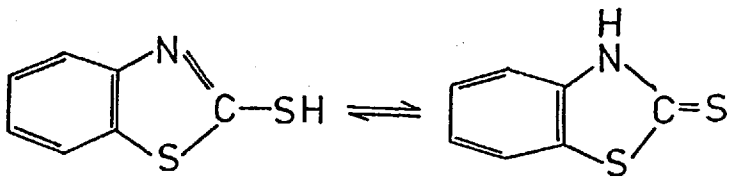
(a) monosulphide crosslink

(b) polysulphide crosslink ($x \geqslant 2$)

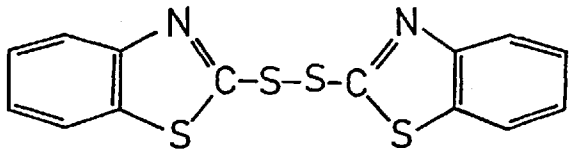
(c) vicinal polysulphide crosslink ($a,b \geqslant 2$)

(d) cyclic monosulphide

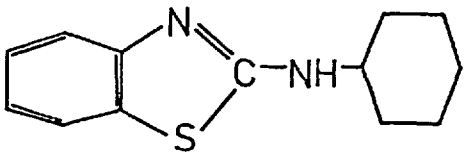
figure 4·1



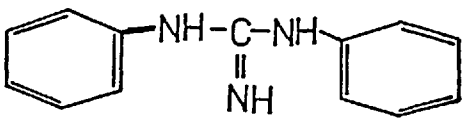
2-Mercaptobenzothiazole (MBT)



2-Mercaptobenzothiazole disulphide (MBTS)

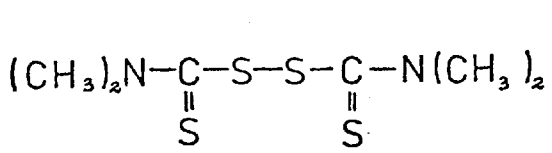


N-Cyclohexylbenzothiazole-2-sulphenamide (CBS)

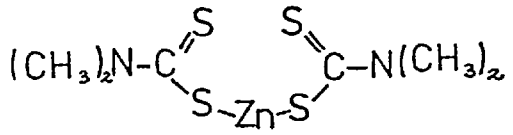


Diphenylguanidine (DPG)

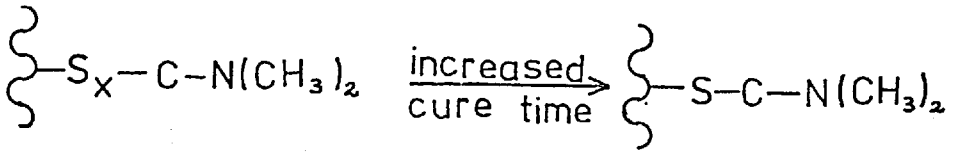
figure 4·2



Tetramethylthiuramdisulphide (TMTD)



Zinc Dimethyldithiocarbamate (ZDMC)



(a) (b)

figure 4·3: Sulphur Donor Cure Systems.

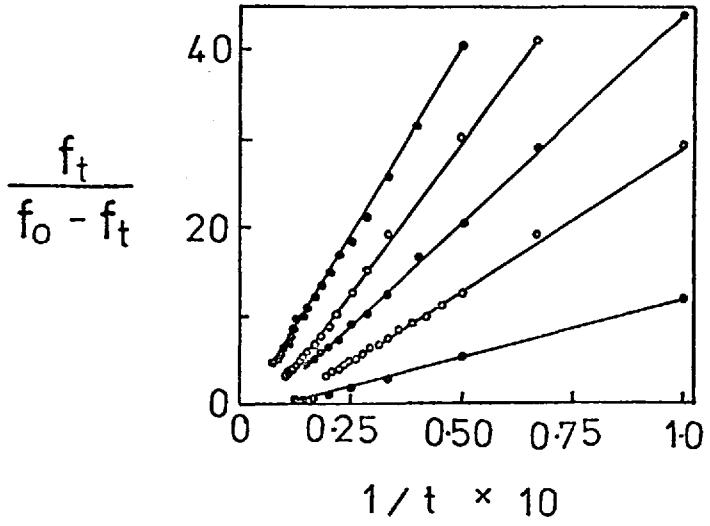


figure 4·4: Plot of Oxidative Stress Relaxation Data According to Equation 4·1 – • highly purified natural rubber; ∘ deproteinized crepe. (ref.86)

sufficiently long. Also produced are pendant groups whose structure depends on the cure time as is shown in figure 4.3. The structure shown in figure 4.3a is unstable and leads to further crosslinking during ageing and ultimately gives that shown in figure 4.3b.

(iii) Those using organic peroxides or γ-radiation.[104] These vulcanizates contain crosslinks that are carbon-carbon bonds although there is often some main chain scission and some extra unsaturation introduced into the main chain; cure proceeds via a free radical process.

(iv) Those using organic peroxides in combination with free sulphur.[105] This system gives carbon-carbon crosslinks in addition to di and polysulphide crosslinks and a greater amount of main chain scission than process (iii). It is used to produce vulcanizates of saturated hydrocarbons that are broadly similar to sulphur cured olefinic rubbers.

(4.2.1) The Oxidation of Hydrocarbon Elastomers

(4.2.1.1) Chemical Stress Relaxation of Peroxide or Radiation Vulcanizates

The relaxation behaviour of these vulcanizates has been widely studied because they have the simplest structure and should be the easiest to interpret. Natural rubber has been most extensively studied providing insight into the mechanism of the oxidation of hydrocarbon rubbers.[86] It was soon established that, provided natural antioxidants were removed, the continuous stress relaxation of natural rubber could be described by the autoxidative mechanism proposed by Bolland, Bateman and others.[15,86,107-111]

Initiation: $2ROOH \longrightarrow$ Radicals (e.g. $RO_2^{\cdot}$, $RO^{\cdot}$, $R^{\cdot}$, $HO_2^{\cdot}$ etc)

Propagation: $R^{\cdot} + O_2 \longrightarrow RO_2^{\cdot}$

$RO_2^{\cdot} + RH \longrightarrow R^{\cdot} + ROOH$

Termination: $2R^{\cdot} \longrightarrow R - R$

$RO_2^{\cdot} + R^{\cdot} \longrightarrow RO_2R$

$2RO_2^{\cdot} \longrightarrow 2RO^{\cdot} + O_2$

$RO^{\cdot} \rightarrow$ Carbonyl + $R'^{\cdot}$

Stress relaxation data obeyed the following equation [86,112]

$$f_t/(f_o - f_t) = a/t - b \qquad (4.1)$$

where a and b were constants (see figure 4.4). This is a second order kinetic equation (equation 3.74, section 3.5.2) which was derived assuming second order decomposition of ROOH and cleavage during either initiation or propagation. Scission apparently took place in the main chain.

Equation (4.1) was only obeyed if highly purified, deproteinised rubber was used, otherwise natural antioxidants (i.e. proteins) inhibited the reaction, so that autocatalytic degradation was preceeded by an induction period or relaxation was not autocatalytic at all. [86,113] The effect of natural and artificial antioxidants explained the earlier results of Tobolsky.[15] Dunn and Scanlan[66] suggested that termination was likely to be due to reaction of free radicals with traces of natural antioxidants rather than the processes suggested in the autoxidative mechanism, even when highly pure rubber was used.

Thirion and Chasset[114] showed that equation (4.1) could be expanded to give

$$f_t/f_o = 1 - t/a - (b - 1)(t/a)^2 \qquad (4.2)$$

which reduced to

$$f_t/f_o = 1 - t/a \qquad (4.3)$$

for slow rates of reaction. This pseudo zero order behaviour has been observed by both Thirion and Chasset[114] and Scheele and Hillmer[115-117] (see figure 4.5). Since 1/a has the character of a rate constant it obeys the following equation (see figure 4.6).

$$a = a_0 \exp(\Delta H/RT) \qquad (4.4)$$

The activation energy, ΔH, obtained by Thirion and Chasset[114] was 105kJ mole^{-1}; this compares with 125kJ mole^{-1} from Tobolsky[15] and 84 to 107kJ mole^{-1} from Scheele and Hillmer[115-117].

The same mechanism operates for u.v. light initiated oxidation[86,118] except that the initiation step becomes

$$ROOH \xrightarrow{\text{u.v. light}} RO^{\cdot} + \dot{O}H$$

The stress relaxation data now obeys the equation

$$f_0/f_t = 1 - a + a \exp(k't) \qquad (4.5)$$

which gives excellent agreement for u.v. light of wavelength 365 mμ at 25°C. Morand[119] showed that similar behaviour took place at wavelengths between 500 and 369 mμ, the rate being greatest at the lowest wavelengths. At wavelengths lower than these deviations were observed, and Dunn, Scanlan and Watson[118] observed non-oxidative relaxation at 313 mμ; Morand[119] suggested that direct photolysis of carbon-carbon bonds might be responsible.

Measurements have been made to evaluate the relative effectiveness of antioxidants since small amounts of these can reduce severely the rate of relaxation.[86] Antioxidants can be classified into groups; those that suppress the propagation step and those that suppress initiation.

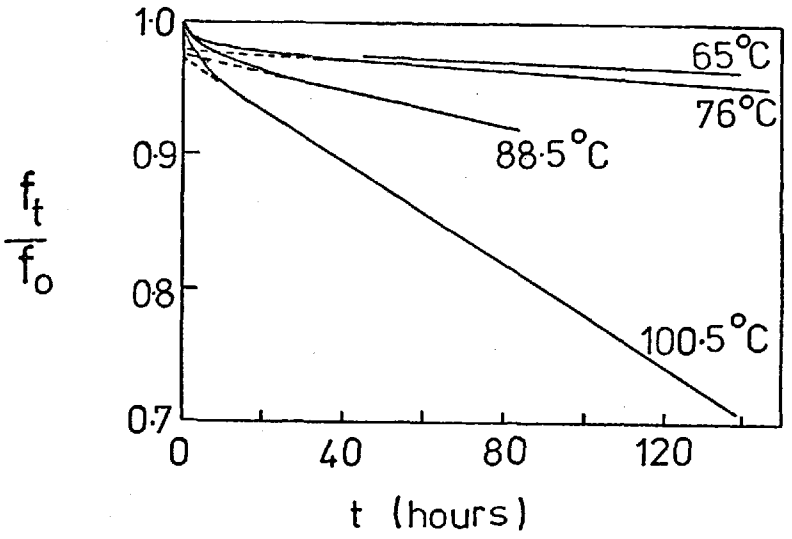


figure 4·5: Stress Relaxation of a Peroxide Cured Natural Rubber Vulcanisate Showing Zero Order Behaviour (ref. 114)

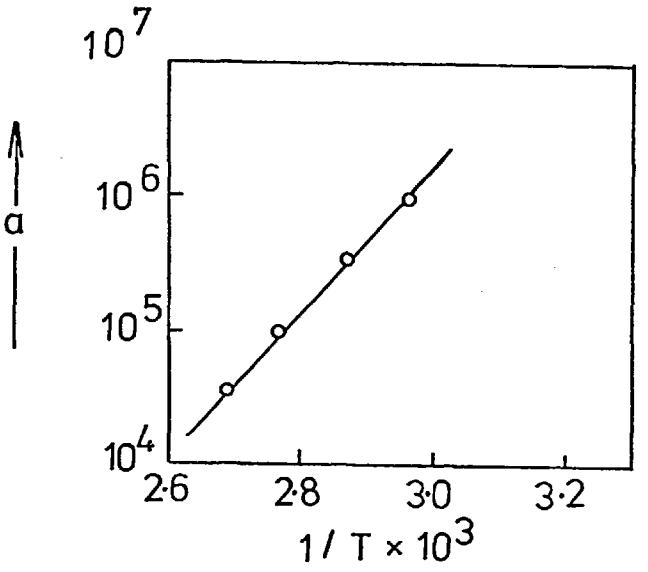


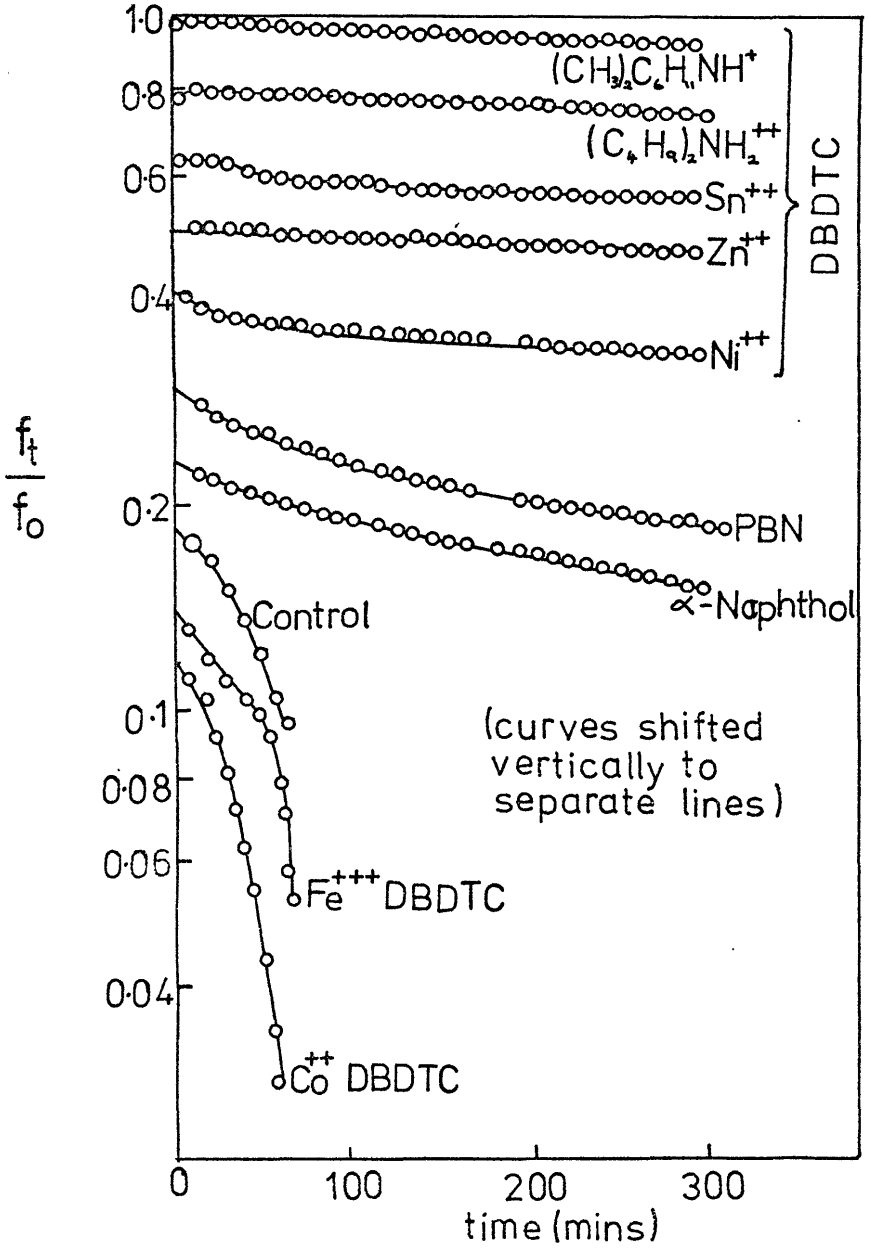
figure 4·6: Arrhenius Plot for Thermooxidative Stress Relaxation of a Peroxide Cured Natural Rubber Vulcanisate (ref. 114)

The first group contains the conventional phenolic and amine antioxidants both of which give rise to a prolonged induction period, where relaxation is slow, prior to auto-catalytic decay;[86,120-122] in some cases relaxation did not become autocatalytic at all.

Dunn[123,124] studied the effect of substituted p-phenylene diamines on the rate of u.v. initiated oxidation. These behaved in the expected manner, with the exception of diphenyl ethylene diamine; additional protection was probably provided by the reduced transmittance caused by the intense colour developed by the samples during the slow period.

Scheele and Hillmer[122] showed that for thermal oxidation during the slow period, the inhibitor concentration was inversely proportional to the relaxation rate, which was zero order for both phenyl-β-naphthylamine and N-phenyl-N-cyclohexyl-p-phenylenediamine in accord with the theory of inhibited oxidation.[122] They showed that phenolic antioxidants behaved in the same way as the amines, although Dunn[123] showed that for photochemical degradation, their behaviour depended on substitution patterns; good antioxidants are those with blocked ortho positions. The presence of a u.v. absorber prolonged the active life of phenolic antioxidants[123,124] in photochemical oxidation.

Apart from phenolic and amine antioxidants, metal salts of dialkyldithiocarbamates, dialkyldithiophosphates and dialkylxanthates are good antioxidants. Their efficiency depends on the identity of the metal ion (see figure 4.7)[86,126,126] and they are thought to decompose hydroperoxides giving non-radical products, interfering with the initiation steps.



DBDTC = Dibutyldithiocarbamate
DMDTC = Dimethyldithiocarbamate
DBODTP = Dibutoxydithiophosphate
DPODTP = Dipropoxydithiophosphate
DS = $(S-\overset{\overset{S}{\|}}{C}-N\langle^{CH-CH_2}_{CH-CH_2}\rangle O)_2$
PBN = Phenyl-β-naphthylamine

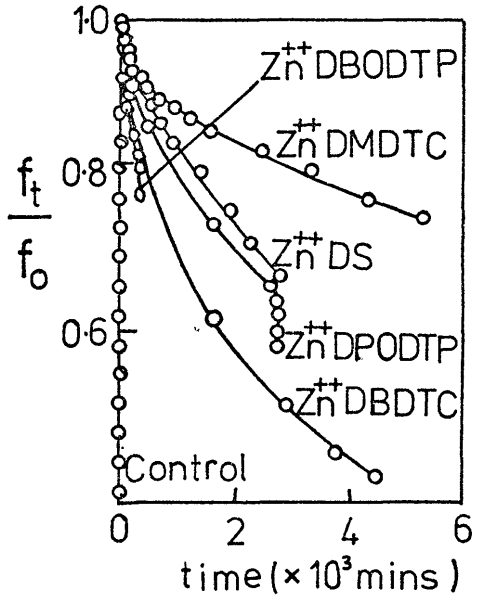


figure 4·7 : Effect of antioxidants on continuous relaxation of natural rubber (ref. 86)

Some examples of synergism[127] have been observed by combining antioxidants from the two groups; that is a hydroperoxide decomposer with a free radical scavanger.

The intermittent and continuous relaxation curves were almost identical for peroxide cured natural rubber, indicating very little crosslinking.[86] The radiation vulcanizates showed a little more crosslinking,[120] probably due to vinylidene groups introduced during cure.[128] Maisey and Scanlan showed that, like scission, crosslinking was a free radical process since it was inhibited by amine and phenolic antioxidants.

Other hydrocarbon rubbers behave similarly to natural rubber, the relative relaxation rates depending on the amount of main chain unsaturation[15]: the greater the amount of unsaturation, the higher the rate. Completely saturated hydrocarbons, such as ethylene-propylene rubber, are the most stable whilst the olefinic hydrocarbons, such as natural rubber, polybutadiene, butyl rubber and styrene-butadiene rubber, are the least stable. Materials such as ethylene-propylene terpolymers with pendant unsaturation are marginally less stable than the saturated rubbers.

The continuous stress relaxation of synthetic polyisoprene, polybutadiene and styrene-butadiene rubber is very similar to that of natural rubber but is generally accompanied by a more pronounced crosslinking reaction.[15,86,129,130]

Recent interest has been concentrated on the stress relaxation of the low unsaturation rubbers, since these could provide high temperature hydrocarbon rubbers. The continuous stress relaxation of ethylene-propylene co-[131] and terpolymer[132-134] rubbers comprised an initial period of slow relaxation followed

by a period of autocatalytic decay. Relaxation during the slow period was first order (i.e. the relaxation curves could be described by the equation $\ln f_t/f_o = -kt$) for both EP and EPT rubbers. The duration of the slow period was reduced by increasing temperature.

In EPT cleavage took place in the crosslinks, since the rate of relaxation was independent of crosslink density; this was to be expected since crosslinking takes place in the vicinity of the pendant double bonds. In EP rubber there was evidence of cleavage both in the main chain and at the crosslinks.

The behaviour of these rubbers can be described in terms of the autoxidative mechanism already discussed, but with the inclusion of an induction period where the concentration of hydroperoxide and free radicals builds up, until they can support the autocatalytic period. Thomas[131] obtained an activation energy of 155 kJ mole^{-1} for the relaxation of EP rubber whilst Imoto et al[134] obtained a value of 130 kJ mole^{-1} for EPT.

Imoto et al[134] studied the relaxation of EPT cured with peroxide in the presence of N,N' - (m-phenylene)-bismaleimide, diallylphthalate or N,N'-methylene bisacrylamide giving C-R-C as well as C-C crosslinks; these vulcanizates behaved in the same way as the simple peroxide cured samples, except that they were slightly less stable.

Very little crosslinking took place in either the EPT[132] or EP[131] rubbers although measurements on the EP rubber were difficult to interpret because of physical relaxation during the intermittent experiment. This lack of crosslinking is at odds with the results, obtained by Narkis and Tobolsky[135,136], for low density polyethylene where there was a high rate of

crosslinking that was further increased in the presence of carbon black.

Tobolsky[111,137] has studied the relaxation of hydrocarbon rubbers where initiation is caused by the decomposition of an added organic peroxide so that the rate of initiation is known. For EP, EPT, polypropylene, SBR and natural rubber the initial rate of scission was found to be proportional to the initial initiator concentration and the scission efficiency (i.e. the initial rate of scission divided by the initial rate of initiation) was between 0.6 and 0.7. In the case of an externally initiated autoxidation reaction, the scheme already presented must be modified by the replacement of the initiation steps by

$$\text{Init} \longrightarrow 2I^{\bullet}$$

$$I^{\bullet} + RH \longrightarrow R^{\bullet} + IH$$

These results led Tobolsky to suggest that cleavage took place during initiation or termination, although this may be a consequence of the abnormally high free radical concentration present in these extremely initiated systems.

(4.2.1.2) Chemical Stress Relaxation of Sulphur Donor Vulcanizates

These vulcanizates (i.e. TMDT cured samples) of natural rubber give autocatalytic decay similar to that for the peroxide cured samples provided that they have been well cured and extracted.[86] If undercured, relaxation is slower than autocatalytic and accompanied by a considerable amount of crosslinking; unextracted samples also give a reduced rate of relaxation. This is because undercured samples contain a pendant bound structure (figure 4.3a), that causes further crosslinking

and reacts with zinc oxide, also present, to give zinc dimethyldithiocarbamate, a good antioxidant; this antioxidant is always produced during cure and is, hence, present in well cured unextracted samples.

When autoxidative degradation does occur, cleavage takes place in the main chain with activation energies of 124 and 117 kJ mole^{-1} respectively for TMTD and TETD vulcanizates[115,117,138]; these are in good agreement with the values obtained for peroxide cures.

EPT may be cured by TMTD and the continuous stress relaxation of these vulcanizates has been studied by several workers. Tobolsky[132,133] found that after an induction period the rate approached that of the peroxide cured samples. Tamura and Murakami's[139.140] results were in general agreement with Tobolsky's[132,133] and showed that, as in the peroxide cured samples, scission took place at the crosslinks.

The results of Imoto el al[134] did not agree with those of Tobolsky[132,133] and Tamura and Murakami[139,140] as relaxation was slower and reduced on extraction. The activation energy obtained was 121 kJ mole^{-1} and relaxation was accompanied by a substantial crosslinking reaction suggesting that the samples might have been undercured.

(4.2.1.3) Chemical Stress Relaxation of Sulphur Vulcanizates

Unaccelerated or accelerated sulphur cured natural rubber vulcanizates contain polysulphide crosslinks which are thermally and rheologically labile; that is, they undergo interchange reactions when heated or stressed.[15,86]

$$RS_aS_bR + R\ S_cS_dR \xrightarrow[\text{stressed}]{\text{heated or}} RS_aS_dR + R\ S_cS_bR$$

This type of reaction, which will be discussed later, has a considerable effect on the relaxation of a rubber network, but can be distinguished from the oxidative reactions since it will occur in a vacuum. In sulphur cured rubber the interchange reaction includes the production of free sulphur and di and monosulphide crosslinks. The concentration of polysulphide crosslinks and, hence, the amount of non-oxidative relaxation can be reduced by extending the cure time, using precisely the optimum concentrations of curing ingredients, or an extensive postcure. Since polysulphide interchange takes place in air and vacuum (or nitrogen) [86] it may be subtracted from the overall relaxation curve in air. Scheele, Hillmer and Bruderman [138] have suggested another approach, applicable when the polysulphide interchange is the only reaction leading to the formation of crosslinks. They did intermittent stress relaxation in which the time that the sample was stretched, t_d, and the time that it was unstretched, t_u, were varied until the sample showed no relaxation in nitrogen. An experiment was then done in air using the same t_d and t_u values; the curve obtained could be attributed solely to cleavage reactions, other than the interchange reaction. This method is difficult to apply, required a large number of experiments to be done and is not applicable in cases where there are additional crosslinking reactions.

The oxidative relaxation of both accelerated and unaccelerated sulphur cured natural rubber vulcanizates is not, in general, autocatalytic [86]. It has been shown that the structure of MBT and CBS natural rubber vulcanizates are critically dependent on the relative concentrations of curing

ingredients and the temperature and time of cure. If these variables are carefully chosen, vulcanizates that are almost polysulphide and cyclic monosulphide free, can be prepared; these give similar, and autocatalytic intermittent and continuous stress relaxation curves.

Other sulphur cured natural rubber vulcanizates generally behave like peroxide or TMTD vulcanizates that contain mild antioxidants. It was suggested [86] that the dialkenyl and dialkyl polysulphides and free sulphur present function as antioxidants and react with free radicals; alkenyl-t-alkyl sulphides also behave as antioxidants and these are present in unaccelerated sulphur vulcanizates. Conventional amine and phenolic antioxidants do give protection to the oxidation of sulphur cured natural rubber [86,128] but they do not affect relaxation due to polysulphide interchange. Metal dialkyl dithiocarbamates increase the rate of relaxation by catalysing the polysulphide interchange reaction.

Morand [119] has studied the photodegradation of natural rubber; at 25°C the rate of relaxation depends critically on wavelength and vulcanising ingredients.

Bauman and Bom [141] investigated the γ-radiation induced relaxation of sulphur cured natural rubber in air and nitrogen and in particular the effect of antioxidants; the antioxidants reduced the rate of relaxation by reacting with $RO_2^{\cdot}$ and $R^{\cdot}$ free radicals.

Cis - 1, 4-polybutadiene can also be vulcanised with sulphur, with or without accelerators, although rather less sulphur is required. [86] Polysulphide interchange gives rise to continuous relaxation under vacuum as for natural rubber but

autocatalytic oxidative degradation is observed unless excessive amounts of sulphur are deliberately included, when the behaviour mirrors that of natural rubber. The structure of the polysulphide crosslinks appears to be different in the low sulphur samples from the high sulphur samples since only in the latter is the interchange catalysed by metal dithiocarbamates and so the crosslinks act as antioxidants. In general terms the rate of relaxation of sulphur cured elastomers is increased by increased unsaturation in the material in the same way as peroxide cured samples so that, in order of stability:[142]

Butyl rubber > SBR > Natural Rubber

Recently sulphur cured EPT has been studied, its relaxation behaviour[133,143] includes polysulphide interchange and oxidative degradation taking place in the vicinity of the double bonds. The reduced amount of unsaturation minimises cyclic monosulphide formation and main chain modification. As with natural rubber the polysulphide crosslinks behave as antioxidants.

EP rubbers cannot be cured by accelerated or unaccelerated sulphur systems but they can be cured with peroxide/sulphur systems giving broadly similar vulcanizates as the more conventional sulphur cures.[105] Dunn has found that the relaxation of these depends upon the concentration of sulphur used; 0.75 to 2.5 pph of sulphur must be used to give an appreciable concentration of polysulphide crosslinks. When high sulphur concentrations are used there is a non-oxidative polysulphide interchange reaction as well as an oxidation reaction. The rate of oxidation, for high sulphur samples,

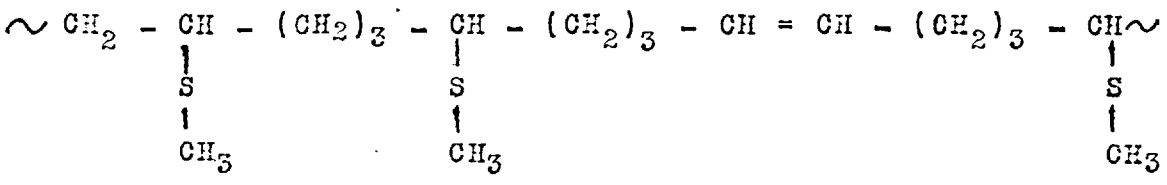
was concentration dependent and slower than for low sulphur samples. Free sulphur inhibited the oxidative relaxation of peroxide cured EP rubber for a period, after which the rate increased until it was the same as that in the absence of sulphur. Dunn[105] proposed that inhibition in the high sulphur vulcanizates was due to free sulphur liberated during polysulphide interchange although it could also be due to the antioxidant nature of the polysulphide crosslinks.

(4.2.2) The Effect of Non-Hydrocarbon Elements on the Oxidation of Hydrocarbon Elastomers

(4.2.2.1) The Presence of Sulphur

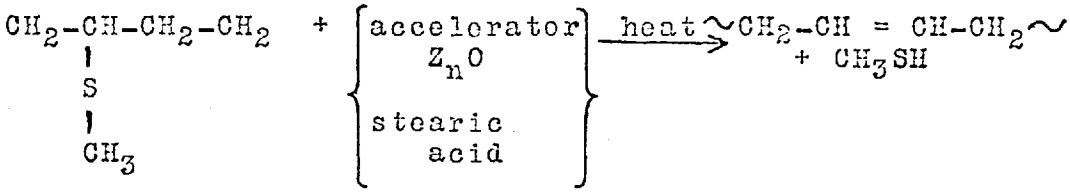
The effect of sulphur on hydrocarbon oxidation has been discussed in section (4.2.1.3). Polysulphide crosslinks and free sulphur inhibit the oxidation of the elastomer; Dunn[105] proposed that free sulphur is most important and as this will be liberated during the polysulphide interchange reaction the polysulphide crosslinks act as a resevoir for free sulphur. There was no evidence that sulphur crosslinks were oxidised to any appreciable extent.

Sulphur can also be present as part of a pendant group as in adduct rubber; this is a polybutadiene that has most of its double bonds saturated with methyl mercaptan, and has the structure



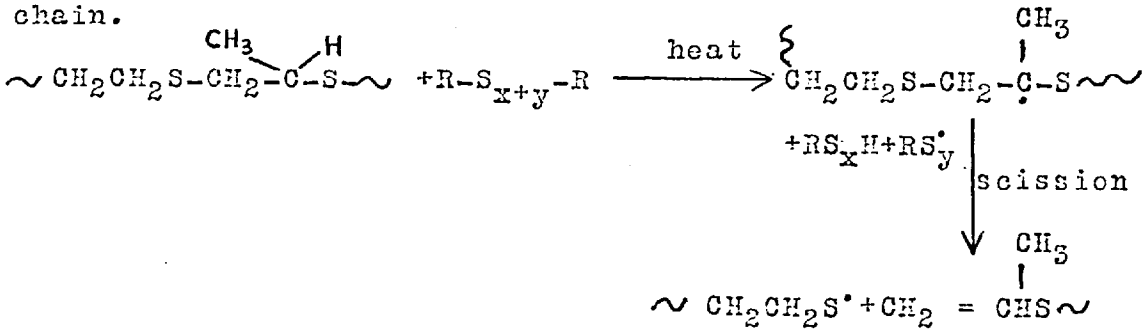
Peroxide cured adduct rubber was found to be highly resistant to oxidation[15] whilst an accelerated sulphur cured sample was less stable. Meyer has shown that a consequence of the accelerated

sulphur cure is the following reaction:[133]

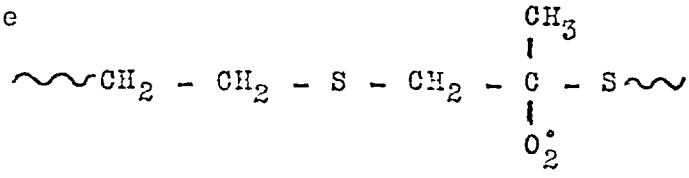


so that the decreased stability was probably due to the increased unsaturation introduced during cure.

Sulphur can also be present in the main chain, and Tobolsky[133] has studied the chemical stress relaxation of an ethylene sulphide-propylene sulphide terpolymer (ESPST) cured with an accelerated sulphur system or a dithiocarbamate salt; the latter leads to a vulcanizate with monosulphide crosslinks only. The dithiocarbamate cured sample was much more resistant than that cured with sulphur, where there was a high rate of scission and crosslinking in both air and nitrogen; the rate in nitrogen was greater than that in air. Tobolsky[133] proposed that this fast rate of non-oxidative degradation resulted from a reaction involving both polysulphide crosslinks and the main chain.



The intermediate free radical could react with oxygen, when present, to give



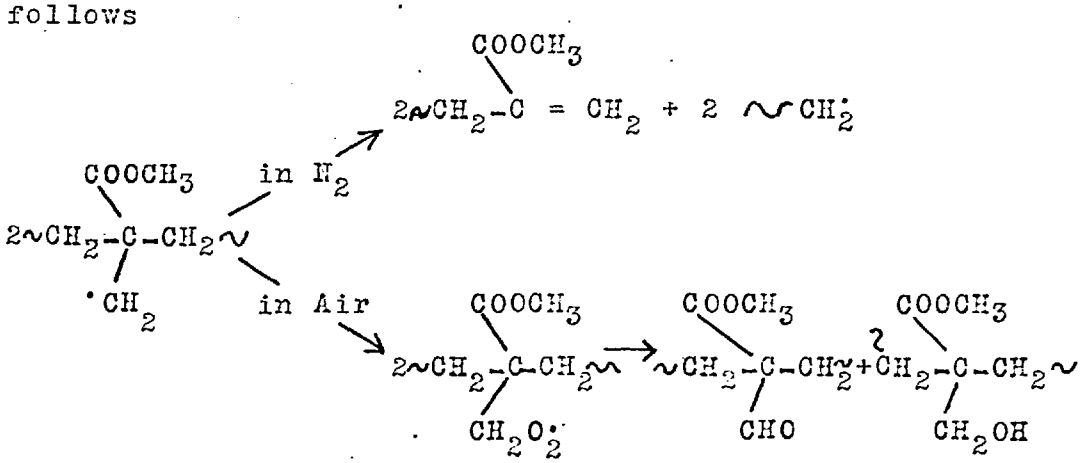
when degradation would occur via the normal autoxidative mechanism.

. . .

(4.2.2.2) The Presence of Oxygen

The polyethers, polyesters and polyacrylates contain both hydrocarbon segments and oxygen atoms; the oxygen may be either in the main chain or in pendant groups.

Tobolsky[111,144] has studied the chemical stress relaxation of a series of peroxide cured ethyl acrylate/methyl methacrylate copolymers; methyl methacrylate was found to be quite stable at 160°C whilst ethyl acrylate relaxed rapidly and autocatalytically. The rate of relaxation of the copolymers increased as the ethyl acrylate concentration was increased. Dicumyl peroxide, present in the samples, led to scission in methyl methacrylate under nitrogen but not in air, whilst ethyl acrylate underwent scission in air and crosslinking in nitrogen. Tobolsky concluded that ethyl acrylate oxidation was due to autoxidative degradation. Methyl methacrylate was assumed to react with dicumyl peroxide to give a free radical, which reacted as follows



The fast termination reaction in air was thought to take place because of the known[111] instability of primary hydroperoxide radicals.

Experiments[144] on ethyl acrylate/methyl methacrylate and ethyl acrylate/methyl-α-chloroacrylate copolymers showed that methyl

substitution retarded oxidative cleavage more than chlorine substitution. The externally initiated relaxation[111] of these copolymers and of a series of n-alkyl acrylate elastomers indicated the same behaviour as in the pure hydrocarbon rubbers. In the n-alkyl acrylate rubbers the relaxation rate decreased as the length of the n-alkyl chain increased due, presumably, to increased scission in the alkyl side chain.

The high rate of oxidation of ethyl acrylate elastomers was undoubtedly due to the tertiary hydrogen formed as a consequence of the acrylic substitution. When this hydrogen was replaced by a methyl group or a chlorine atom the rate of oxidation was considerably reduced.

Singh and Weissbein[145] studied the effect of fillers, antioxidants and different curing systems on acrylate elastomers. A TMTD cure gave the most stable vulcanizates which were further stabilised by the presence of amine antioxidants.

In the polyether rubbers, polypropylene oxide for example, the oxygen is frequently present in the main chain, although it can be in a pendant group as in poly (methylvinyl ether). Tobolsky[133] showed that a poly(propylene oxide) copolymer containing a few mole percent unsaturation underwent a very rapid rate of continuous stress relaxation in both air and nitrogen when cured with peroxide. This cleavage reaction was believed to be due to the decomposition of hydroperoxide groups formed during cure. An accelerated sulphur cured vulcanizate gave a continuous relaxation curve typical of an inhibited oxidation reaction in addition to a polysulphide interchange reaction.

The externally initiated oxidation[146] of poly(propylene oxide) and poly(methylvinyl ether) gave linear relationships between the initial scission rate and the initiator concentration as did the hydrocarbon and acrylic rubbers. In the case of poly(methylvinyl ether) the scission efficiency was slightly reduced because the ether group could react to give inert products without scission.

Polyester rubbers, where the ester group is in the main chain, were shown to be very inert to oxidation[15,130] when cured with peroxide. When cured with sulphur they relaxed slowly due to crosslink scission but the polymer backbone was still extremely resistant to oxidation.

(4.2.2.3) Miscellaneous Substituents

(i) Chlorsulphonated Polyethylene

Haaf and Johnson[147] studied the chemical stress relaxation of chlorsulphonated polyethylene cured by divalent metal oxide/sulphur accelerator or m-phenylene-bis-maleimide systems. The metal oxide/sulphur accelerator cure gives a vulcanizate with metal sulphonate and polysulphide crosslinks whilst m-phenylene-bis-maleimide gives covalent C-R-C type links. The maleimide vulcanizates underwent first order, oxidative continuous stress relaxation (i.e. $\log f_t/f_o = - k_1 t$) with an activation energy of 130 kJ $mole^{-1}$; cleavage took place in the main chain. The metal oxide/accelerator vulcanizate relaxed due to non-oxidative polysulphide and metal sulphonate interchange reactions, in addition to an oxidative main chain scission process with an activation energy of 125 kJ $mole^{-1}$. The response to antioxidants was much the same as for natural rubber with N-dibutyldithiocarbamate decreasing oxidation but

catalysing the interchange reactions. Phenolic and phosphite antioxidants decreased scission but gave increased crosslinking. Oxidation of these rubbers is similar to that of the hydrocarbon rubbers, being largely unaffected by the chlorsulphonic acid side groups and chlorine substitution.

(ii) Nitrogen and Chlorine Substituents

Tobolsky[146] studied the stress relaxation of butadiene/dichlorostyrene and butadiene/vinylpyridine copolymers and of a butadiene/styrene/vinyl pyridine terpolymer. The vinylpyridine rubbers were less stable than the dichlorostyrene rubber but all were more stable than an isoprene/styrene copolymer.

(4.2.3) The Thermal Degradation of Hydrocarbon Elastomers

The thermal degradation of hydrocarbon elastomers is rather difficult to study since hydrocarbon elastomers will relax in an inert atmosphere due to the breakdown of hydroperoxide groups present, without giving useful information about the overall thermal stability of the network. Recently, techniques have been developed that have led to the production of polymers with low hydroperoxide concentrations; hydroperoxides can also be removed by heating the samples under vacuum. Most studies were made on polyethylene, EP and EPT rubbers at temperatures in excess of 250°C.

Tobolsky and Shaw[149] studied the continuous stress relaxation of peroxide and radiation cured polyethylene and EPT vulcanizates in the range 300-350°C. The overall thermal stability was in the order

peroxide cured EPT > peroxide cured low density polyethylene > peroxide cured high density polyethylene > radiation cured high density polyethylene.

This order of stability is the reverse of what would be expected on the basis of increasing branching and unsaturation and is attributed to weak links introduced during cure. The kinetics of relaxation are slower than first order, except for EPT, and the activation energies are given in Table 4.1 below [149,150]

TABLE 4.1

Material	Cure	H kJmole^{-1}
high density polyethylene	radiation	238
high density polyethylene	peroxide	230
low density polyethylene	peroxide	217

The relaxation of EPT was found to be almost first order in agreement with the previous work of Lee, Sperling and Tobolsky [151], who obtained activation energies of 222 kJmole^{-1} above 280°C and 38 kJmole^{-1} below 280°C. No explanation of the low temperature process was offered; its activation energy is considerably lower than that for oxidative degradation.

Yu and Wall [152] studied the thermal relaxation of an EP rubber and a polyethylene under vacuum at 260-320°C and obtained activation energies of 176 and 305 kJmole^{-1} respectively. They suggested that degradation was due to the random scission of backbone C-C bonds.

Tobolsky and Takahashi [153] recently studied the thermal degradation of natural rubber cured with dicumyl peroxide or TMTD at 100-250°C. The activation energies obtained were 266 and 230 kJmole^{-1}, respectively and scission occured in the main chain for the peroxide vulcanizate and at the crosslink for the TMTD vulcanizate. These activation energies suggest that the

presence of unsaturation has little effect on thermal stability since the value of 268 kJmole^{-1} is comparable with the values obtained for EPT, EP and the crosslinked polyethylenes.

(4.2.4) The Radiolytic Stability of Hydrocarbon Elastomers

Bauman and Bom[141] and Evans, Morgan and Stapleton[154] studied the γ-radiation induced scission of radiation and accelerated sulphur cured natural rubber. Continuous stress relaxation was slower than first order and the presence of free radical scavengers reduced the relaxation rate further, indicating that cleavage was a free radical process.

Yu and Wall[155,156] showed that EP rubber also underwent γ-radiation induced main chain cleavage although no general mechanism was proposed to explain their observations.

(4.2.5) The Mechanical Degradation of Hydrocarbon Elastomers

Kusano, Suzuki and Murakame[157] studied the recombination of free radicals, produced in the mechanical deformation of natural rubber below its glass transition temperature, by intermittent stress relaxation. The study highlighted the relatively high stability of the free radicals; complete recombination taking up to 200 minutes at 65°C.

(4.3) THE CHEMICAL STRESS RELAXATION OF ELASTOMERS CONTAINING LABILE LINKS

The relaxation behaviour of networks containing labile links is particularly interesting; these links are chemical bonds that break and reform so that there is no net chemical change in the network.

If the interchange reactions are taking place in an elastomer, the method of chemical stress relaxation may be used, since the intermittent and continuous experiments will give

the rates of bond formation and cleavage.

(4.3.1) Polysulphide Rubbers

Polysulphide elastomers can be prepared [158] by the condensation polymerisation of a dichloroalkane and sodium polysulphide.

$$n\ Cl\text{-}R\text{-}Cl + n\ Na_2S_x \longrightarrow (R\text{-}S_x)_n + 2n\ NaCl$$

Crosslinks can be introduced using a mixture of dichloroalkane and polychloroalkane. The polymer is then treated with sodium sulphite and sodium mercaptan which reduces the polysulphide links to disulphide and thiol groups. The product is a liquid branched polymer containing disulphide links and thiol terminated chains that can be oxidised with metal oxides to give a solid elastomer [15,102,158]

$$\sim SH + M_nO_2 + HS\sim \longrightarrow \sim S - S\sim + M_nO + H_2O$$

if PbO_2 is used this reaction is accompanied by mercaptide formation

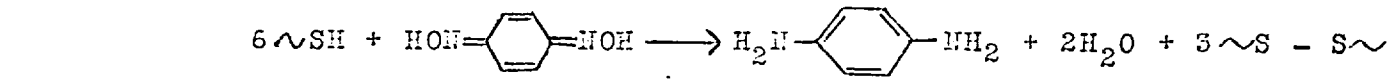
$$\sim SH + PbO + HS\sim \longrightarrow \sim SPbS\sim + H_2O$$

which may be decomposed in two ways:

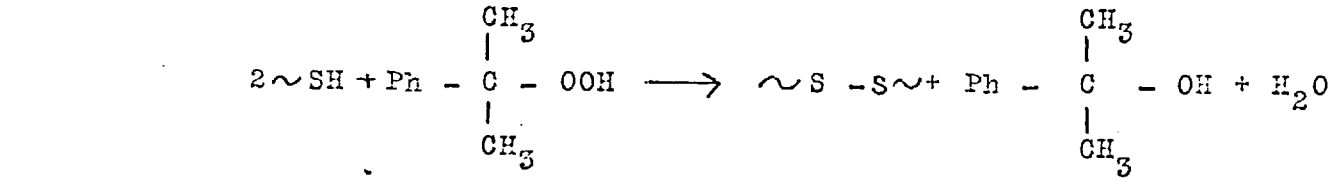
$$\sim SPbS\sim + S \longrightarrow \sim S - S\sim + PbS$$

$$\sim SPbS\sim \xrightarrow[\text{(prolonged)}]{\text{heat}} \sim S\sim + PbS$$

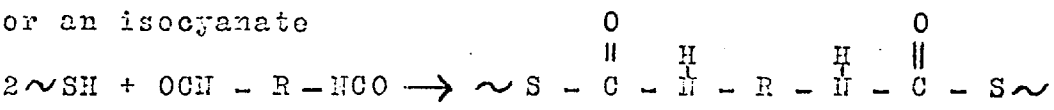
Another curing agent is paraquinone dioxime [15,102,158]



or an organic peroxide



or an isocyanate

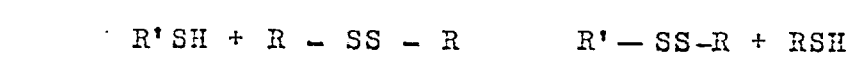


The relaxation behaviour of these polymers was first studied by Stern and Tobolsky[159] and Mochulsky and Tobolsky[160] who made the following observations:

(i) The intermittent stress relaxation data showed that $(f_t/f_o)_i$ was equal to unity at all times indicating that the overall network chain density did not change with time (see figure 4.8)

(ii) Continuous stress relaxation curves were approximately first order (i.e. $\ln(f_t/f_o)_c = -kt$) (see figure 4.8).

(iii) If residual thiol groups were present, relaxation appeared to be due to an exchange reaction involving terminal thiol groups and disulphide links.



This reaction was catalysed by acids or bases.

(iv) If terminal thiol groups were excluded, relaxation took place due to a polysulphide/polysulphide interchange reaction. The rate of relaxation was reduced by chloro - 2,4 - dinitrobenzene and chloro - 2,4 - dinitronaphthalene which are radical terminators indicating that the interchange reaction was a free radical process.

Owen, MacKnight and Tobolsky[102,161] studied a series of isocyanate terminated polyester-urethane rubbers cured with 1,2,6 hexanetriol, 1,2,6 hexanetriol and dithioglycol, and 1,2,6 hexanetriol and tetrathioglycol respectively, such that the networks were identical except that one contained no sulphide links, one contained some disulphide links and the third contained some tetrasulphide links. The continuous stress

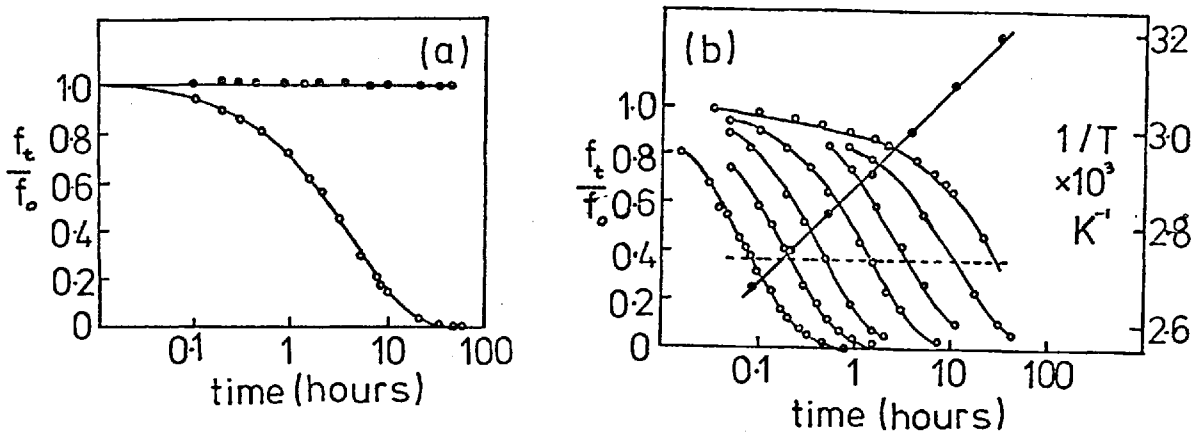


figure 4·8 : Stress relaxation of polysulphide rubber (ref.159)
(a) relaxation at 60°C - ∘ continuous, • intermittent
(b) relaxation curves and Arrhenius plot at 40-100°C

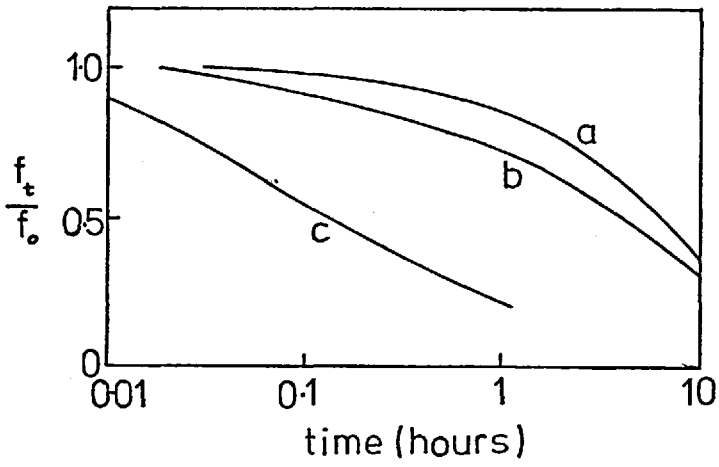


figure 4·9 : Continuous relaxation of urethane elastomers containing sulphide links; a - no sulphide links, b - disulphide links, c - tetrasulphide links. (ref.161)

relaxation data showed that there was little difference between the stabilities of the elastomers containing no sulphide links and disulphide links, but the network containing tetrasulphide links was much less stable (see figure 4.9). Also the specific rate constant for tetrasulphide breakdown in the urethane/tetrasulphide rubber was very similar to that obtained by Tobolsky, Beevers and Owen[99,162] for a polyethylene tetrasulphide rubber. The activation energy obtained for cleavage of the urethane/tetrasulphide elastomer[102,161] was 102 kJ mole^{-1} which compares favourable with the value of 100 kJ mole^{-1} obtained by Stern and Tobolsky[159] for a polysulphide rubber and 108 kJ mole^{-1} obtained by Tobolsky, Beevers and Owen[99,162] for polyethylene tetrasulphide.

The close agreement between these results indicates that the same mechanism is operating. Gee, Fairbrother and Merrall[163] have suggested that this involves a three electron bond as follows:

$$R - S_4 - R \longrightarrow 2RS - S^{\cdot} \longrightarrow 2RS\ldots S$$

On the basis of these results Tobolsky, MacKnight and Takahashi[164] suggested that the high rate of relaxation sometimes observed in disulphide rubbers resulted from the presence of a small number of higher sulphides.

Sulphur swollen into disulphide rubbers increased the rate of relaxation[160,164,165] and a mechanism to explain this was proposed[164]

$$S_8(\text{ring}) \longrightarrow {}^{\cdot}S_8^{\cdot} \quad (\text{diradial chain})$$

$${}^{\cdot}S_8^{\cdot} + RSSR \longrightarrow RS_q^{\cdot} + RS^{\cdot}$$

If this mechanism operates then

$$(1/\tau_{ch}) = k\left\{ m + (8/3)([S_8]/\nu_o) \right\}$$

where τ_{ch} is the observed relaxation time, k is the specific rate constant for tetrasulphide interchange, m is the number of disulphide links per network chain, $[S_8]$ is the sulphur concentration and ν_o is the initial network chain density. The observed τ_{ch} values agreed well with values calculated from this equation.[164]

The disulphide interchange reaction was slow unless sulphur or thiol groups were present;[102,160,161] a reasonably high rate of relaxation was observed, however, when the rubber contained ionic materials and relaxation was particularly high when catalysed by cobalt ions.[15,165] Very rapid relaxation was observed when the rubber contained lead mercaptides.[15,165] These observations and conclusions were confirmed by Bertozzi, Davis and Fettes.[166]

The polysulphide interchange in sulphur cured hydrocarbon rubber[86] may also be rationalised in terms of the mechanisms discussed.

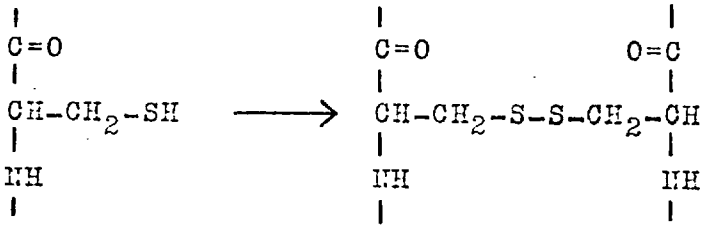
$$R - S_{x+y} - R \rightleftharpoons R - S_y^{\bullet} + R - S_x^{\bullet}$$

$$R - S_y^{\bullet} + R - S_x^{\bullet} \rightleftharpoons R - S_{x+y-8}R + {}^{\bullet}S_8^{\bullet} \text{ (diradical chain)}$$

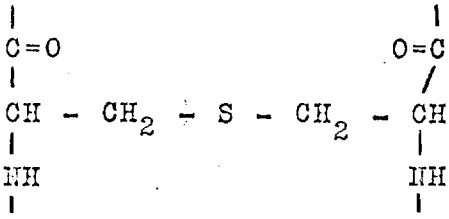
$${}^{\bullet}S_8^{\bullet} \text{ (diradical chain)} \rightleftharpoons S_8 \text{ (ring)}$$

(4.3.2) Chemical Stress Relaxation of Wool and Allied Fibres

Wool is a polymeric solid comprising, in essence, a helical protein chain derived from a wide variety of amino acids.[167,168] One such amino acid, cysteine, gives rise to disulphide crosslinks as follows:[167,168]



If this is reacted with KCN [169] it gives a lanthionine crosslink:



Materials containing such disulphide and monosulphide crosslinks and thiol groups may undergo interchange reactions that can be studied by chemical stress relaxation [169-172] (see section 4.3.1). The experimental conditions used to study wool and other fibres are rather different from those generally used for elastomers; the relaxation of woollen fibres being conducted under conditions of high humidity or under water. This is done because woollen goods are usually pressed under steam during laundering and it is of interest to see how stress relaxation under these conditions leads to the setting of the grements (i.e. a process analogous to the permanent set of rubbers) [170]. Setting of woollen garments generally only lasts until the garments are laundered again, although chemical treatment can lead to the permanent set of the fibres [170]. Two theories were proposed to explain the stress relaxation of woollen fibres under these conditions, the theory of Speakman [173] and the thiol/disulphide interchange theory. [15,102,169-172]

Speakman's theory [173] involves the hydrolysis of the disulphide bond followed by reaction with other amino acid residues to give a variety of new crosslinks; this theory has been severely criticised [174] and has very little experimental support. [171]

The thiol/disulphide interchange reaction is essentially that proposed by Tobolsky [15,102] (see section 4.3.1) although it is complicated when chemical setting agents, such as alkalis or

bisulphites,[170] are present. This explanation has been preferred in the description of the chemical stress relaxation of wool.

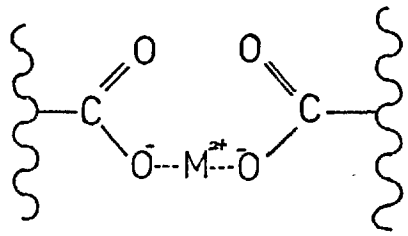
The most comprehensive study of the chemical stress relaxation of wool was made by Weigmann, Rebenfield and Dansizer;[171] they observed two processes taking place when wool was continuously relaxed under water. The first process was rapid with an activation energy of 17-33 kJ $mole^{-1}$, which was attributed to the cleavage of H-bonds, salt links and Van der Waals interactions. The second process was a slow, long term one which was attributed to the thiol/disulphide interchange reaction; this had an activation energy of 96 kJ $mole^{-1}$ which compares favourably with the values of about 100 kJ $mole^{-1}$ obtained by Tobolsky.[15,102] The rate of the long term relaxation process was very much reduced when experiments were conducted in solutions of N-ethylmaleimide[171] or divinylsulphone[172] both of which block thiols, preventing their participation in the interchange reaction.

Miyanchi et al[169,175] have shown that the same type of relaxation behaviour takes place in N-mercaptomethyl poly-capryolactam fibres and that relaxation of this and wool is reduced after treatment with KCN, as the monosulphide crosslinks produced cannot undergo interchange.

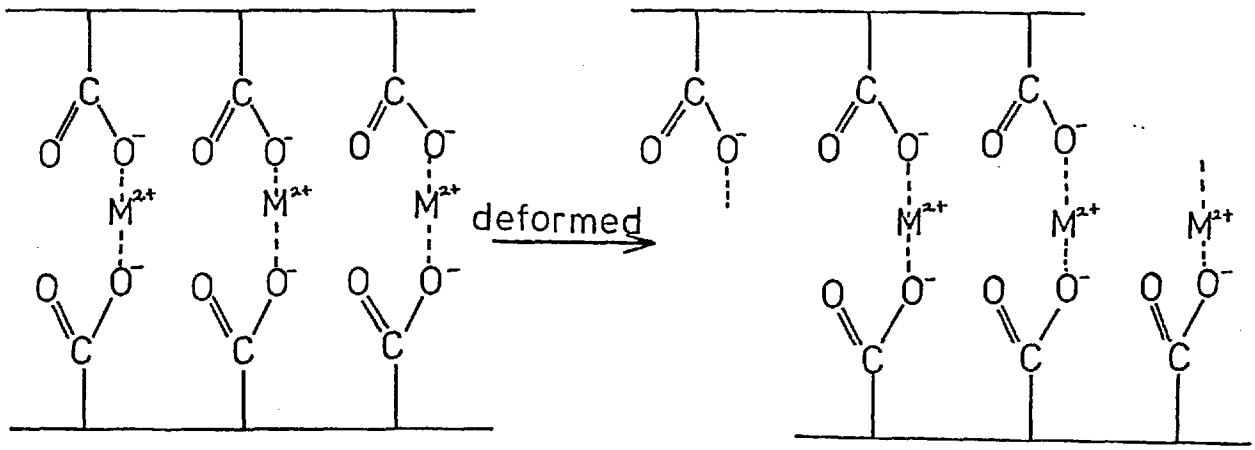
(4.3.3) Rubbers Containing Salt Links

Rubbers containing pendant carboxylic acid groups may be cured by divalent metal oxides to give vulcanizates containing crosslinks with the structure shown in figure 4.10a.[176]

It was suggested that these might undergo interchange by breaking and remaking ionic bonds (see figure 4.10b).[176]



(a) a salt linkage



(b) deformation of a network containing salt links

figure 4·10: Networks of salt links

Tarasova and Dogadkin[177] reported that the stress relaxation of such networks could be explained by such a mechanism, although Ward and Tobolsky[178] found that the behaviour was not this simple; relaxation being due to both interchange and viscous flow.

(4.4) THE CHEMICAL STRESS RELAXATION OF HIGH TEMPERATURE ELASTOMERS

In recent years the demand for elastomers that can be used at elevated temperatures has increased; in particular the aero-space industry requires materials that will withstand temperatures in excess of 120°C. Few materials will withstand these temperatures, the principal ones being the silicones and the fluoro-elastomers.

(4.4.1) The Chemical Stress Relaxation of Silicone Rubbers

(4.4.1.1.) The Chemical Stress Relaxation of Polydimethyl Siloxane

Polydimethyl siloxane can be cured by organic peroxides or radiation; vinyl groups are often substituted for a few of the methyl groups to facilitate crosslinking.[179] The crosslinks produced are simple carbon-carbon bonds as in the hydrocarbon rubbers.

Polydimethyl siloxane has the structure

$$\left[\begin{array}{c} CH_3 \\ | \\ -Si-O- \\ | \\ CH_3 \end{array}\right]_n$$

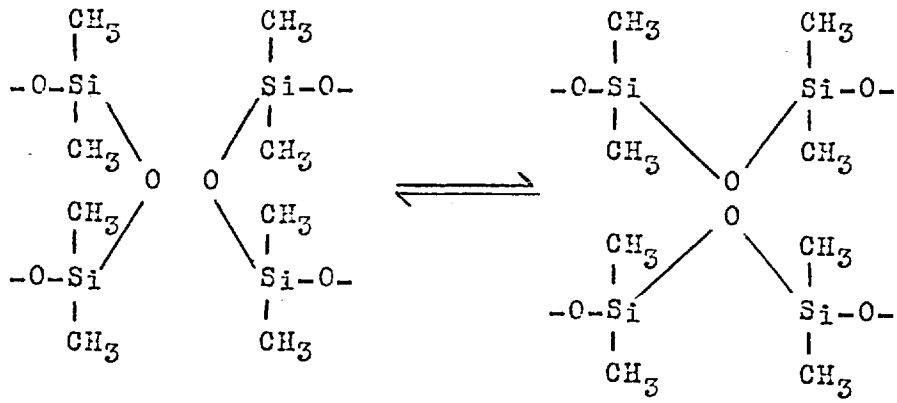
so that the polymer backbone contains only S_i - O bonds.

The chemical stress relaxation behaviour of pdms was first studied by Osthoff, Bueche and Grubb[180] who found that

an extracted, radiation cured pdms vulcanizate underwent continuous stress relaxation at 150-260°C in anhydrous argon with an activation energy of 95 kJ $mole^{-1}$; the rate of relaxation in argon or nitrogen was not increased by the presence of moisture. The continuous stress relaxation of benzoyl peroxide cured samples containing potassium hydroxide and acid residues relaxed at a faster rate than the radiation cured sample in dry nitrogen, with an activation energy of only 21 kJ $mole^{-1}$; the rate was increased still further in air, CO_2 and moist nitrogen at 130°C. Turner and Lewis's[181] results, where comparable, were in broad agreement with those of Osthoff, Beuche and Grubb.[180] Turner and Lewis[181] showed that the rates of both intermittent and continuous relaxation were higher under moist conditions and indicated that simultaneous scission and crosslinking was taking place.

It was concluded, from the results of Osthoff, Beuche and Grubb and Turner and Lewis, that stress relaxation resulted from two chemical processes:

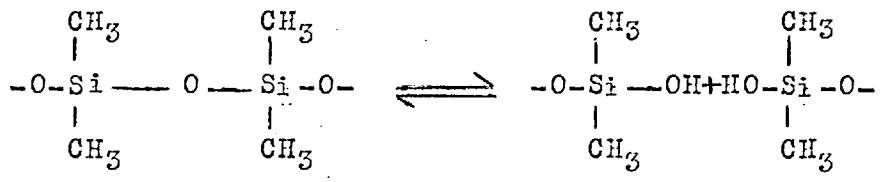
(i) Siloxane bond interchange



that took place under anhydrous conditions and was catalysed by the presence of acids or bases; it was thought[179] that this

reaction might also have been catalysed or co-catalysed by water.

(ii) Siloxane bond hydrolysis via silol formation.



The equilibrium position of this reaction would be pushed to the right hand side as the concentration of water increased; the rate of scission being proportional to the concentration of water.

Tobolsky, McLoughlin and Johnson[182] prepared a series of pdms films containing an acid catalyst which underwent rapid relaxation at 60°C under anhydrous conditions. The rate of continuous relaxation of these vulcanizates was reduced by increased humidity; this stabilising effect of water was reversible, permanent stabilisation being brought about by soaking in pyridine. Since the effect of water was opposite to that expected if siloxane hydrolysis were taking place, Tobolsky[15] suggested that siloxane bond interchange was occurring, catalysed by the acid, which was stabilised by water, and neutralised by pyridine. As these results are different from those of all the other workers they must be due to the unique structure of the vulcanizates.

Several workers studied the relaxation of pdms where some of the methyl groups were replaced by vinyl groups. Lee, Sperling and Tobolsky[151] and Thomas[179,183,184] investigated the relaxation of peroxide cured samples. Continuous stress relaxation was very slow at 250°C in a vacuum and in dry very pure nitrogen with activation energies of 217[150] and 146[151] kJ mole^{-1} respectively.

Thomas[179,183,184] showed that relaxation in dry air was faster than the vacuum rate and could be reduced by the incorporation of an antioxidant (see figure 4.11), partially polymerised trimethyldihydroquinone (TMDHQ), indicating that some of the relaxation was due to oxidative scission of the crosslinks. The rate of continuous stress relaxation was further increased in moist air and became first order (see figure 4.11); this first order reaction had an activation energy of 61 kJ $mole^{-1}$, was unaffected by extraction except at high temperatures, and was apparently due to a main chain cleavage reaction.

Controvesy exists regarding the effect of a fume silica filler; Thomas[179,183,184] found that the water content and the acidity of the filler caused the relaxation rate to be increased, but Tobolsky and Shaw[185] found that the relaxation rate was reduced. Red oxide improved the stability of the vulcanizates.

These results could also be explained in terms of the siloxane bond hydrolysis and interchange reactions already discussed. Thomas[179] concluded that siloxane bond interchange was not important because of the very slow rate of relaxation in a vacuum. He suggested that relaxation under moist conditions was due to siloxane bond hydrolysis although it could be due to water catalysed siloxane bond interchange.

(4.4.1.2) The Chemical Stress Relaxation of Modified Silicone Rubbers

To produce higher stability elastomers several attempts have been made to modify pdms, by substitution both of pendant methyl groups and within the main chain.

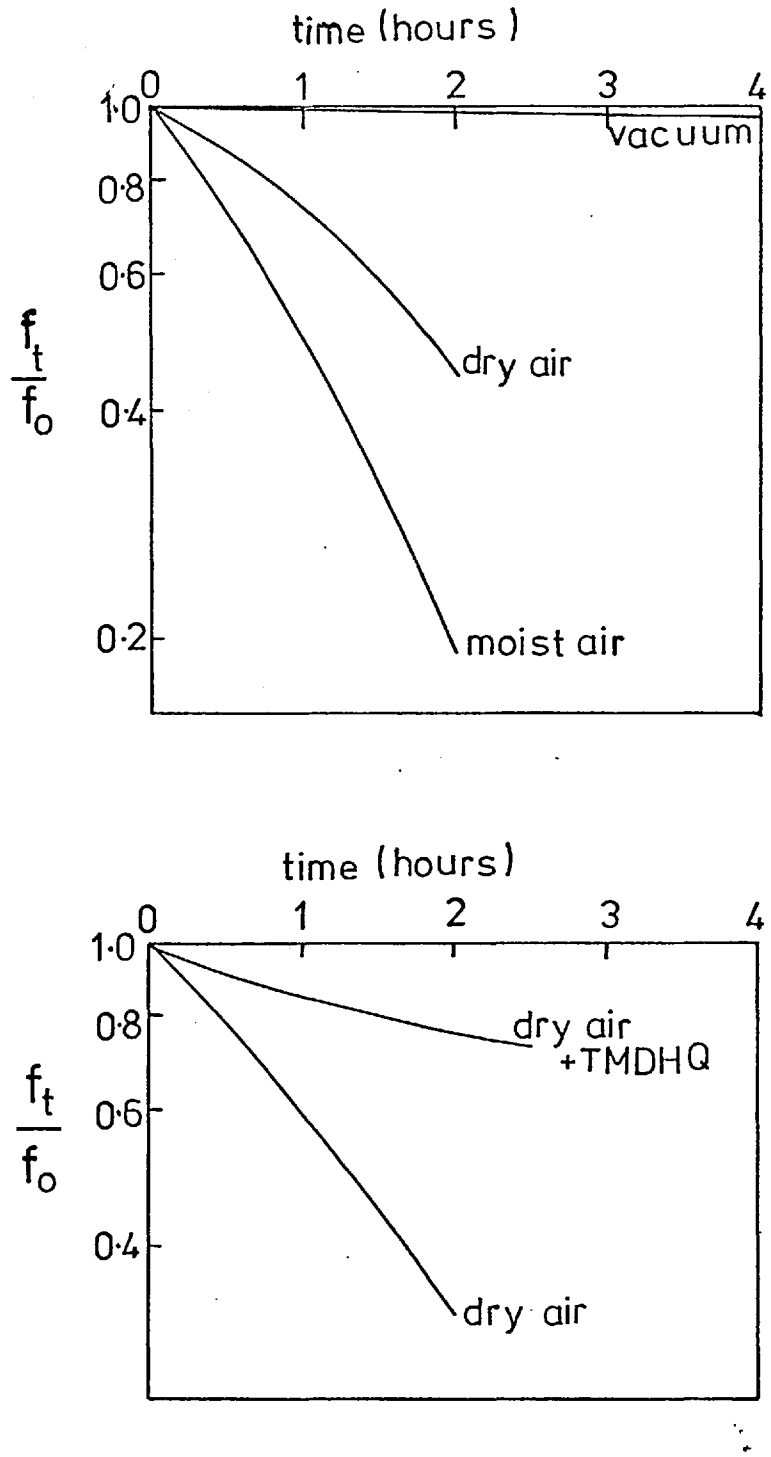


figure 4·11 : Effect of different atmospheres and antioxidant on the continuous stress relaxation of a peroxide cured methyl vinyl silicone rubber (ref.184)

The flurosilicones are an example of methyl group substitution in which some of them are replaced by trifluoropropyl groups. Thomas[186] and Tobolsky and Shaw[185] have shown that the fluorosilicone elastomers were considerably less stable than conventional pdms. Thomas[186] showed that the stability of fluorosilicone rubbers was critically dependent on the peroxide used to cure the material and that the order of vulcanizate stability was

Dichlorobenzoyl peroxide > 2,5 dimethyl -2, 5-ditertiary butyl peroxyhexane > Benzoyl peroxide > Dicumyl Peroxide.

This was explained in terms of the neutralisation of basic residues from the polymerisation of the base polymer, by residues resulting from the crosslinking system. These conclusions were supported by experiments on samples that had been deliberately doped with dichlorobenzoic acid or acidic silica fillers. Tobolsky and Shaw[185] showed that the presence of iron oxide led to a considerable stabilisation of the vulcanizates.

The m-carborane/pdms rubbers are examples of in chain modified silicone rubbers; these involve replacement of oxygen atoms with m-carborane units either in a regular or a random manner. Zaganiaris, Sperling and Tobolsky[187] and Sperling, Cooper and Tobolsky[188] studied several peroxide cured m-carborane/pdms rubbers including SiB - 1 with the structure

$$\{Si - CB_{w}H_{10}C - Si - O\}_{n},$$

SiB - 2[187,188] with the structure

$$\{Si - CB_{10}H_{10}C - Si - O - Si - O\}_{n}$$

and SiB - 1.5, a 50:50 copolymer of these two. The relative stabilities of these were characterised by a "maximum

temperature", defined as the maximum temperature at which the samples maintained $(f_t/f_o)_c$ values of at least 1/e(0.368) or did not undergo "excessive" crosslinking for 24 hours [187] (see Table 4.2).

TABLE 4.2

Sample	Useful Maximum Temperature °C	
	In Air	In N_2
SiB - 2	260	325
SiB - 1.5	275	-
SiB - 1	285	-
pdms	230	280
SiB - 2 filled with fume silica	300	416

In the SiB rubbers there were very high rates of crosslinking at higher temperatures than those listed in Table 4.2.

Tobolsky and Shaw [185] studied the continuous relaxation of a random SiB - 2 rubber in nitrogen; in common with the other m-carborane/pdms rubbers, relaxation was slower than first order and was interpreted by the multi-exponential procedure described in section 3.5.2 in terms of two first order processes. It is interesting that the short time process had an activation energy of 217 kJ $mole^{-1}$ whilst the long term process had a smaller activation energy of 175 kJ $mole^{-1}$; both these processes were associated with crosslink scission and Tobolsky and Shaw [185] proposed that they were due to the thermal decomposition of two different types of crosslinks.

Since the nitrogen relaxation was due to cleavage of

the crosslinks then the oxidation of the crosslinks and pendant hydrocarbon segments was probably the cause of the scission and crosslinking that occurs in air. The differences between the relaxation of the elastomers containing different amounts of m-carborane is then due to differences in simultaneous siloxane bond interchange. The stabilising effect of silica (see Table 4.1) may be due to its neutralisation of basic polymerisation residues as in the fluroelastomers.

The SiB polymers can be cured without peroxides, so that cure proceeds by displacing methyl groups resulting in the production of networks without SiCSi or SiCCSi bonds; these networks are more stable[185] than the peroxide cured vulcanizates.

Other modifications of the methyl substitution type have involved replacement of some methyl groups by phenyl groups or by vinyl-o-carborane groups[185]. Pendant phenyl groups do not provide the same degree of protection as main chain m-carborane groups against thermal scission and the use of pendant vinyl-o-carborane groups as crosslinking sites has a detrimental effect on thermal stability.

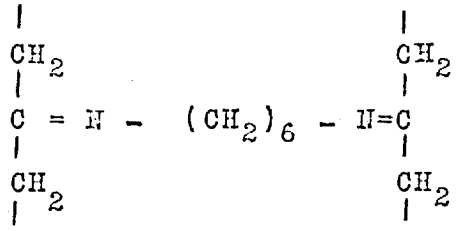
(4.4.2) The Chemical Stress Relaxation of Fluoro-Elastomers

The fluoro-elastomers or "vitons" are copolymers of vinylidene fluoride and hexafluropropylene having the structure

$$-CH_2-CF_2-(CH_2-CF_2)_s(CF_2-\underset{\displaystyle F}{\overset{\displaystyle CF_3}{\overset{|}{C}}})_t-CH_2-CF_2- \ ,$$

which is cured commercially by diamines such as hexamethylene

diamine carbamate (HMDC)[189] in conjunction with magnesium oxide. This gives crosslinks with the structure



Viton can also be cured by exposure to γ-radiation; this gives C-C crosslinks and introduces some main chain unsaturation into the polymer.

Thomas[189-193] studied the continuous stress relaxation of HMDC/viton vulcanizates which at 250°C underwent a rapid oxidative cleavage reaction in the vicinity of the crosslinks. The rate of relaxation was unaffected by extraction or by the presence of carbon black fillers and was first order at $(f_t/f_o)_c$ values of 0.8 or more. The activation energy for the oxidation reaction was 97 kJ $mole^{-1}$.

The continuous relaxation behaviour of dicinnamylidene - 1,6 - hexanediamine (DCHD)/viton vulcanizates was identical with that of the HMDC vulcanizates, giving points that fitted on the same Arrhenius plot.

The intermittent relaxation of both HMDC and DCHD vulcanizates showed that there was a high rate of crosslinking; for every 100 crosslinks removed by cleavage, 85-90 were introduced by crosslinking (see figure 4.12). Thus the original or "first" network was replaced, during oxidative ageing, by a "second" network.

The continuous stress relaxation of p-phenylenediamine (PPD) vulcanizates took place at a slower rate than was the case for HMDC or DCHD cured samples although it was also

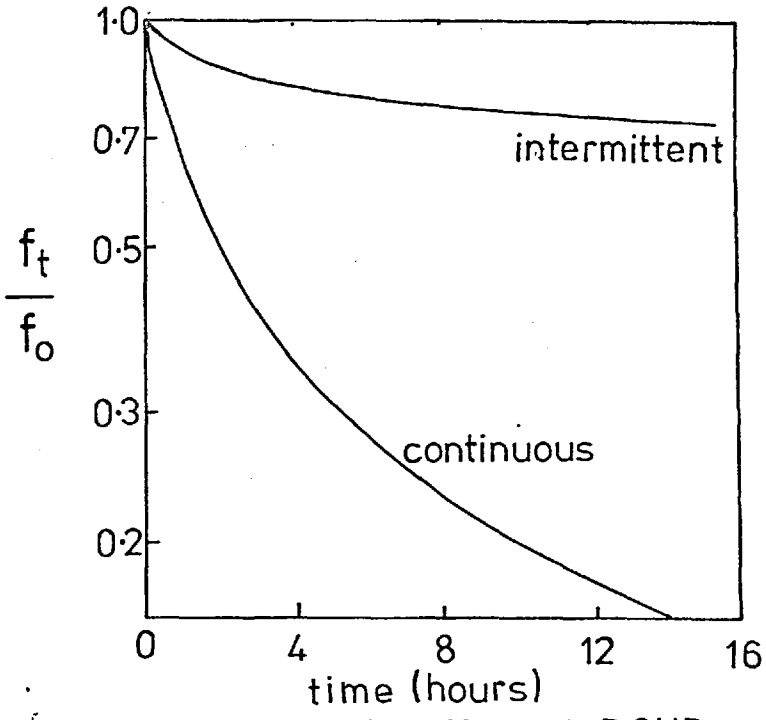


figure 4·12: Chemical stress relaxation of DCHD cured Viton B in air at 250°C (ref.193)

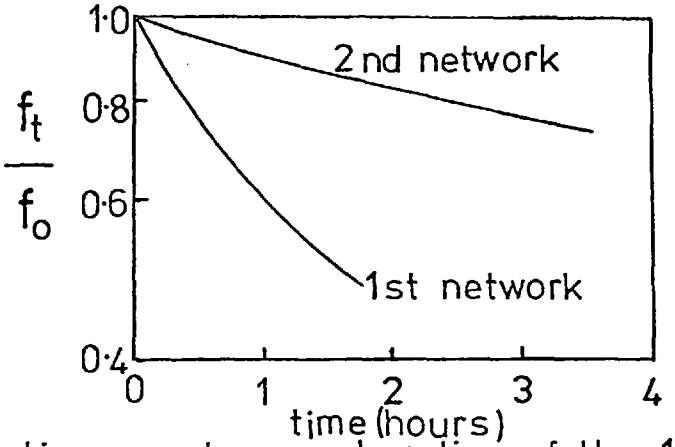


figure 4·13: Continuous stress relaxation of the 1st and 2nd networks of Viton elastomers (ref.193)

accompanied by an efficient crosslinking reaction. Thomas concluded that in HMDC or DCHD cured samples scission took place both in and at the crosslinks but that scission in the crosslinks was prevented in PPD vulcanizates by the higher oxidative stability of the aromatic ring.

A prolonged post cure in air at 250°C resulted in the complete replacement of the first network, by the second network; the stability of the second network was much greater than the first (see figure 4.13) and was the same whatever amine was used for the original cure. The second network underwent a first order main chain scission reaction with an activation energy of 115 kJ $mole^{-1}$; these results were essentially the same as those obtained for radiation cured samples where the activation energy was 117 kJ $mole^{-1}$, although a higher rate of relaxation was observed because of the main chain unsaturation present.

The presence of 2 - 3% of an antioxidant, TMDHQ, improved the stabilities of both first and second networks although 0.55% of polymerised phenylene diamine was better, since this maintained a constant network chain density for 10 times longer than TMDHQ at 250°C.

Yoshida, Florin and Wall [194] studied the radiation induced oxidation of Viton and Kel-F(3700), a copolymer of vinylidene fluoride and chlorotrifluromethylene. Both of these were cured with γ-radiation and relaxed at 25°C in air and nitrogen. under dose rates of 0.3 - 2.7 Mr hr^{-1}; physical relaxation effects were factored out and linear f_o/f_t vs t curves observed.

The G factors (i.e. the number of scissions per 100 eV absorbed) obtained are given in Table 4.3.

TABLE 4.3.

Sample	Crosslinking Dose (Mr)	G factor at stated Dose Rate					
		0.31 Mr/hr		0.8 Mr/hr		2.7 Mr/hr	
		Air	N_2	Air	N_2	Air	N_2
Viton A	4	13.2	4.6	8.9	7.1	12.5	7.7
	8	12.5	5.2	8.4	7.3	15.2	7.0
	16	12.2	5.6	10.2	7.9	-	6.9
Kel-F-3700	4	6.2	4.1	3.6	4.1	-	-
	8	4.8	1.9	-	2.4	-	-
	16	3.7	2.1	-	4.8	-	-

For Viton A, the G values in air are generally greater than those in N_2, although there is a considerable amount of difference between the results at different dose rates. The independence of the G factors on the crosslinking dose indicates that scission takes place at the crosslinks. No intermittent data was obtained and so it was not possible to consider the effect of simultaneous crosslinking reactions that must have been taking place at an appreciable rate, especially at the higher dose rates.

The scission reaction in Kel-F was not appreciably different in nitrogen from that in air and Yoshida, Florin and Wall suggested that this was a result of the low permeability of Kel-F to oxygen.

(4.4.3) The Chemical Stress Relaxation of Nitroso Rubber

Nitroso rubbers are copolymers of polytetrafluroethylene and trifluronitrosomethane that is reputed to be curable with a mixture of triethylene tetramine (TETA) and HMDC.

Thomas [195] found that continuous stress relaxation curves of a TETA/HMDC vulcanizate were first order, after an initial

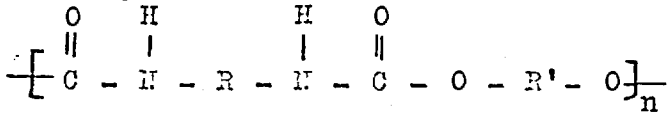
period of fast relaxation, in the temperature range 22 - 150°C. The linear portion was unaffected by changing the concentrations of TETA and HMDC, or by changing the atmosphere from air to nitrogen; the activation energy was 27 kJ mole^{-1}. Intermittent stress relaxation indicated an initial period of crosslinking.

It was concluded that TETA/HMDC was a largely ineffective curing system, and the relaxation behaviour resulted from viscous flow with some TETA and HMDC induced scission and chain branching superimposed upon it.

(4.5) THE CHEMICAL STRESS RELAXATION OF POLYURETHANE ELASTOMERS

The polyurethane elastomers do not fit into any of the previous three groups of rubbers although a discussion of their stability will include some aspects of hydrocarbon oxidation and labile bond reactions. However, their properties are, in general, quite different.

Polyurethane elastomers comprise glycol terminated polymer chains (typically polyethers or polyesters) and diisocyanates; these basic ingredients are reacted together to give a polyurethane which has the structure



where R is usually an aromatic group and R' is a polyester or a polyether.

The first studies of stress relaxation were made by Offenbach and Tobolsky[16] and Colodny and Tobolsky[17] and are summarised in Table 4.5. Soaking sample 1 in water did not affect the relaxation at 90°C although soaking sample 2 in polyethylene glycol reduced τ ch at 110°C from 19 to 6.8 hours. The intermittent stress relaxation of all the samples

TABLE 4.4

Polyol	Other Reactants	Constituent Links	τ_{ch} at 120°C (hours)	ΔH kJ mole^{-1}	Sample No.	Ref.
ethylene/ propylene adipate polyester	diphenyl methane diisocyanate and water	ester, urethane, disubstituted urea, biuret	3.3 *	125	1	16
	naphthalene-1,5-diisocyanate and butan-1,4-diol	ester, urethane	6.9 *	146	2	16
	toluene-2,4-diisocyanate and an aromatic diamine	ester, urethane disubstituted urea, biuret	4.9 *	142	3	16
	methyl triphenyl tri-isocyanate	ester, urethane	14	116	4	17
	reacted with toluene dissocyanate to give isocyanate terminated polymer: 1,2,6 hexanetriol	ester, urethane	9.7	119	5	17
	reacted with toluene dissocyanate to give isocyanate terminated polymer: water	ester, urethane disubstituted urea, biuret	1.6	122	6	17
Commercial polyether (Adiprene B)		ether, urethane + other links	2.1	127	7	16

* approximate values obtained from figure 4 of ref.16

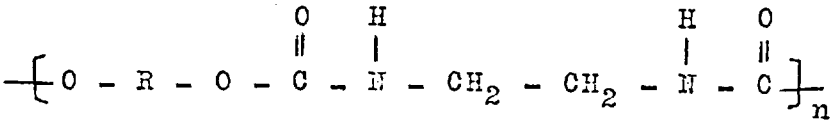
indicated that a substantial bond reformation or crosslinking reaction was taking place.

The results summarised in Table 4.3 indicate that vulcanizates containing disubstituted urea and biuret links are less stable than those containing just ester and urethane links; Tobolsky[15] did not consider that these networks might also contain allophanate links but these could be present in all of them.

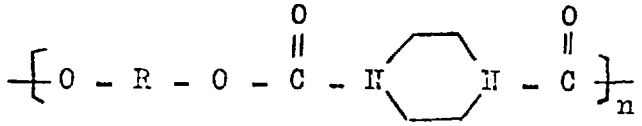
Tobolsky and Peterson[196] evaluated the specific rate constant for urethane cleavage in sample 4 (Table 4.3) which contains two urethane links; they obtained

$$k_1 = 1/2\,\tau_{ch} = 2.5 \times 10^{10} \exp - 116000/RT$$

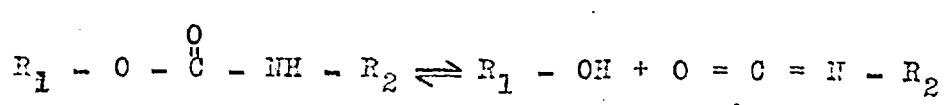
To investigate further the stability and mechanism of urethane cleavage, Tobolsky, Yu and Thach[20] studied two sulphur cured urethane rubbers; one prepared from ethylene diamine and the other prepared from piperazine. The structures of these elastomers were:



and



The continuous stress relaxation curves for these two rubbers are shown in figure 4.15; the much greater stability of the piperazine network was attributed to the fact that it cannot undergo dissociation by the reaction



These early results of Tobolsky et al showed that the continuous stress relaxation of polyurethane elastomers was not, in general, first order and it was demonstrated by Weissbein and Singh[18,19] and Tobolsky, Johnson and MacKnight[197] that the curves could be analysed using the multi-exponential equation discussed in section (3.5.2). The curves could be described quite well using two terms (see Figure 4.14).

Using this approach Tobolsky, Johnson and MacKnight[197] analysed the data for a triol cured, isocyanate terminated polyester prepolymer and obtained activation energies of 195 and 172 kJ $mole^{-1}$ for the slow and fast processes respectively. The intermittent modulus remained unchanged with time indicating that a new chain was produced for every one broken; this could have resulted from cleaved bonds regenerating.

Weissbein and Singh[18,19] also analysed their results in this way and obtained good fits for a number of polyurethanes. They prepared samples from an isocyanate terminated prepolymer that was cured with 1,2,6 hexanetriol, trimethylolpropane or mixtures of trimethylolpropane and butanediol. The use of mixtures of butanediol and trimethylolpropane enabled the number of urethane groups per chain to be varied in a systematic manner; the continuous relaxation rate increased as the number of urethane groups per network chain increased. These results confirmed further the association of cleavage with the urethane group in networks where more readily cleaved bonds (i.e. biuret etc.,) were absent. The presence of ferric acetyl acetonate, a catalyst that increases urethane breakdown, considerably increased the rate of relaxation; but the

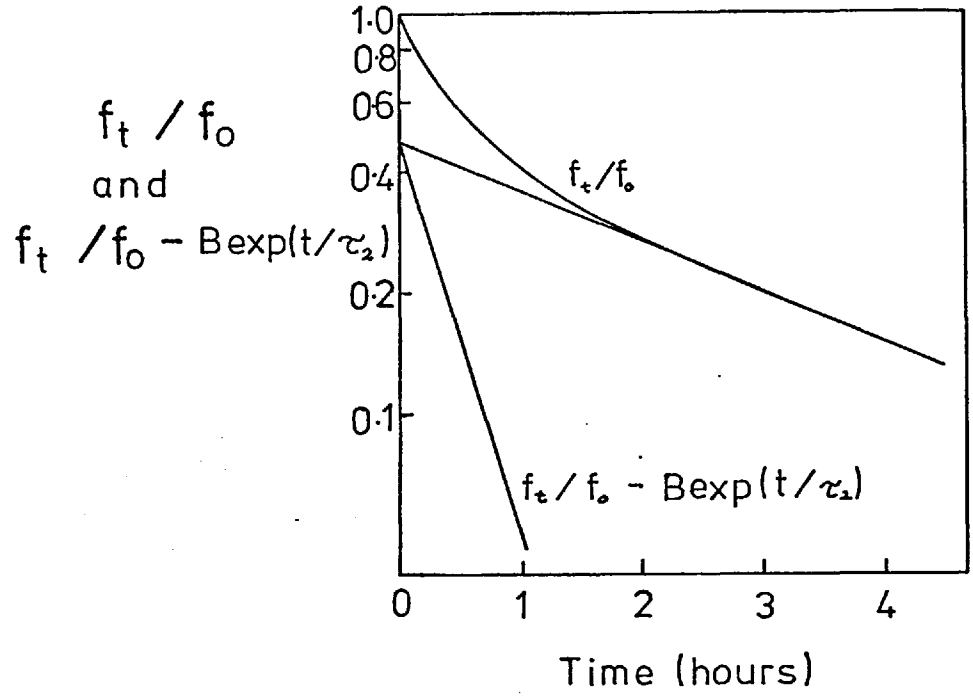


figure 4·14 : Multi-exponential analysis of a triol cured polyurethane elastomer relaxed at 160°C (ref. 197)

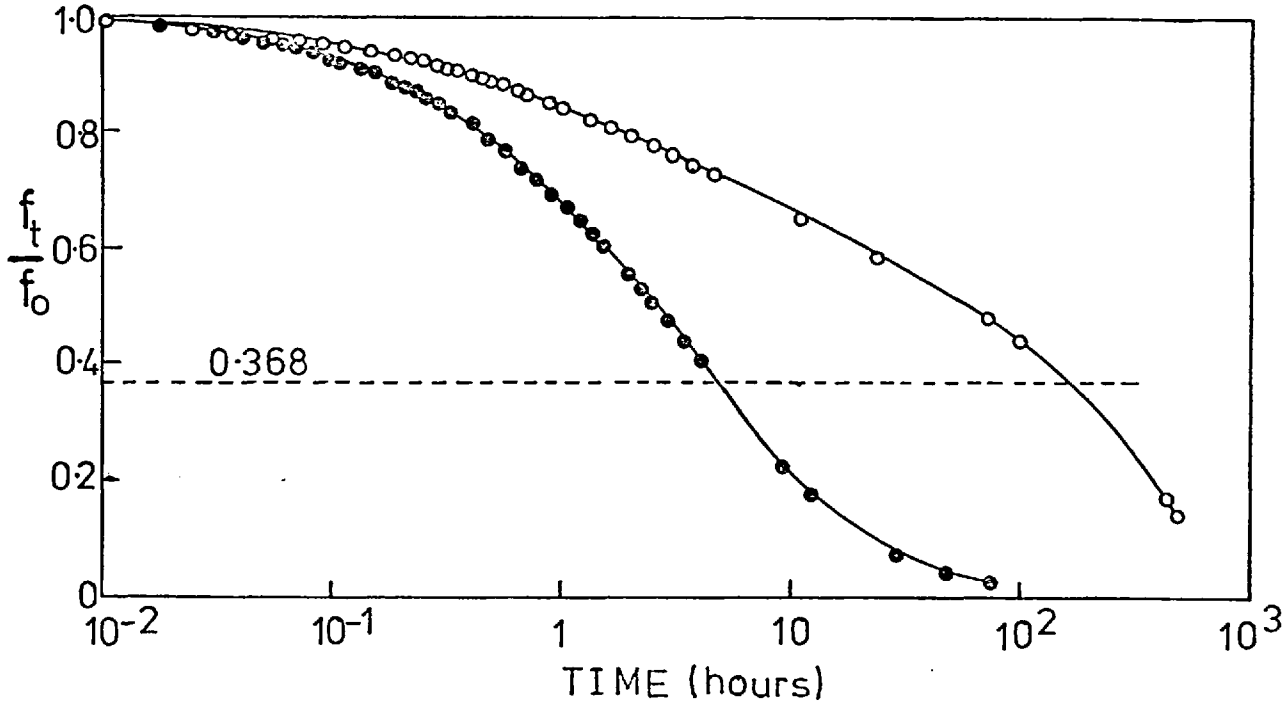
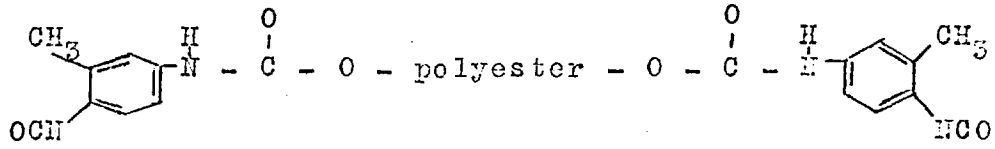


figure 4·15: Relaxation of piperazine (o) and ethylenediamine (•) extended urethane elastomers at 120°C (ref. 20)

relaxation curve could now only be adequately described by a three term exponential equation.

A number of model polyurethanes were prepared by Weissbein and Singh[19] with the structure:



the only difference between the model polymers was the number average molecular weight of the polyester which was varied in the range 1000 - 4000. This isocyanate terminated prepolymer was cured with trimethylolpropane to give elastomers with exactly four urethane links per chain.

The continuous relaxation curves were resolved using the two term exponential equation (see page 76); the slowest process gave the same activation energy of 124 kJ $mole^{-1}$ and approximately the same rate; irrespective of polyester molecular weight. The faster process did not give identical rates, except at 150°C, and the activation energies for the samples varied between 80 and 121 kJ $mole^{-1}$. The slow process was attributed to urethane cleavage whilst the fast process was attributed to the cleavage of undefined weak links as had been proposed by Tobolsky et al.

+ + + + + +

CHAPTER 5

THE PHYSICAL AND CHEMICAL PROPERTIES OF POLYURETHANES

(5.1) INTRODUCTION

The work described in this thesis is concerned with solid polyurethane elastomers,[1-8,198,199] in particular, those that can be handled on a rubber mill.[2,3] The millable polyurethanes are not, however, the only type of urethane elastomers, but are chemically similar to many of the other types, which include castable, thermoplastic, cellular, sprayable and poromeric polyurethanes and spandex fibres. In addition the chemical similarities extend to the flexible and rigid foams, coatings and adhesives.[1,7]

The physical properties, on the other hand, are quite different from the other urethane elastomers, except for the castable urethanes,[1-3] and the other polyurethane materials.

The characteristic component of polyurethane polymers is the urethane group,[1,3,7,8,199] which has the structure:

$$R - NH - \overset{O}{\overset{\|}{C}} - O - R'$$

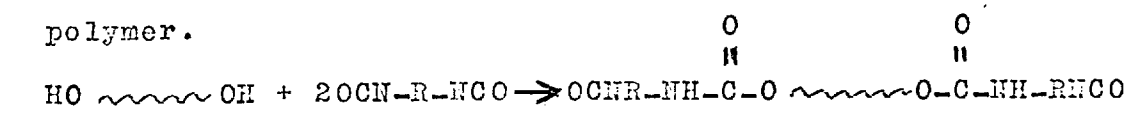
although this group is by no means the major component of the polymer.

The polymer comprises glycol terminated polymer molecules with fairly low molecular weights, that are reacted with diisocyanates to give polyurethanes. The molecular weight of the glycol would generally be 3000 or less and is usually a polyether or a polyester, although more recently glycol tipped polybutadienes or polydimethylsiloxanes have been used.[3]

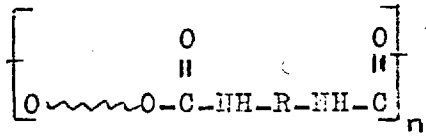
(5.2) THE PREPARATION AND CURE OF URETHANE ELASTOMERS

The exact method of preparation depends upon the required product, but it can be visualised as comprising two stages which may sometimes be combined into one:[1,3]

(i) Prepolymer preparation comprises the reaction of an excess of diisocyanate with a glycol terminated polyether or polyester; the product is an isocyanate terminated prepolymer.



(ii) Chain extension comprises the reaction of this prepolymer with an active hydrogen compound such as water, amines or a glycol. If the glycol terminated polyether or polyester is used, the product is a simple linear polyurethane with the structure:



This may be hydroxyl or isocyanate terminated depending on which reactant was present in excess; hydroxyl terminated polymers are the most stable.

If an amine chain extender or water were used the product would contain disubstituted urea linkages in addition to urethanes. Several other chain extenders such as amino alcohols, hydrogen sulphide or dicarboxylic acids have been used but are not commercially important.

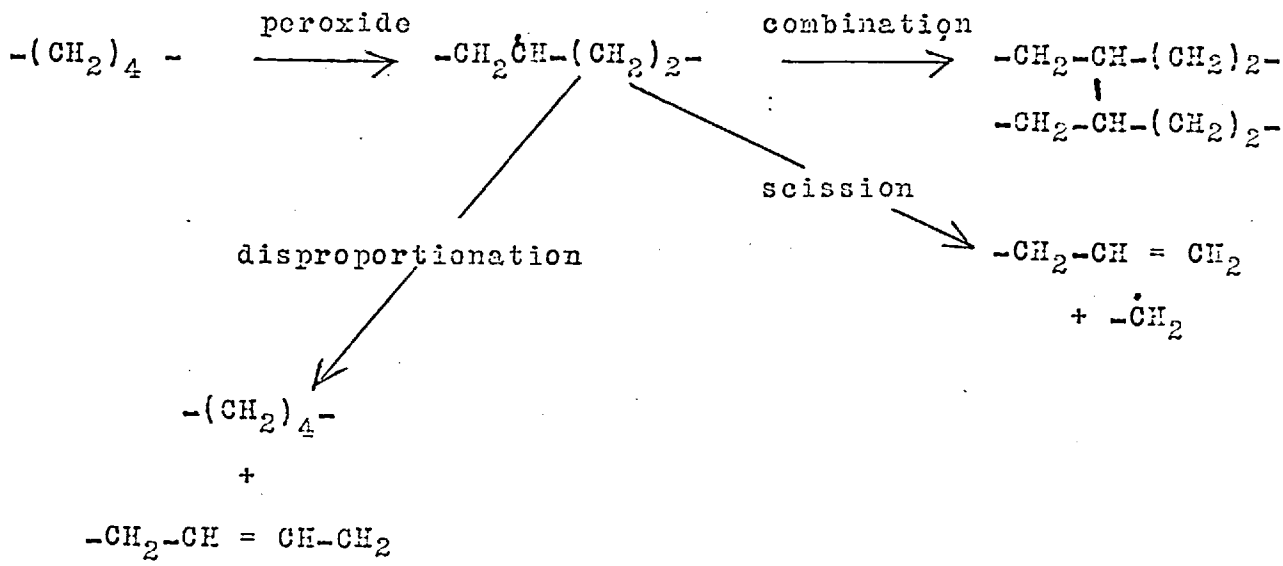
The crosslinking[1-3] of urethane polymers can be accomplished in several ways. Perhaps the most obvious method is the use of triol or triamine chain extenders giving urethane or urea linkages. Crosslink density can then be varied if mixtures of triol and diol or triamine and diamine etc. are used. Apart from the urethane or urea links the terminal isocyanate groups can react with urethane or urea groups in the chain to give allophanate or biuret crosslinks, or with other isocyanate groups to produce isocyanate dimers or trimers. This means that polymers containing terminal isocyanates or added diisocyanate in addition to urethane or urea groups can be

crosslinked simply by heating to 120°-150°C. The hydroxyl terminated urethanes may be cured in this way by addition of diisocyanate, when the crosslinks will be allophanates, biurets and isocyanate trimers; alternatively a triisocyanate can be used when there will be predominantly urethane crosslinks.

The structures of these types of crosslinks are shown in figure 5.1.

Other systems include the peroxide or sulphur cure of suitably modified polyurethanes.[200] Peroxide cures can be used whenever the polymer contains some hydrocarbon segments, since the cure involves abstraction of hydrogen and combination of the free radicals so formed. Hydrogen can be most readily abstracted from a CH group followed by CH_2 and CH_3, the ease of abstraction being approximately 17:6:1.[201] However, terminal CH_2 groups or CH_2 groups that are α to a double bond are more highly reactive.

The free radicals formed do not have to combine to give a crosslink[104] but can result in main chain scission or the production of double bonds by a disproportionation reaction; these wasteful side reactions are more important in fully saturated hydrocarbons than in olefins.



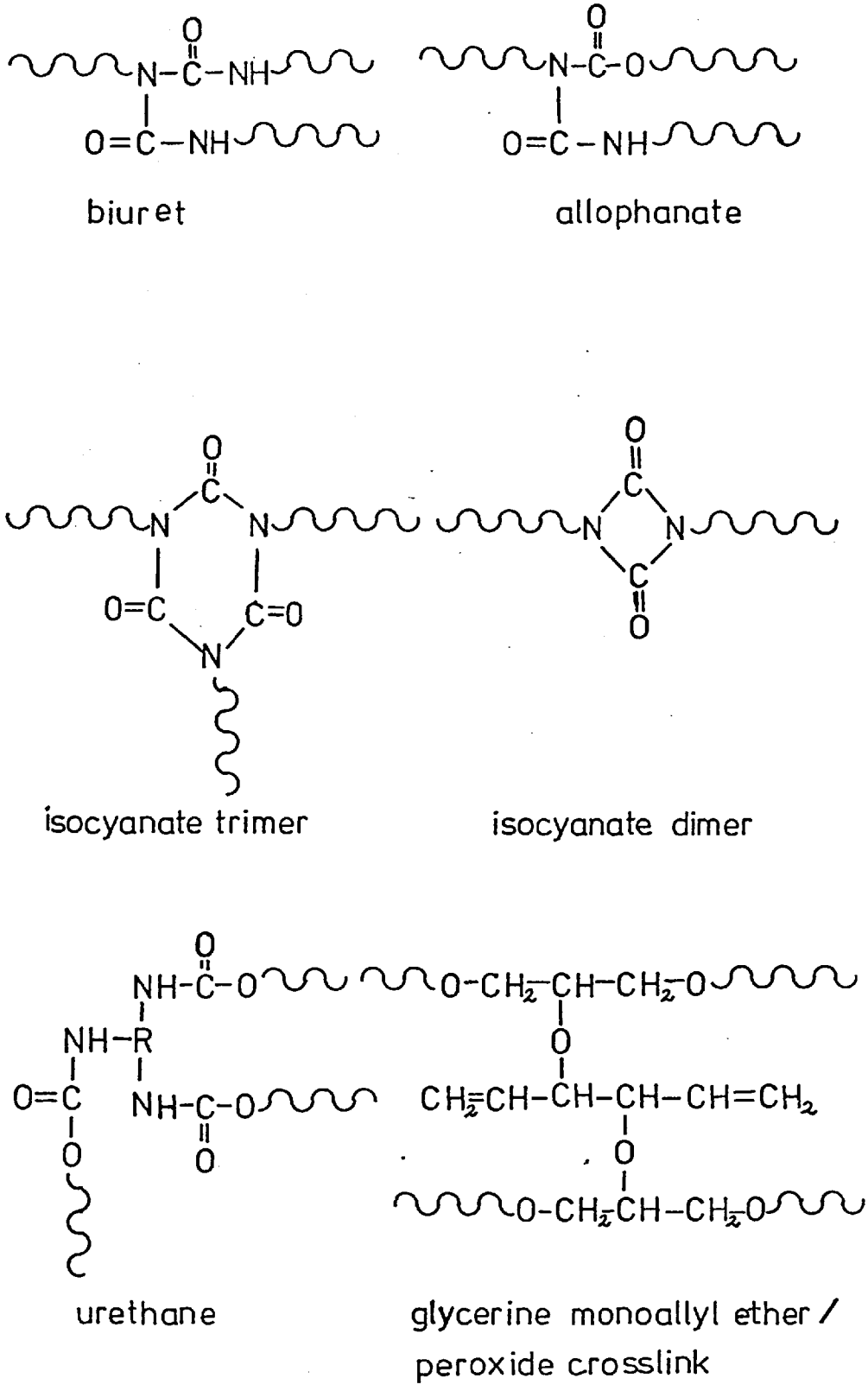
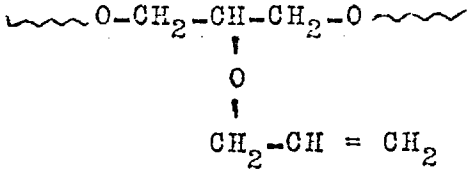


figure 5·1 : Crosslinks in urethane elastomers

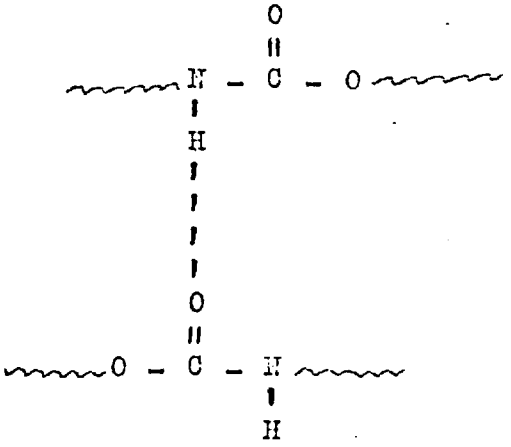
Small amounts of unsaturation are often included in the polymer to aid peroxide curing and to enable the materials to be sulphur cured; this is frequently done by the addition of glycerine monoallyl ether [1-3,6] which gives the structure



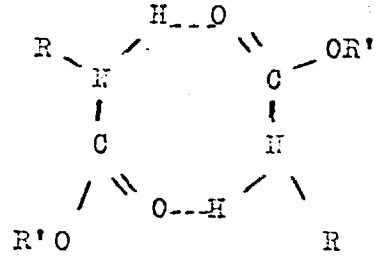
(5.3) HYDROGEN BONDING IN POLYURETHANE ELASTOMERS

The primary chemical structure of polyurethane elastomers was discussed in section (5.2), apart from this there is evidence of an extensive secondary bonded structure resulting from hydrogen bonding. [1,3,202,203,204]

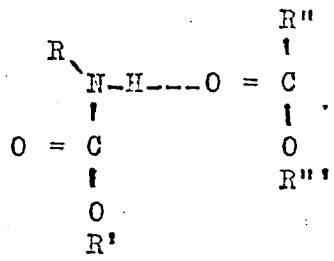
The hydrogen bonds formed are usually assumed to be similar to those in amides so that they will have the following structure: [1,202]



A recent study, using ultrasonic methods, has suggested that in simple urethanes a dimer is formed which has the structure: [202]

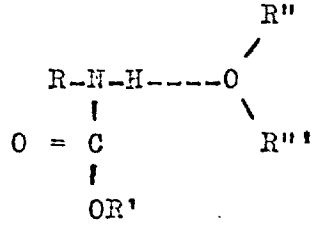


This has an activation energy for dissociation of 16 kJ mole^{-1} per bond. The same technique was used to show that in polyester and polyether solvents there was both urethane/urethane and urethane/solvent hydrogen bonding. The urethane/solvent bonds would presumably have the structures:



for the polyester

and



for the polyether

The ester/urethane and urethane/urethane bonds will form preferentially with the carbonyl oxygen rather than the other oxygen as carbonyl groups are known to form strong hydrogen bonds.[204]

All these bonds are likely to be formed in polyurethane elastomers and the hydrogen bonded structure of the polymers undoubtedly affects their stress relaxation at low temperatures and their compression set behaviour.[1,2,3]

(5.4) THE ENVIRONMENTAL STABILITY OF POLYURETHANE ELASTOMERS

Several studies have been made[1-5,198] to determine the thermal,[205,206] photolytic,[207,208] thermooxidative,[205] photooxidative,[207,208] hydrolytic and fungal or bacteriological stability of urethane elastomers.[3] All of these factors were known to reduce the service life of polyurethane elastomers[3] although most interest has been concentrated on the thermal, thermooxidative and hydroyltic stability of the elastomers.

(5.4.1) The Thermal Stability of Polyurethane Elastomers

(5.4.1.1) The Urethane Link

Thermal dissociation of the urethane link [1,198] would seem to follow three pathways. Firstly, degradation can lead to the production of an isocyanate and an alcohol; this will be a reversible reaction:

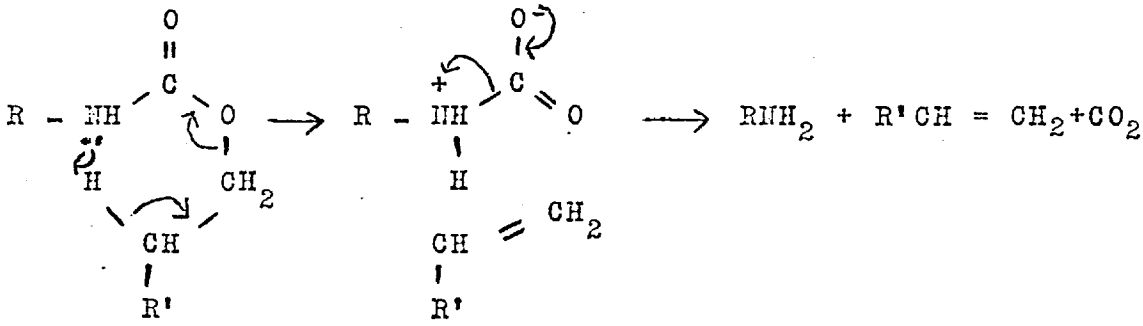
$$RNHCOOR' \rightleftharpoons RNCO + R'OH$$

Secondly, an olefin and a primary amine can be formed:

$$RNHCOOCH_2CH_2R' \longrightarrow RNH_2 + R'CH = CH_2 + CO_2$$

[209]

this may proceed via a cylic intermediate.

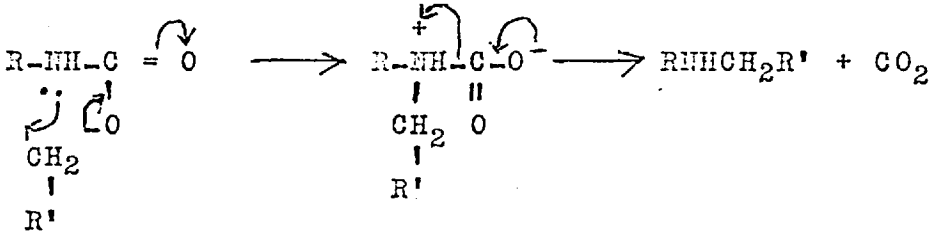


Thirdly, decomposition may lead to the production of a secondary amine: [1,198,209]

$$RNHCOOH_2R' \longrightarrow RNH\ CH_2R' + CO_2$$

[209]

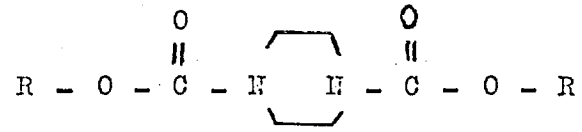
which may also involve a cyclic intermediate:



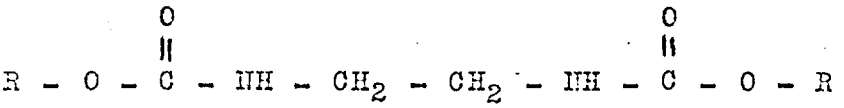
This reaction involves no net scission of the polymer chain in which it takes place.

The most common of these decomposition pathways seems to be the first. The hydrogen atom plays an important role in the decomposition process since Beachell [210] and others [20] have shown that the rate of decomposition is reduced when this hydrogen atom is removed. Beachell and Ngoc Son [210] showed that

an N substituted urethane, where the hydrogen atom was replaced by a methyl group was more stable than an unsubstituted urethane.[20] Tobolsky, Yu and Thach showed that the continuous stress relaxation of a piperazine extended polyether with the structure



was much slower than that of an ethylene diamine extended polyether (see figure 4.15) which has the structure:



This again indicates the importance of the urethane hydrogen.

When gross degradation occurs many different products are formed; however, most of these result from the reaction of the simple products, already mentioned, with themselves or with other groups present in the polymer. The most complicated reaction products[205,206,211-216] appear only when the reaction is continued for a very long time or at a very high temperature and are hence, unlikely to play any part in the degradation processes that are measured by chemical stress relaxation (see section 1.4)

(5.4.1.2) Other Nitrogen Containing Links

In general, the thermal decomposition of the other nitrogen-containing links present in urethane elastomers leads to the production of the materials from which the links were formed.[1,2,198] Substituted ureas revert to an isocyanate and an amine, biurets to a substituted urea and an isocyanate, allophanates to urethane and an isocyanate, and isocyanate dimers to isocyanates.

Biurets and allophanates are both rather unstable, [1,198] the biuret being the slightly more stable, isocyanate dimers are moderately stable, although catalysts can bring about rapid degradation at low temperatures.

Substituted urea links are fairly stable [1,2,198] requiring temperatures of about 170°C to get an appropriate rate of dissociation. Isocyanate trimers are very stable to both heat and chemicals although they do decompose above 300°C giving a carbodiimide.

(5.4.1.3) Polyester and Polyether Segments

The thermal stability of the ester group is extremely high except at very high temperatures, in excess of 300°C, where some cracking to unsaturated compounds occurs. [1,198]

$$R - \overset{O}{\overset{\|}{C}} - O - (CH_2)_2 - R' \longrightarrow R - \overset{O}{\overset{\|}{C}} - OH + R - CH = CH_2$$

The formation of cyclic esters of low molecular weight has also been reported; [1] this may require the participation of terminal hydroxyl groups most of which will have been converted to urethane groups in this case.

Polyethers are much less stable than polyesters, they dissociate to give low molecular weight hydrocarbons, ketones, aldehydes and ethers. [1,198,217,218] The first step in this process is the scission of the C-O bond. [217,218]

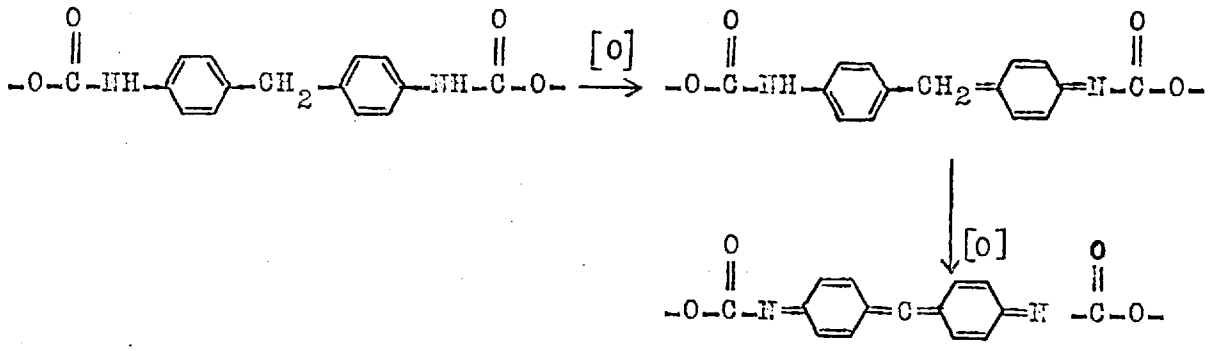
$$R - CH_2 - O - CH_2 - R \longrightarrow R\dot{C}H_2 + RCH_2 - O^{\cdot}$$

(5.4.2) The Thermooxidative Stability of Polyurethane Elastomers

(5.4.2.1) The Urethane Link

Urethane links are very stable to oxidation although Schollenberger [2,219,220] showed that in urethanes prepared from 4,4' diphenylmethane dissocyanate (MDI), oxidation in the presence of u.v. light led to the production of a quinone-imide structure

as follows:



This reaction presumably involves production of a free radical, $R\dot{N}COOR'$ followed by a rearrangement to form the stable structure shown above; because of this it is probably limited to materials that can undergo a stabilising rearrangement of this type.

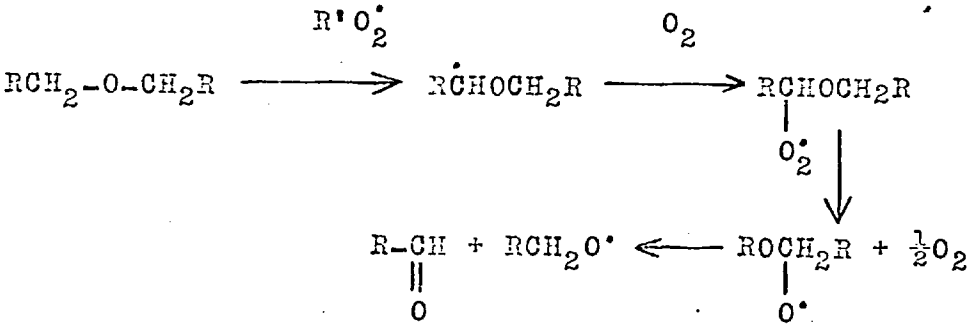
. . This reaction does not result in scission but it may interfere with the thermal decomposition of the urethane group discussed in section (5.4.1.1).

(5.4.2.2) Other Nitrogen Containing Links

Substituted urea, allophanate, biuret and isocyanate dimer and trimer links are not oxidatively unstable although some of the products of their thermal decomposition may undergo oxidation.[1]

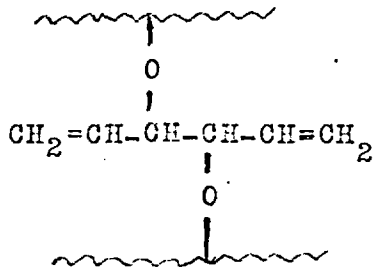
(5.4.2.3) Polyether and Polyester Segments

Polyethers are subject to fairly fast oxidation; the C-O bond undergoes cleavage by the following mechanism[1-3,198,217,218]



This oxidation of the ether linkage is considerably reduced when antioxidants are present.[217]

Polyesters are very stable to oxidation[142] unless unsaturated groups are present and the oxidation of polyethers is also increased when unsaturated. When the elastomer contains glycerine monoallyl ether (see section 5.2), the unsaturated nature of this group will result in an increased rate of oxidation. A peroxide cured sample will contain crosslinks with the structure



so that oxidation can lead to cleavage of the crosslink. Antioxidants will reduce the rate of oxidation of these unsaturated groups.

(5.4.3) The Hydrolytic Stability of Polyurethane Elastomers

(5.4.3.1) The Urethane Link

The urethane group is subject to hydrolytic cleavage[1,3,196] which is catalysed by both acids and bases. Saunders and Frisch[1] concluded that urethane hydrolysis took place less readily than ester hydrolysis.[221] This agreed with the work of Athey, who showed that the tensile strength of a polyester-urethane fell much more rapidly than that of a polyether-urethane when both were immersed in water at 50-70°C. The cure system used did not affect the rate of hydrolysis

However, the urethane link does undergo hydrolytic cleavage giving an amine and an alcohol under basic conditions and a mixture of products, such as amines, ureas, etc., under acid conditions.

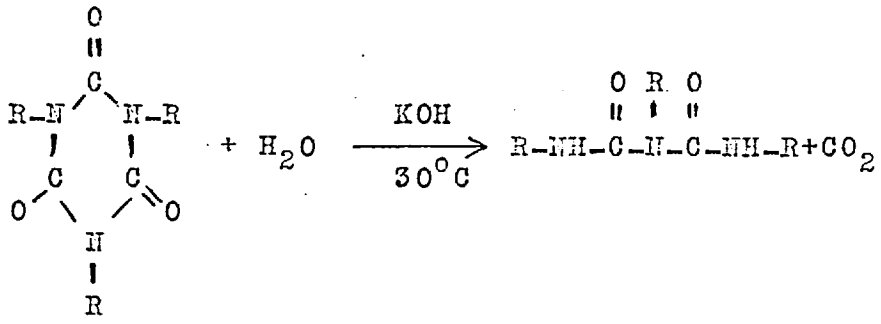
(5.4.3.2) Other Nitrogen Containing Links

There ~~is~~ are very little data on the hydrolysis of urea,

allophanate, biuret and isocyanate dimer and trimer links; the available experimental evidence is contradictory.[3] An early study indicated that biuret links were less stable than urethane.[221] Athey has shown that an amine cured polyether-urethane is less stable than a glycol cured material, indicating that the urea and biuret links are less stable than urethane.[222] However, Magnus has reported that amine cured polether-urethanes are more stable than glycol cured ones.

In any event, urea hydrolysis is known to be catalysed by both acids and bases.

Isocyanate trimers are fairly stable to hydrolysis but will react slowly to give a biuret linkage[198]

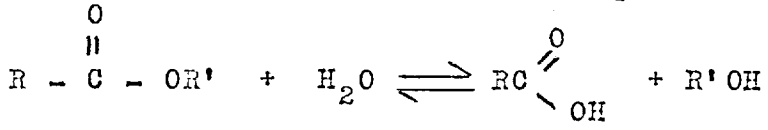


Isocyanate dimers react slowly with alcohols to give allophanates and if the same reaction occurs with water, a disubstituted urea will be formed.

(5.4.3.3) Polyester and Polyether Segments

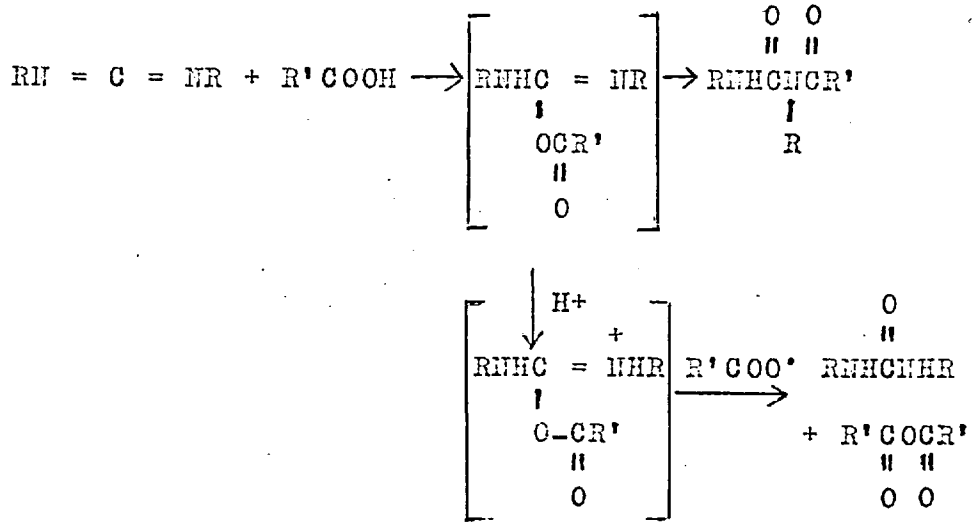
The polyether chain is resistant to hydrolysis and, in general, polyether-urethanes are much more resistant to hydrolysis than polyester-urethanes; this has prompted Athey and others to propose that the ester group is more susceptible to hydrolysis than the urethane group.

Ester hydrolysis is a very well known reaction that proceeds according to the following equation:[1,3,198]



This reaction is catalysed by both acids and bases.

In the case of an acid catalysed reaction the carboxylic acid produced in the reaction will further catalyse the decomposition reaction. To prevent this and reduce the rate of hydrolysis, carbodiimides have been added;[3] these act by neutralising the acid produced.[1,198]



Carbodiimides have not been entirely successful and have failed in long term weathering tests over water under ambient conditions where they acted as accelerators of degradation. This behaviour was thought to be due to the fungal attack of the samples where the carbodiimide was acting as a nutrient[3] and hence aided fungal growth. When fungal attack was excluded the carbodiimides reduced the rate of hydrolysis.

+ + + + + +

CHAPTER 6

THE CHARACTERISATION OF ADIPRENE CM AND GENTHANE S

(6.1) INTRODUCTION

To develop meaningful interpretations of the chemical stress relaxation data, it is important to characterise, fully, the materials under study.

It is apparent from section (3.3) that the network chain densities of the samples must be known in order to distinguish between crosslink and main chain cleavage. Apart from this, it is important to know the chemical composition and structure of the elastomers in order to identify likely sites for crosslinking or cleavage, and then to design experiments to establish which of these sites are responsible for the stress relaxation.

The results presented in this chapter are concerned with the characterisation both of the backbone polymer and the cured elastomer.

(6.2) THE MATERIALS USED

The two polymers used were commercially available materials that were supplied and cured by the Materials Department, Royal Aircraft Establishment, Farnborough, Hampshire. They were:

(i) Adiprene CM (E.I. du Pont de Nemours and Co.), a polyether based urethane prepared from poly (oxybutylene)glycol and a 2,4 and 2,6 isomer mixture of tolylene diisocyanate (TDI)[1,2,6] plus about 5 to 10% of glycerine monoallyl ether.

(ii) Genthane S (General Tyre and Rubber Co.), a polyester based urethane prepared from a glycol terminated 80:20 poly (ethylene/propylene adipate) and methylene-p, p-diphenyl diisocyanate (MDI)[1,2,6].

In both cases excess polyol was used to give a hydroxyl terminated polyurethane.

The two polymers were cured with dicumyl peroxide; four different peroxide concentrations were used; 1.0, 1.5, 2.0 and 2.5 pph gum. The samples were milled and then press cured for 30 minutes at 160°C.

(6.3) CHARACTERISATION OF THE UNCURED POLYMER

(6.3.1) The Chemical Composition

(6.3.1.1) Nuclear Magnetic Resonance Spectra

Deuterochloroform solutions of the two polymers were prepared and proton magnetic resonance spectra obtained using a Varian A 60, 60 MHz n.m.r. spectrometer. The spectra were obtained at ambient temperature (~30°C) and an internal reference compound, tetramethyl silane, was used to give a peak at $\delta = 0$ ($\tau = 10$); the spectra were electronically integrated.

The spectra and integrals are shown in figure (6.1)

The spectra could be interpreted in terms of the reported compositions (see section 6.2) of the polymer, except that the glycerine monoallyl ether, present in small amounts, could not be detected since it was masked by other peaks; the peak assignments are given in table (6.1).

The integrals (fig 6.1) were used to determine the relative molar concentrations of the various groups present; this is possible because the intensity of a peak is directly proportional to the number of protons responsible for it. The results of this calculation are shown in table (6.2).

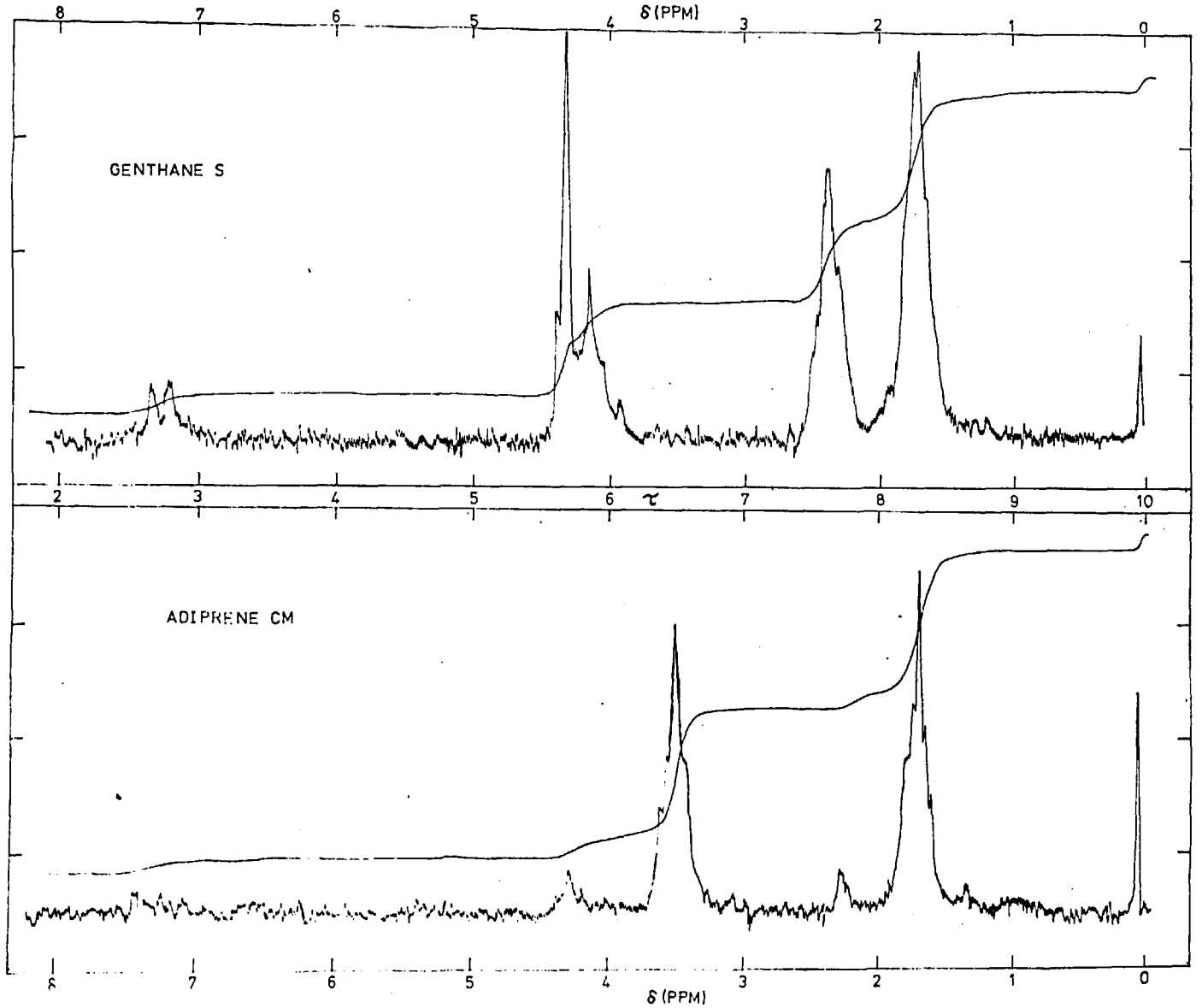
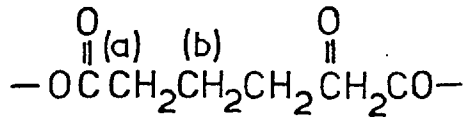
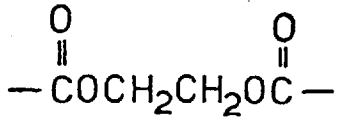
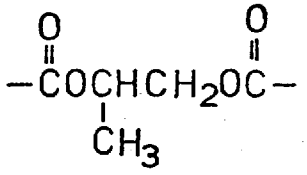
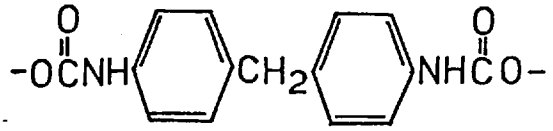


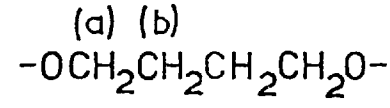
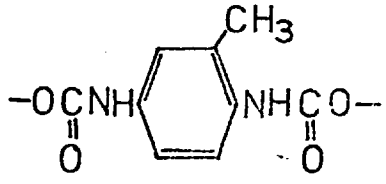
fig. 6-1 NUCLEAR MAGNETIC RESONANCE SPECTRA (PROTONS) OF $CDCl_3$ SOLUTIONS OF ADIPRENE CM AND GENTHANE S

TABLE 6·1

GENTHANE S

STRUCTURE	GROUP	δ (PPM)
	CH_2(a)	2·3
	CH_2(b)	1·6
	CH_2	4·2
	CH_3	1·3
	CH_2	4·2
	CH	4·7
	CH_2	3·9
	CH	7·1 & 7·3

ADIPRENE CM

STRUCTURE	GROUP	δ (PPM)
	CH_2(a)	3·6
	CH_2(b)	1·6
	CH_3	2·1
	CH	7·1 & 7·3

(6.3.1.2) Infra-Red Spectra

The infra-red spectra of chloroform solutions, and of films cast from chloroform solutions, were obtained for both polymers using a Perkin Elmer 157G spectrometer, a Perkin Elmer 457, a Perkin Elmer 257 and a Unicam SP200 were also used during this study.

The chloroform solution spectra were obtained in the usual way, using two matched cells, one containing the solution and the other containing pure solvent; the spectrometer then subtracted the solvent spectrum from the solution spectrum leaving the spectrum of the polymer. The chloroform had been distilled and dried over a molecular sieve type 4A; it was, hence, water and ethanol free as was confirmed by the absence of an OH peak in its infra red spectrum.

The film spectra used films, cast from chloroform solutions, on salt plates mounted in small teflon collars. The teflon collars fitted into a brass mount that fitted the cell mount of the spectrometer. This method had the advantage that films cast on the salt plates, mounted in the teflon collars could be heat aged and the spectrum of the same film taken repeatedly after different times of ageing.

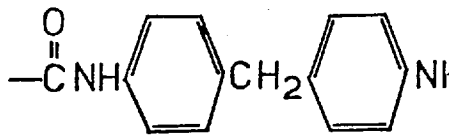
The spectra are shown in figs. 6.2 and 6.3, they confirmed the published structures of the polymers,[1,2,6,223] the assignments of the principal peaks being given in table (6.3)[1,2,3,198]

It is clear from a comparison of the solution and film spectra for each polymer that the NH peak at 3 microns changes. In the film this appears as a broad peak centred on 3 microns with a small shoulder at 2.9 microns. The solution spectra were slightly different; the NH band comprised a narrow, sharp

Table 6·2

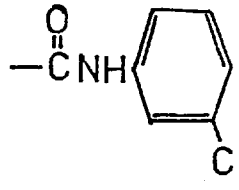
Chemical Composition of Urethane Polymers

Genthane S



to $-CHCH_2O-$ (with CH_3) to $-CH_2CH_2O-$ to $-C(=O)(CH_2)_4C(=O)O-$ is 18 to 65 to 118 to 165

Adiprene CM



to $-(CH_2)_4O-$ is 26 to 192

Table 6·3

Infra Red Band Assignments for Polyurethanes

Microns	Functional Group
2·94-3·13	-NH stretch (H-bonded)
2·86-2·94	-NH stretch (free)
3·3-3·7	-CH stretch
5·75-5·88	-C=O stretch (urethane)
5·71-5·83	-C=O stretch (ester)
6·20	C=C skeletal stretch of benzene ring
6·41-6·58	-NH deformation (Amide II band)
≈8·2	-C(=O)-O-C stretch of ester or urethane
≈9·3	-C-O-C stretch of aliphatic ether

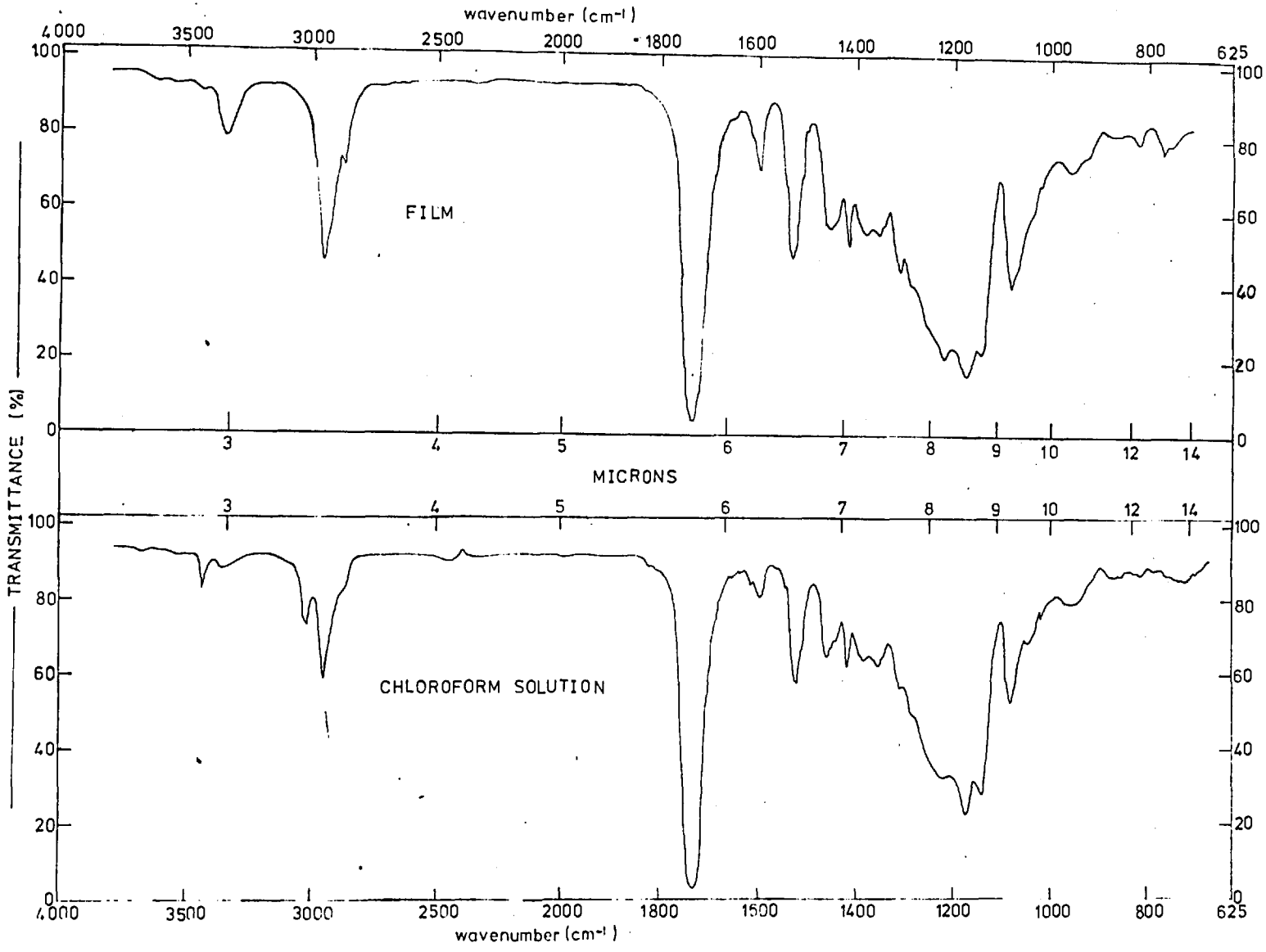


fig. 6·2 INFRA-RED SPECTRA OF GENTHANE S

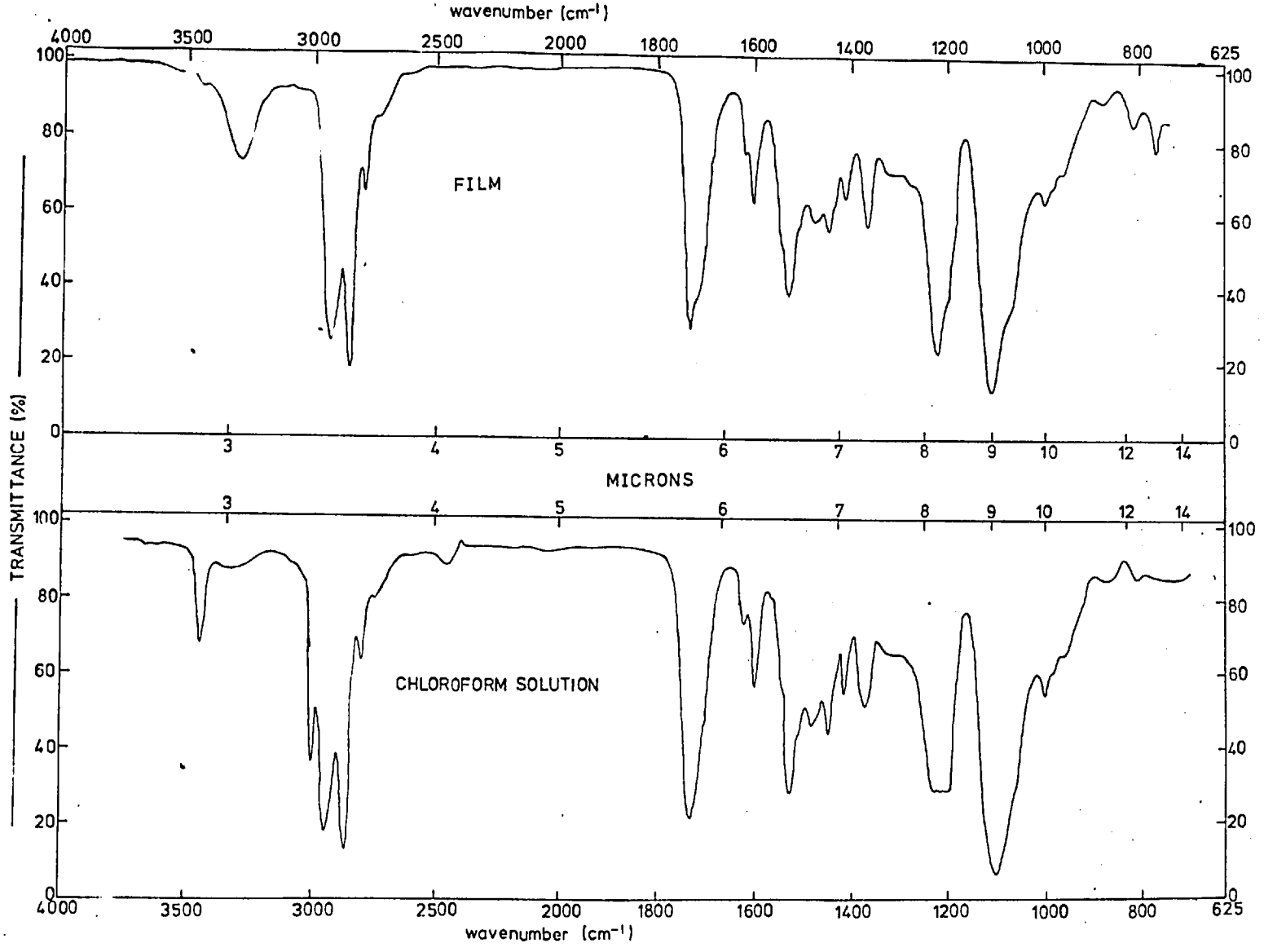


fig.6·3 INFRA-RED SPECTRA OF ADIPRENE CM

peak centred on 2.9 microns and a broad hump centred on 3 microns. This shift to higher frequency accompanied by peak sharpening on going from a film to a solution is typical of a system in which there is hydrogen bonding and indicates that hydrogen bonds involving the -NH group are present in these two polyurethanes. This observation is in agreement with the published work concerning polyurethanes.[1,3,202,203,204]

(6.3.2) Physical Characterisation

(6.3.2.1) Number Average Molecular Weight

Samples of Genthane S and Adiprene CM were sent to the "Polymer Supply and Characterisation" centre at Shawbury, Shrewsbury, (RAPRA) for analysis by membrane osmometry. The Osmometer used was a Melabs; tetrahydrofuran solutions of the polymers were used, the most concentrated being 5gl^{-1}. Measurements were made at 20°C using a regenerated cellulose membrane (W.A. Howe Hygrocella 11539).

Measurements were also made by J.H. Sexton, Polymer Characterisation Laborotory, Imperial College using a Mechrolab 502 membrane osmometer. Chloroform solutions of the two polymers were used, the most concentrated being 10gl^{-1}. 0.8 cellulose acetate membranes were used at 25°C, these membranes have been reported as suitable for use with chloroform, but were found to swell on prolonged immersion in chloroform, so that they had to be cut down to fit the osmometer.

The number average molecular weights obtained from these two studies are given in table (6.4); there is a considerable amount of difference between those obtained by RAPRA and those obtained at Imperial College.

TABLE 6.4

Number Average Molecular Weights of Genthane S and Adiprene CM

Origin of Data	Genthane S	Adiprene CM
$\bar{M}_n$ from Mecrolab ($\times 10^{-3}$)	92± 5	230 ± 30
$\bar{M}_n$ from Melabs ($\times 10^{-3}$)	31	140

The Imperial College results were based on four experiments for Adiprene CM and two experiments for Genthane S and were fairly reproducible as indicated by the spread of results. The large differences between the sets of results are difficult to explain, but it should be noted that RAPRA have reported[224] that their osmometer has consistently given good agreement with instruments in other laboratories, whilst the Imperial College instrument has been unreliable giving consistent, but inaccurate results for polystyrene standards.[225] In view of the difficulties regarding the membrane and osmometer used at Imperial College and the satisfactory nature of the RAPRA instrument, the results obtained by RAPRA would seem to be favoured.

(6.3.2.2) Molecular Weight Distribution

Samples of the two polymers were sent to the "Polymer Supply and Characterisation Centre" for analysis by Gel Permeation Chromatography.

(i) The Method of Gel Permeation Chromatography

Gel Permeation Chromatography is a method that separates molecules on the basis of their molecular size.[226-233] It utilises apparatus similar to that used for liquid chromatography except that the columns are filled with solvent swollen, crosslinked, polystyrene beads. The material under investigation is dissolved in a suitable solvent and introduced into the top of the column. Any molecules that are larger

than the maximum pore size of the polystyrene beads elute through the column via the interstitial volume. The remainder of the molecules will diffuse into the beads, the smallest penetrating furthest so that they elute last.

By using appropriate columns or combinations of columns polymers can be studied and a fairly accurate determination of their molecular size distributions obtained.[234]

For linear polymers these will be equal to their chain length distributions and hence to their molecular weight distributions.

(ii) Calibration for Gel Permeation Chromatography

The measured quantities[229,230] are the elution volume (i.e. the volume of solvent passing through the column between sample injection and elution) and the concentration of the eluting solution. In order to obtain chain length distributions the columns must be calibrated with well characterised and preferably monodisperse samples of the polymer under investigation (monodisperse samples are not usually available, so narrow molecular distribution samples are used[235]).

As this would severely limit the analytical use of GPC it has been suggested[230,234,235] that the columns should be calibrated for polystyrene (as narrow molecular weight distribution samples are readily available). A calibration curve of the extended length, in angstroms, of the polystyrene molecules against elution volume can then be constructed. If it is assumed that this calibration curve is universally correct,[227] chain length distributions may be determined.

Also, if the molecular weight per angstrom length of polymer is known, the molecular weight distribution can be calculated from the chain length distribution.

(iii) Evaluation of the Molecular Weight per Angstrom Length of Polymer

The molecular weight per angstrom length of polymer is usually denoted Q.

The number, weight and z average chain lengths and molecular weights are respectively An, $\bar{M}n$, Aw, $\bar{M}w$, Az and $\bar{M}z$ (An, Aw and Az can be obtained from the chain length distribution)[236]

By definition:

$$\bar{M}n = QAn$$

$$\bar{M}w = QAw$$

$$\bar{M}z = QAz$$

Q may be determined in several ways:

(a) By direct evaluation, based on a knowledge of the composition of the polymer and on known bond lengths and angles.[234,236,237]

(b) By the determination of the repeat distance of the polymer by X-ray diffraction analysis of crystalline samples.[236]

(c) By determining one or more of the molecular weight averages by another physical method[236] (e.g. light scattering, osmometry, viscometry etc.) whence:

$$Q = \bar{M}i/Ai$$

where i = n, w, z etc.

(iv) Gel Permeation Analysis of Adiprene CM and Genthane S

The apparatus used was supplied by Waters Associates and 0.25% solutions of Adiprene CM and Genthane S in tetrahydro-

furan were used. The column arrays were:

Column A: 1 x 4', 100-350Å; 700-2000Å; 5×10^3 - 1.5×10^4Å; 7×10^5 - 5×10^6Å

Column B: 1 x 4', 700-2000Å; 1.5×10^4 - 5×10^4Å; 7×10^5 - 5×10^6Å; 5×10^6 - 10^7Å

These mean that each array comprised four columns in series, each one being four feet long. The range of chain lengths, in angstroms, resolved by each column is given by the four sets of figures.

The average chain lengths obtained and the ratios An:Aw:Az are given in table (6.5); three sets of results were obtained.

Set 1: Results not entirely satisfactory because the peaks were rather small.

Set 2: Results were quite good for Genthane S but the sharp cut off on the high molecular weight side made the Adiprene CM results rather unsatisfactory.

Set 3: Different solutions were used and the experiments were done at least 6 weeks after those for sets 1 and 2. The Genthane S results were quite good but the Adiprene CM did not seem to be entirely soluble and some gel was filtered off.

Genthane S: The best value probably lies between those of sets 2 and 3 but nearer to set 2.

Adiprene CM: The best value probably lies between sets 1 and 2 but nearer to set 1.

It should be noted that

$$\bar{M}n : \bar{M}w : \bar{M}z = An : Aw : Az$$

To obtain $\bar{M}n$, $\bar{M}w$ and $\bar{M}z$ it is necessary to evaluate Q; of the methods outlined earlier, methods (a) and (c) were used.

The evaluation of Q by method (a) utilised the chemical compositions of the polymers obtained from the n.m.r. data (section 6.3.1.1), and bond lengths and angles obtained from reference 237 . The calculation of the extended lengths of the various groups that comprise the polymers is illustrated in figure 6.4 and the Q values obtained are given in table (6.6).

The Q values determined by method (c) were obtained from the number average molecular weight evaluated by osmometry; these Q values are also given in table (6.6).

The average chain lengths and the An : Aw : Az values are given in table (6.5). The molecular weight averages other than the number average were calculated using the Q values calculated by method (c); these are given in table (6.7). It is clear from tables (6.5) and (6.7) that reasonably consistent results were obtained. The discrepancy between the Q values obtained by methods (a) and (c) shows that the urethane polymers behave differently in solution from polystyrene; the state of coiling is probably different because of the strongly polar nature of the urethanes.

The An : Aw : Az values (table 6.5) indicate that the molecular weight distributions of both polymers are broad, Adiprene CM having a broader distribution, than Genthane S.

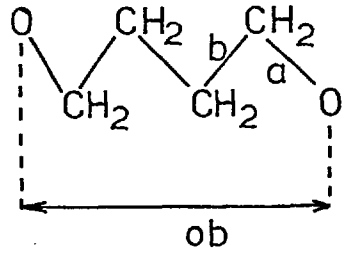
Figure 6·4

Extended Length Calculation

a = 1·46 Å b = 1·54 Å c = 1·52 Å d = 1·36 Å e = 1·33 Å f = 2·8 Å

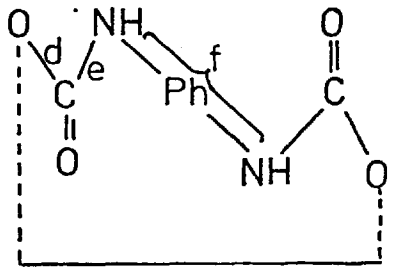
$\hat{ab}$ = 113° $\hat{ac}$ = $\hat{cd}$ = 114° $\hat{de}$ = 118·5° $\hat{ef}$ = 124° $\hat{ff}$ = 119°

Adiprene CM



ob = 6·23 Å

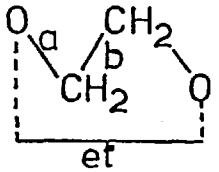
mol. wt. = 72



td = 9·55 Å

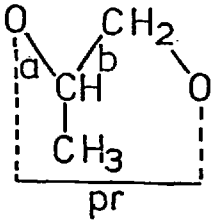
mol. wt. = 192

Genthane S



et = 3·73 Å

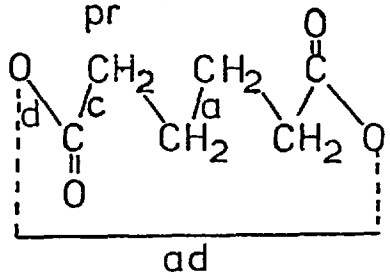
mol. wt. = 44



pr = 3·73 Å

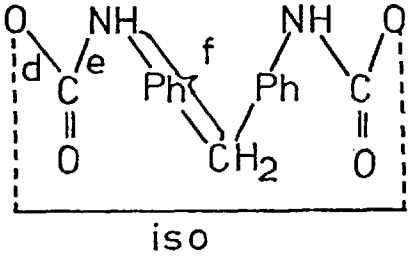
pr* = 4·98 (see pg.)

mol. wt. = 58



ad = 8·59 Å

mol. wt. = 128



iso = 14·5 Å

mol. wt. = 268

TABLE 6.5

G.P.C. Results for Adiprene CM and Genthane S

Average Chain Lengths x 10^{-3} etc.	Genthane S	Adiprene CM	Column Array	Set
An	1.69	2.20	B	1
Aw	3.99	10.2		
Az	12.6	35.0		
An:Aw:Az	1:2.36:7.46	1:4.64:15.91		
An	1.34	2.34	A	2
Aw	3.22	20.2		
Az	7.72	937		
An:Aw:Az	1:2.41:5.78	1:8.64:40.1		
An	1.05	3.18	B	3
Aw	2.88	19.7		
Az	6.04	91.1		
An:Aw:Az	1:2.75:5.75	1:6.20:28.6		

TABLE 6.6

A Comparison of Q Values Calculated by Different Methods

Polymer	Q estimated from bond angles and lengths	Q estimated from Melabs $\bar{M}n$		
Genthane S	14.8 (Q^x = 14.3)	18.34	23.13	29.52
Adiprene CM	13.02	63.6	59.3	44.0

pr^x and Q^x were calculated for a 1,3 propylene glycol as it was suggested that pendant methyl groups behave like in-chain methylene groups.

TABLE 6.7

Molecular Weight Averages Calculated from G.P.C. Data

Average Molecular Weight	Genthane S	Adiprene CM	Set
x 10^{-3}			
$\bar{M}n$	31*	140*	
$\bar{M}w$	73	653	1
$\bar{M}z$	231	1240	
$\bar{M}n$	31*	140*	
$\bar{M}w$	74	1192	2
$\bar{M}z$	178	56400t	
$\bar{M}n$	31*	140*	
$\bar{M}w$	86	880	3
$\bar{M}z$	177	1276	

* Values obtained from osmometry

t probably incorrect because of column array used

(6.3.2.3) Glass Transition Temperatures and Densities

A Du Pont differential thermal analyser was used to determine the glass transition temperatures of the two polymers, which were - 57.5°C for Adiprene CM and - 46°C for Genthane S. The reference thermocouple was immersed in glass beads and a heating rate of 10°C/min was used.

The densities of the polymers were found to be 0.973 g cm^{-3} for Adiprene CM and 1.143 g cm^{-3} for Genthane S.

(6.3.2.4) Solubility

Several of the experiments described in the previous three sections required solutions of the polymers. This meant that suitable solvents for the materials were needed and a large number of solvents were investigated. Solvents were rapidly screened by placing small pieces of polymer in a few ml of solvent in a stoppered bottle. The polymer was left for several days at ambient temperature to dissolve and then checked several times at intervals of about 24 hours. The solvents were then classified into one of the four following groups:

A = Complete dissolution of polymer in solvent

B = Partial dissolution; the polymer was swollen by the solvent which became coloured by the polymer or slightly more viscous indicating that some material had dissolved.

C = The polymer was swollen moderately by the solvent but the dissolution of material was not apparent.

D = Little or no swelling occured

The results of these experiments are presented in tables (6.8) and (6.9).

TABLE 6.8

Solubility of Adiprene CM

A	B	C	D
Tetrahydro-furan	Toluene	Carbon Tetra-chloride	2,3,4 Tri-methylpentane
Dioxan	Benzene	Methyl Formate	Nitromethane
Proprio-phenone	Ethyl Acetate	Tetrachloro-ethylene	Cyclohexane
Mesityl Oxide	Styrene	Dimethyl Sulphoxide	Water
Bromobenzene	Methyl Meth-acrylate	Vinyl Acetate	Glycerol
Dichloro-methane	Acetone	n-Propanol	i-Propanol
Chloroform	Chloro-benzene	n-Butanol	n-Heptane
Pyridine	n-Propyl Formate	n-Pentanol	sec-Butanol
Chloral	1,1,1 tri-chloro-ethane	Napthyl-Isocyanate	Cyclohexanol
Ethyl Methyl Ketone	Dimethyl Formamide	Nitrobenzene	Butyl Phthalate
α-Methyl Benzylamine	Cyclopenta-none	i-Butanol	
Butryophenone	i-Propyl Acetate	Phenyl Acetate	
n-Butylamine	Cyclohexano	Tetrachloro-ethane	
n-Octylamine		Tricresyl-phosphate	
Divinyl Benzene		Piperidine	
Dichloro-ethane		Aniline	
1,2 epoxypro-pane		n-Propyl Chloride	
Acetic acid		m-Cresol	
Trichloro-ethylene			

TABLE 6.9

Solubility of Genthane S

A	B	C	D
Methyl Acetate	n-Butyl Acetate	n-Amyl Acetate	Cumene
Ethyl Acetate	Benzene	Toluene	n-Hexadecane
n-Propyl Acetate	Dimethyl-sulphoxide	Ethyl Benzene	2,2,4-trimethyl-pentane
Methyl Formate	Styrene	Xylene	Water
Ethyl Formate	Acetic Acid	Divinyl Benzene	Ethanol
Ethyl Acrylate	Phenyl Acetate	Carbon Tetra-chloride	Methanol
Bromobenzene	Aniline	1,4-Divinyl-oxy butane	Carbon di-sulphide
Dichloromethane	Chlorobenzene	Napthyl Iso-cyanate	Diethyl ether
Nitromethane	Nitrobenzene	Tricresyl Phosphate	n-Octyalde-hyde
Ethyl Methyl Ketone	Piperidine	m-Cresol	Didecyl-phthalate
Chloral	1,1,1-tri-chloroethane	Cyclohexane	n-heptane
α-Methyl Benzylamine		i-Propyl Acetate	Amyl alcohol
Mesityl Oxide		n-Propyl Chloride	n-Butanol
Butryophenone			i-Propanol
Propriophenone			n-Propanol
2-Methoxy-ethanol			Glycerol
n-Butylamine			sec-Butanol
Acetone			Tetrachloro-ethylene
Vinyl Acetate			iso-Butanol
Methyl Methacrylate			Cyclohexanol
Dimethyl Formamide			Butylphthalate
1,2-epoxy-propane			
1,2-dichloro-ethane			
n-Propyl Formate			
Trichloro-ethylene			
Cyclopentanone			
Chloroform			
Tetrahydro-furan			
Dioxan			

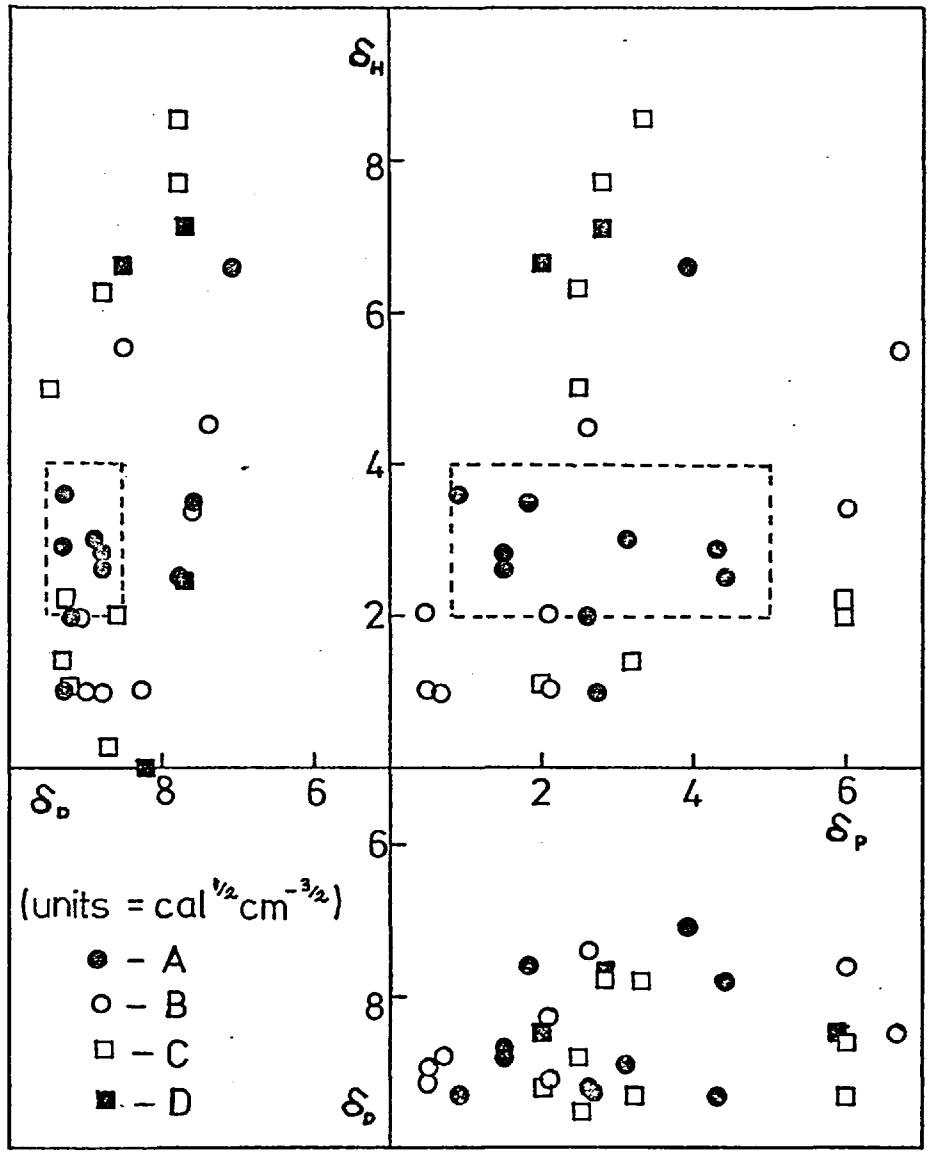


figure 6·5: Solubility data for Adiprene CM.

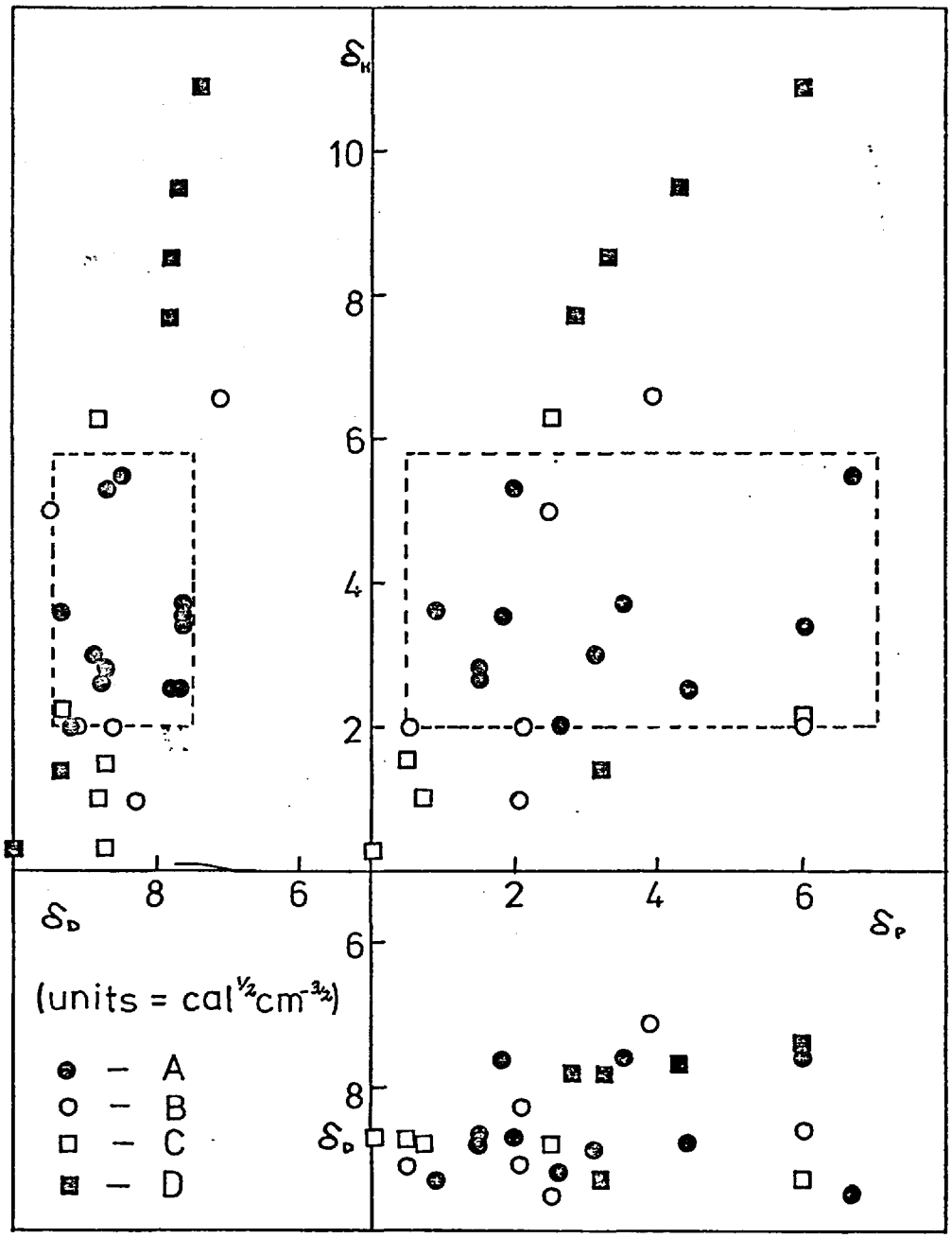


figure 6·6: Solubility data for Genthane S

Whilst these experiments were done to find solvents for the polymer, the results can be interpreted in terms of the solubility parameters of solvent and polymer. The data can be plotted in the way proposed by Beerbower and Dickey[14] when the solubility parameter is split into three components δ_P, δ_H and δ_D.

The maximum solubility will occur when the three component solubility parameters of the solvent are equal to those of the polymer. To determine the required information a four dimensional plot must be made involving δ_D, δ_P, δ_H and solubility; this can be reduced to a three dimensional plot by classifying solvents into a number of groups[14], each group representing a range of solubilities, as has been done in this study. If each group is represented by a different symbol and the data plotted as three projections of δ_D, δ_P, δ_H space, then there will be regions in the three resultant plots (i.e. δ_D vs δ_P, δ_P vs δ_H and δ_D vs δ_H) in which the majority of the good solvents lie. Plots have been constructed for both Adiprene CM and Genthane S and regions containing solvents in which the polymer is soluble can be discerned in the δ_D vs δ_H and δ_H vs δ_P plots; this cannot however be done in the δ_P vs δ_D plots. The regions identified in the δ_D vs δ_H and δ_H vs δ_P plots are centred on a point ($\delta_D = 9.0$, $\delta_H = 3.0$, $\delta_P = 3.0$) for Adiprene CM and ($\delta_D = 9.5$, $\delta_H = 3.9$, $\delta_P = 3.2$) for Genthane S, this implies that the overall δ values will be $10.0(\text{cal cm}^{-3})^{\frac{1}{2}}$ for Adiprene CM and $10.8(\text{cal cm}^{-3})^{\frac{1}{2}}$ for Genthane S. Although these values are of qualitative interest only, the plots (figs. 6.5 and 6.6) are quite useful since any solvent that

falls within the dotted region in the δ_D vs δ_H and δ_H vs δ_P plots is very likely to be a good solvent for the polymer, so that, were further solvents required, the search for them could be eased by restricting attention to those that lie within these regions.

In addition the δ_H values obtained for the two polymers are quite large as would be expected for a system in which there is hydrogen bonding.

(6.4) CHARACTERISATION OF THE CURED ELASTOMER

(6.4.1) The Swelling of the Elastomers in Solvents

Swelling measurements were made on the elastomers in a more quantitative manner than that used to investigate the solubility of the polymers (section 6.3.3.4).

Small pieces of thin rubber sheet weighing about 0.1 g were accurately weighed and placed in stoppered bottles containing enough solvent to immerse the sample. The bottles were placed in a thermostatically controlled water bath at 25°C. The samples were left for several days to equilibrate and then removed from the bottles, surface dried and quickly weighed. Several weighings were made on each sample, 24 hours being allowed between each and the procedure continued until constant weights were obtained; this ensured that equilibrium had been reached.

The sample was then placed in a glass vessel which was evacuated to remove the solvent, the sample was removed and weighed again. This final weight was generally very close to the initial weight of the sample before it had been swollen as the samples had all been extracted with a benzene/cyclohexane

TABLE 6.10

The Swelling of Gonthane S in Various Solvents

Solvent	Volume Fraction of Rubber in Swollen Sample, ϕ_2			
	2.5% DCP in cure	2.0% DCP in cure	1.5% DCP in cure	1.0% DCP in cure
Methyl Acetate	0.23	-	-	-
Ethyl Acetate	0.35	0.31	0.28	0.19
n-Propyl Acetate	0.40	-	-	-
n-Butyl Acetate	0.48	-	-	-
n-Amyl Acetate	0.55	-	-	-
Methyl Formate	0.33	-	-	-
Ethyl Formate	0.30	-	-	-
Cyclohexane	0.88	0.88	0.85	0.83
Toluene	0.49	-	-	-
Methanol	0.81	-	-	-
Ethanol	0.83	-	-	-
Propan-1-ol	0.82	-	-	-
Propan-2-ol	0.84	-	-	-
Butan-1-ol	0.86	-	-	-
Pentan-1-ol	0.87	-	-	-
Glycerol	0.98	-	-	-
Water	0.96	-	-	-
Chloroform	0.13	0.12	0.09	0.07

TABLE 6.11

The Swelling of Adiprene CM in Various Solvents

Solvent	Volume Fraction of Rubber in Swollen Sample, ϕ_2			
	2.5% DCP in cure	2.0% DCP in cure	1.5% DCP in cure	1.0% DCP in cure
Toluene	0.35	0.32	-	-
Benzene	0.34	0.29	0.28	0.26
Cyclohexane	0.71	0.68	0.67	0.64
Carbon Tetrachloride	0.38	0.33	0.30	0.25
Chloroform	0.21	0.21	0.20	0.17
Carbon Disulphide	0.40	0.37	0.34	0.32
Acetone	0.47	0.43	0.41	0.40
Ethyl Methyl Ketone	0.38	-	0.30	0.24
Pyridine	-	0.18	-	-
Tetrahydrofuran	-	0.22	-	0.17
Dioxan	-	0.22	-	-
Methyl Formate	0.58	-	-	-
Methyl Acetate	0.46	-	-	-
Ethyl Formate	0.35	-	-	-
Ethyl Acetate	0.42	-	0.31	-
n-Propyl Acetate	0.51	-	-	-
n-Butyl Acetate	0.39	-	-	-
n-Amyl Acetate	0.36	-	-	-
Ethanol	0.59	0.57	0.55	0.54

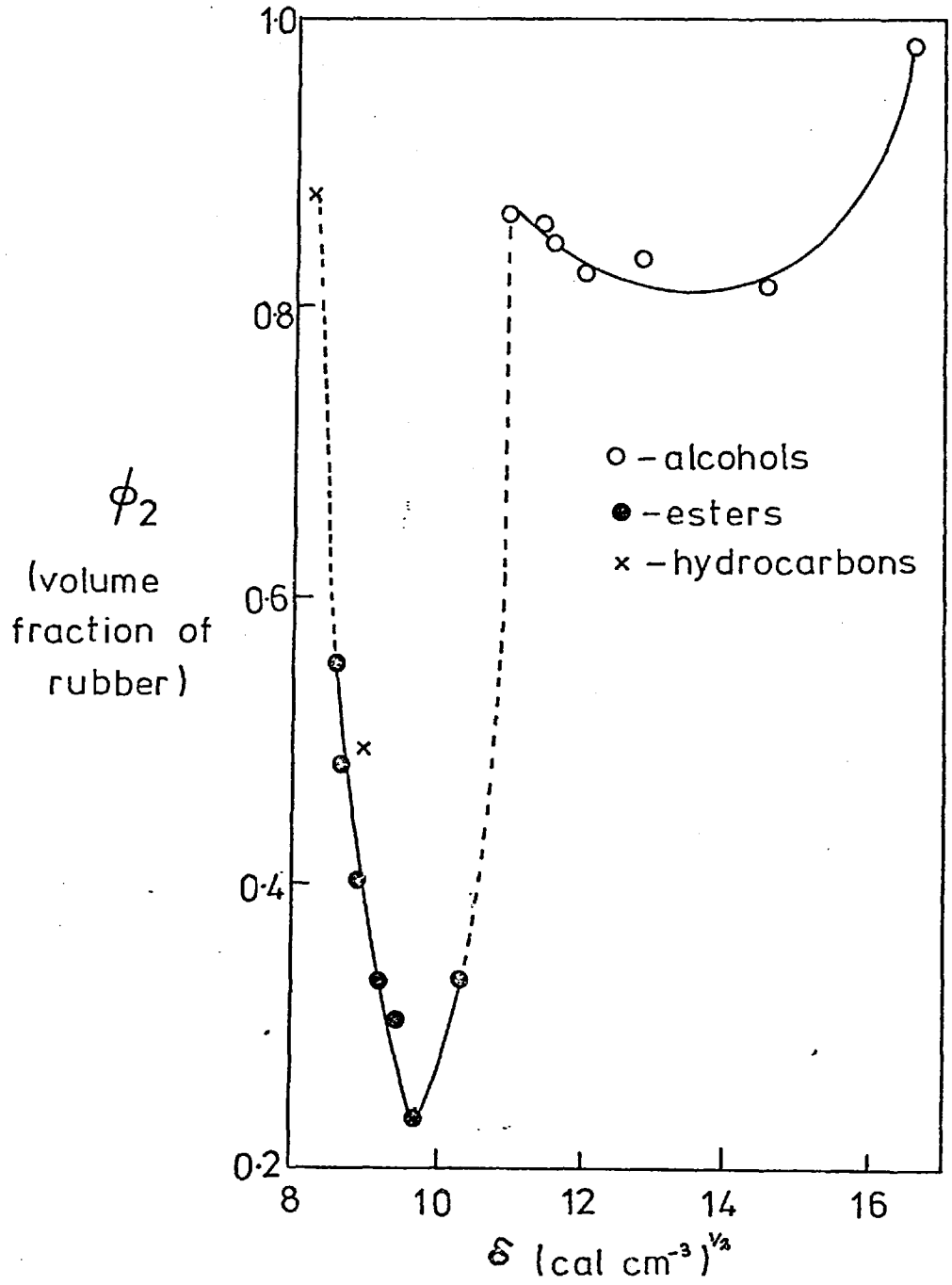


figure 6·7: Plot of ϕ_2 vs δ for Genthane S

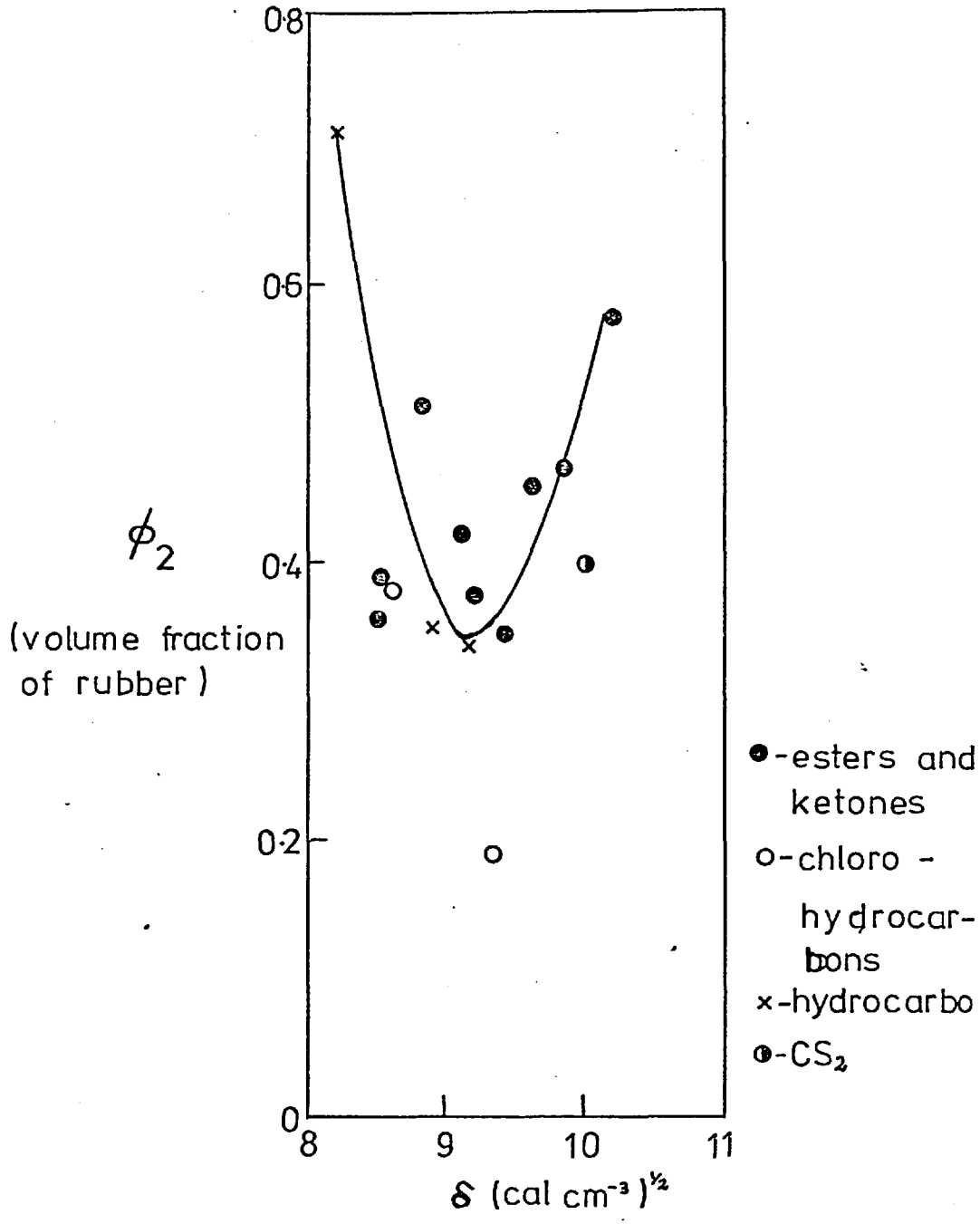


figure 6·8: Plot of ϕ_2 vs δ for Adiprene CM

mixture in a soxlet extractor to remove residual cure ingredients and any low molecular weight material not joined to the network.

The swelling of the elastomers was characterised by the volume fraction of rubber in the swollen sample, ϕ_2, and the results are summarised in tables (6.10) and (6.11).

The swelling data can also be used to investigate the solubility parameters of the elastomers; there was insufficient data to apply the method of Beerbower and Dickey[14] and so the more usual method of plotting the degree of swelling against the overall δ values of the solvents was employed.[47,48,49] These plots are shown in figs. (6.7) and (6.8); the δ values obtained were 9.2 $(\text{cal cm}^{-3})^{\frac{1}{2}}$ for Adiprene CM and 9.6 $(\text{cal cm}^{-3})^{\frac{1}{2}}$ for Genthane S which are both smaller than those obtained in section 6.3.2.4. However, in view of the nature of the correlation and the experiments there is reasonable agreement between the two sets of values and in both cases the Genthane S value is greater than that of Adiprene CM.

(6.4.2) The Stress-Strain Properties of the Elastomers in Simple Elongation

(6.4.2.1) An Apparatus for Measuring the Tensile Properties of Dry and Swollen Elastomer Samples

The apparatus is illustrated in fig. 6.9, it consists essentially of a force measuring unit and a means of extending the rubber sample which is in the form of a long thin strip. The force measuring unit or transducer and spring assembly is shown in more detail in fig. 6.10.

The sample is held at one end by the bottom clamp (15), the other end is held in a similar clamp that slots into the

block (21) of the transducer and spring assembly. Extension of the sample is accomplished by moving the whole transducer and spring assembly in a slot formed by the main spars of the apparatus, (11) and (22).

Movement of the transducer and spring is achieved by rotating a threaded rod (25); as the hole in the transducer and spring assembly, through which this rod passes, is threaded, rotation of the rod raises or lowers the transducer and spring assembly. The threaded rod is turned by rotating the knob (1) at the top end of it.

The length of the sample is obtained by measuring the distance between indian ink marks on the rubber with a travelling microscope.

The transducer and spring assembly contains a flat cross shaped phospher-bronze spring (29) that is tightly clamped at the four ends of the cross. The force is applied to the centre of the spring via the rod (32), this causes the centre of the spring to be displaced by an amount that depends on the size of the force. This displacement is measured by an electrical transducer capable of measuring displacements of up to ± 0.010 inch. The transducer is a linear variable differential transformer (LVDT), Schaevitz type 010 MS-LT, which gives an a.c. output and requires a low voltage, high frequency a.c. input (e.g. 3 volts at 1 kHz); the a.c. excitation and the conversion of the a.c. output to a d.c. output was effected by a Sangamo C52 transducer meter. The d.c. output was measured on a voltmeter incorporated into the transducer meter.

The output of the transducer can be "backed off" to zero using the controls on the transducer meter, provided the transducer is near to its mechanical zero. Mechanical zero is

achieved when the core of the transducer is positioned inside it so as to give zero electrical output; the core is attached to the top of rod (32). To allow the transducer to be mechanically zeroed there is a micrometer adjustment (30) which allows the body of the transducer to be moved up and down without affecting the position of the core. When a force is applied the spring is displaced, this causes movement of the core away from its zero position resulting in an electrical signal, whose magnitude depends on the distance moved by the core.

The apparatus is used with a load of about 120g (20) permanently on the spring. Overdisplacement of the spring, likely to cause damage can be prevented by two guard rings, (31) and (35), that can be set with the aid of a travelling microscope.

The transducer and spring assembly was calibrated by placing weights in a small load pan suspended from the top sample clamp. Typical calibration curves, that is plots of load vs reading on the voltmeter of the transducer meter, are shown in fig. 6.11.

It is clear from fig. 6.11 that calibration curves can be of two types, either convex with respect to the load axis or S shaped. This is because it is very difficult to get the spring into its holder so that it is perfectly flat; it will generally be slightly bowed as shown in fig. 6.12. If bowed as in fig. 6.12(a) an S shaped curve will be obtained whilst if bowed as in fig. 6.12(b) a curve that is convex with respect to the load axis results.

The entire apparatus fits inside a glass jacket, (9) and (14), shown in fig. 6.13. The glass jacket has a side-arm

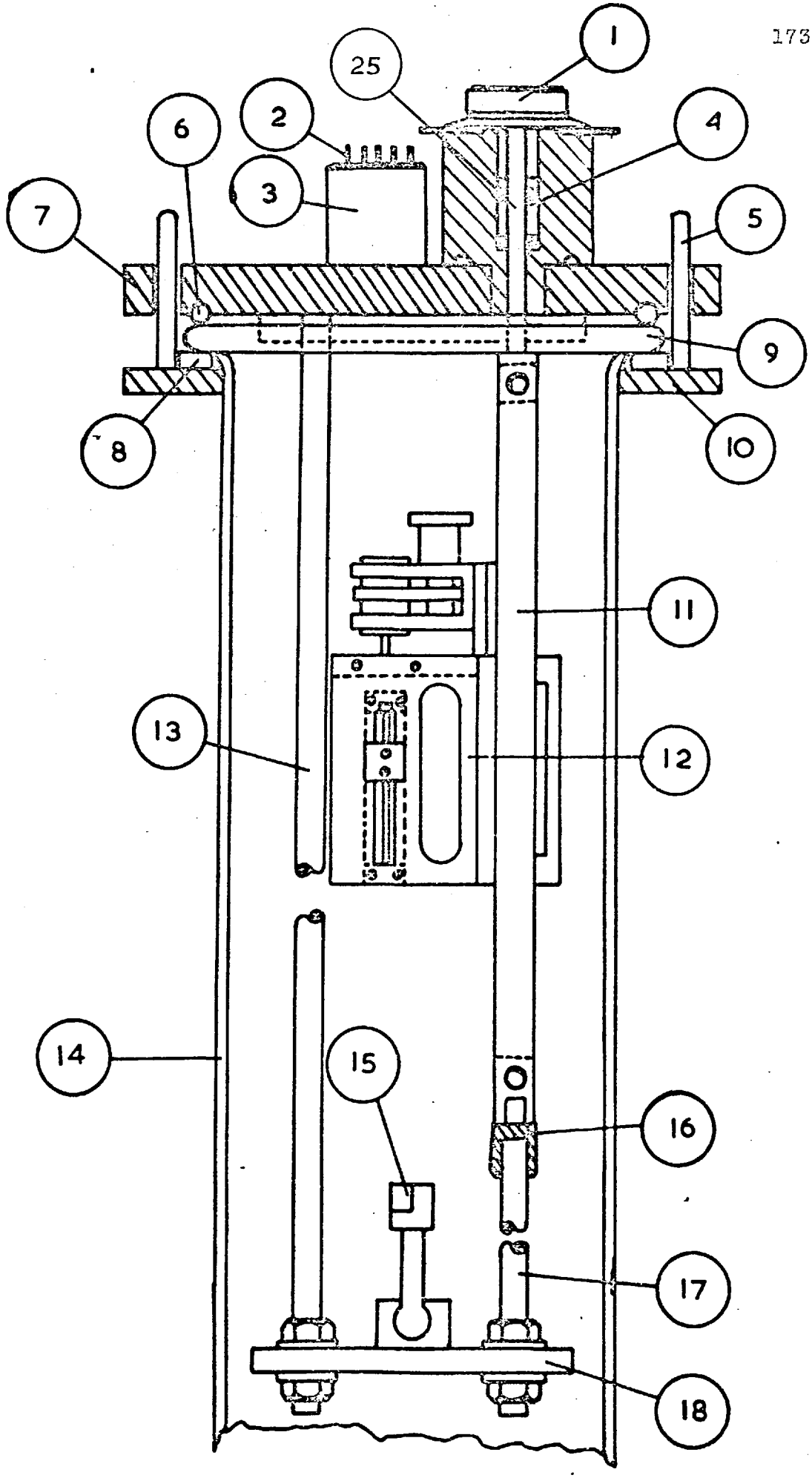


fig.6-9: TENSILE STRESS-STRAIN APPARATUS

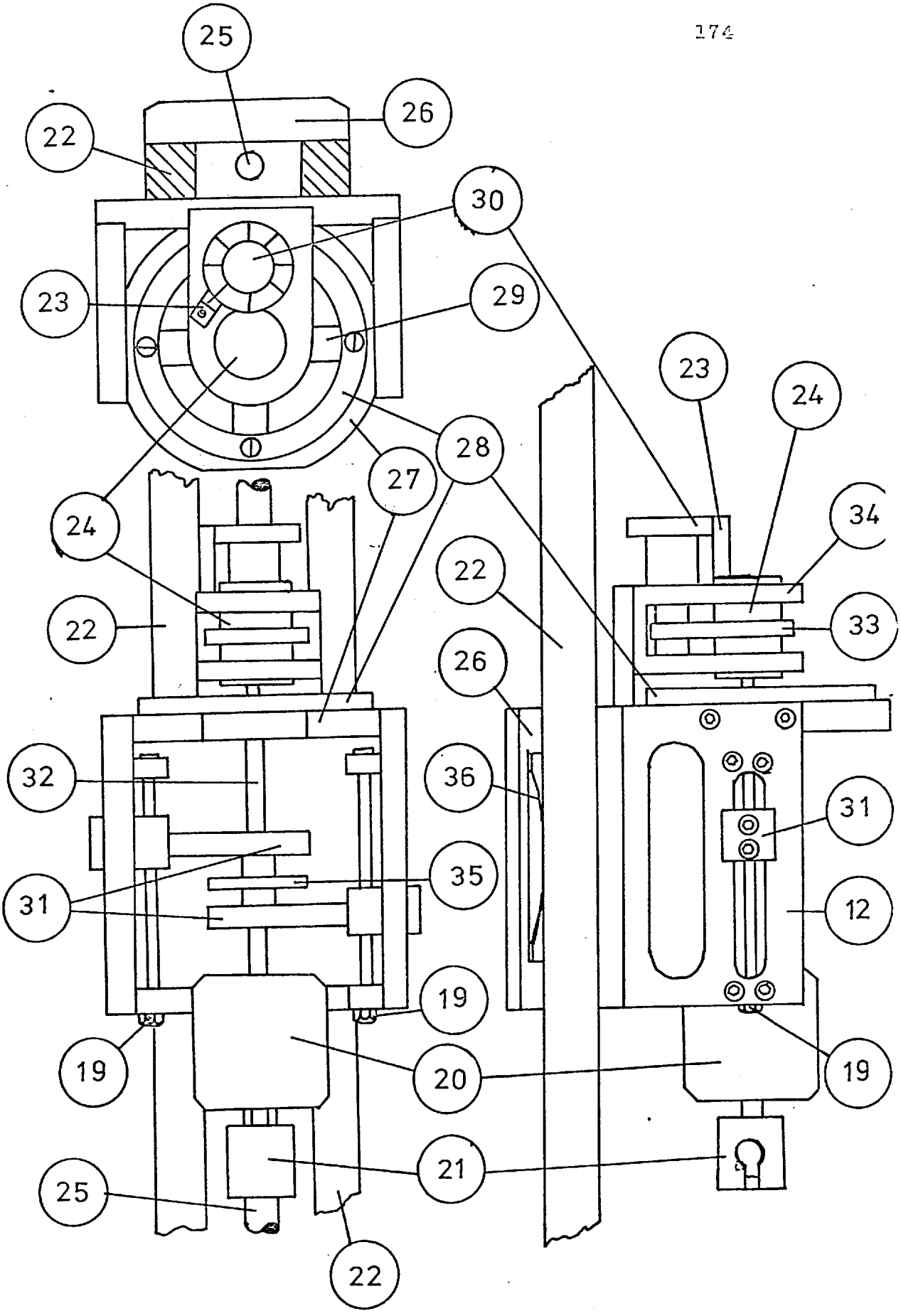


fig. 6-10:
DETAILS OF TRANSDUCER AND SPRING ASSEMBLY

Key to Figures 6.9 and 6.10

1 Drive shaft knob
2 Metal/glass lead outs for electrical connections
3 Chimney mount for 2
4 O-ring vacuum seal
5 Threaded studs
6 O-ring
7 Top plate of apparatus
8 Rubber seat
9 Ground lip of glass jacket
10 Ring to allow glass jacket to be clamped in place
11 Main spars of apparatus that form the slot in which the transducer and spring assembly moves
12 Transducer and spring assembly
13 Supporting spars
14 Glass jacket
15 Bottom sample clamp (sandwich type)
16 End of square section spars 11
17 Circular section supporting spars
18 Bottom plate of apparatus
19 Knobs that wind the guard rings, (31) up and down
20 Starting load on spring (about 120 g)
21 Block that holds top sample clamp
22 Main spars of apparatus (no. 11 in fig. 6.9)
23 Line to indicate position of 30
24 Transducer holder
25 Threaded rod on which whole assembly moves
26 Back plate
27 Block on which spring is mounted
28 Top retaining ring for spring
29 Phosphor bronze spring
30 Knob for micrometer transducer adjustment
31 Guard rings to prevent overstraining of spring
32 Pull rod, connects sample through to the spring
33 Transducer holder mount
34 Bracket holding transducer adjuster
35 Stop, used with 31 to prevent overstraining of spring
36 Spring

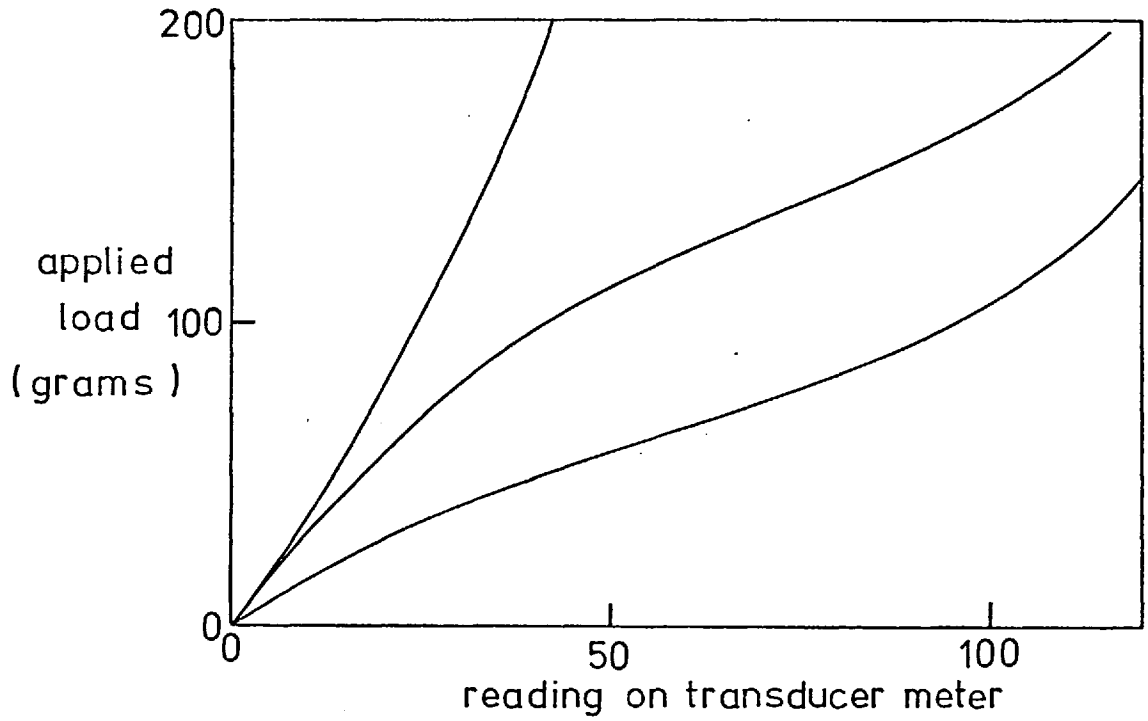


figure 6·11: Calibration curves for transducer and spring assembly

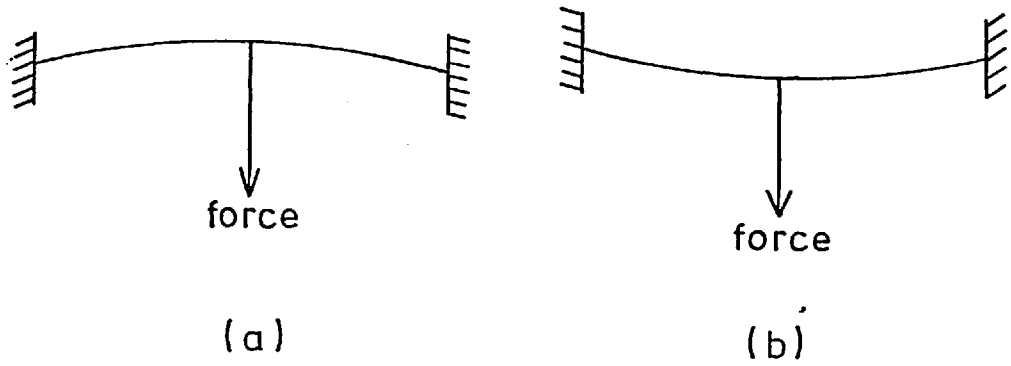
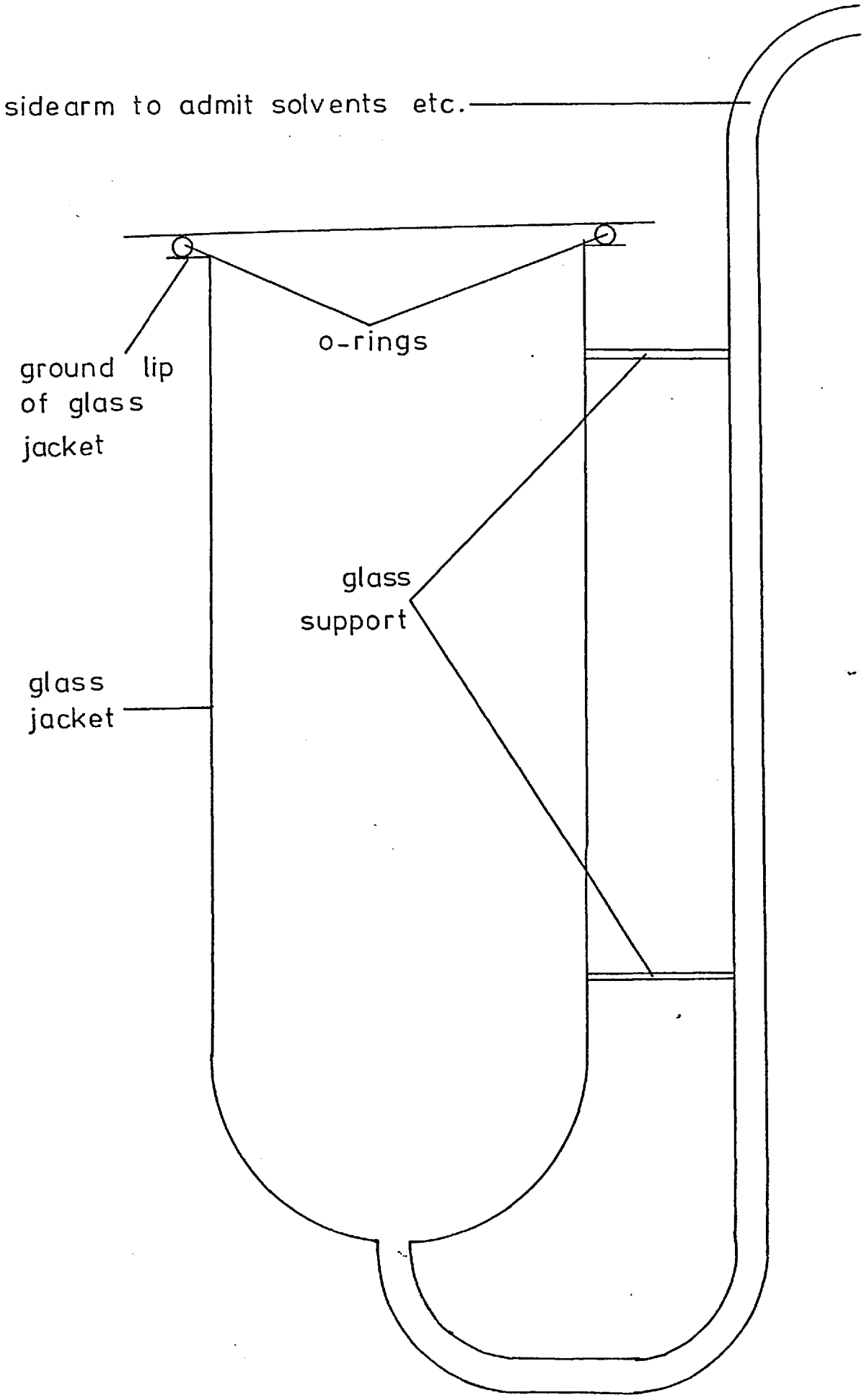


figure 6·12: Sectional view of spring showing its two positions

figure 6·13: Glass jacket for apparatus



through which solvents can be admitted so that experiments can be done on samples that are swollen and immersed in a solvent. When doing these experiments highly degreasing solvents should be avoided whenever possible.

The assembled apparatus, complete with glass jacket, is placed in a glass sided, thermostatically controlled water bath ready for use. It is important that the apparatus should be mounted vertically in the tank, otherwise the calibration will alter. This was accomplished by a three point levelling device used in conjunction with a spirit level, the device being connected to the apparatus by two steel rods screwed into the top plate (7).

(6.4.2.2) The Tensile Properties of Adiprene CM and Genthane S

Stress-strain measurements in simple elongation were made on both elastomers in the dry state or swollen in a suitable solvent. For Adiprene CM two sets of experiments were made on dry samples. In the first set the sample was extended and the force exerted by the sample and the sample length measured. The sample was then extended further and the process repeated. This procedure was repeated until sufficient points were obtained; in this experiment the sample was continuously loaded.

In the second set of experiments the sample was extended and the force and length measured, the sample was then retracted and allowed to recover for 10 minutes. The procedure was then repeated using different extensions until sufficient points were obtained; in this experiment the sample was intermittently loaded.

Since the elastic behaviour of dry rubber networks is time dependent, see section (2.5.3)[106], it is standard practice to wait for the same length of time between extending a sample and measuring its force; in all these experiments a time interval of 5 minutes was used.

To interpret these measurements in terms of any of the equations discussed in Chapter 2, the extension ratio , λ, is required which means that both l and l_0, the deformed and undeformed lengths of the sample, must be known. l was measured with a travelling microscope during the stress-strain experiment and l_0 was obtained by extrapolating the l vs force curve to zero force.

It can be shown that a small error in l_0 has a profound effect on $(\lambda - \lambda^{-2})$ that is most pronounced at λ values close to unity; errors may well arise in the evaluation of l_0 simply because it does involve extrapolation. Because of these difficulties a computer programme was written in which l_0 was allowed to vary by a small amount on either side of the extrapolated value. The programme then selected the l_0 value that gave the best fix to either the Kinetic Theory or the Mooney-Rivlin Equation; this l_0 value was always very close to the extrapolated value. Since an error in l_0 has a larger effect on $(\lambda - \lambda^{-2})$ as λ approaches unity, a weighting scheme was used that gave the greatest weighting to λ values further removed from unity. The computer programme is presented in Appendix C.

The other parameters required were the volume fraction of rubber in the swollen sample (unity for a dry sample), the width and thickness of the sample. The volume fraction was measured in the way described in section 6.4.1, the width was

measured with a travelling microscope and the thickness was measured with a micrometer.

The results of the continuous and intermittent loading experiments are shown in figs. 6.14 and 6.15 plotted according to the Mooney-Rivlin equation; it is evident that the data are fairly well described by this equation giving C_1 and C_2 constants shown in table (6.12) below.

TABLE 6.12

C_1 and C_2 Constants for Tension of Dry Adiprene CM

% DCP in cure	Continuous Loading			Intermittent Loading		
	$C_1 \times 10^5$ Nm^{-2}	$C_2 \times 10^5$ Nm^{-2}	C_1/C_2	$C_1 \times 10^5$ Nm^{-2}	$C_1 \times 10^5$ Nm^{-2}	C_1/C_2
1.0	1.66	1.39	1.19	2.45	0.90	2.72
1.5	2.41	1.53	1.57	2.90	0.90	3.22
2.0	3.23	1.71	1.89	3.25	1.50	3.62
2.5	4.56	2.00	2.28	3.69	1.54	3.94

Tension experiments were alwo conducted on Adiprene CM samples that were swollen to equilibrium in ethanol, the results are shown in fig. 6.16 plotted according to the Mooney-Rivlin equation. In this case intermittent and continuous loading gave the same results which were independent of the time interval between loading and measuring. It is clear from fig. 6.16 that C_2 was zero; the C_1 values obtained are shown in table (6.13) below:

TABLE 6.13

C_1 Values for Tension of Ethanol Swollen Adiprene CM

% DCP in cure	$C_1 \times 10^5$ Nm^{-2}
1.0	2.80
1.5	4.70
2.0	5.60
2.5	6.10

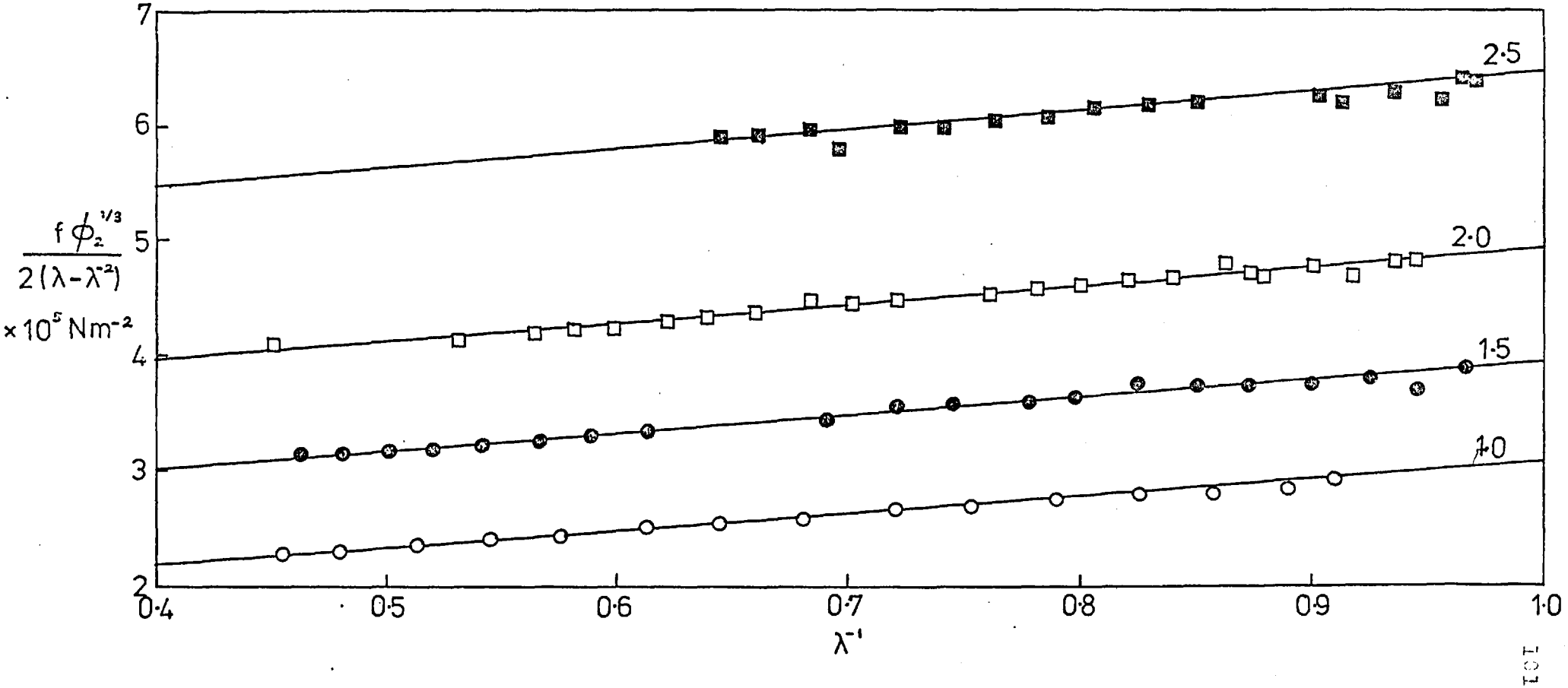


figure 6·14 : Tension experiments on dry Adiprene CM plotted according to the Mooney-Rivlin equation (numbers on lines are percentages of dicumyl peroxide in cure). Continuous loading experiment.

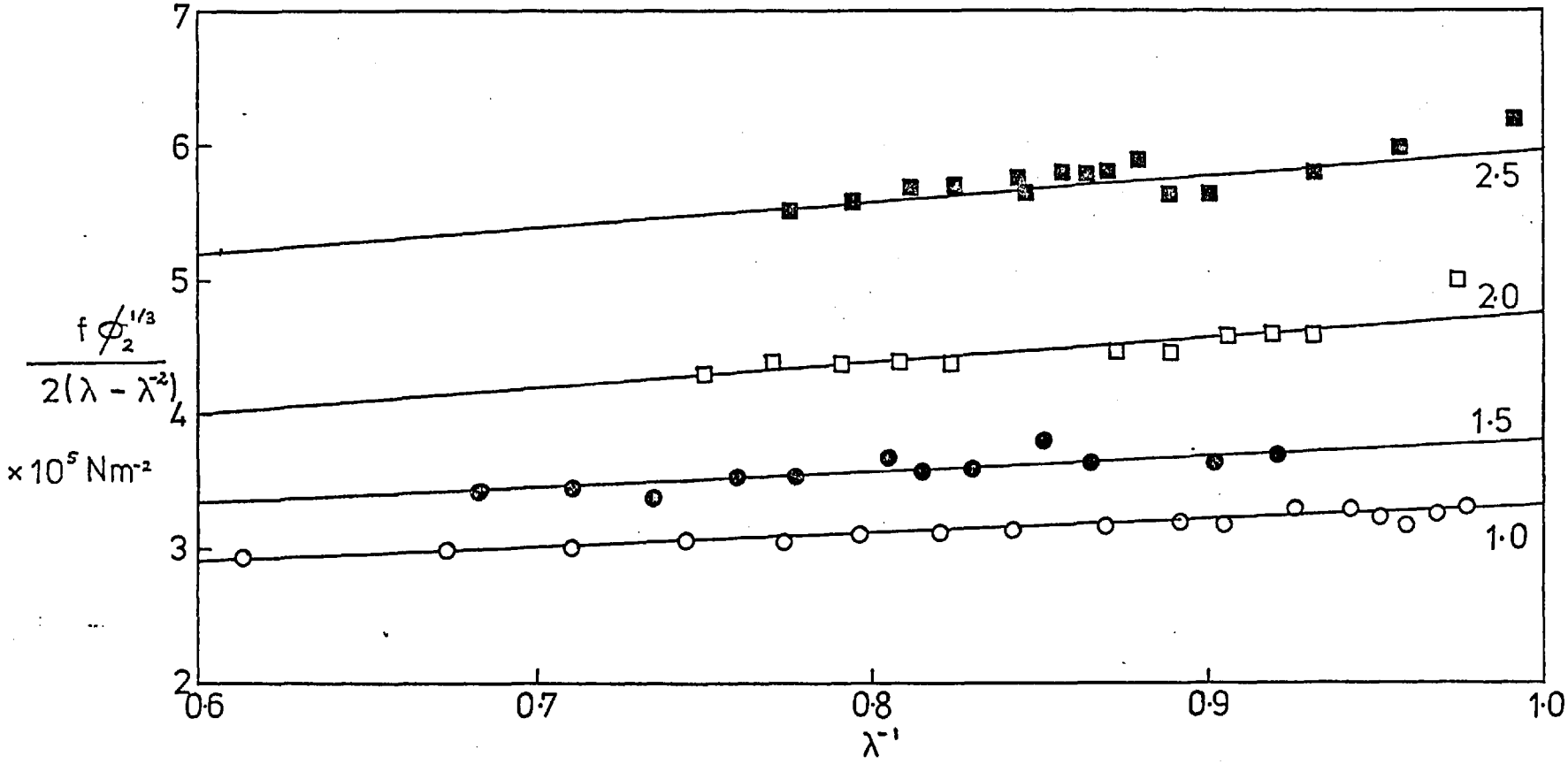


figure 6·15 : Tension experiments on dry Adiprene CM plotted according to the Mooney-Rivlin equation (numbers on lines are percentages of dicumyl peroxide in cure). Intermittent loading experiment

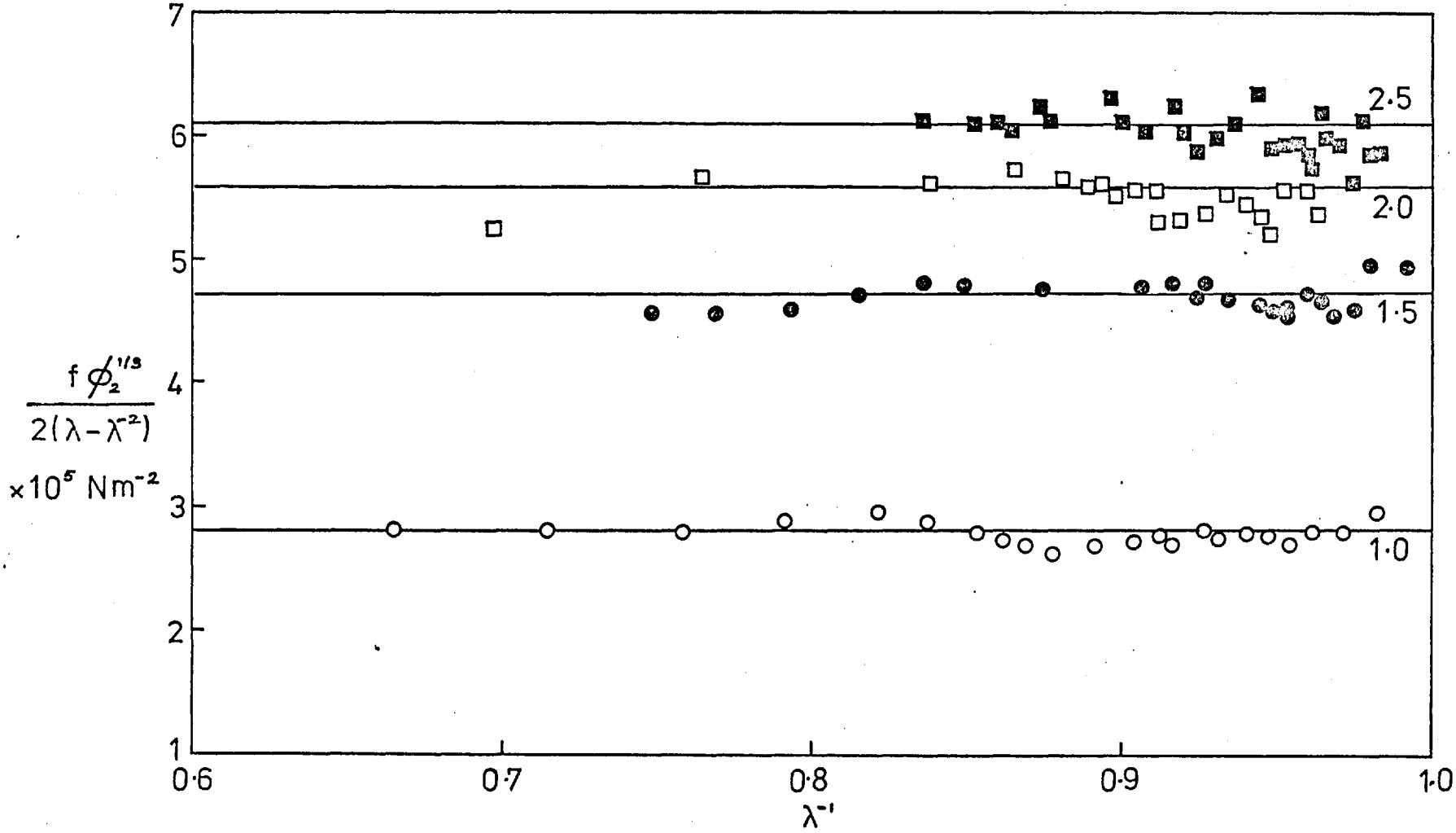


figure 6·16: Tension experiments on Adiprene CM swollen to equilibrium in ethanol plotted according to the Mooney-Rivlin equation (numbers on lines are percentages of dicumyl peroxide in cure)

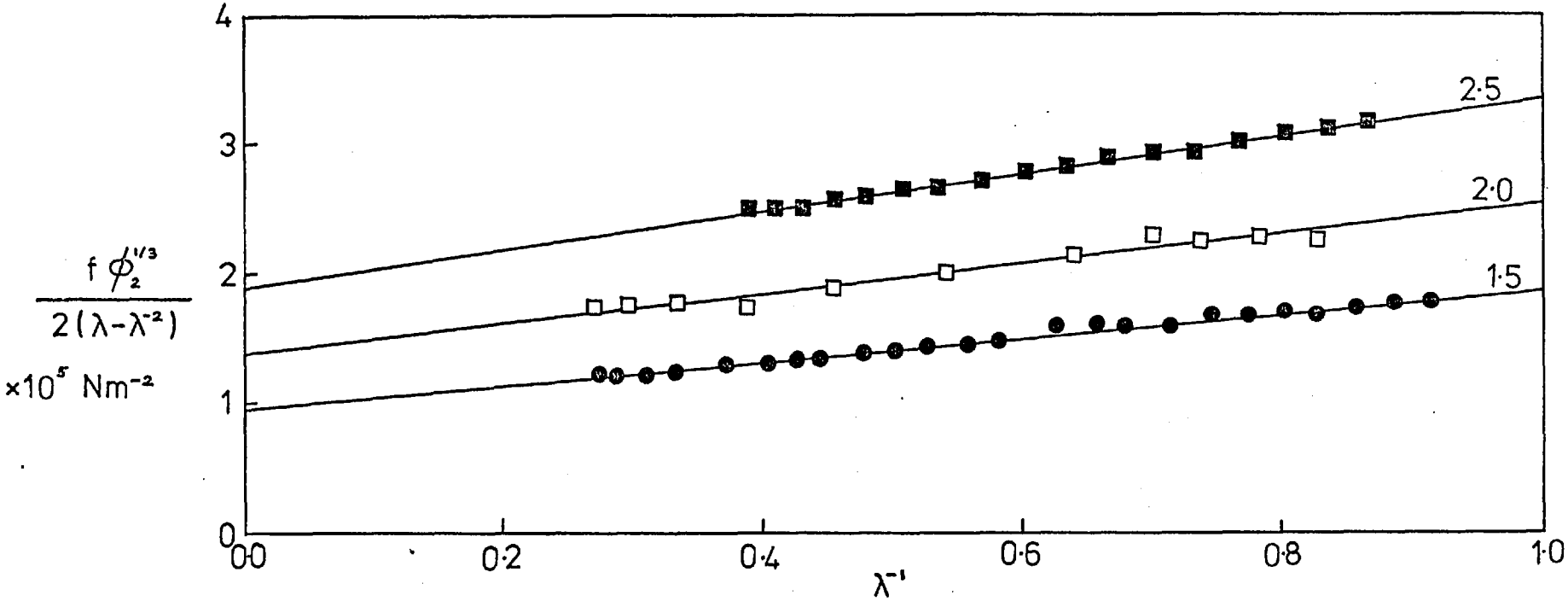


figure 6·17: Tension experiments on dry Genthane S plotted according to the Mooney-Rivlin equation (numbers on lines are percentages of dicumyl peroxide in cure)

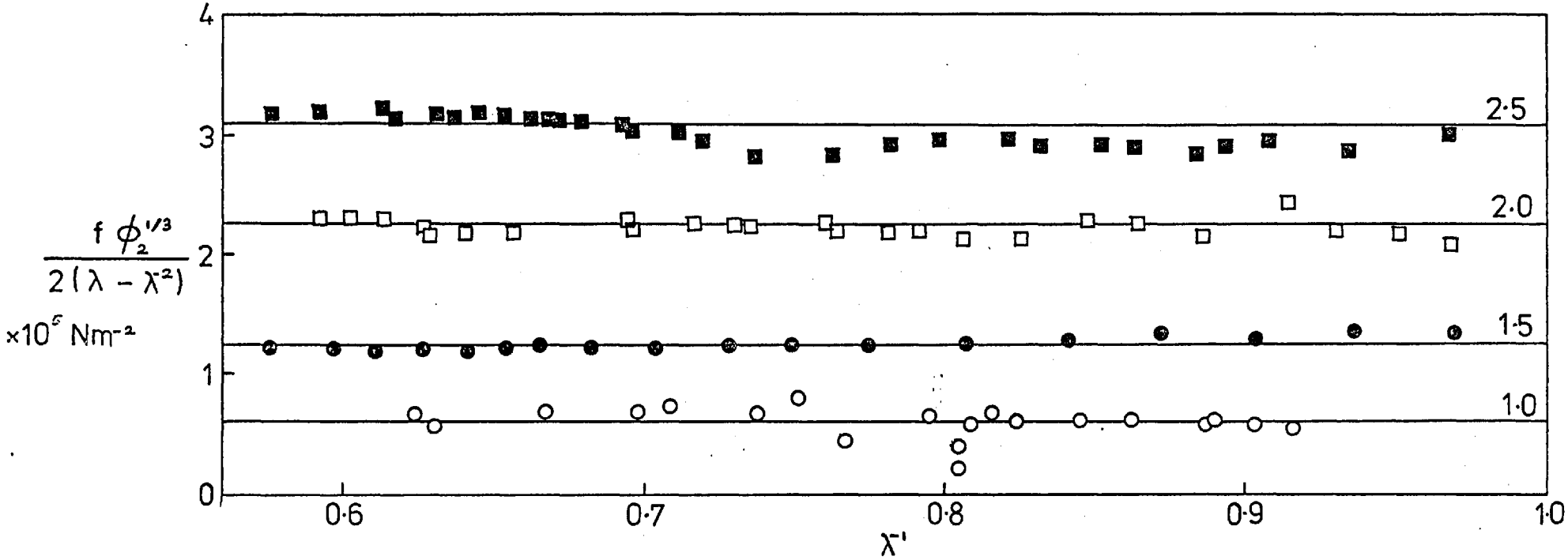


figure 6·18: Tension experiments on Genthane S swollen to equilibrium in ethyl acetate plotted according to the Mooney-Rivlin equation (numbers on lines are percentages of dicumyl peroxide in cure)

In the case of Genthane S only continuous loading experiments were conducted on the dry samples; it was not possible to conduct an experiment on the sample cured with 1.0% dicumyl peroxide since this underwent rapid stress relaxation for more than 24 hours; this did not occur in any of the other samples where stress relaxation was undetectable. The results for the other samples are shown in fig. 6.17 and table (6.14)

TABLE 6.14

C_1 and C_2 Constants for Tension of Dry Genthane S

% DPC in cure	$C_1 \times 10^5$ Nm^{-2}	$C_2 \times 10^5$ Nm^{-2}	C_1/C_2
1.5	0.95	0.92	1.03
2.0	1.40	1.15	1.22
2.5	1.91	1.44	1.33

Measurements were also made on Genthane S samples swollen to equilibrium in ethyl acetate; C_2 was zero (see fig. 6.18) and the C_1 values obtained are shown in table (6.15).

TABLE 6.15

C_1 Values for Tension of Ethyl Acetate Swollen Genthane S

% DCP in cure	$C_1 \times 10^5$ Nm^{-2}
1.0	0.68
1.5	1.22
2.0	2.26
2.5	3.05

(6.4.3) The Stress-Strain Properties of the Elastomers in Uniaxial Compression

(6.4.3.1) Apparatus and Experimental Method

The apparatus used for making the compression measurements was essentially the same as that of Cluff, Gladding and Pariser[239] and Thomas[240] and is illustrated in figure 6.19.

All the compression measurements were made on swollen samples which were in the form of small cylindrical buttons. These buttons were swollen to equilibrium in solvent and placed in a small beaker with an optically flat bottom so that the anvil of a sensitive dial gauge rested on the top flat side of the button as is shown in fig. 6.19; the dial gauge was a "Wallace Dial Gauge" measuring to 0.002 mm. Weights were placed on the load pan of the dial gauge and the gauge used to measure the height of the buttons. The gauge itself, which is virtually friction free, exerts a load of 58 g on the button.

Swelling the buttons had to be done gradually when high degrees of swelling were anticipated. If the buttons were simply immersed in the required solvent they frequently underwent mechanical degradation; to prevent this mixtures of the required solvent and a solvent that did not swell the material very much were used. The poor solvent used was generally cyclohexane so that if the required solvent was chloroform the sample would first be swollen in cyclohexane. It would then be swollen in turn in cyclohexane/chloroform mixtures containing increasing proportions of chloroform and would be fimally transferred to pure chloroform.

As for the tension experiments it is necessary to know the zero load height of the sample in order to evaluate λ. This was obtained in the same way as in the tension experiments and the results optimised using the computer programme in Appendix C.

The volume fraction of rubber in the swollen vulcanizate was obtained as described in section 6.4.1 and the radii of the buttons were determined with a travelling microscope.

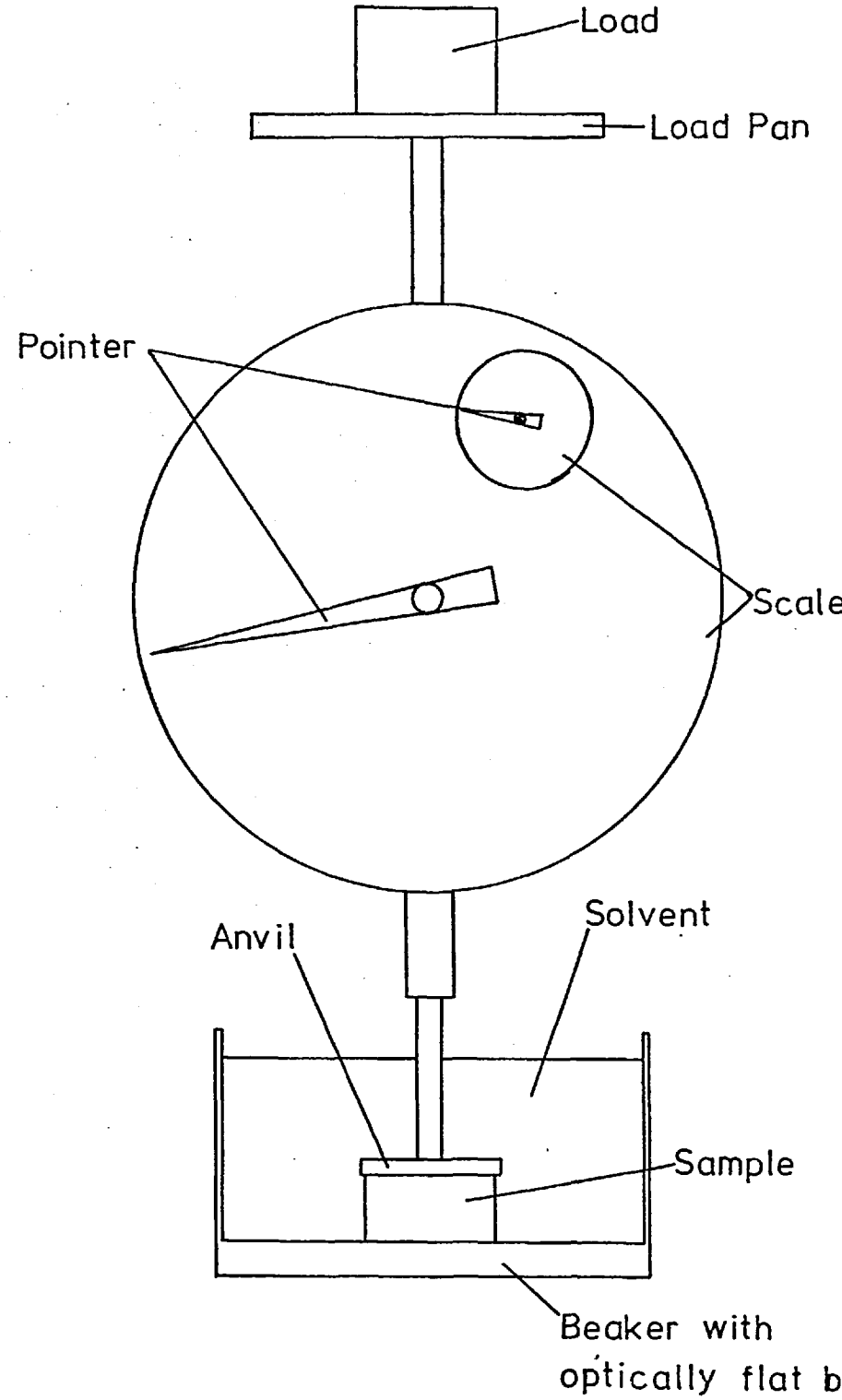


figure 6·19 : Dial gauge set up for compression experiment on a swollen sample

(6.4.3.2) Compression of Adiprene CM and Genthane S

Uniaxial compression experiments were conducted on Adiprene CM samples swollen to equilibrium in cyclohexane, benzene, chloroform and ethanol and the results, plotted according to the Mooney-Rivlin equation, are shown in figs. 6.20, 6.21, 6.22 and 6.23. C_2 is zero in all cases and the C_1 values obtained are shown in table (6.16) below.

TABLE 6.16

C_1 Values from the Compression of Adiprene CM Samples Swollen to Equilibrium in Various Solvents

Solvent	$C_1 \times 10^5$ Nm^{-2}			
	1.0% DCP	1.5% DCP	2.0% DCP	2.5% DCP
Cyclohexane	3.55	-	5.50	6.25
Benzene	3.50	4.70	5.45	6.10
Chloroform	3.15	4.65	5.20	5.95
Ethanol	3.45	4.75	5.30	6.65
Average Values	3.41	4.70	5.35	6.25

Compression measurements were made on Genthane S samples swollen to equilibrium in cyclohexane, chloroform and ethyl acetate and the results are shown in figs. 6.24, 6.25 and 6.26. C_2 was zero and the C_1 values obtained are shown in table (6.17)

TABLE 6.17

C_1 Values from the Compression of Genthane S Samples Swollen to Equilibrium in Various Solvents

Solvent	$C_1 \times 10^5$ Nm^{-2}			
	1.0% DCP	1.5% DCP	2.0% DCP	2.5% DCP
Cyclohexane	1.29	2.02	2.92	3.56
Chloroform	0.45	0.95	2.10	-
Ethyl Acetate	0.33	1.23	1.82	2.95

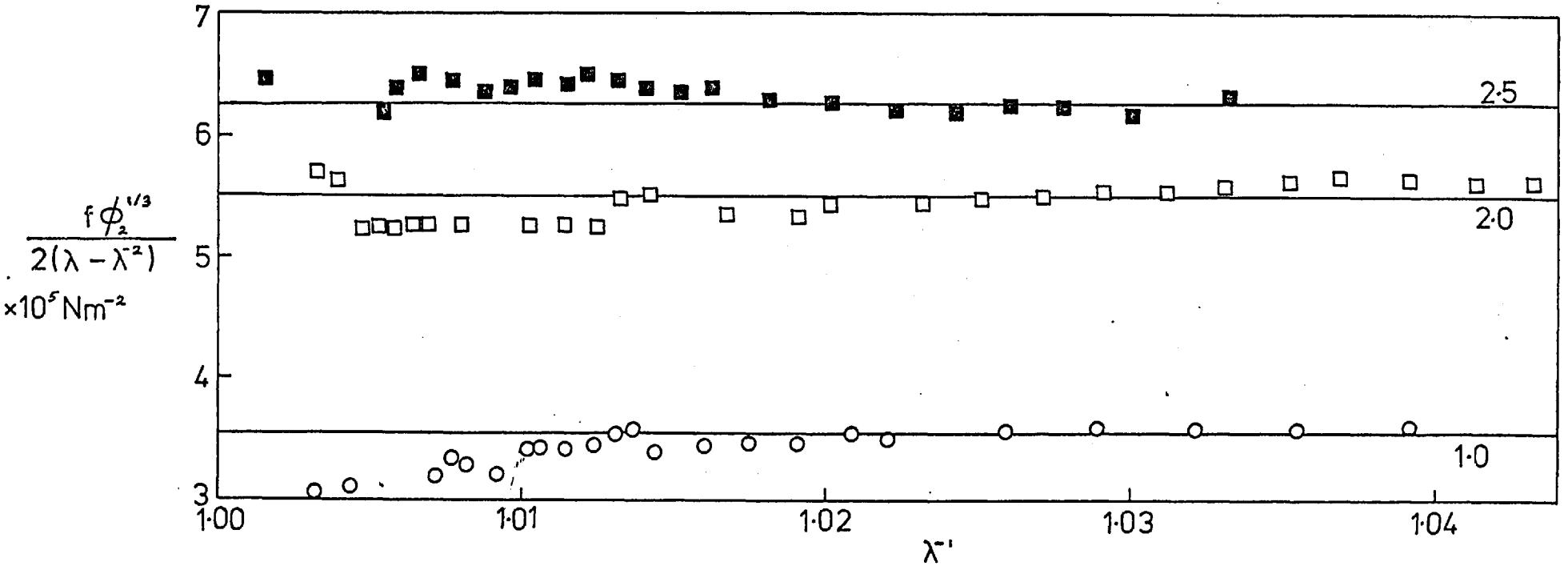


figure 6·20 :Compression experiments on Adiprene CM swollen to equilibrium in cyclohexane plotted according to the Mooney-Rivlin equation (numbers on lines are percentages of dicumyl peroxide in cure)

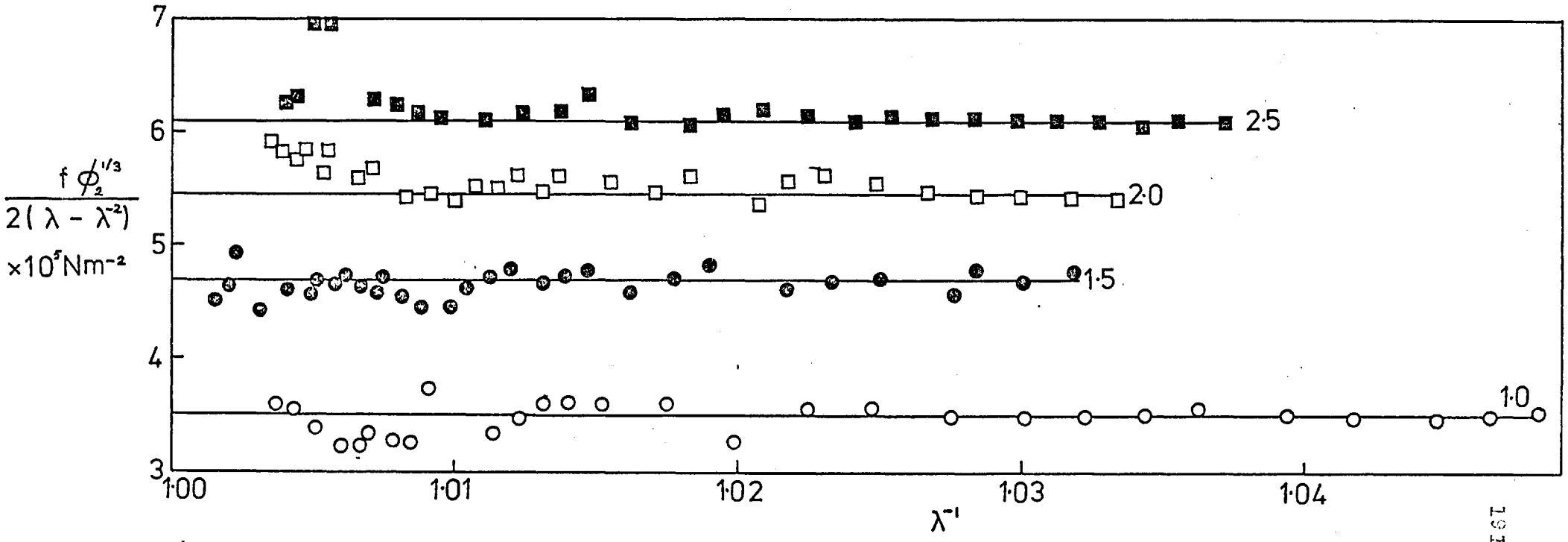


figure 6·21 : Compression experiments on Adiprene CM swollen to equilibrium in benzene plotted according to the Mooney-Rivlin equation (numbers on lines are percentages of dicumyl peroxide in cure)

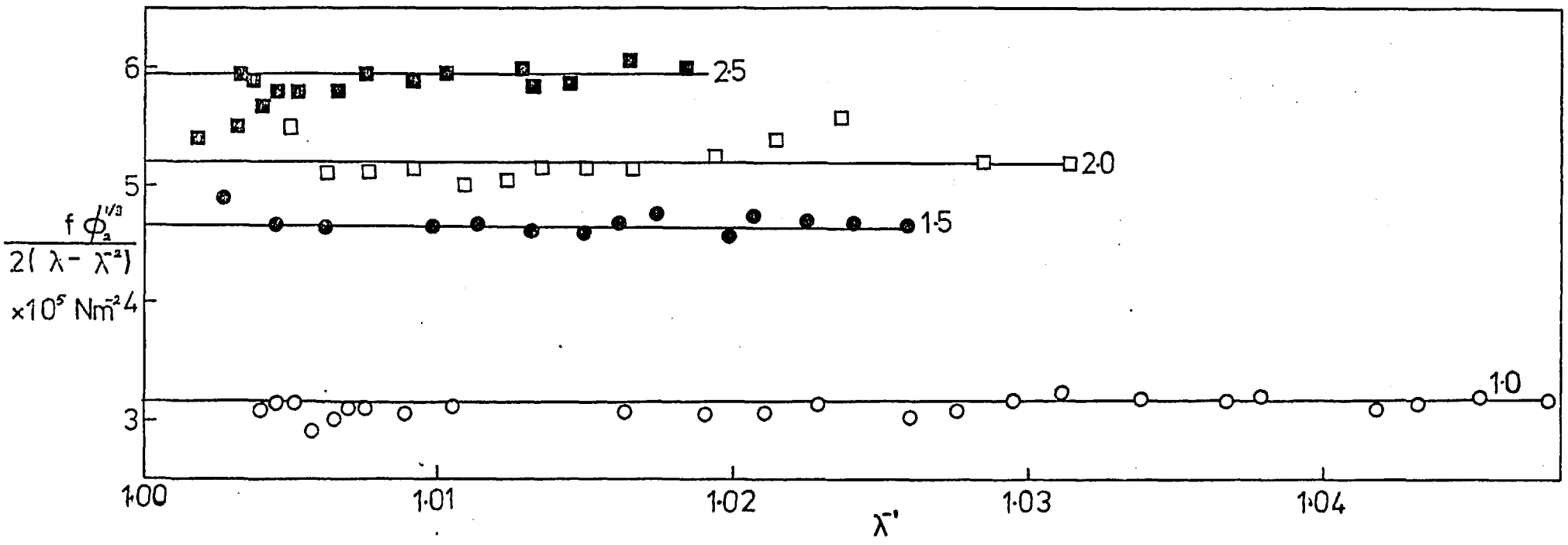


figure 6·22 : Compression experiments on Adiprene CM swollen to equilibrium in chloroform plotted according to the Mooney-Rivlin equation (numbers on lines are percentages of dicumyl peroxide in cure)

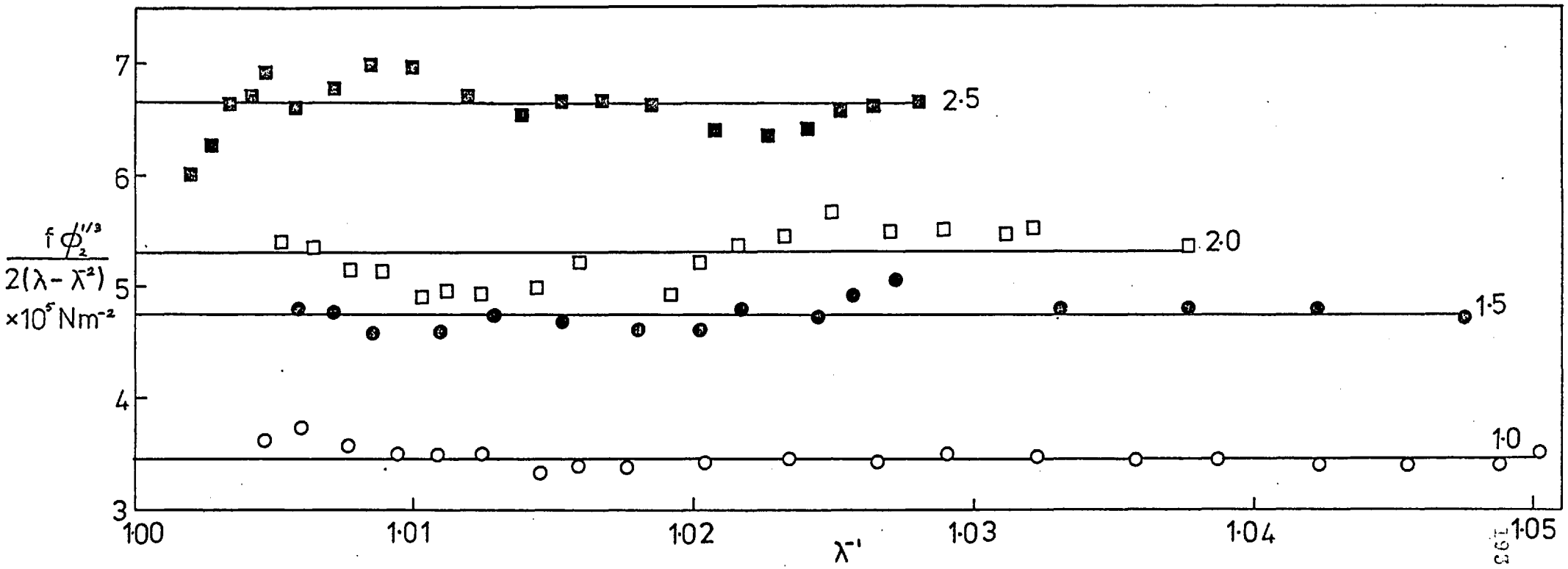


figure 6·23 :Compression experiments on Adiprene CM swollen to equilibrium in ethanol plotted according to the Mooney-Rivlin equation (numbers on lines are percentages of dicumyl peroxide in cure)

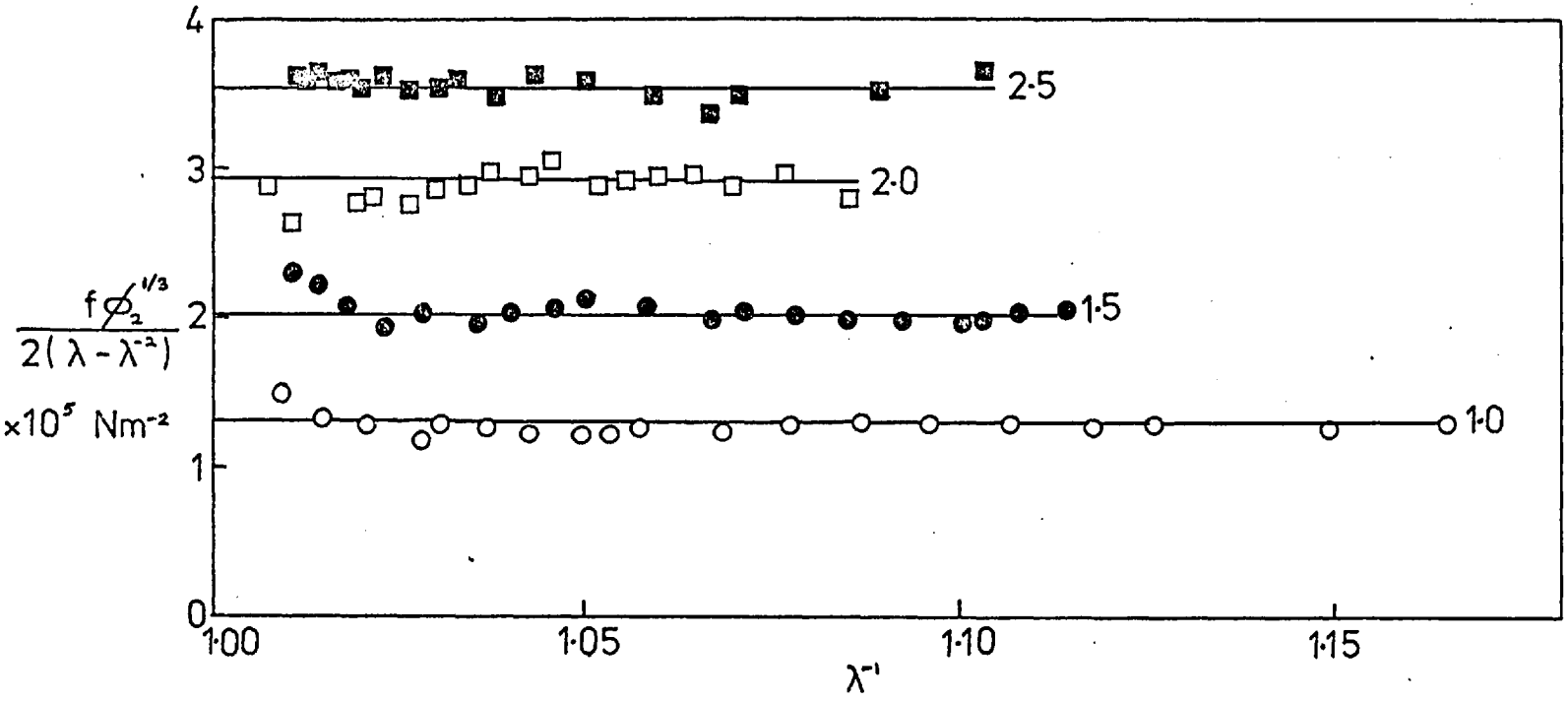


figure 6·24: Compression experiments on Genthane S swollen to equilibrium in cyclohexane plotted according to the Mooney-Rivlin equation (numbers on lines are percentages of dicumyl peroxide in cure)

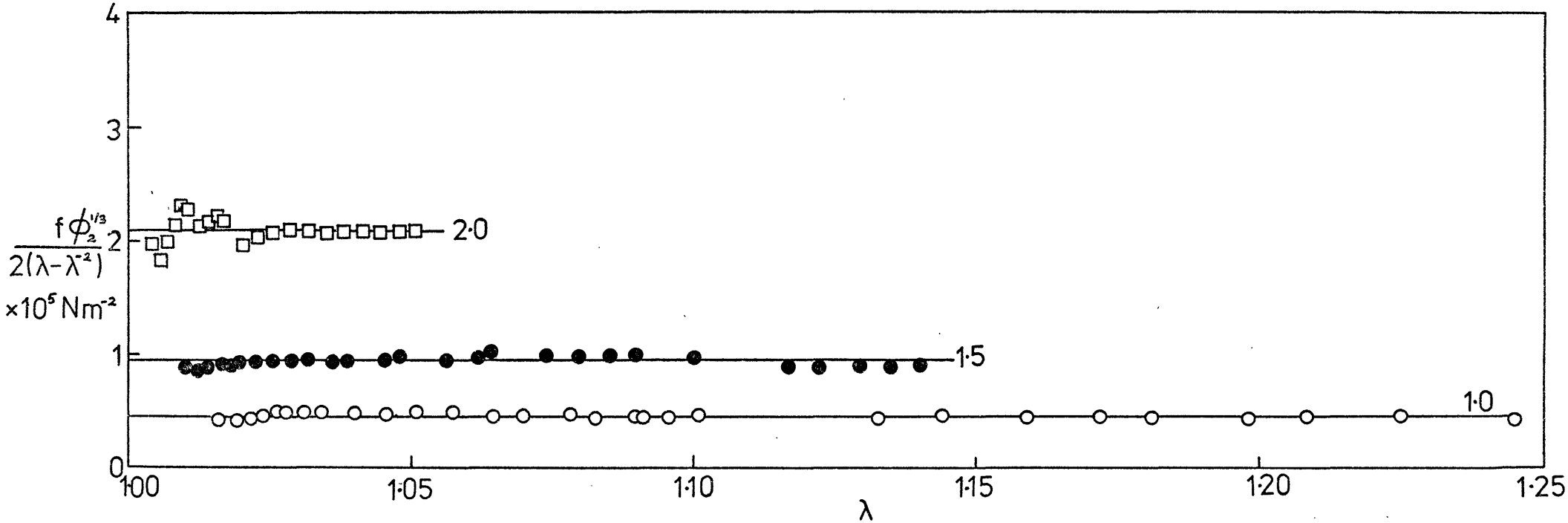


figure 6·25: Compression experiments on Genthane S swollen to equilibrium in chloroform plotted according to the Mooney-Rivlin equation (numbers on lines are percentages of dicumyl peroxide in cure)

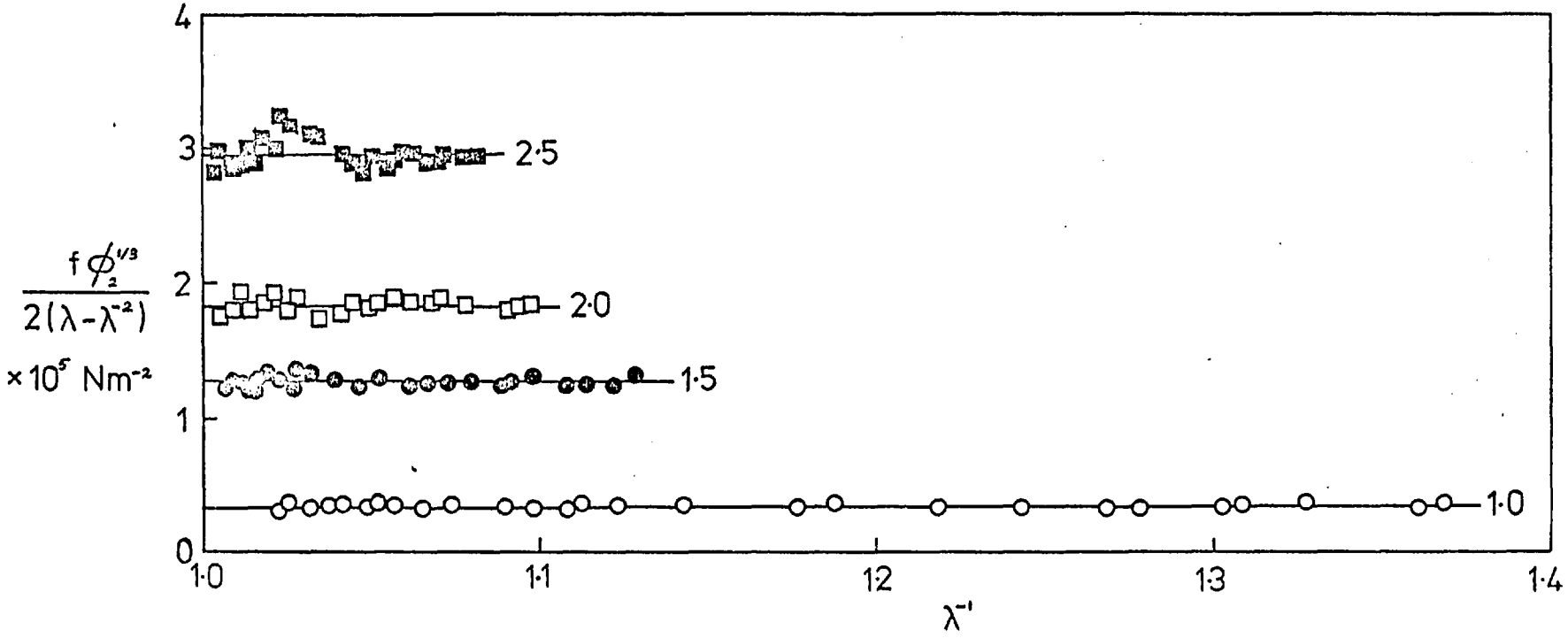


figure 6·26: Compression experiments on Genthane S swollen to equilibrium in ethyl acetate plotted according to the Mooney-Rivlin equation (numbers on lines are percentages of dicumyl peroxide in cure)

(6.5) DISCUSSION OF RESULTS

(6.5.1) The Composition and Structure of the Polymers

The infra-red and n.m.r. spectra of the polymers confirmed that their chemical structure is as reported in the literature (see section 6.3.1). However, the n.m.r. data also allow the calculation of the relative concentrations of the various groups, that comprise the polymer molecules; of particular interest is the urethane group concentration given in table (6.18) below.

TABLE 6.18

The Urethane Group Concentration in Adiprene CM and Genthane S

	Adiprene CM	Genthane S
Weight fraction of $\{O-\overset{O}{\overset{\|}{C}}-NH\}_2R$	0.265	0.138
Mole fraction of $\{O-\overset{O}{\overset{\|}{C}}-NH\}_2R$	0.120	0.049
Mole fraction of urethane groups	0.240	0.098
Molecular weight per urethane group	362	970

The urethane group concentration is greater in Adiprene CM than in Genthane S by a factor of two to three, the mole per cent of diisocyanate used to prepare the polymers is fairly small, 12% in Adiprene CM and 5% in Genthane S, as was stated in section 5.1

(6.5.2) The Stress-Strain Properties of the Elastomers

Several facts emerge from the stress-strain results described in sections 6.4.2 and 6.4.3:

(i) C_2 is zero for swollen samples of Adiprene CM and Genthane S for both tension and compression measurements

(ii) There is good agreement between the C_1 values for the compression of Adiprene CM and Genthane S swollen in various solvents except in the case of cyclohexane swollen Genthane S.

(iii) The C_1 values obtained in tension and compression of samples swollen in the same solvent for both Genthane S and Adiprene CM show reasonable agreement with one another.

(iv) The C_1 values for dry Genthane S and Adiprene CM in tension were smaller than the values for swollen samples and the C_2 values were not zero. For Adiprene CM the C_1 and C_2 values depended on the way the experiment was done.

These facts indicate that tension experiments on dry samples are a poor way of characterising networks since the C_1 and C_2 values depend on the way the experiment is done and the C_1 values do not agree with those obtained for swollen samples where C_2 is zero, and the data can be described by the simple kinetic theory. The variable and method dependent C_1 and C_2 values presumably result from the viscoelastic properties of the materials which are probably dependent on the hydrogen-bonding present in these materials. This may also be the cause of the abnormally high C_1 values obtained for cyclohexane swollen Genthane S.

The good agreement between the C_1 values for the swollen samples and the zero C_2 values suggests that viscoelastic effects are unimportant and that the C_1 values obtained are a true measure of the equilibrium elastic properties of the network. Since C_2 is zero the data can be described by the

simple kinetic theory equation so that C_1 can be identified with $\frac{1}{2}A\,\nu^{*}RT\,q_o^{-2/3}$ where ν^{*} is the number of moles of crosslinks per unit volume of rubber. Assuming that q_o is unity, (see section 2.4.2), and A is unity, (see section 2.4.1) ν^{*} can be calculated.

The number average molecular weight of the network chains is given by

$$\bar{M}c = \rho/\nu^{*}$$

where ρ is the density of the rubber.

These parameters are listed in table (6.19).

TABLE 6.19

Network Parameters for Genthane S and Adiprene CM

Genthane S

% DCP in cure	C_1^{*} x 10^5 Nm^{-2}	ν^{*} x 10^{-5} moles cm^{-3}	$\bar{M}c$
1.0	0.48	3.88	30700
1.5	1.15	9.29	12800
2.0	2.06	16.63	7160
2.5	3.00	24.21	4920

Adiprene CM

% DCP in cure	C_1^{*} x 10^5 Nm^{-2}	ν^{*} x 10^{-5} moles cm^{-3}	$\bar{M}c$
1.0	3.41	21.63	3540
1.5	4.65	37.58	2590
2.0	5.35	43.05	2260
2.5	6.25	50.47	1930

* C_1 values averaged over acceptable sets of data.

The molecular weight between crosslinks for the Genthane S sample cured with 1.0% dicumyl peroxide is very large and almost the same as the number average molecular weight of the primary polymer molecules, (see section 6.3.2.1).

This means that the number of crosslinks per primary polymer molecule will be small and hence explains the fast stress relaxation observed when attempting to conduct stress-strain measurements on the dry sample. The network will be able to relax quite considerably before being constrained by the small number of crosslinks present.

It has been pointed out, (see sections 2.5.2.3 and 3.3.2), that the network chain density derived from stress-strain measurements is the elastically effective network chain density and does not include loose ends. This means that $\bar{M}c$ as calculated from the elastically effective network chain density will be in error if there are a large number of loose ends. Flory and others, (section 3.3.2), have proposed corrections for this; use of Flory's equation, which has been shown to be reasonably correct when there are a lot of loose ends, gives:

$$1/\bar{M}c = 1/(\bar{M}c)_e + 2/\bar{M}n$$

where $\bar{M}c$ is the true number average molecular weight of network chains, $(\bar{M}c)_e$ is the value calculated from the number of elastically effective network chains and given in table (6.19), and $\bar{M}n$ is the number average molecular weight between crosslinks. Once the true $\bar{M}c$ values have been evaluated, the number of urethane groups per network chain can be calculated. These parameters are given in table (6.20).

It is clear that this correction is very much more important in Genthane S than in Adiprene CM.

+ + + + + +

TABLE 6.20

Network Parameters for Genthane S and Adiprene CM Corrected for Loose Ends

Genthane S

% DCP in cure	$(\bar{M}c)_e$	$\bar{M}c$	urethane groups per network chain
1.0	30700	10300	10.6
1.5	12800	6990	7.2
2.0	7160	4910	5.1
2.5	4920	3750	3.9

Adiprene CM

% DCP in cure	$(\bar{M}c)_e$	$\bar{M}c$	urethane groups per network chain
1.0	3540	3450	9.5
1.5	2590	2550	7.2
2.0	2260	2220	6.1
2.5	1930	1910	5.3

CHAPTER 7

CHEMICAL STRESS RELAXATION IN ADIPRENE CM AND GENOCHANE S

(7.1) APPARATUS

The results presented here were obtained using two different sets of apparatus. One set is in use at the Materials Division, Royal Aircraft Establishment, Farnborough, Hampshire whilst the other set was designed and built at Imperial College as part of this study. Approximately half the results were obtained on each set of apparatus, both gave identical results.

The R.A.E. apparatus has been described fully elsewhere [241,242] and the I.C. apparatus will be fully described in this chapter.

(7.1.1) The Relaxometer

The most important part of the apparatus is the relaxometer which is shown in figure 7.1.

The relaxometer was a developed version of the tensometer described in section (6.4.2.1), the force being measured by an almost identical spring and transducer assembly. As in the tensometer, this assembly could be moved up and down by means of a threaded rod, however, this was not done to extend the sample but to accommodate samples of different lengths. It was used to take up the "slack" in long samples or to "slacken off" short ones.

The sample was held between the clamps, (13) and(15). Extension was effected by rotating the cam, (26), through 180°C so that the carriage, (16), was moved from its uppermost to its lowest position. The distance between these positions could be varied by adjusting the position of

the pivot (25), at the bottom end of the connecting rod (21), in the slot in which it was fixed. A further rotation of 180° returned the sample to its original, undeformed state by returning the carriage (16) to its uppermost position.

This extension method allowed both continuous and intermittent stress relaxation measurements (see Chapter 3) to be made. In a continuous experiment the sample was extended at the beginning of the experiment and remained in this state for the duration of the experiment. In an intermittent experiment the sample was maintained in the undeformed state and at regular intervals, usually one hour, was stretched, the force measured, and the sample retracted. The cam rotation method ensured that the sample was always extended by exactly the same amount.

The relaxometer was mounted on a frame and was slid up into a furnace (see section 7.1.2) when is use. When in position in the furnace the relaxometer and furnace were vacuum tight as the connections between the furnace and the relaxometer and between the demountable parts of the relaxometer were sealed with O-rings. The O-ring in contact with the furnace was cooled by water circulating through holes drilled in the block (19) at the bottom of the relaxometer. The drive shaft for the cam (37) and the bottom end of the rod (27), used to adjust the position of the spring and transducer assembly, left the apparatus via vacuum seals. The electrical leads to the transducer, the resistance bulb thermometer (see section 7.1.2) and the thermocouple used to measure the temperature close to the sample, were passed out of the apparatus via glass/metal vacuum seals. The sealed nature of the apparatus allowed

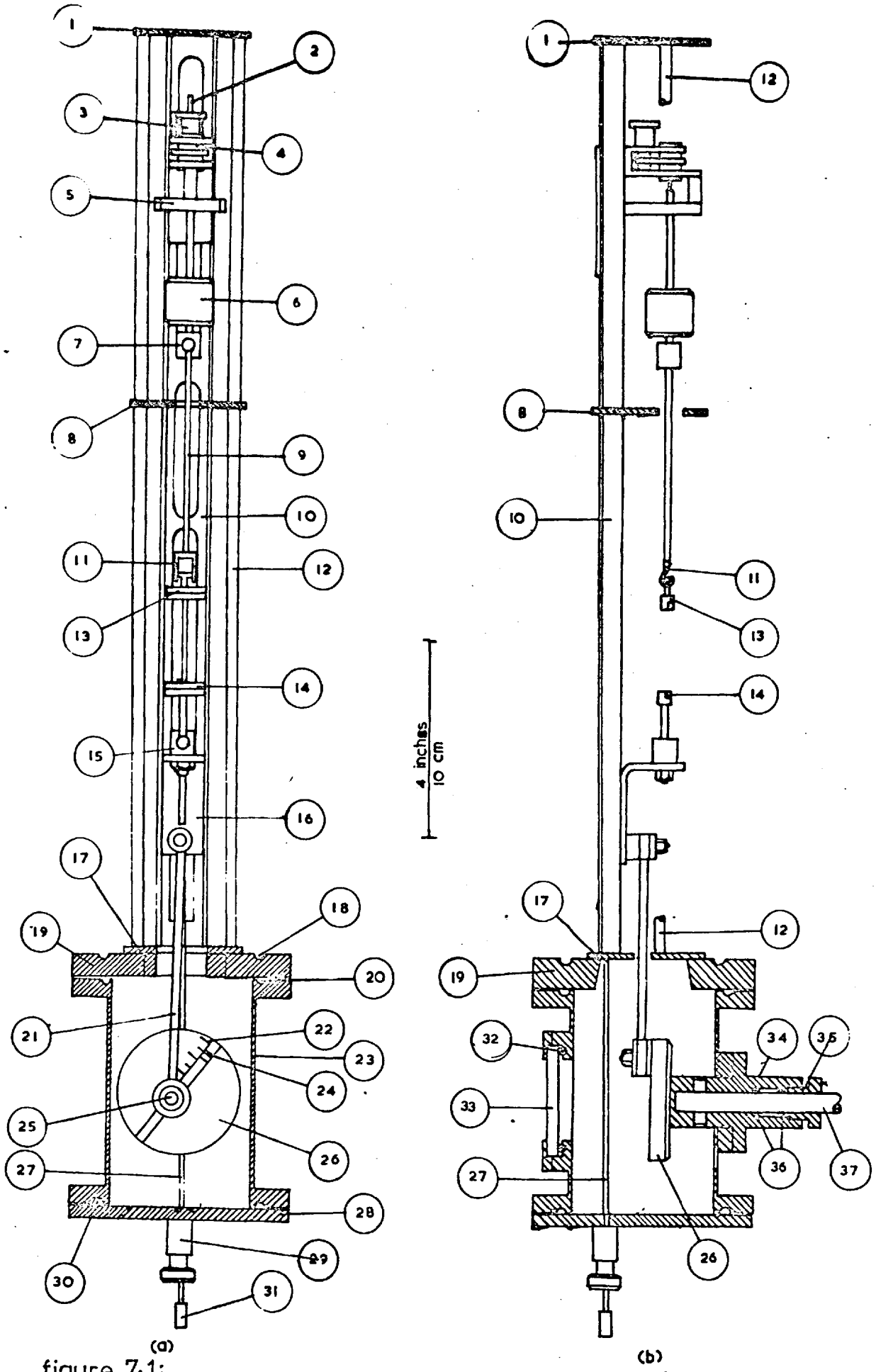


figure 7·1:
STRESS RELAXOMETER: cam reversed in (a) to show details of travel adjustment.

KEY TO FIGURE 7.1

1. Top Plate
2. Threaded Rod to allow the transducer and spring assembly to be moved up and down
3. Micrometer adjustment of transducer
4. Transducer holder
5. Spring support
6. Zero load weight (as in tensometer fig. 6.10)
7. Block for mounting rod connecting top sample clamp to spring
8. Centre Plate
9. Rod connecting top sample clamp to spring
10. Main frame of apparatus
11. Hook for supporting top sample clamp
12. Supporting spars
13. Top sample clamp
14. Bottom sample clamp
15. Mount for bottom sample clamp
16. Carriage on which bottom sample clamp travels
17. Bottom Plate
18. Recess for O-ring
19. Water cooled block
20. O-ring seal
21. Connecting rod
22. Millimeter scale on cam
23. Casing of bottom end of relaxometer
24. Scribe line to mark travel of cam
25. Pivot
26. Cam
27. Bottom of threaded rod (2)
28. Bottom Plate
29. Vacuum seal
30. O-ring seal
31. Knob to turn threaded rod (2)

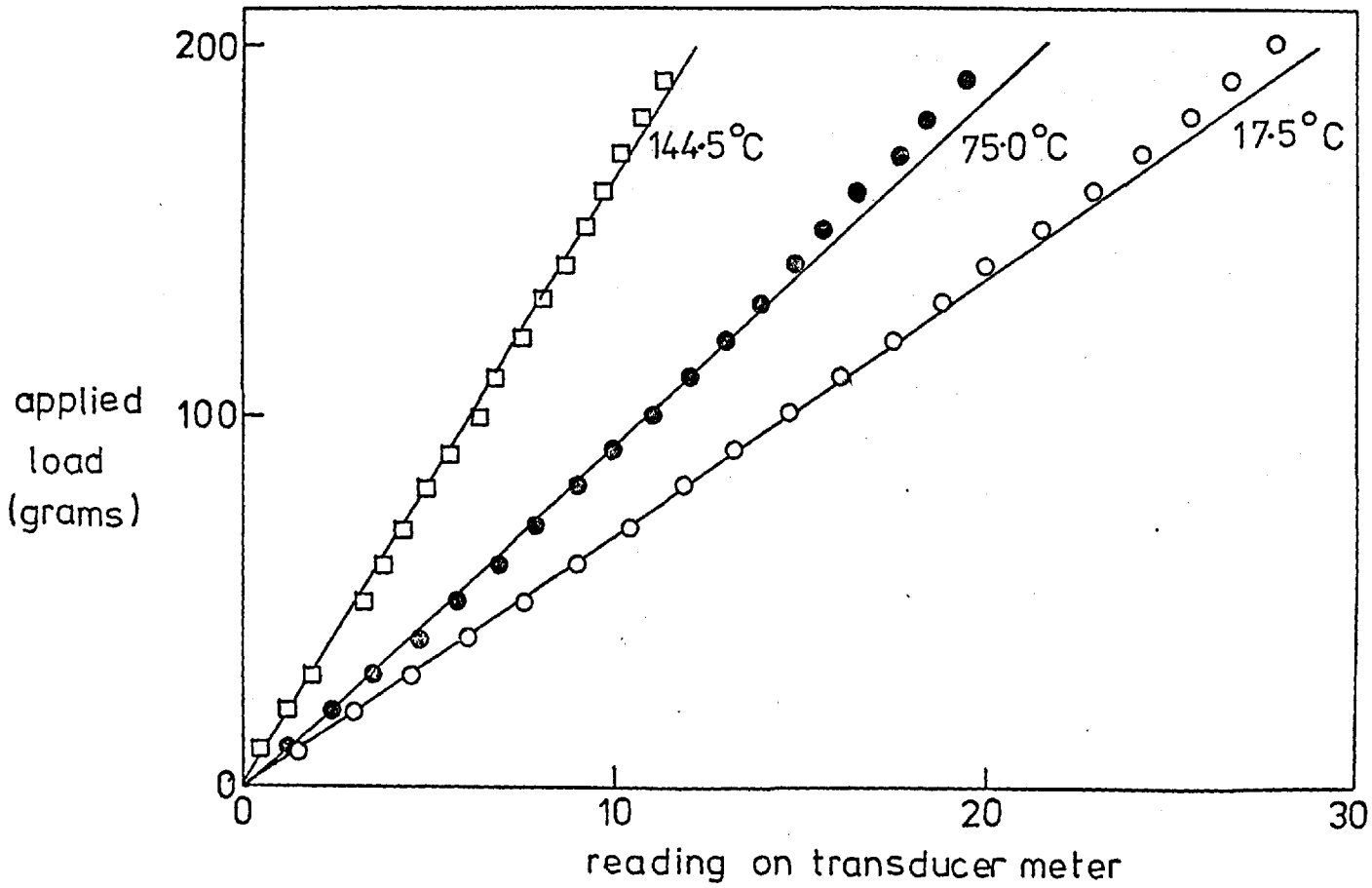


figure 7. 2 :Calibration curves for transducer and spring assembly at different temperatures

experiments to be conducted either in a vacuum or in a controlled atmosphere.

The cam used to extend the sample was driven round by an electric motor mounted outside the relaxometer, the motor was geared down to provide a final drive speed of 5 r.p.m. so that rotation of the cam through 180^{o} took 6 seconds. A double ended cam was mounted on the motor shaft outside the relaxometer; this opened a microswitch and stopped the motor after it had driven through precisely 180^{o}. In the original design an electromagnetic brake was included to ensure that the motor stopped dead as soon as the power was cut off; in practice this was found to be unnecessary as the microswitch could be adjusted so that the high friction in the system caused the motor to stop at the same position every time. The motor was started by momentarily shorting out the microswitch used to stop it; this allowed the cam to move sufficiently so that the microswitch closed and restored power to the motor.

The spring and transducer assembly was almost identical to that described earlier (see section 6.4.2.1) but gave a linear load vs transducer output curve (see fig. 7.2) unlike the tensometer. This was probably because in the relaxometer the spring was clamped into position when the assembly was at a higher temperature than that at which measurements were made. This meant that the spring was under tension at the operating temperature as it had contracted slightly; the spring was, thus, perfectly flat.

(7.1.2) The Furnace

The furnace (see fig. 7.3) was a thin walled stainless steel tube with a main winding over the whole length of it

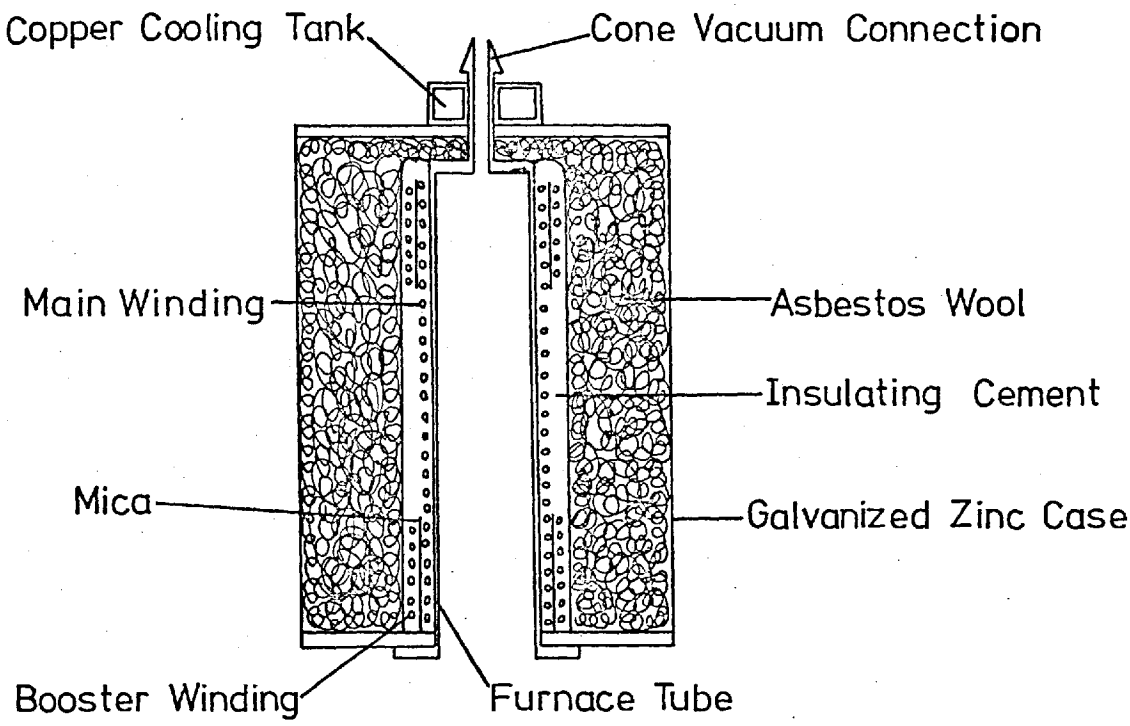


figure 7·3 :Cross-section of furnace

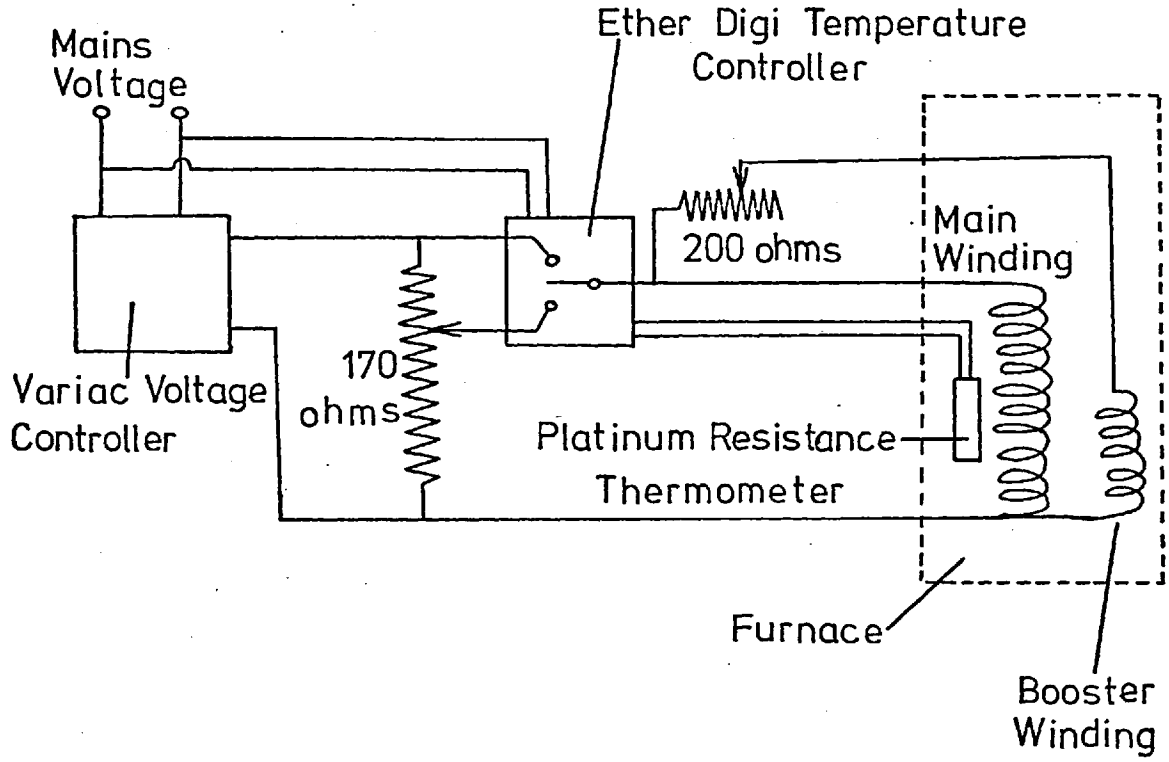


figure 7·4 : Temperature Control Circuit

and booster coils wound over the main winding at each end to compensate for end losses. In practice it was possible to keep the temperature constant over the whole length of the sample using just the main and bottom booster windings. The temperature of the furnace dropped off as the top of it was approached but the temperature at any point remained constant. This is important since the characteristics of the spring and transducer are temperature dependent.

The furnace control circuit is shown in figure 7.4; the temperature controller was an Ether Digi 1971/1 which is a relay based proportional controller. A platinum resistance thermometer was used to measure the temperature, this formed one of the arms of a Wheatstone bridge in the controller; the resistance thermometer was mounted on the main frame of the relaxometer, adjacent to the sample.

The applied voltage was supplied by the variac, and could be varied from 0 - 270 volts. This voltage was applied to a 170 ohm resistor from which a voltage that was 80 - 90% of the applied voltage was tapped off. This reduced voltage was supplied continuously to the main coil of the furnace. The applied voltage was adjusted so that the reduced voltage caused the furnace to heat up to a temperature that was about $5^{o}C$ lower than the required temperature. Control was effected by switching on and off the small voltage that was the difference between that supplied by the variac and that fed continuously to the main coil. A fraction of the voltage supplied to the main coil was fed to the booster winding via a 200 ohm resistor.

The overall stability of the furnace and the temperature control circuit was good, the furnace was always within 0.5°C of the set temperature.

(7.1.3) The Vacuum System

A standard glass vacuum system containing ground glass, greased taps was used (see fig. 7.5). Connections to the furnaces were made via B19 cones and sockets; the covers at the top of the furnaces were kept cool by cold water circulating in copper tanks mounted just below the cones (see fig. 7.3) The vacuum line allowed the furnaces to be evacuated to outgas the samples or to do experiments in a vacuum (i.e. 10^{-5} cm Hg). The incorporated gas handling line allowed experiments to be done in controlled atmospheres.

(7.1.4) The Control and Measuring Systems

The measuring system is illustrated schematically in figure 7.6, it comprises the two transducers (one for each relaxometer) which are connected, in turn, to the transducer meter via the Ledex switch. The output from the transducer meter is attenuated by the "resistive network" and then passed into a Honeywell Electronik 15, 4 point, potentiometric recorder.

The Ledex switch is an electromagnetic rotary stepping switch, that steps on one position on receipt of a 24 volt pulse.

The "resistive network" is shown in figure 7.8; it allows the output from the transducer meter (0 to 1 volt) to be attenuated to give a signal of 0 - 10 mV for the Honeywell recorder. It also adjusts impedances as the transducer meter has an output impedance of about 2500 ohms whilst the Honeywell recorder has an input impedance of only 400 ohms.

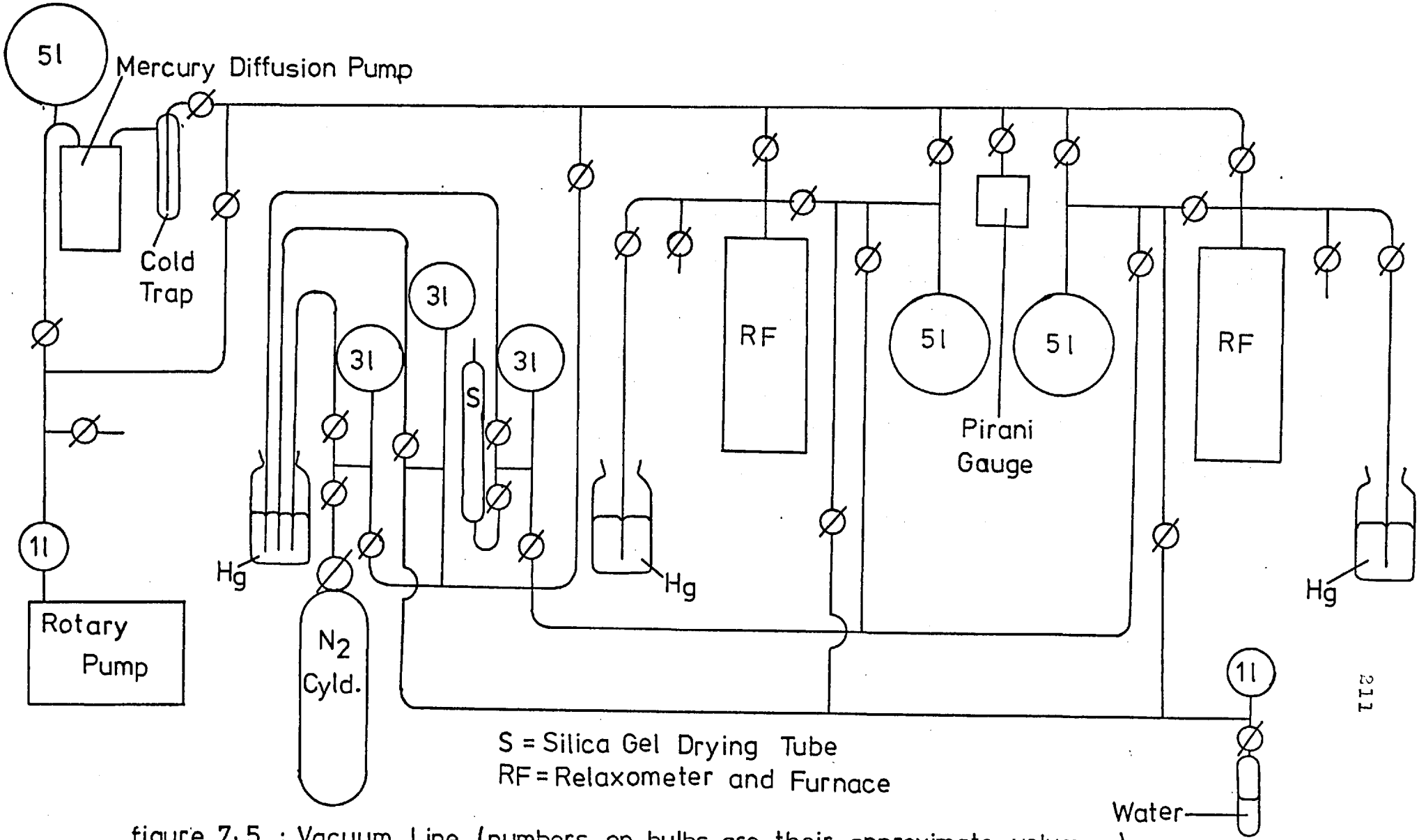


figure 7·5 : Vacuum Line (numbers on bulbs are their approximate volumes)

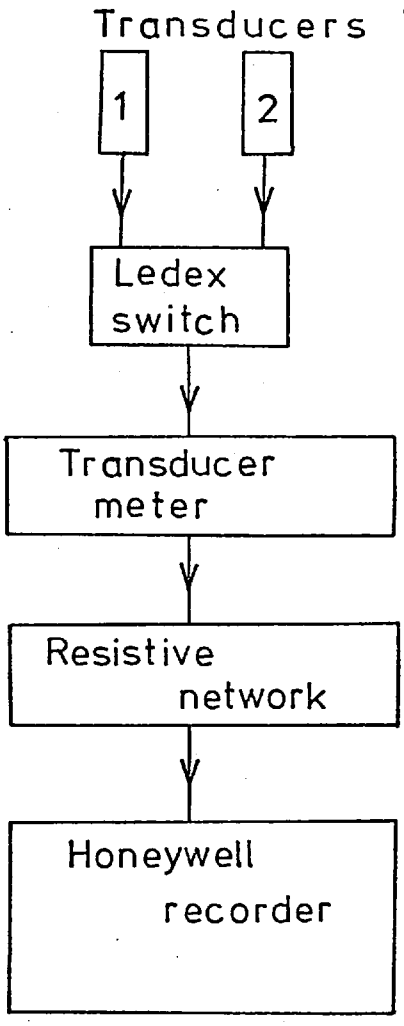


figure 7·6 : Measuring circuit - block diagram

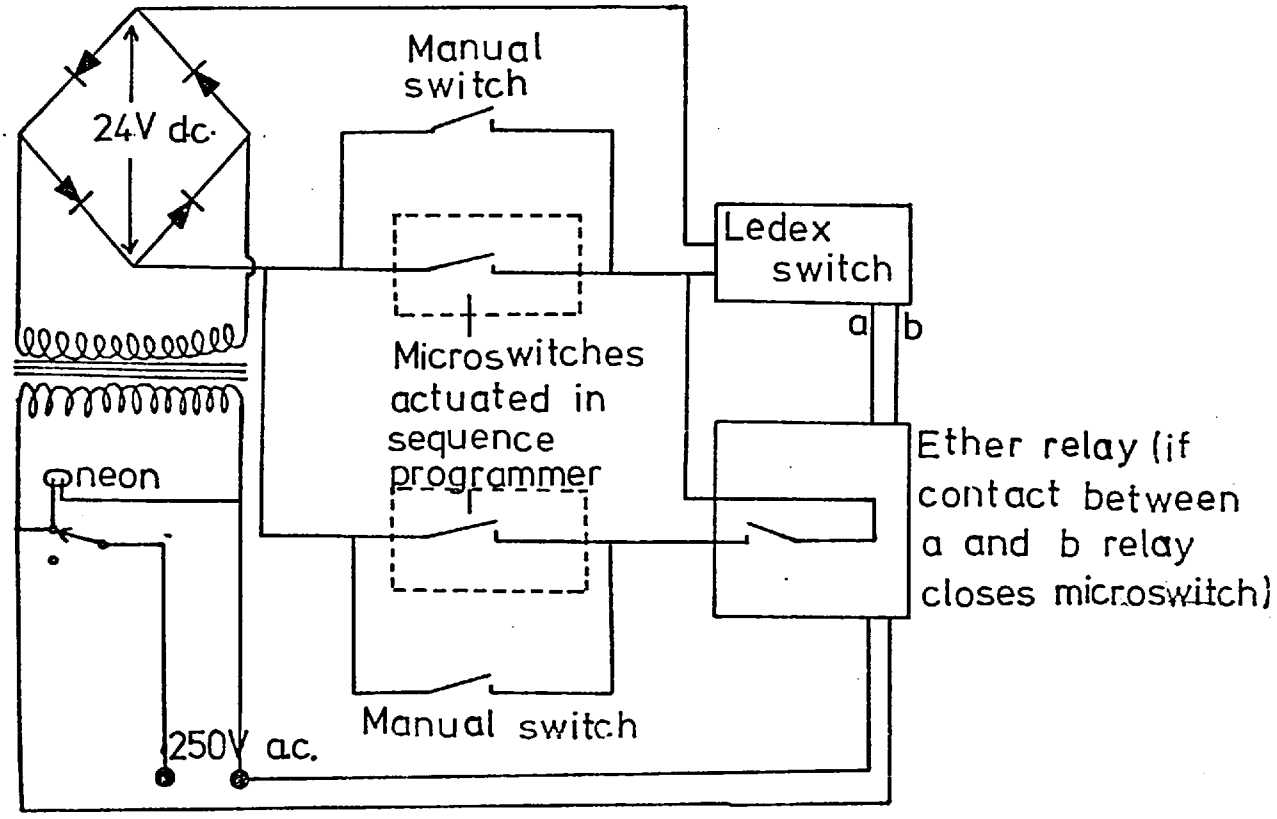


figure 7·7 : Control circuit for Ledex switch

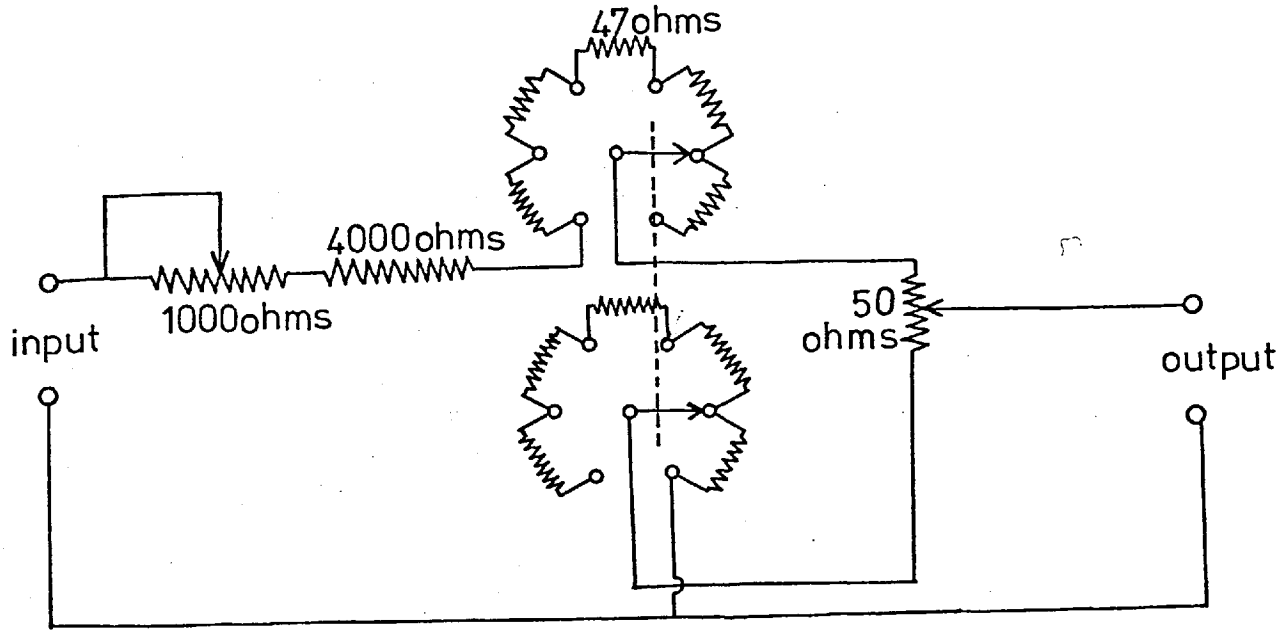


figure 7·8 : Circuit of resistive network

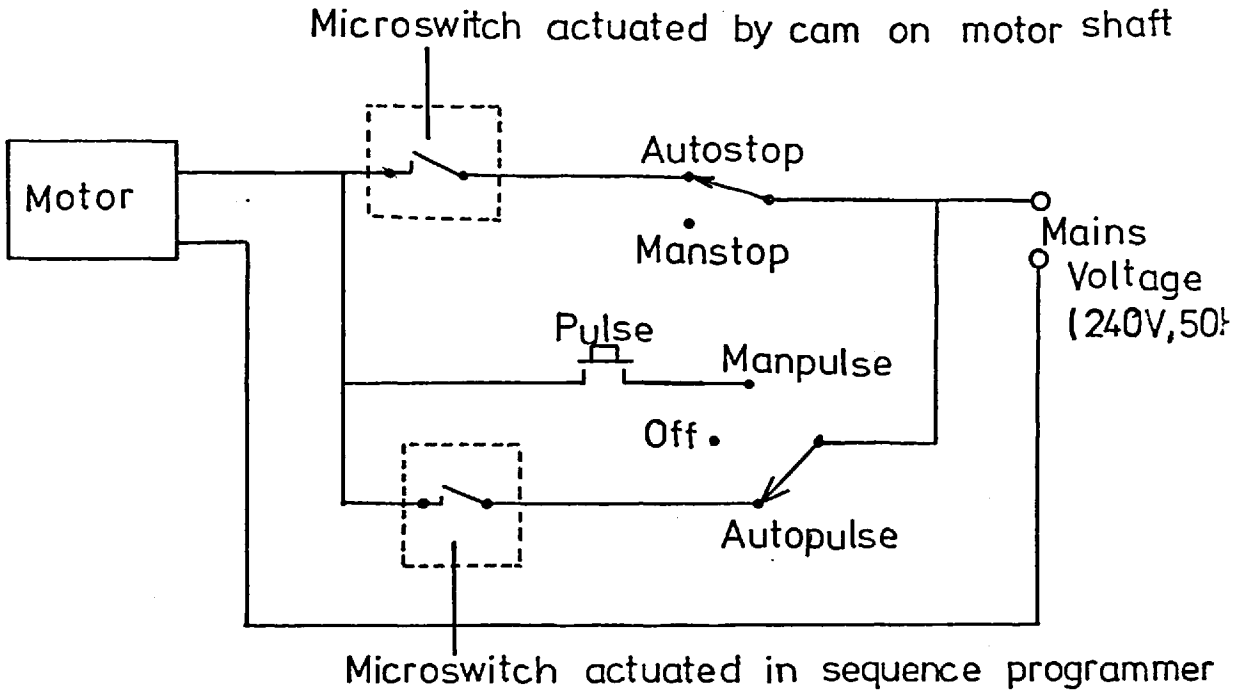
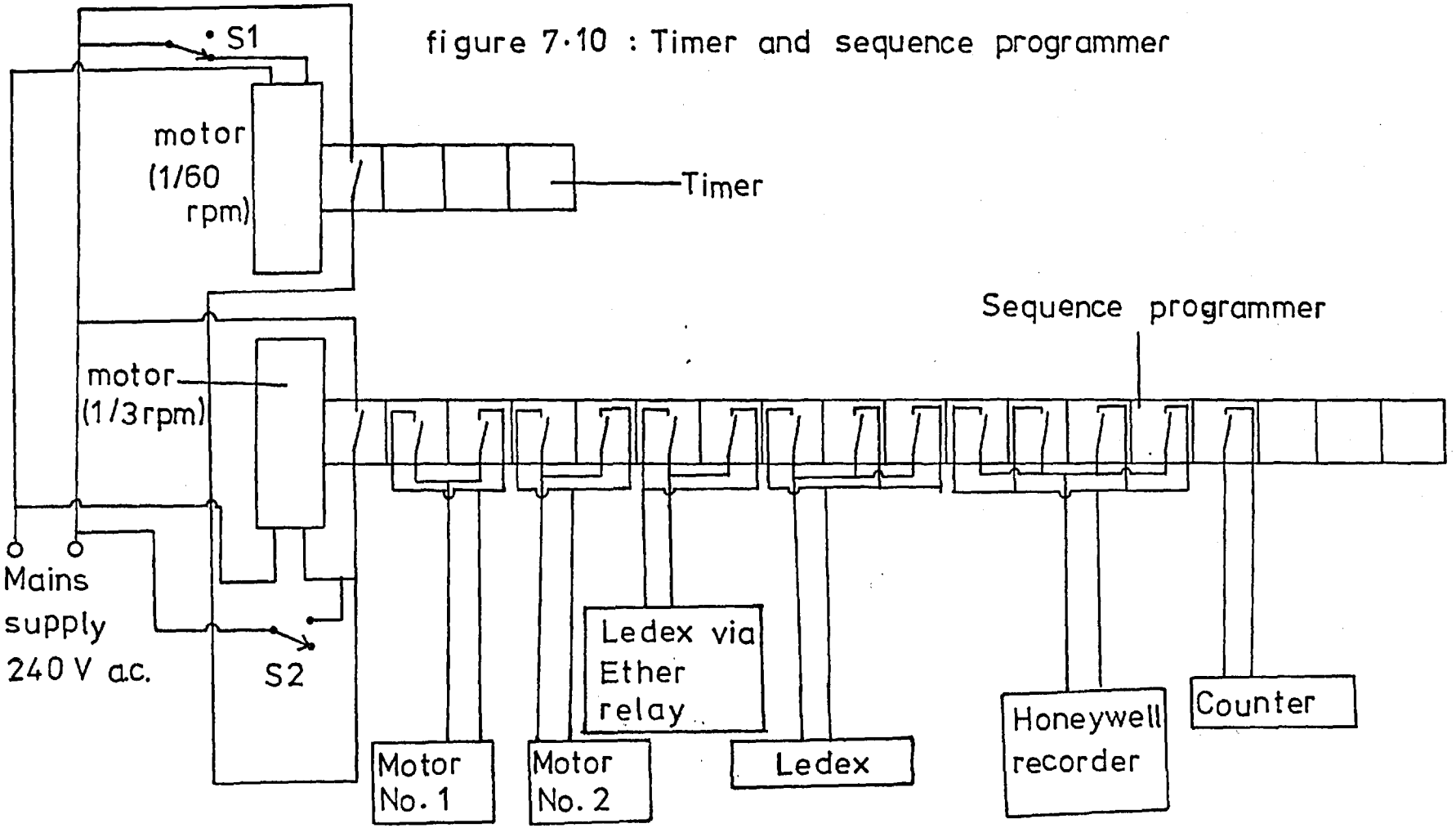


figure 7·9 : Extension control circuit

figure 7·10 : Timer and sequence programmer



The Honeywell recorder has been slightly modified so that printing can be controlled externally, that is the recorder prints one point when an external contact is made; the recorder can also be operated continuously in the usual way.

The overall control centre of the apparatus is the "sequence programmer". This is an electric motor with a speed of 1/3 r.p.m.; on the drive shaft of the motor are 18 plastic, adjustable cams which depress a set of microswitches as the shaft rotates. By setting the cams correctly the unit can be made to depress the microswitches in a desired order and for desired intervals of time. These units can thus be used to control any process comprising a sequence of different operations; they are used commercially in vending and automatic washing machines. In this instance the unit is used to operate the motors used to extend the samples in the relaxometer, to actuate the Ledex switch so that the required transducer is connected to the transducer meter, to control the printing mechanism of the Honeywell recorder and to pulse two electromagnetic counters which record the number of experimental points taken. One complete revolution of the programmer represents a complete run through the measuring sequence of the apparatus. The sequence programmer is started by a pulse from another motor and microswitch assembly that acts as a timer (this second assembly has a speed of 1/60 r.p.m.), when the programmer has completed one revolution it switches itself off, the measuring sequence being restarted on receipt of another pulse from the timer. The timer and sequence programmer are shown in figure 7.10.

The control circuit for the Ledex switch is shown in fig. 7.7, the switch may be operated in two ways. If pulsed directly the switch moves on one position, alternatively it can be pulsed via another relay which causes the switch to step on one position if there is contact between leads a and b, if after stepping there is still contact between a and b the switch will step on one more position; this will continue until the switch finds a position in which there is no contact between a and b. One of the wafers of the Ledex switch is used to provide contact between a and b, this wafer is wired so that when pulsed via the Ether relay, the switch will step on until in the position where number 1 transducer is connected to the transducer meter.

Pulsing of the Ledex switch in either mode of operation can be done manually or by the sequence programmer.

The control circuit for the motors used to extend the rubber samples in the relaxometer is shown in fig. 7.9. The switches allow the motors to be operated automatically, by the sequence programmer, or manually, by depression of the "pulse" switch. The Manpulse/off/autopulse switch is switched to "autopulse" for automatic operation and to "manpulse" for manual operation. The Autostop/manstop switch allows the motor to run until stopped by the cam mounted on the drive shaft (see section 7.1.1), when the switch is at "autostop", or until the pulse ends, when the switch is at "manstop". This second option allows the extension in a continuous experiment to be set manually by depressing the "pulse" switch until the desired extension is obtained.

In a continuous experiment the "manpulse" option is used and the sample extended either to the preset value

determined by the cam (26) of the relaxometer by using the "autostop" option, or to any desired extension using the "manstop" option described above. Once extended the manpulse/off/autopulse switch is set to "off" and the sample retained in the stretched condition for the duration of the experiment.

In an intermittent experiment the switches are set to "autopulse" and "autostop" respectively and so the sample is stretched and retracted at regular intervals to the same preset extension as required for the experiment, these actions being controlled by the sequence programmer. The interval used for intermittent experiments was one hour although there are sufficient microswitches on the timer to use intervals of 15 or 30 minutes if required.

The sequence programmer and control circuits etc, cause the following sequence of operations to take place.

1) Return Ledex to position with transducer 1 connected to the transducer meter.

2) Print two points on the Honeywell recorder, the output from transducer 1 and the termperature inside furnace 1.

3) Switch Ledex on one position so that transducer 2 is connected to the transducer meter.

4) Repeat step 2 for transducer 2 and furnace 2.

5) Close the microswitch that will start the extension motor in relaxometer 1 provided the motor control circuit is set for an intermittent experiment; if this is the case, the rubber sample will be extended.

6) Repeat step 1.

7) Repeat step 2.

8) Repeat step 5, if an intermittent experiment is being done this will cause the retraction of the rubber sample in relaxometer 1.

9) Repeat step 3.

10) Repeat step 5 for relaxometer 2.

11) Repeat step 4.

12) Repeat step 8 for relaxometer 2.

13) Switch the Ledex on one position, there is now no transducer connected to the transducer meter but the terminals are shorted out so that zero output is fed to the transducer meter.

14) Pulse Counters

15) Stop sequence programmer.

This measuring sequence will be repeated when the sequence programmer is pulsed again by the timer after an interval of one hour.

The output obtained on the recorder gives one point and a zero check (i.e. the output obtained from the transducer when the sample is in the relaxed state) every hour for an intermittent experiment and two points per hour for a continuous experiment (see figs. 7.11(c) and 7.11(a) respectively).

If only one relaxometer is being operated continuously the timer and sequence programmer can be switched off, the correct transducer connected to the transducer meter using the manual controls for the Ledex switch, and the Honeywell recorder operated in the usual, continuous mode. A continuous force vs time plot will be obtained such as is shown in figure 7.11 (b).

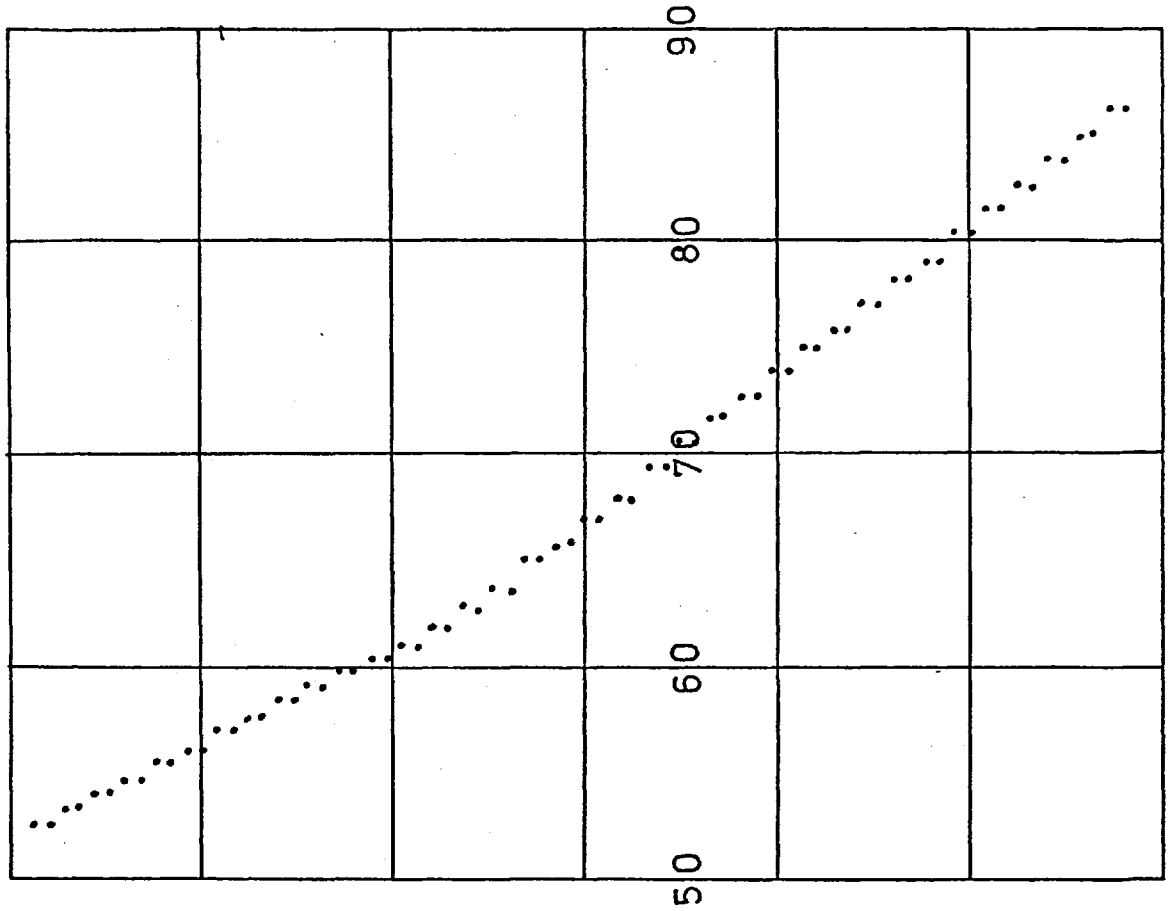


figure 7·11(a): Continuous relaxation of Adiprene CM (recorder pulsed by sequence programmer)

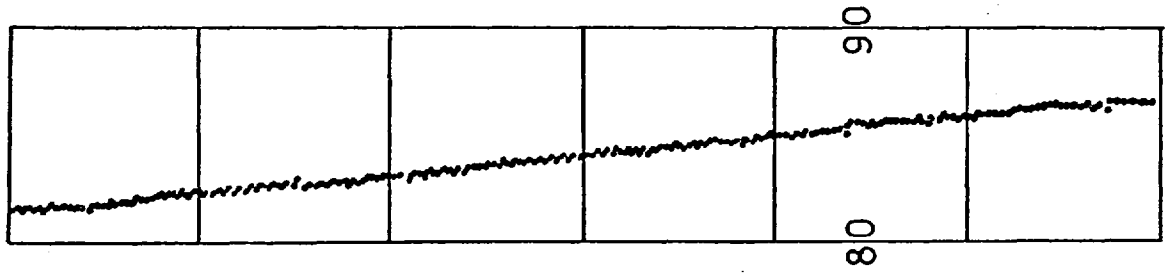


figure 7·11(b): Continuous relaxation of Adiprene CM (recorder running continuously at 1inch/hour)

figure 7·11(c); Intermittent relaxation of Genthane S

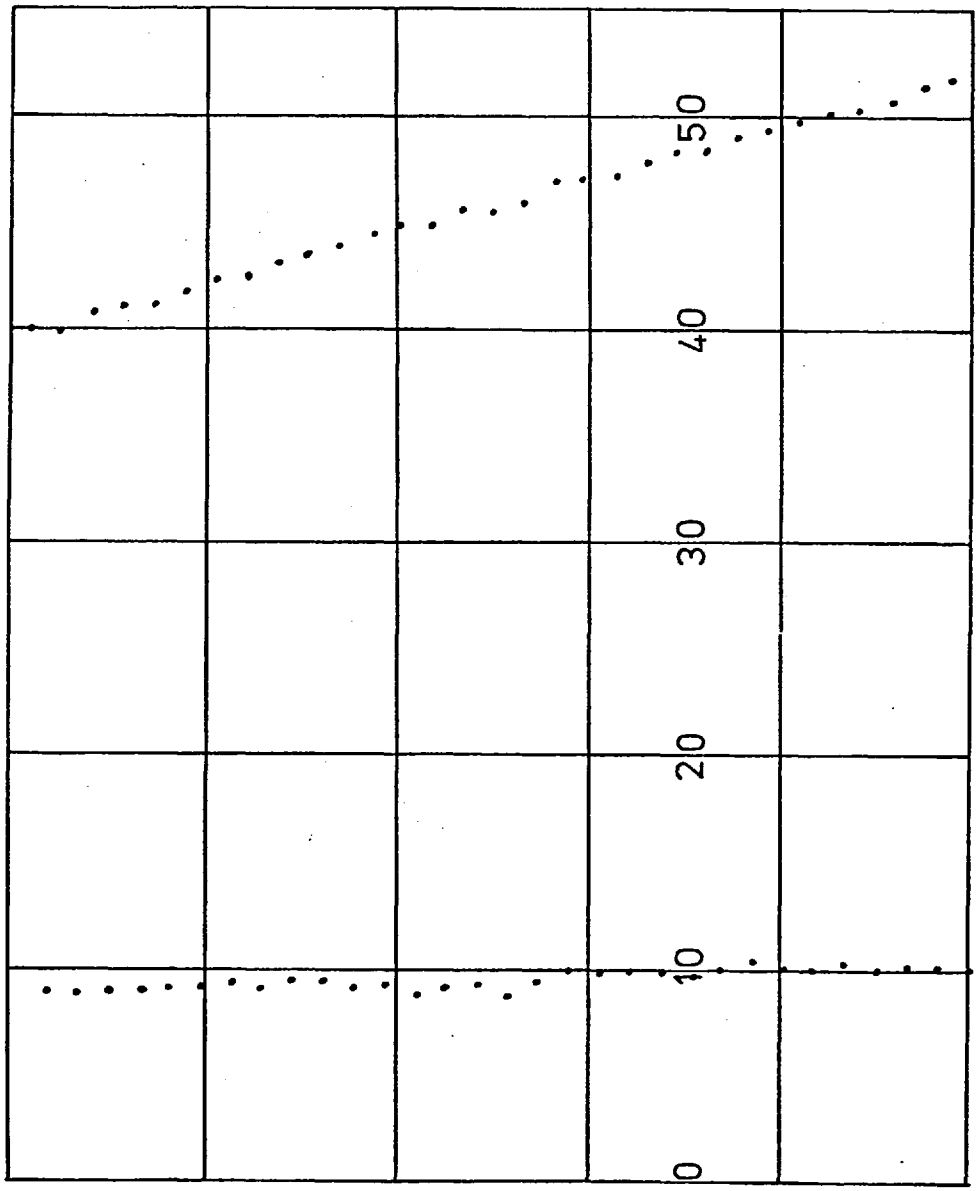


Figure 7.11 shows that the system as a whole gave quite acceptable relaxation curves in the sense that there was very little scatter of points even in the intermittent relaxation experiments.

(7.2) CHEMICAL STRESS RELAXATION OF ADIPRENE CM AND GENTHANE S

(7.2.1) Continuous and Intermittent Stress Relaxation of Genthane S in Air

Continuous stress relaxation measurements on Genthane S in air were made at temperatures of 80-150°C. The results are shown in fig. 7.12 as a first order plot (i.e. ln f_t/f_0 vs t). In common with previous results [18,19,197] the first order plots are curved; Tobolsky [197] has treated this type of result using a multi-exponential equation (eqn. 3.80, section 3.5.2) and a plot using Tobolsky's procedure is shown in fig. 7.13. A two term equation gave good straight lines over the range 80 - 150°C.

Figure 7.14 shows the data plotted according to the second order equation (eqn. 3.79, section 3.5.2), excellent straight lines are again obtained except for a small amount of curvature at short times.

Figures 7.15 and 7.16 show the Arrhenius plots obtained from the multi-exponential and second order analyses. The points for the short time or weak bond relaxation are widely scattered and the best line through these points is parallel to the line through the points for the long time or strong bond relaxation. The second order analysis leads to a good straight line in the Arrhenius plot, the slope of which is different from the slopes of the lines obtained from the Tobolsky analysis. According to the Tobolsky analysis, relaxation is due to the scission of two types of bond, each

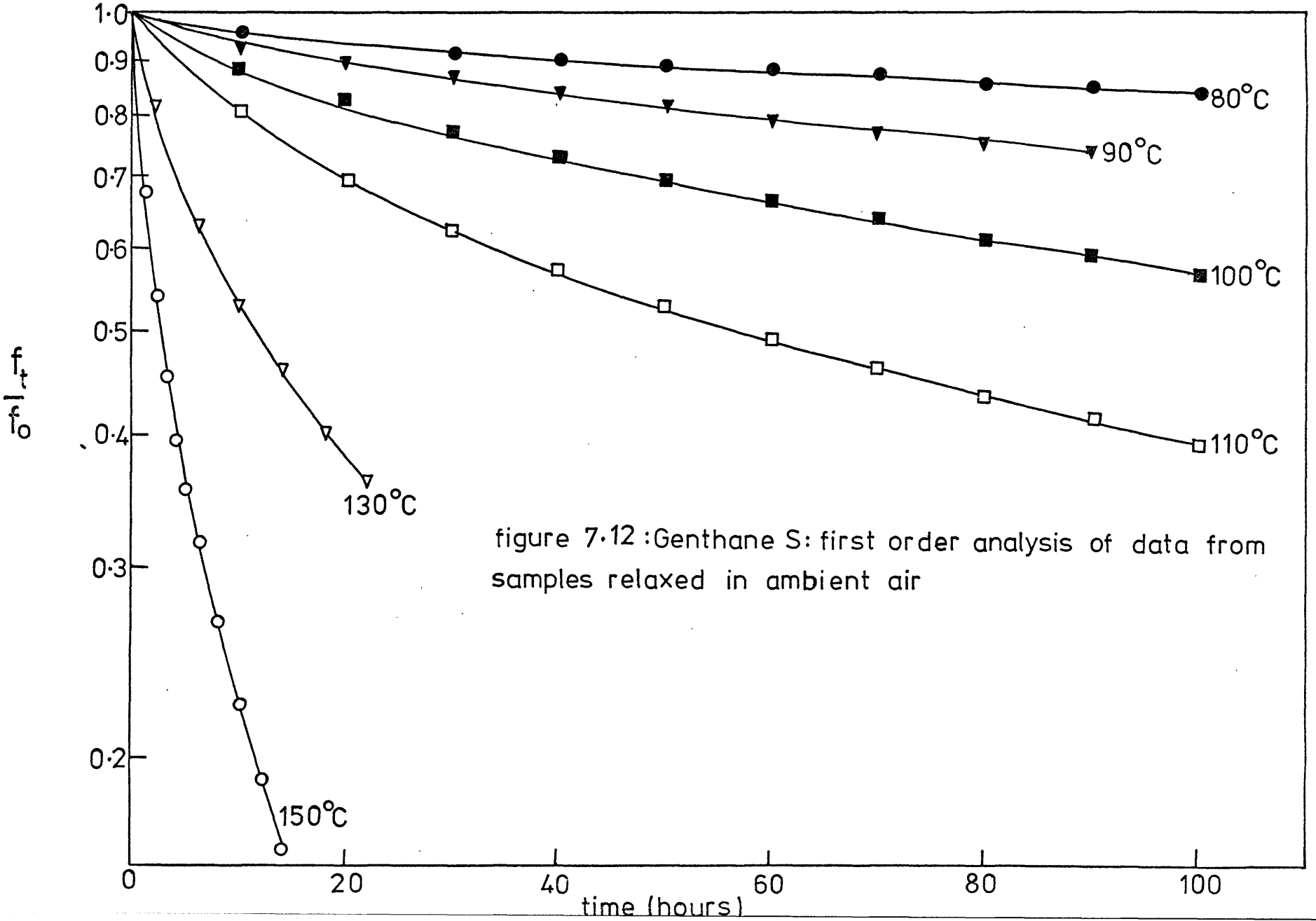


figure 7·12 : Genthane S: first order analysis of data from samples relaxed in ambient air

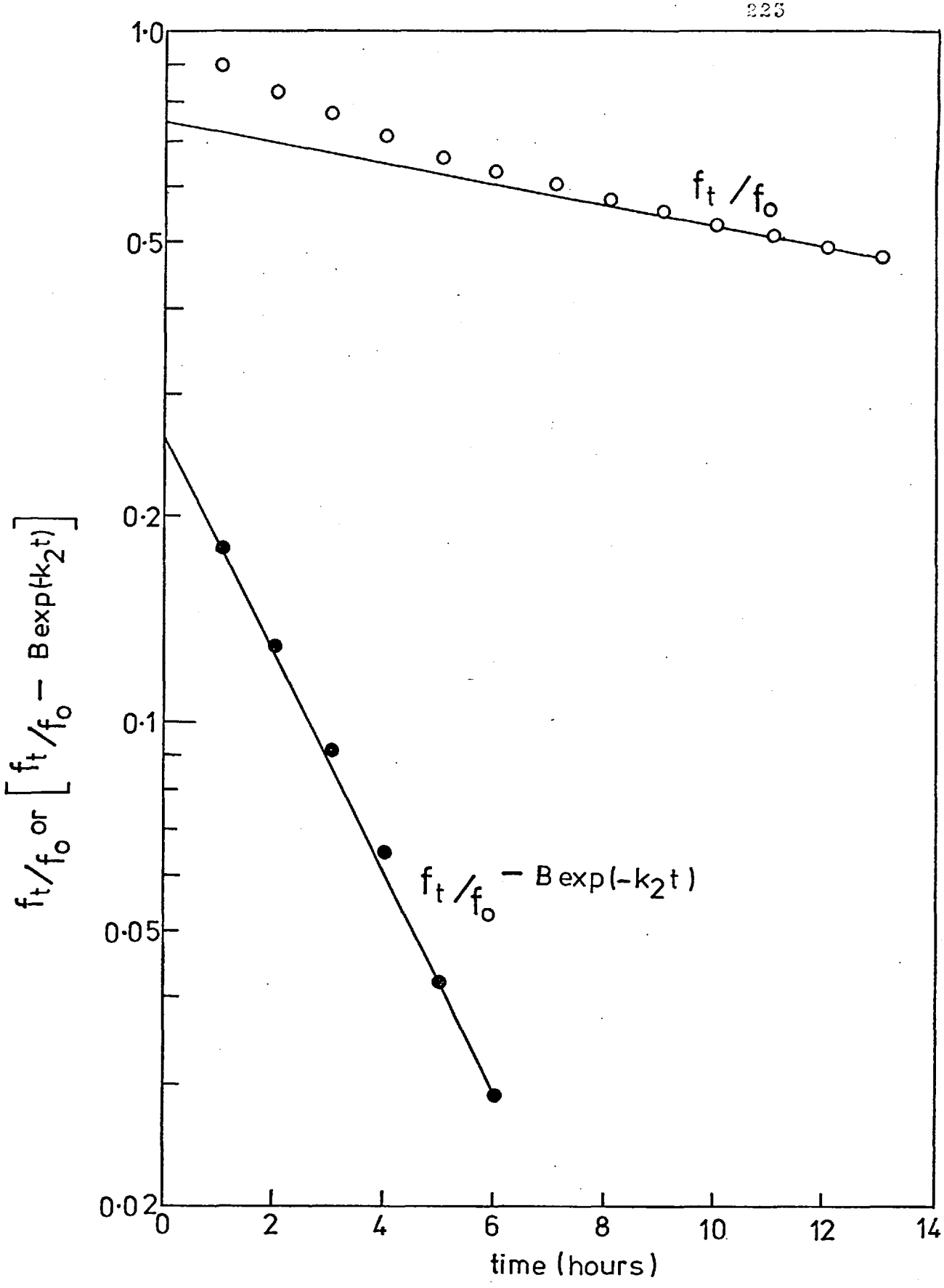


figure 7·13 : Genthane S: Tobolskys "Procedure X" analysis of data from sample relaxed in ambient air at 130°C

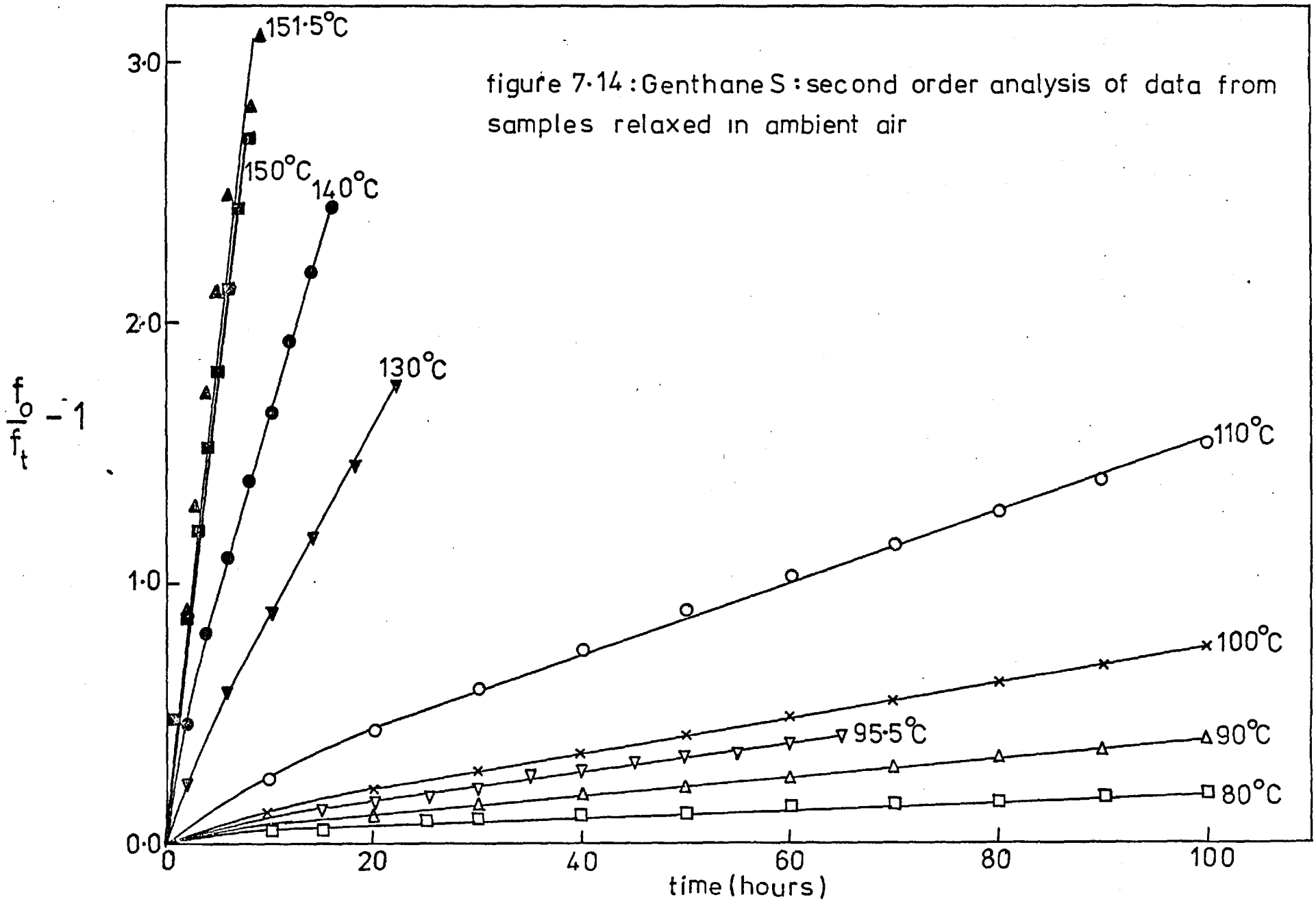


figure 7·14 : Genthane S : second order analysis of data from samples relaxed in ambient air

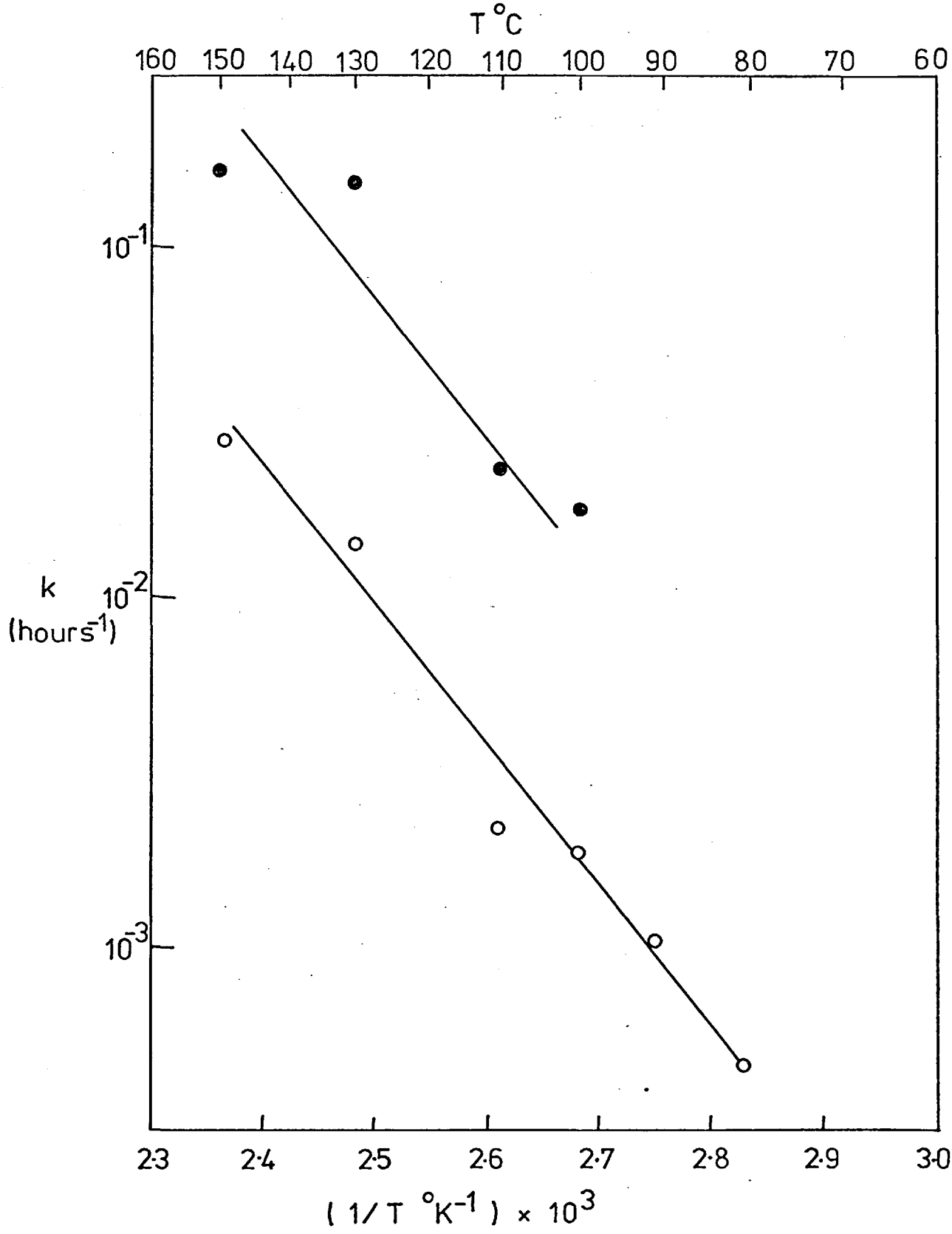


figure 7·15 : Arrhenius plot of the first order rate constants for the continuous relaxation of Genthane S in air (o- strong bond, o-weak bond)

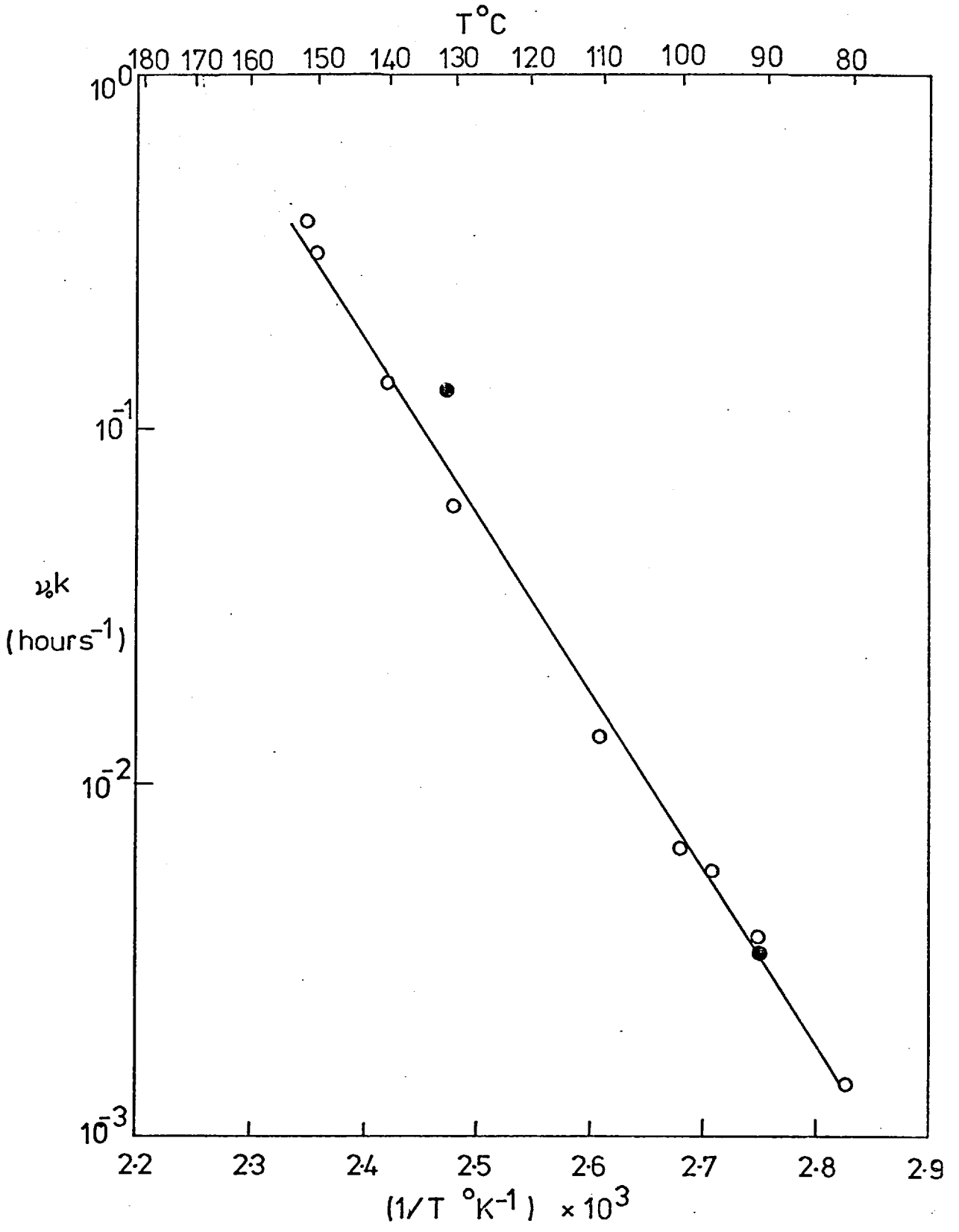


figure 7·16: Arrhenius plot of the second order rate constants for the continuous relaxation of Genthane S (o - ambient air, ● - nitrogen)

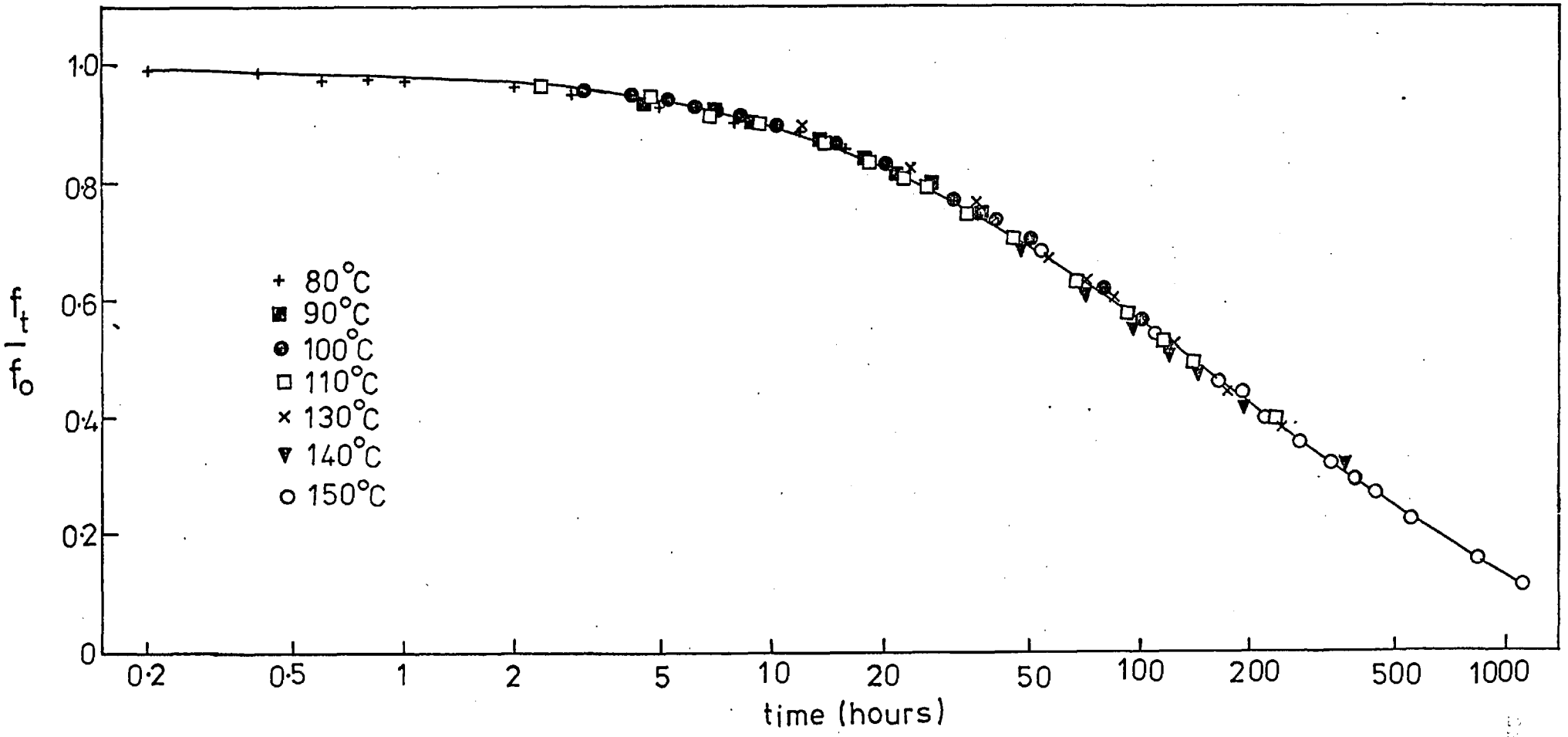


figure 7·17 : Master curve for the continuous relaxation of Genthane S in ambient air at 100°C

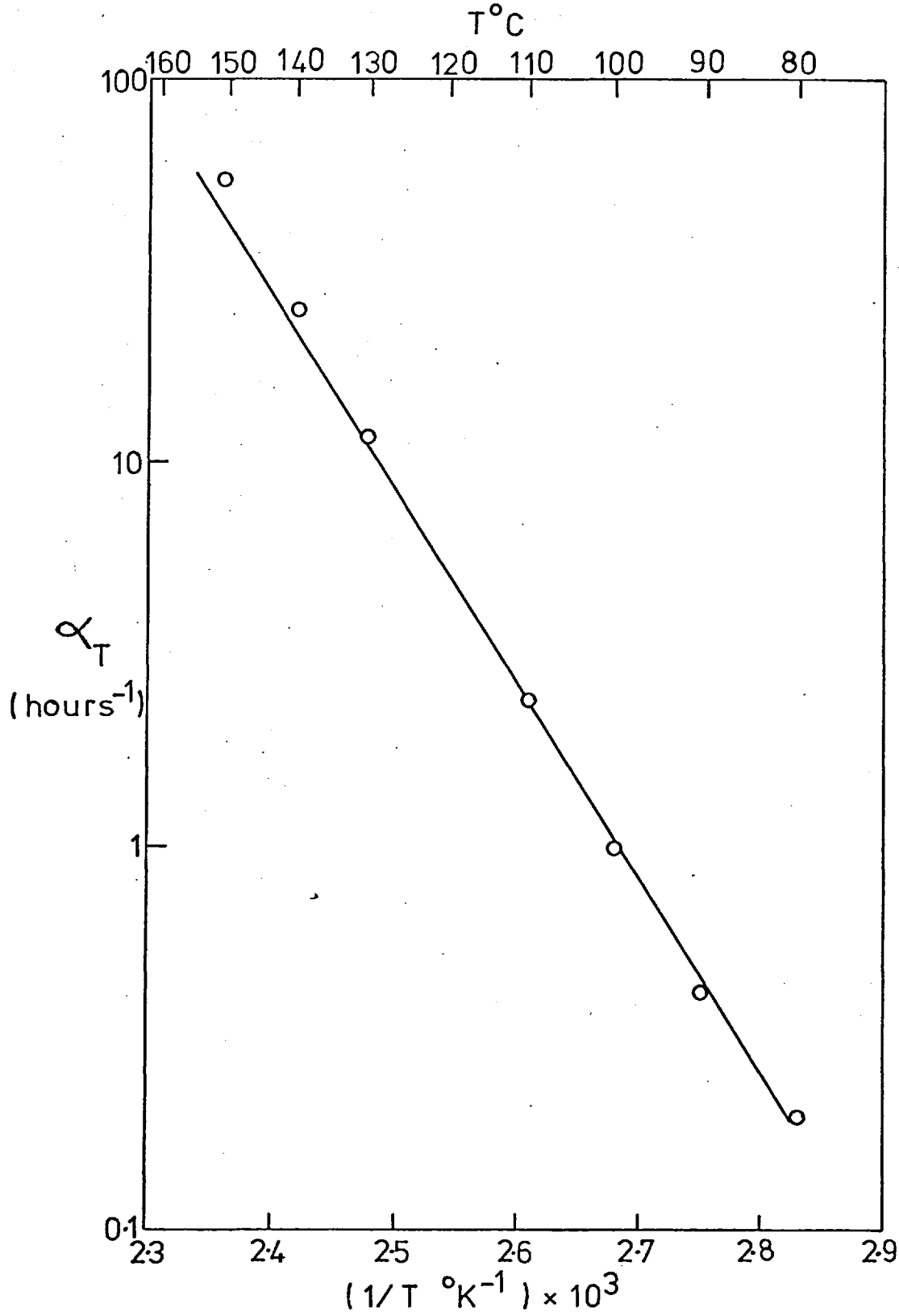


figure 7·18: Arrhenius plot of shift factors, α_T, required to produce a master curve for the relaxation of Genthane S in air at 100°C

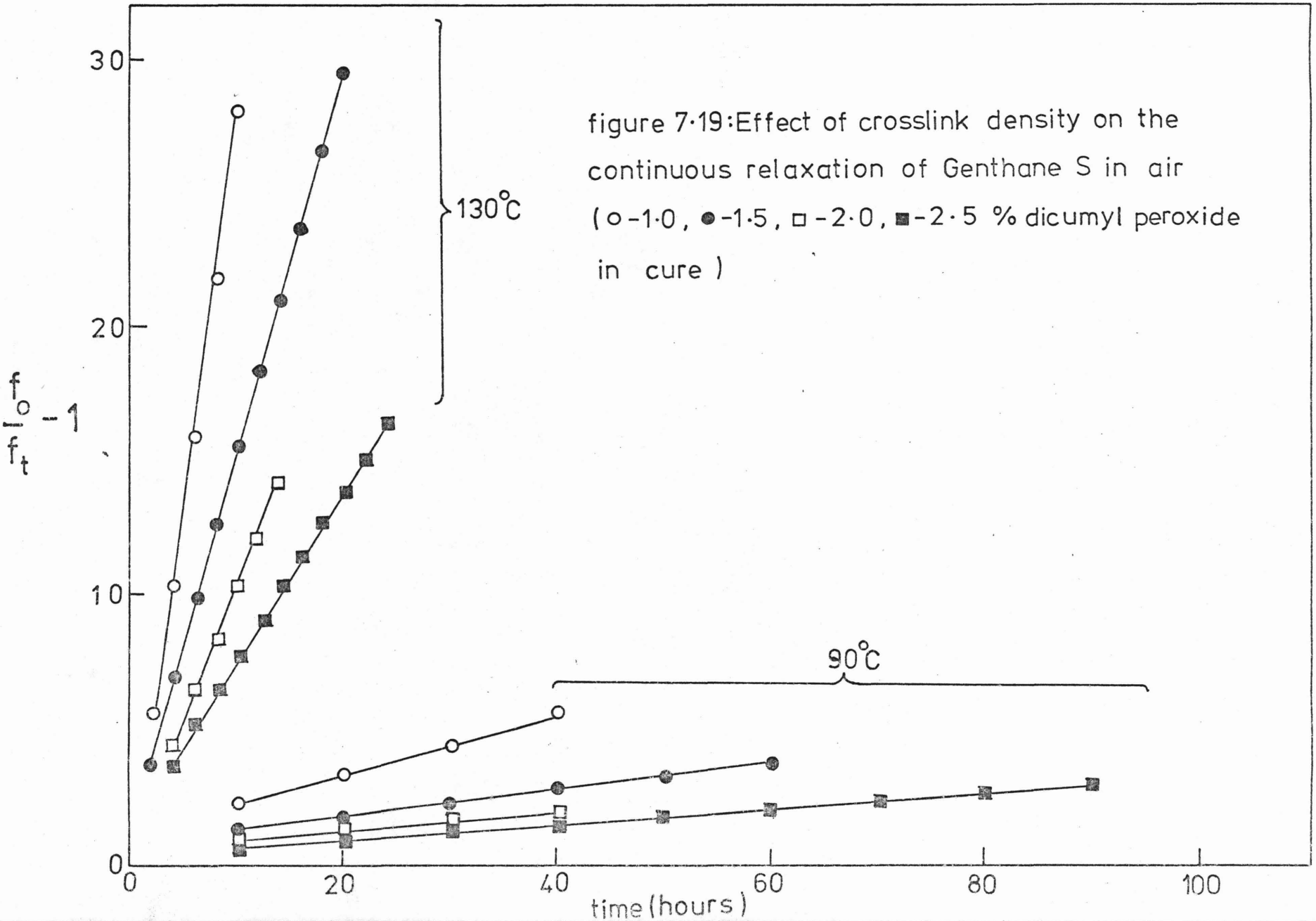


figure 7·19: Effect of crosslink density on the continuous relaxation of Genthane S in air (o - 1·0, ● - 1·5, □ - 2·0, ■ - 2·5 % dicumyl peroxide in cure)

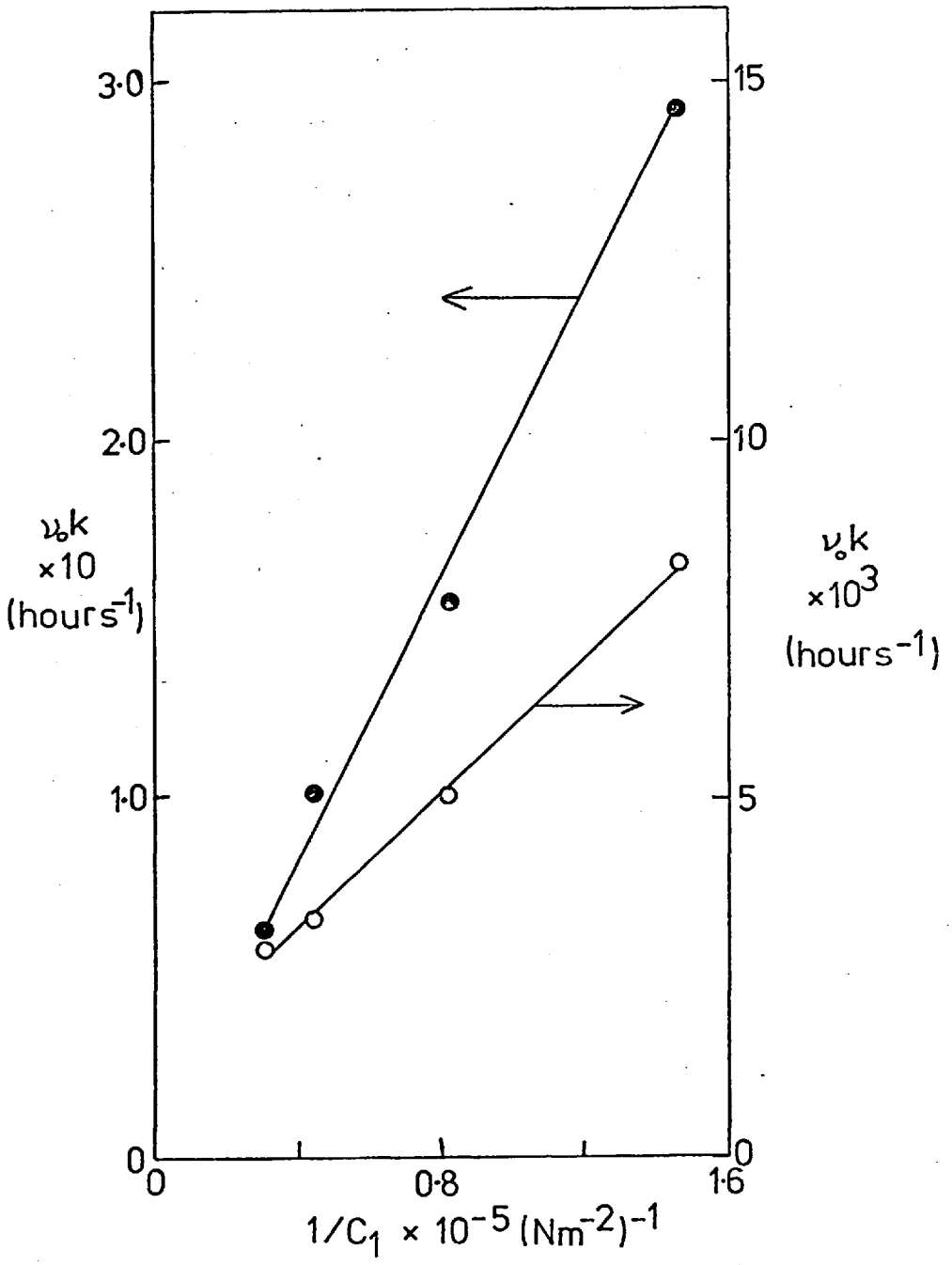


figure 7·20: Genthane S - Effect of crosslink density on relaxation rate (● at 130°C, o at 90°C)

of which give the same activation energy (see table 7.2) so that the differences in the cleavage rates lie in the different pre-exponential factors. The second order analysis shows that the whole relaxation curve can be described in terms of a single rate constant which gives an activation energy that is different to that obtained from Tobolsky's analysis.

The data can be analysed in a third manner, using the time-temperature superposition method (section 3.5.4); the relaxation curves superposed to give a master curve (fig. 7.17) and the shift factors, α_T, gave a good Arrhenius plot (fig. 7.18) The activation energy obtained was the same as that obtained from the second order analysis indicating that this approach is correct whilst that employed by Tobolsky is not. The activation energy obtained from the time-temperature superposition analysis is given in table (7.2).

Continuous relaxation measurements on Genthane S in air were conducted on samples with different initial crosslink densities at 90°and 130°C to determine whether scission took place in the main chain or at the crosslink. A linear relationship between the rate of relaxation and the reciprocal of the crosslink density was obtained (figs. 7.19 and 7.20) indicating that cleavage took place in the main chain (see sections 3.3.1 and 3.3.2).

Intermittent stress relaxation experiments were conducted on Genthane S in air at 80 - 150°C, these were analysed according to the two network theory (section 3.2) andplots of Δ vs log t obtained (fig. 7.21). These curves superposed to give a master curve (fig. 7.22). Points interpolated from the master curve gave a good straight line when plotted

TABLE 7.1

Rate Constants for Continuous Relaxation of Genthane S

$T^{0}C$	$1/T \times 10^{3}$ (K^{-1})	Tobolsky's procedure X				$k \times 10^{3}$ (hrs^{-1})	α_T
		weak bond		strong bond			
		A	$k \times 10^{2}$ (hrs^{-1})	B	$k \times 10^{3}$ (hrs^{-1})		
80	2.83	-	-	0.95	1.31	1.44	0.200
90	2.75	-	-	0.94	3.01	3.62	0.425
95.5	2.72	-	-	-	-	5.61	-
100	2.68	0.14	4.34	0.82	3.53	6.55	1.00
110	2.61	0.29	5.50	0.67	5.45	13.5	2.38
130	2.48	0.26	35.9	0.74	34.1	59.4	11.8
140	2.42	-	-	-	-	134	25.0
150	2.36	0.34	38.5	0.44	69.7	311	55.5
151.5	2.35	-	-	-	-	380	-

TABLE 7.2

Activation Energies for Scission and Crosslinking of Genthane S

Process	Method of Analysis	Δ H kJ $mole^{-1}$
Scission Reaction	Tobolsky { weak bond	77.5
	Tobolsky { strong bond	77.5
	Second Order Plot	94.6
	Time-temperature super pos'n	94.6
Crosslinking Reaction	Time-temperature super pos'n	107.9

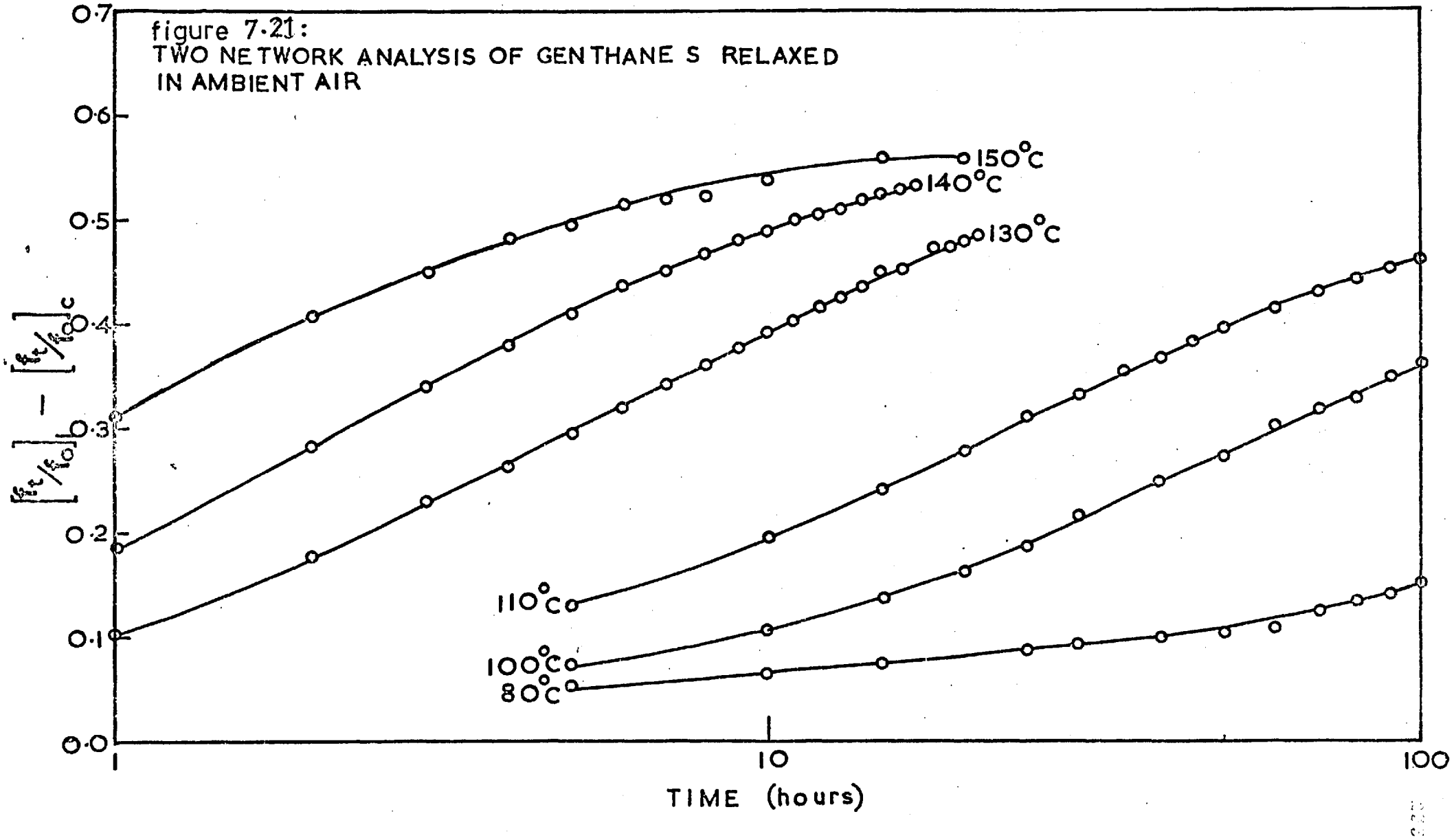
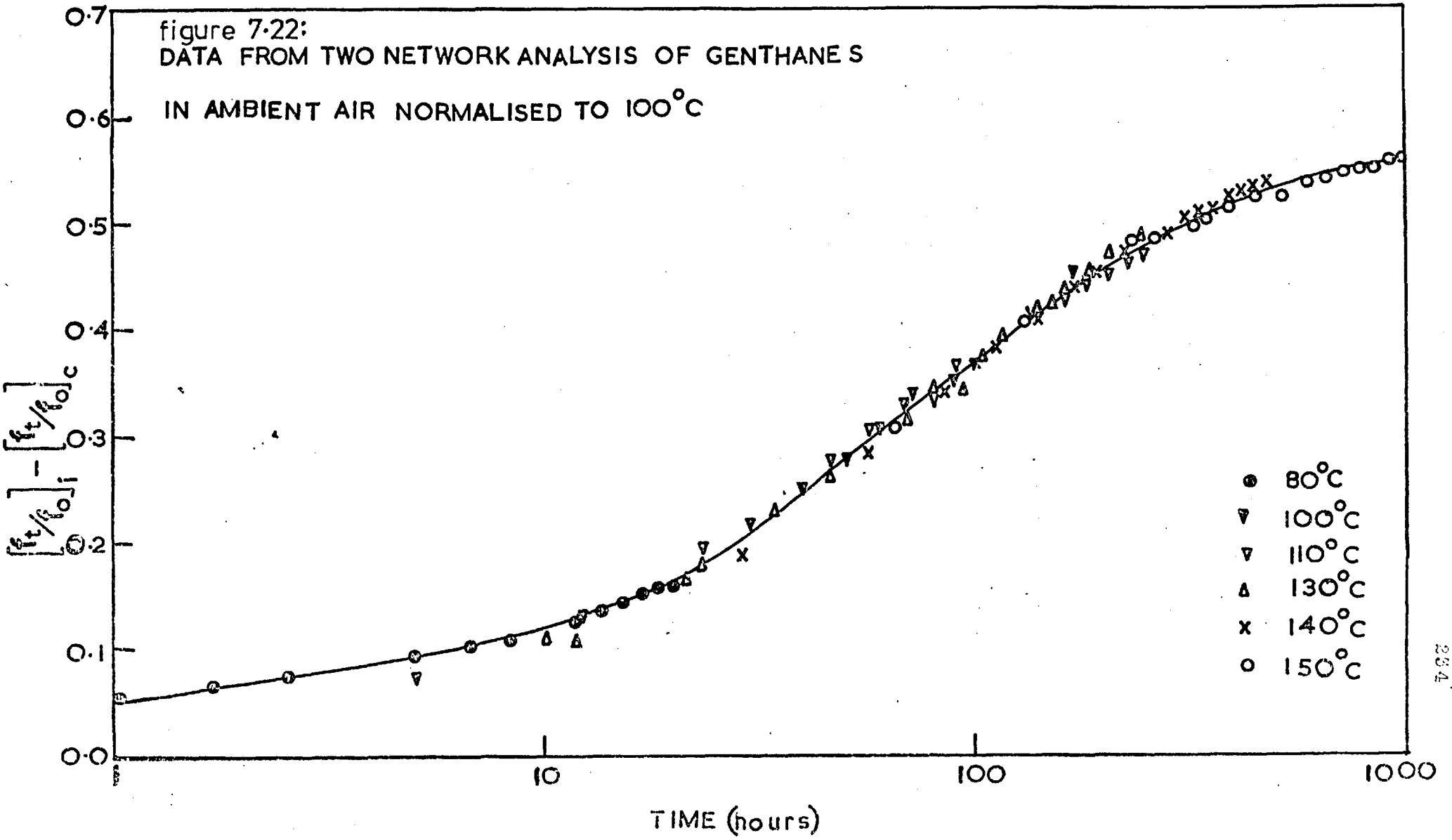

figure 7·21:
TWO NETWORK ANALYSIS OF GENTHANE S RELAXED
IN AMBIENT AIR
0·7
0·6
0·5
0·4
0·3
0·2
0·1
0·0
150°C
140°C
130°C
110°C
100°C
80°C
1
10
100
TIME (hours)

figure 7·22:
DATA FROM TWO NETWORK ANALYSIS OF GENTHANE S

IN AMBIENT AIR NORMALISED TO 100°C



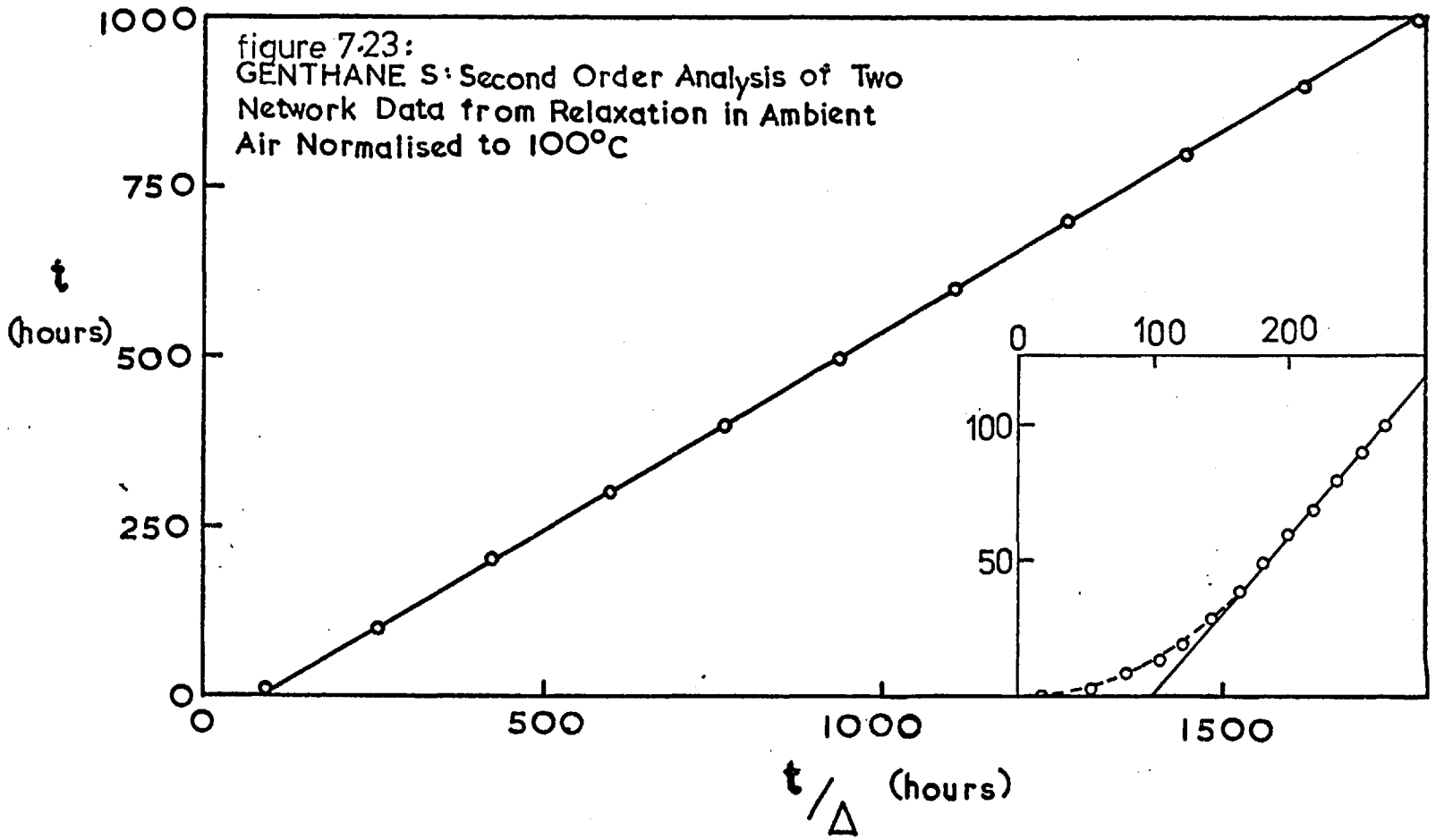


figure 7.23:
GENTHANE S: Second Order Analysis of Two Network Data from Relaxation in Ambient Air Normalised to 100°C

$$\Delta = \left[\frac{f_t}{f_o}\right]_{int} - \left[\frac{f_t}{f_o}\right]_{cont}$$

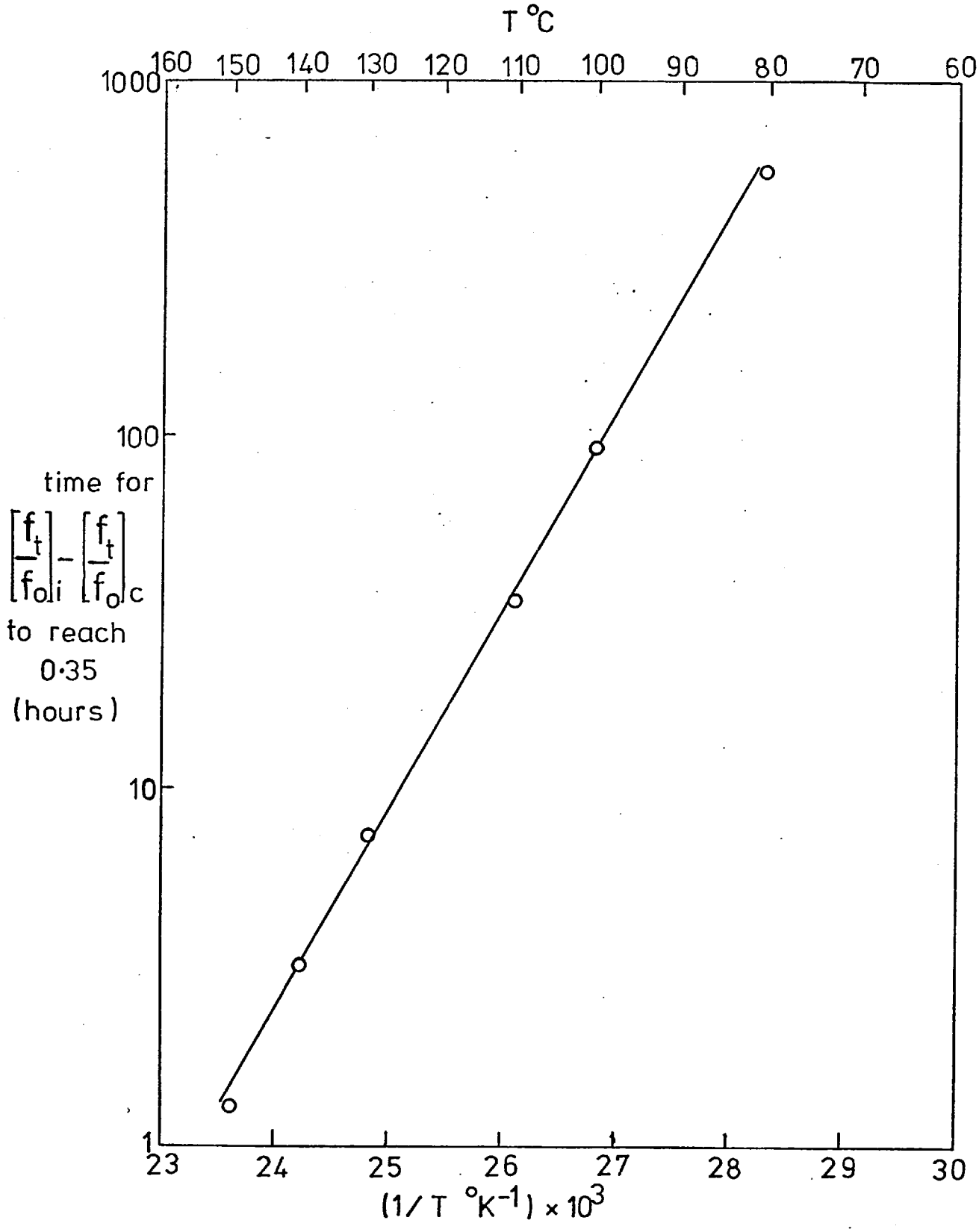


figure 7·24: Arrhenius correlation of intermittent relaxation data for Genthane S in ambient air

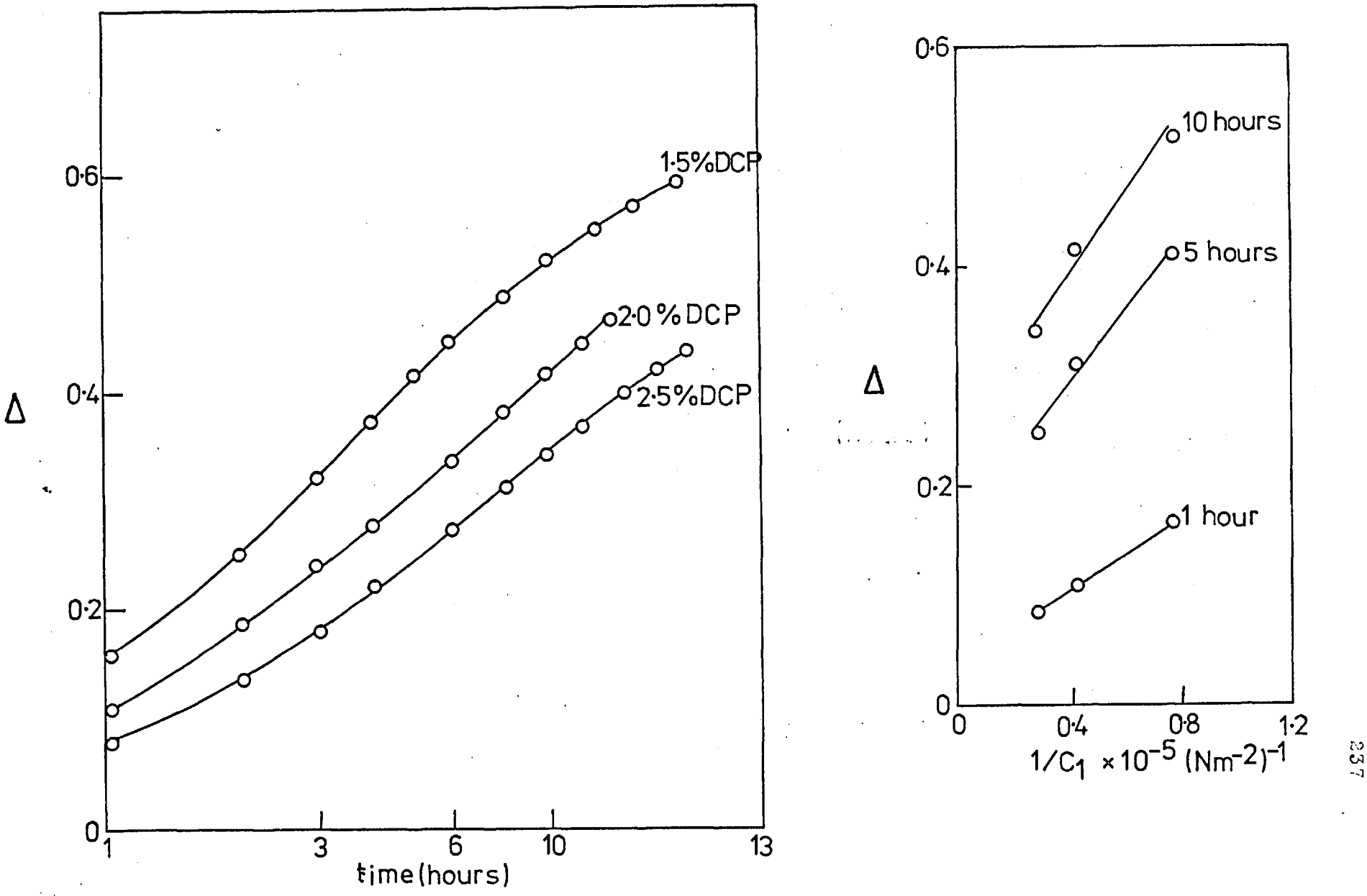


figure 7·25: Effect of crosslink density on the rate of network chain formation in Genthane S at 130°C

TABLE 7.3

Rate Data from Two Network Analysis of Continuous and Intermittent Results

$T^{\circ}C$	$1/T \times 10^{3}$ K^{-1}	Time for Δ to reach 0.35 (hours)
80	2.83	560
100	2.68	92
110	2.61	35
130	2.48	7.4
140	2.42	3.2
150	2.36	1.6

TABLE 7.4

Continuous and Intermittent Results on Genthane S Samples with Different Crosslinking Densities

$C_1 \times 10^5$ Nm^{-2}	$1/C_1 \times 10^{-5}$ $N^{-1}m^2$	Continuous		Intermittent		
		${}_0k$ at $130^{\circ}C$	${}_0k$ at $90^{\circ}C$	Δ at stated time		
				1 hr	5 hrs	10 hrs
0.48	2.08	0.296	0.0087			
1.15	0.87	0.141	0.0050	0.16	0.41	0.52
2.06	0.49	0.104	0.0035	0.11	0.31	0.42
3.00	0.33	0.065	0.0028	0.09	0.24	0.34

TABLE 7.5

Continuous Stress Relaxation of Genthane S Samples Containing Stabaxol PCD

% by weight of Stabaxol PCD	${}_0k$
0.00	0.123
0.46	0.140
0.87	0.085
1.25	0.046
1.70	0.039
3.40	0.036
10.38	0.039

according to equation (5.87) for a second order crosslinking reaction (fig. 7.23) except for a small amount of curvature at short times. The two network data were characterised by the time taken for Δ to reach 0.35. This is equivalent to $\tau_{0.35}$ (section 3.2). An Arrhenius plot of these times gave a good straight line (fig. 7.24) from which the activation energy for the process was obtained (table 7.2).

Intermittent stress relaxation experiments on samples with different initial crosslink densities (fig. 7.25) showed that the reaction leading to the formation of new network chains was independent of the original crosslink density since Δ was inversely proportional to $\nu_1(o)$.

(7.2.2) Further Experiments on Genthane S and the Effect of Additives

The results presented in section (7.2.1) showed that the reactions taking place in Genthane S in air led to a removal of network chains due to scission and to the formation of new network chains; for every 100 chains removed, 60 new chains were formed. Experiments were conducted to investigate the nature of these reactions.

Continuous stress relaxation on samples that had been soxlet extracted with hot benzene for 48 hours showed the same relaxation rate as unextracted samples implying that extractable material had no effect on the relaxation rate.

Continuous and Intermittent stress relaxation in nitrogen showed that at 130°C the rate of scission and network chain formation was slightly faster than in air (see figs. 7.26 and 7.27)

figure 7·26:
GENTHANE S: Effect of Nitrogen, and Postcure on Relaxation in Air at 130°C

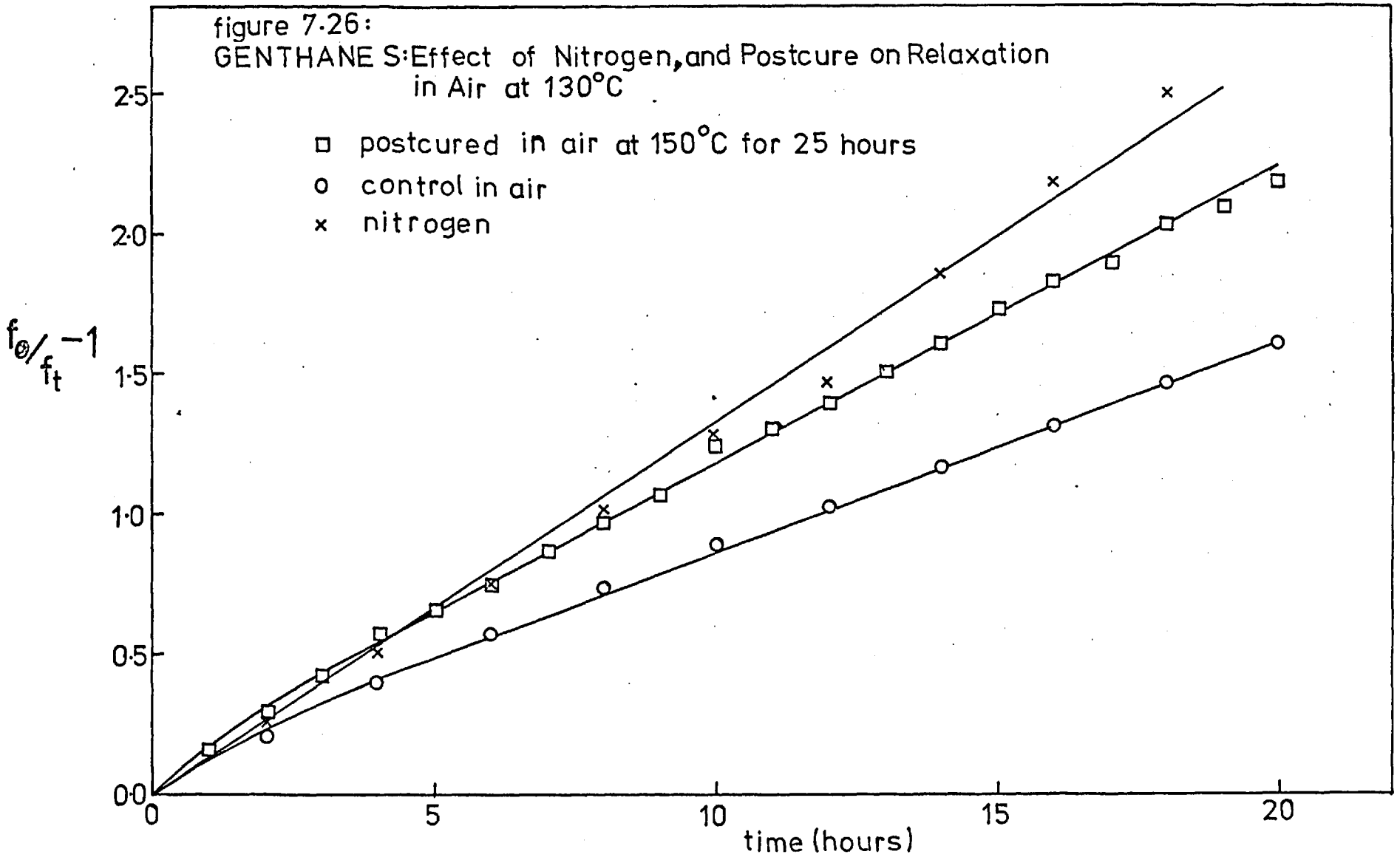
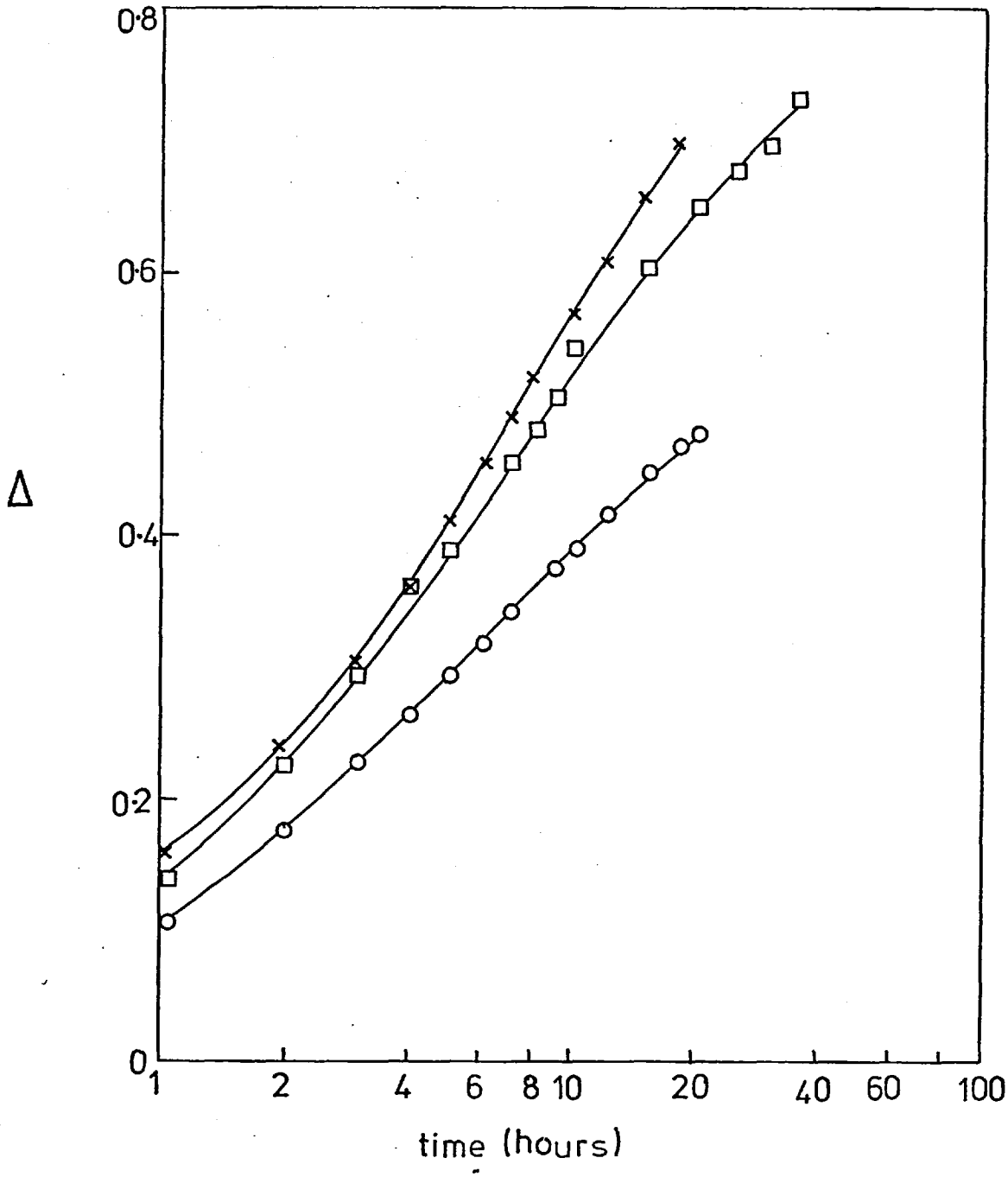


figure 7·27: Genthane S - Effect of nitrogen and postcure on the rate of network chain formation at 130°C (× nitrogen atmospere, □ postcured in air at 150°C for 25 hours and relaxed in air, ○ control in air)



The results described in section (7.2.1) indicated that if the rubber were heated at 150°C for 25 hours in air, all the original network chains would have been cut and replaced by new chains. Samples were postcured in this way after which continuous and intermittent stress relaxation experiments were conducted on them. Figures 7.26 and 7.27 show that the rate of scission and network chain formation was slightly increased over the rates obtained for unpostcured samples, however, these increased rates resulted solely from the decreased initial crosslink density of the samples. These results indicate that the network is unchanged on ageing except that the network chain density is slightly reduced suggesting that most of the cleaved chains regenerate to give a second network that is chemically identical to the first.

The results in nitrogen suggested that the cleavage and network chain formation reactions were largely non-oxidative but that there was a small amount of oxidative inhibition.

To investigate further, the effect of oxygen, continuous and intermittent stress relaxation experiments were conducted in air on Genthane S samples containing an antioxidant, an antioxidant and cispolyisoprene or cispolyisoprene on its own. The cispolyisoprene was included as an oxidisable material that would act as a convenient source of free radicals and the antioxidant used was a quinoline based material, Flectol H (Monsanto).

The rates of scission and network chain formation were unaffected by the presence of polyisoprene but they increased slightly when Flectol H was present, whether in the presence of polyisoprene or not (see figs. 7.28 and 7.29).

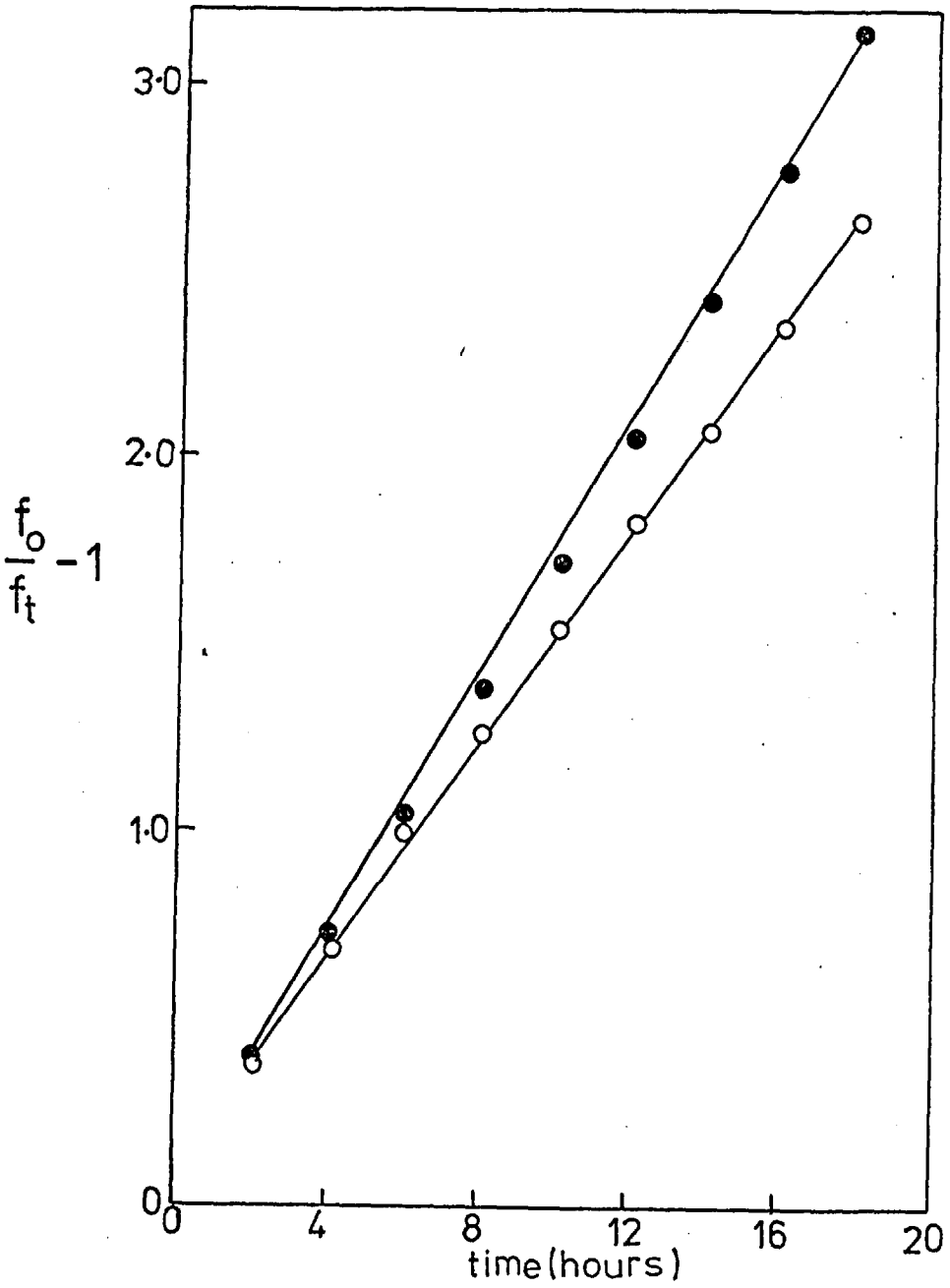
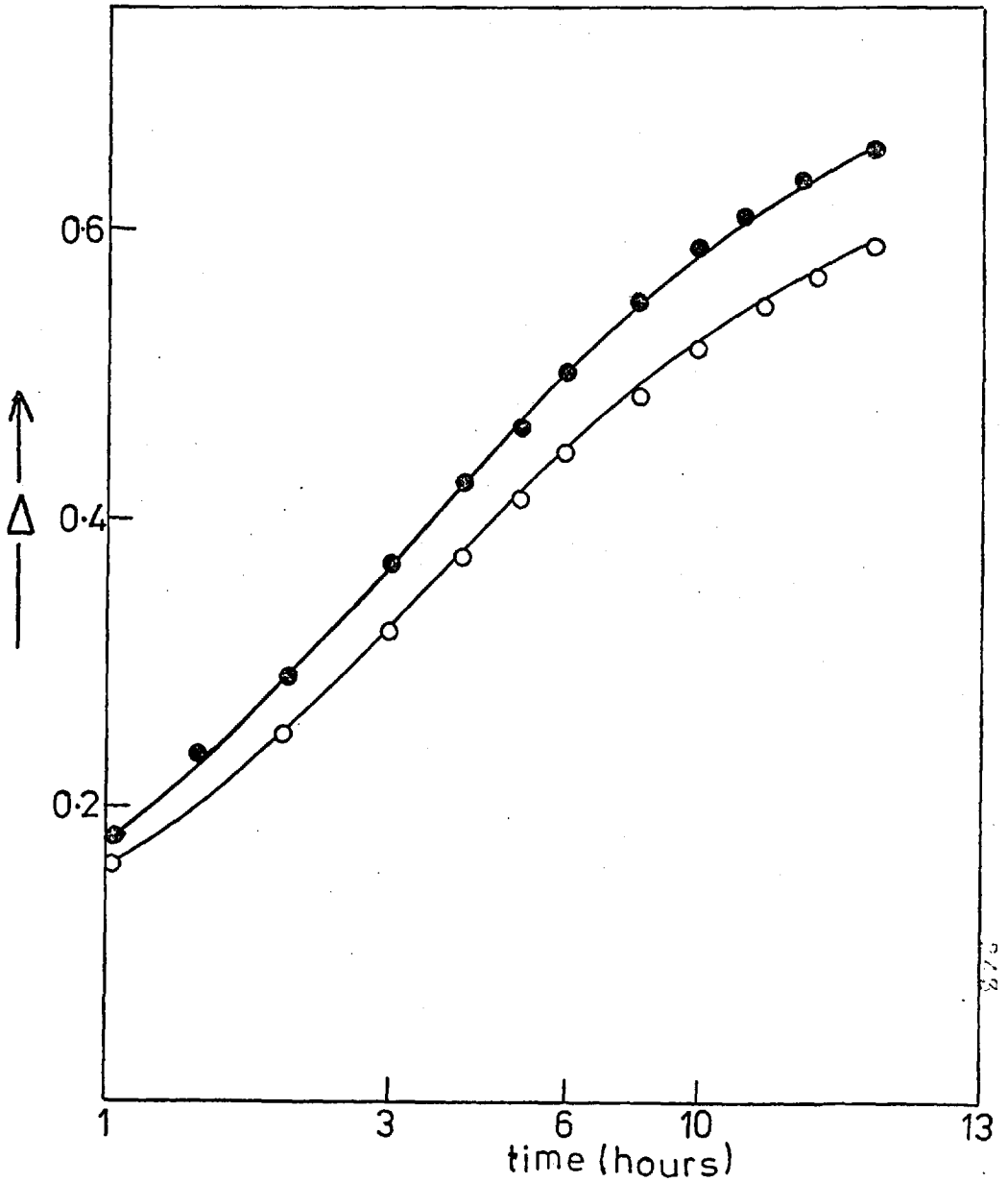


figure 7·28: Stress relaxation of Genthane S samples containing Flectol H in air at 130°C (o with FH, o without FH)



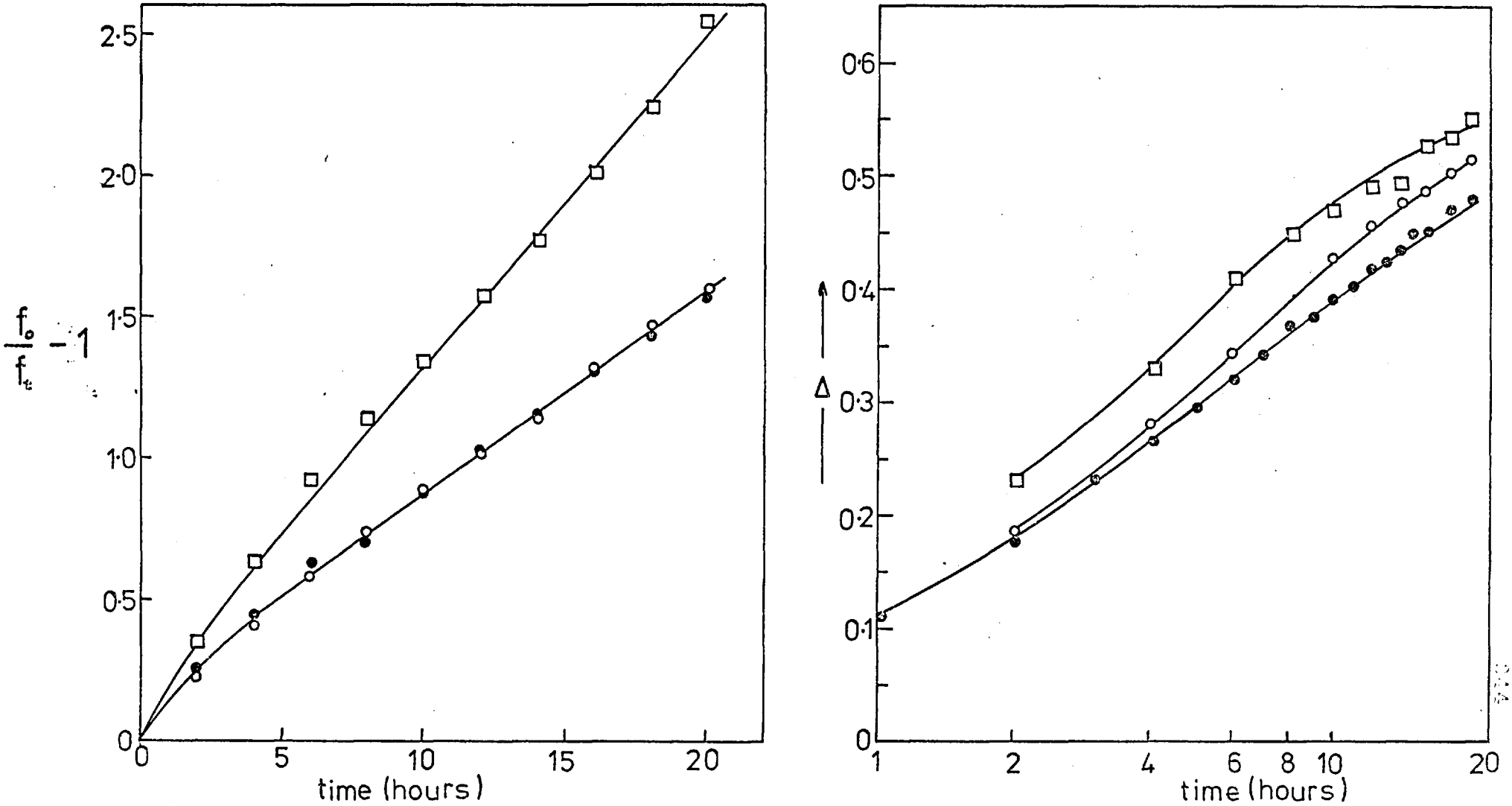


figure 7·29: Continuous and intermittent relaxation of Genthane S under oxidising conditions (● - control o - containing polyisoprene □ - containing polyisoprene and Flectol H) at 130°C

These experiments indicated that the oxidative inhibition was probably a free radical process since its rate was reduced when an antioxidant was present. Curiously it was not affected when a high concentration of free radicals was present, resulting from the oxidation of polyisoprene.

Apart from the comparatively minor oxidative inhibition discussed above, there are largely non-oxidative scission and network chain formation reactions taking place. With respect to these reactions, carbodiimides have been reported to give enhanced stability to hydrolytic attack (section 5.4.3.3), and it is possible that the non-oxidative reactions involve trace amounts of water present in the materials. Also, isocyanates have been reported [210] to give enhanced stability to thermal degradation. To investigate these effects experiments were done on samples containing a carbodiimide, Stabaxol P.C.D. (Bayer), and on samples that had been treated with phenyl isocyanate.

Treatment with isocyanate comprised swelling the rubber in phenyl isocyanate, heating the swollen sample at 130°C for 1 hour, extracting with benzene for 48 hours and removing the benzene by evacuation. Experiments were also conducted on samples treated in this way with Stabaxol P.C.D., figure 7.30 shows that a sample treated with carbodiimide in this way gave an identical relaxation curve to that containing carbodiimide but untreated.

Figures 7.30 and 7.31 show that both carbodiimide and treatment with phenyl isocyanate led to reduced rates of scission and network chain formation, phenyl isocyanate giving the more significant reduction.

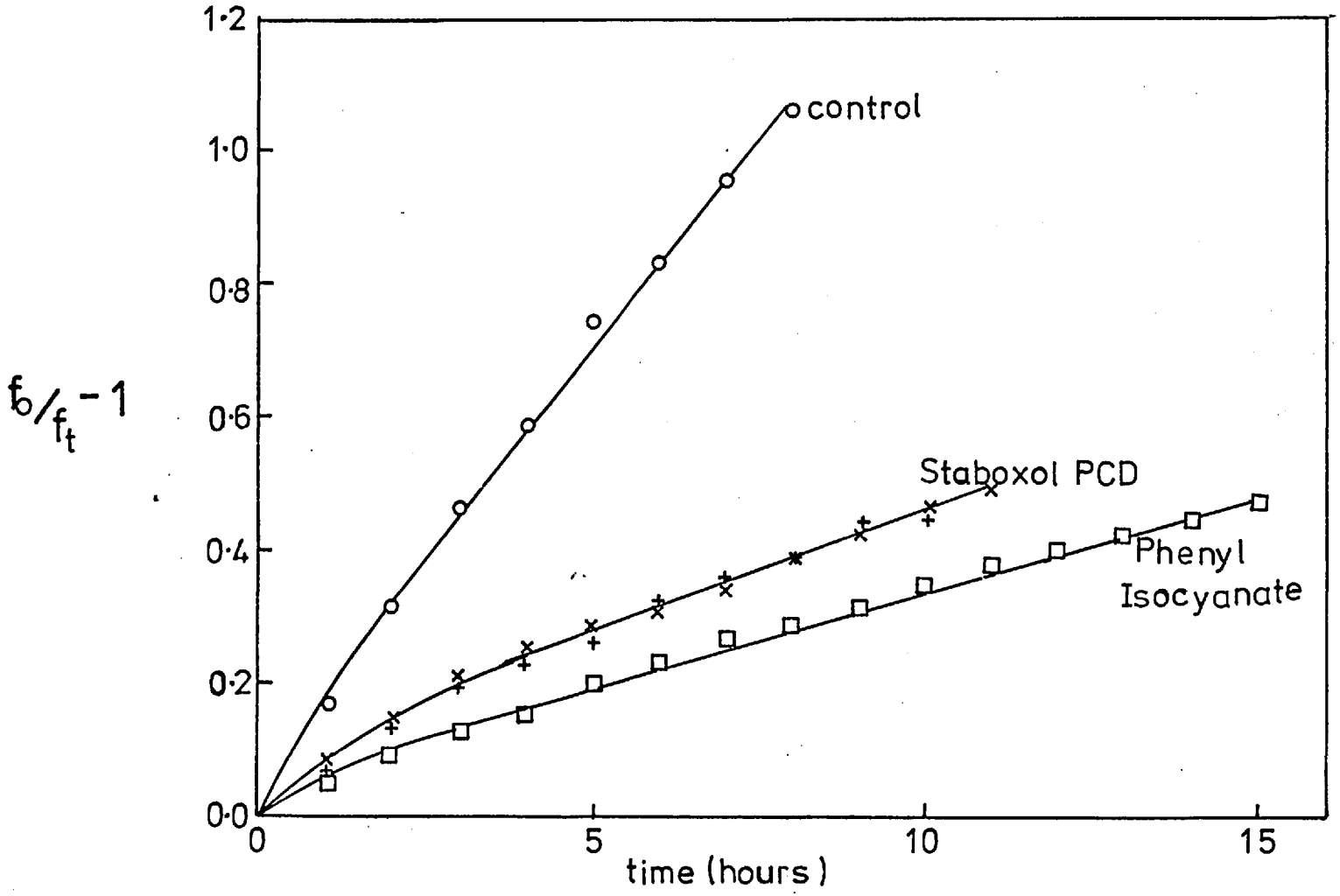


figure 7·30:
GENTHANE S: Effect of Isocyanate Additives on Relaxation Rate in Air at 130°C

× extracted

\+ unextracted

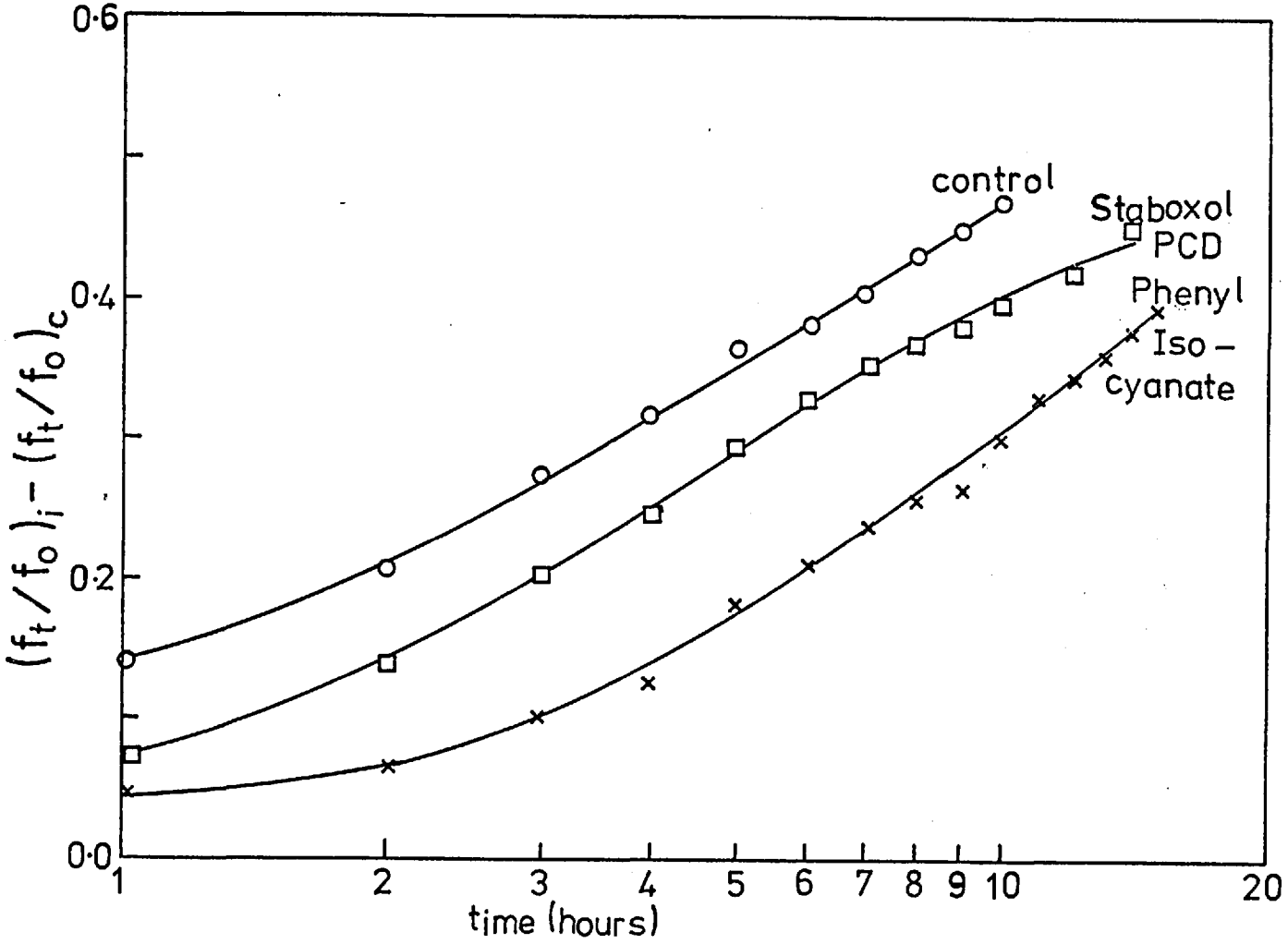


figure 7·31:
GENTHANE S: Effect of Additives on the Crosslinking Reaction in Air at 130°C

The carbodiimide used was an isocyanate terminated material and so it probably acted simply as an isocyanate. Figure 7.32 shows the effect of changing the concentration of carbodiimide on the rate of continuous stress relaxation.

The Flectol H, Stabaxol PCD and polyisoprene were introduced into the samples by swelling them in chloroform solutions of the additive and then removing the solvent by evacuation. The concentration of the additive in the solvent was assumed to be the same inside and outside the sample. As the amount of solution inside the rubber sample could be determined, the amount of additive in the sample could be calculated assuming that only the solvent was removed when the sample was evacuated.

The urethanes are believed to be susceptible to hydrolytic decay (see section 5.4.3.3) and it is possible that hydrolysis in the main chain is responsible for the non-oxidative degradation of Genthane S. However Thomas [243] showed that the rate of continuous relaxation in Genthane S was the same in moist and dry air and the results presented here show that the rate of relaxation is faster in dry nitrogen than in ambient air. These results suggest that hydrolysis is not responsible for the degradation since the rate of relaxation would be expected to increase as the humidity increased. To clarify this further Genthane S was relaxed under water at 95.5°C, the results of this are shown in fig. 7.33; after a short period of fast relaxation the rate decreased until it was approximately the same as that for a dry sample in air.

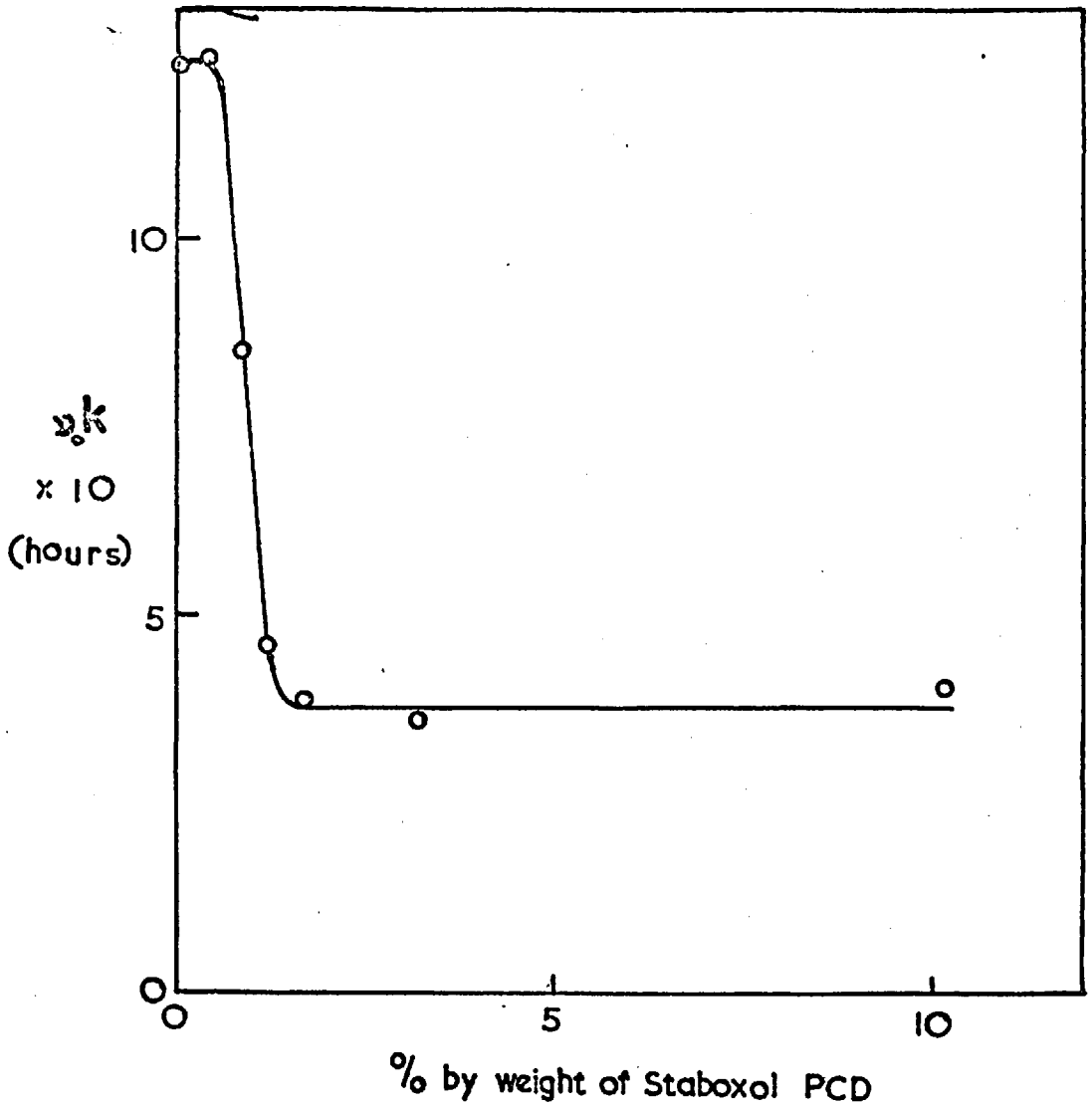


figure 7·32:
Effect of Carbodiimide Additive on the Rate of Relaxation of Genthane S at 130°C in Ambient Air

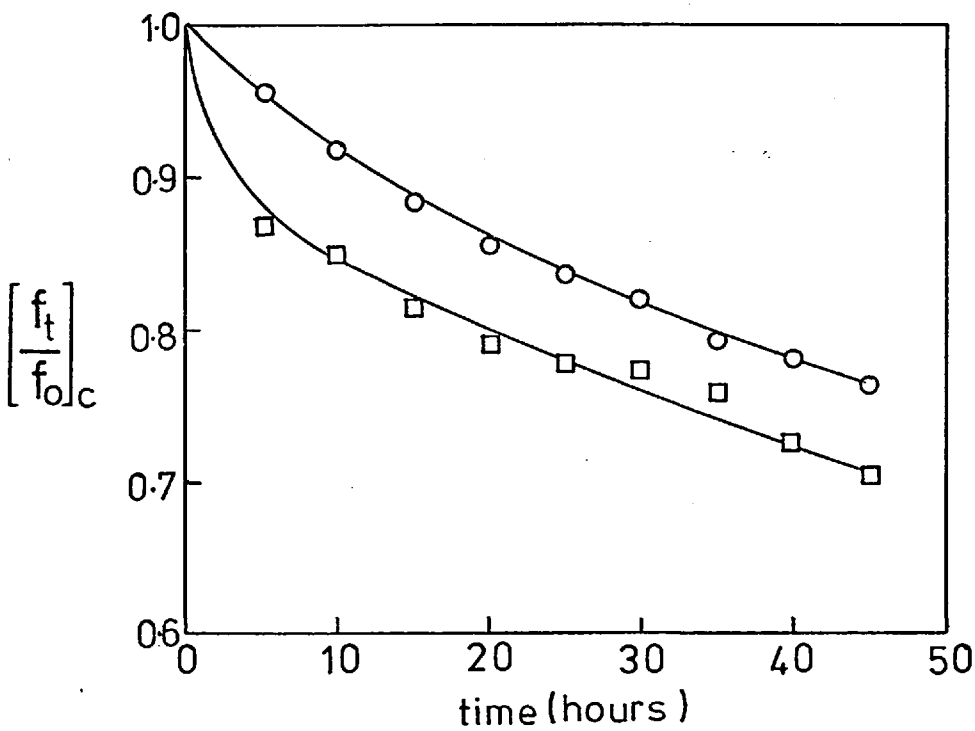


figure 7·33: Effect of water on the relaxation of Genthane S at 95·5°C. (o - relaxation in air, □ - relaxation in water)

TABLE 7.6

Rate Constants for the First Order Continuous Relaxation of Adiprene CH in Air

T°C	1/T x 10^{-3} K^{-1}	k x 10^{4} (hours^{-1})
60	3.03	2.58
70	2.92	4.17
80	2.83	6.79
100	2.68	55.5
105.5*	2.64	108 ± 12
110	2.61	197
120	2.55	374
131	2.48	2430
150	2.36	8300

* Average value, using points at different crosslink densities in Table 7.7 below

TABLE 7.7

Rate Constants for the First Order Continuous Relaxation of Adiprene CH Samples with Different Initial Crosslink Densities in Air at 105.5°C

% DCP in cure	C_1 x 10^{5} Nm^{-2}	$1/C_1$ x 10^{-6} $(Nm^{-2})^{-1}$	k x 10^{2}	
1.0	3.41	2.93	1.64 1.52	unextracted
1.5	4.65	2.15	1.02	unextracted
2.0	5.10	1.96	1.13	extracted in benzene
			1.21	unextracted
2.0	5.35	1.87	1.11 1.01	unextracted
2.5	6.25	1.60	1.05	unextracted

The sample was pre-swollen in water at 40°C but since swelling is temperature dependent the fast initial rate of relaxation was probably due to dimensional changes in the sample brought about by the 55.5°C increase in temperature.

(7.2.3) Continuous and Intermittent Relaxation of Adiprene CM in Air and Nitrogen

Continuous stress relaxation experiments on Adiprene CM in air were conducted at 60 - 150°C. The results are shown in figure 7.34; it is clear that there is a linear log $(f_t/f_o)_c$ vs t relationship except at the lowest temperatures where there is some curvature at short times. The rate constants obtained from the slopes of these lines (see table 7.6) gave a linear Arrhenius plot provided the low temperature points were omitted (see fig. 7.35), the activation energy obtained from the slope was 130.5 kJ $mole^{-1}$.

Experiments were conducted on samples with different initial crosslink densities, the results of these are given in table (7.7), it is evident that the rate of relaxation was independent of initial crosslink density indicating that cleavage occurred in or at the crosslink.

Intermittent stress relaxation experiments showed that there was little or no crosslinking reaction (see fig. 7.36).

Continuous and Intermittent stress relaxation experiments on Adiprene CM in nitrogen or in air in the presence of an antioxidant showed that there was both a much reduced rate of scission and a high rate of crosslinking or network chain formation (see figs. 7.36 and 7.37). These results indicate that the continuous relaxation of Adiprene CM in air is due to an oxidation reaction and that the oxidation reaction or the

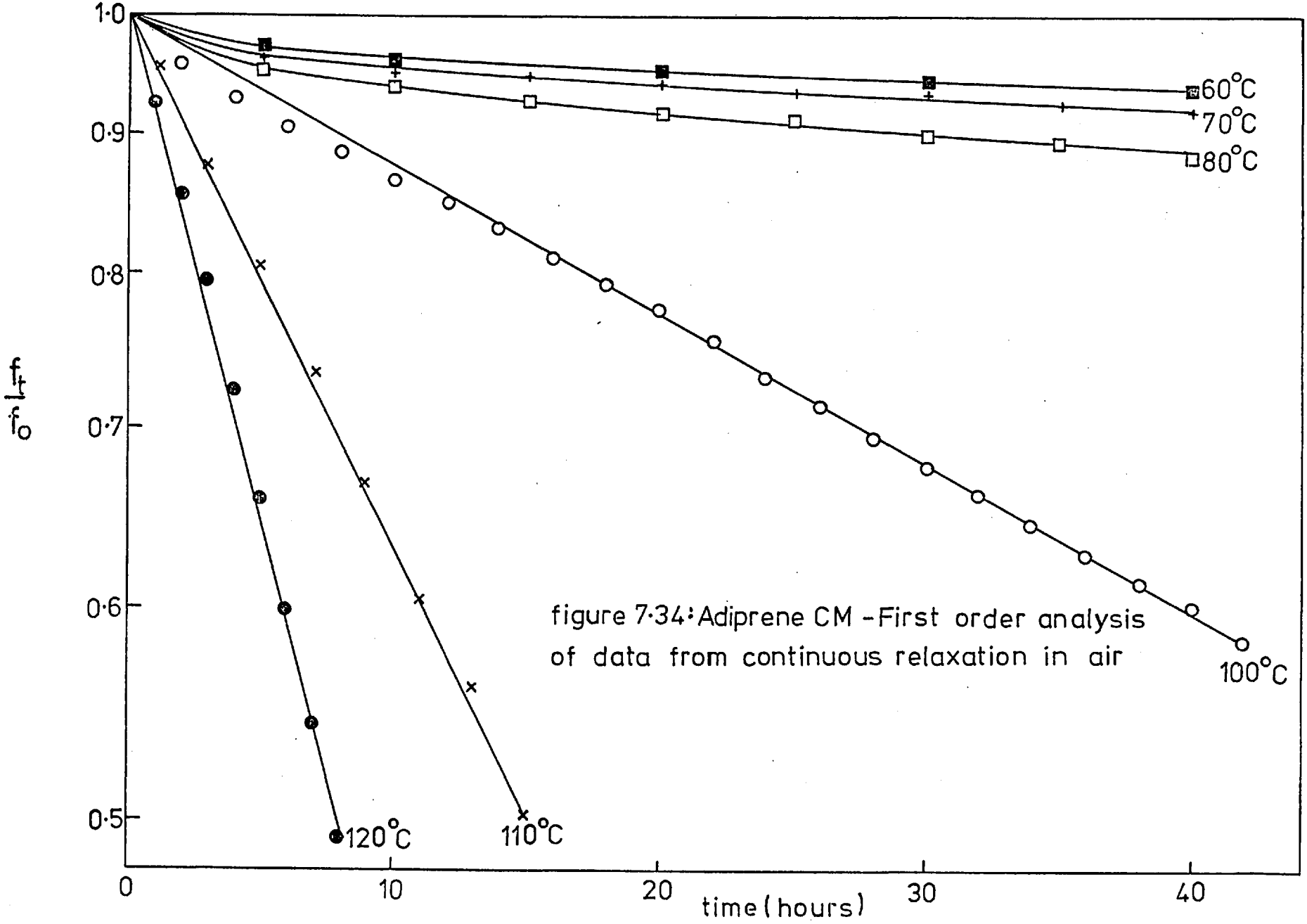


figure 7·34: Adiprene CM - First order analysis of data from continuous relaxation in air

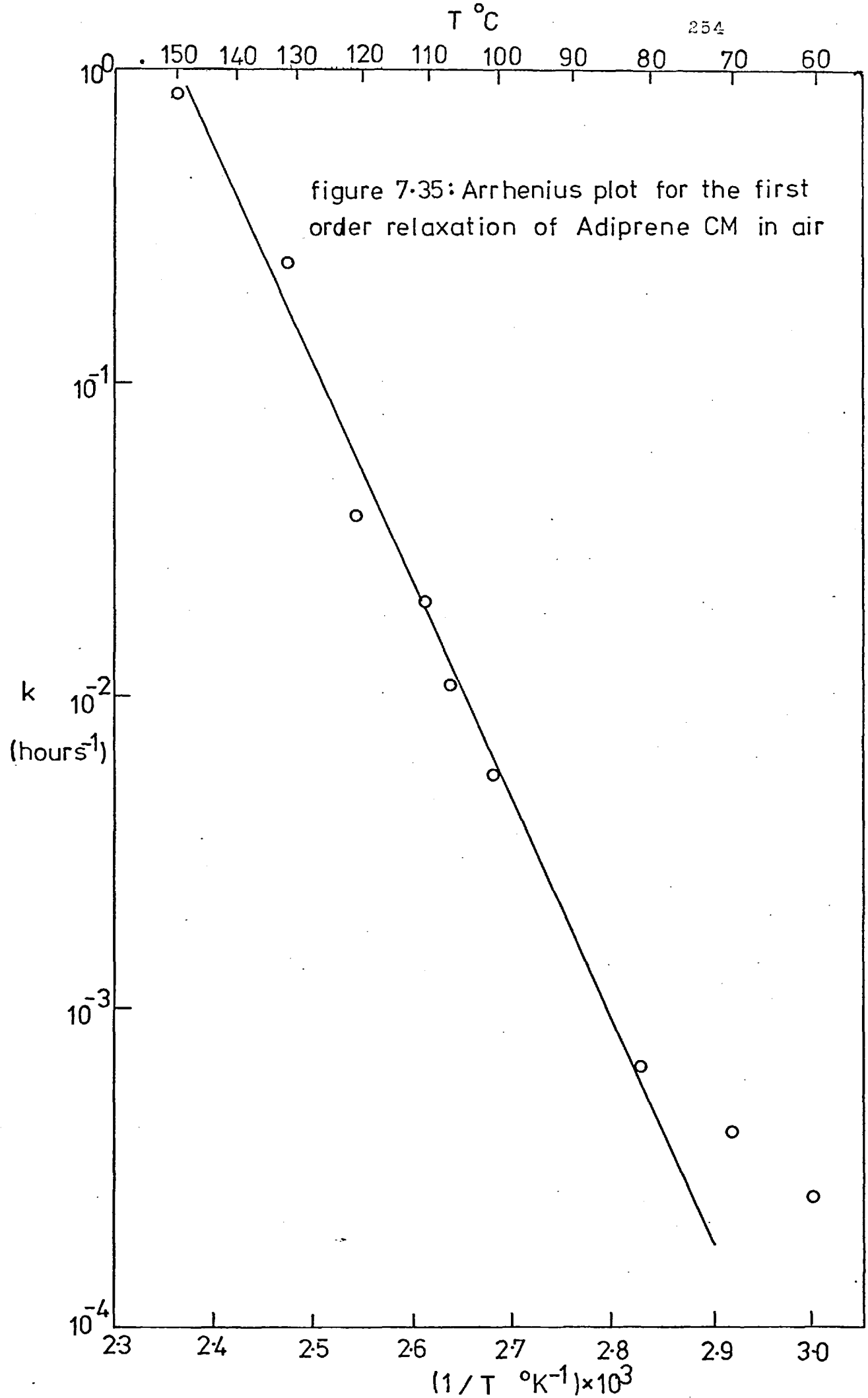
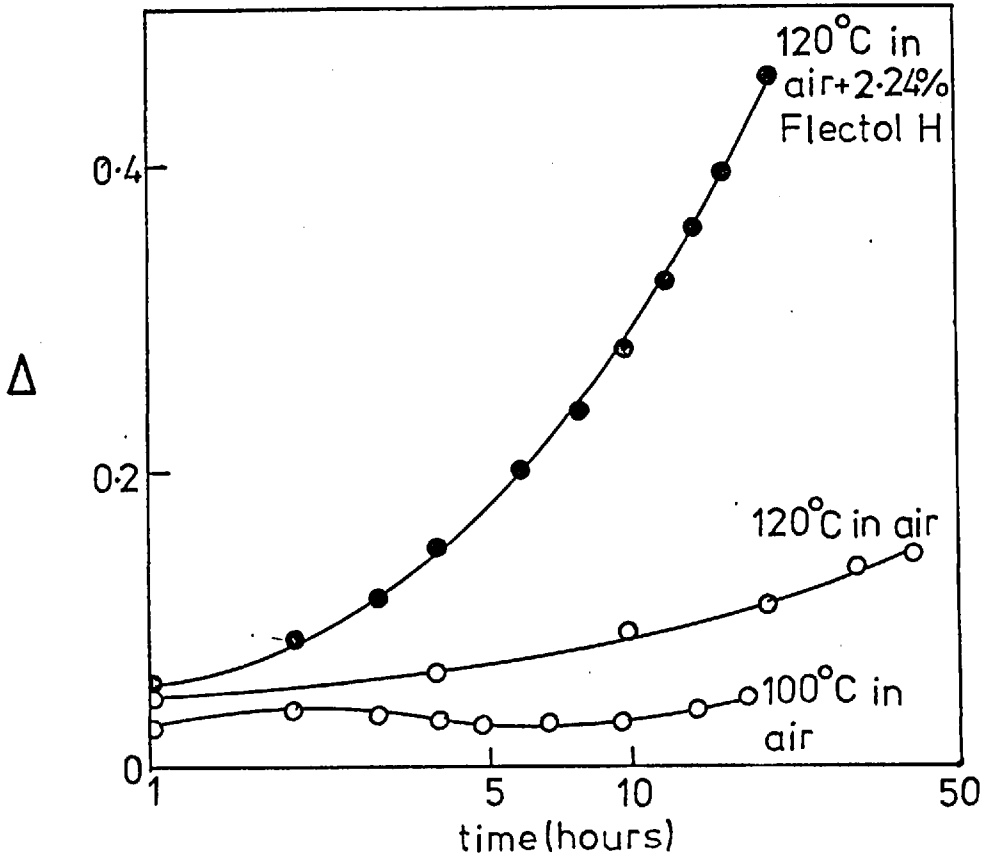
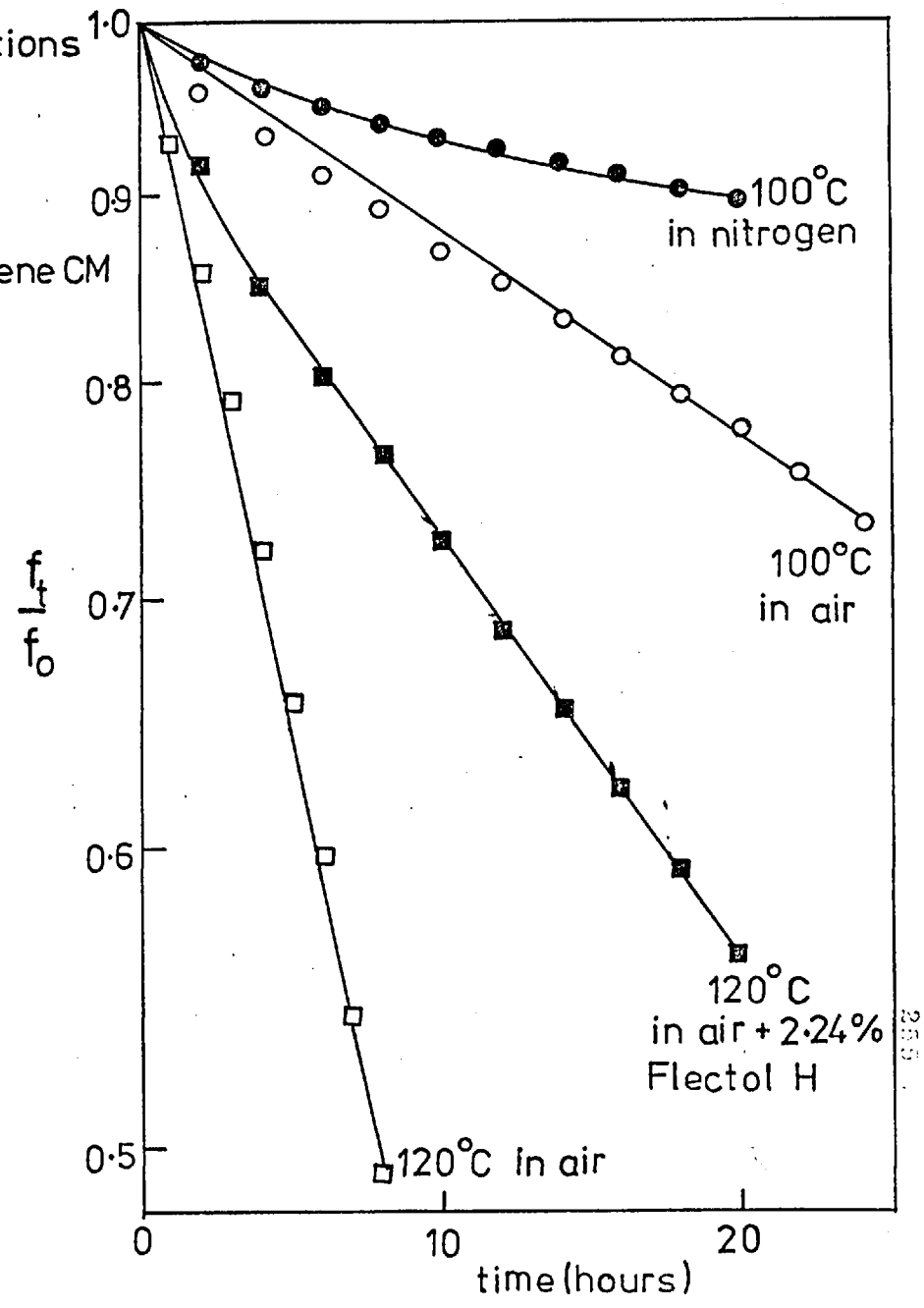


figure 7·35: Arrhenius plot for the first order relaxation of Adiprene CM in air

figure 7·37 (right): Effect of non-oxidising conditions on the continuous relaxation of Adiprene CM

figure 7·36 (below): Effect of non-oxidising conditions on network chain formation in Adiprene CM





presence of oxygen severely inhibits the rate of network chain formation.

The continuous relaxation of Adiprene CM in nitrogen was not first order but obeyed the same kinetics as the cleavage reaction in Genthane S and gave good straight lines when analysed according to second order kinetics (see figs. 7.38 and 7.39). The rate constants obtained are presented in table (7.8), they gave good Arrhenius plots (fig. 7.40) and an activation energy of 110.8 kJ mole^{-1}. Experiments on samples with different initial crosslink densities showed that the relaxation rate was linearly dependent on the reciprocal of the initial crosslink density (figs. 7.41 and 7.42) which was indicative of a main chain cleavage reaction.

The intermittent relaxation results were interpreted using the two network theory and plots of Δ vs log t shown in fig. 7.43. These curves could be superposed to give a master curve (fig. 7.44) and points interpolated from the master curve gave a good straight line when plotted according to equation 3.87 except for a small amount of curvature at short times as can be seen from fig. 7.45. This behaviour is identical with that of Genthane S except that here 136 new chains are formed for every 100 lost due to cleavage.

An Arrhenius plot of the time taken for Δ to reach 0.25, that is $\tau_{0.25}$, gave a good straight line (fig. 7.46) and an activation energy of 95.7 kJ mole^{-1}.

The activation energies obtained are given in table (7.11); the value obtained for the oxidation reaction compares favourably with those obtained for the oxidation of hydrocarbons (see chapter 4) whilst those obtained for the non-oxidative

TABLE 7.8

Rate Constants for the Second Order Continuous Relaxation of Adiprene CM in Nitrogen

$C_1 = 6.3 \times 10^5$ Nm^{-2}			$C_1 = 5.1 \times 10^5$ Nm^{-2}		
T°C	1/T x 10^{-3} K^{-1}	k x 10^{-4} (hours^{-1})	T°C	1/T x 10^{-3} K^{-1}	k x 10^{-4} (hours^{-1})
80	2.83	1.91	68	2.93	3.79
90	2.76	4.90	88	2.77	13.2
100	2.68	10.4	100	2.68	49.5
110	2.61	29.2	108	2.63	161
120	2.55	72.0	126	2.45	825
130	2.48	206	128	2.43	438

TABLE 7.9

Rate Constants for the Second Order Continuous Relaxation of Adiprene CM Samples with Different Initial Crosslink Densities in Nitrogen at 103°C

% DCP in cure	$C_1 \times 10^5$ Nm^{-2}	$1/C_1$ x 10^{-6} (Nm^{-2})$^{-1}$	k (hours^{-1}) x 10^2
2.5	6.25	1.60	0.33
2.0	5.35	1.87	0.75
1.5	4.65	2.15	1.75
1.0	3.41	2.93	3.44

TABLE 7.10

Rate Data from Two Network Analysis of Continuous and Intermittent Relaxation of Adiprene CM in Nitrogen

T°C	1/T x 10^{-3} K^{-1}	Time for Δ to reach 0.25 hours
80	2.83	12.7
90	2.76	32.5
100	2.68	73.8
110	2.61	164
120	2.55	315
130	2.48	750

TABLE 7.11

Activation Energies for Scission and Crosslinking in Adiprene CM

Process	Reaction	ΔH kJ mole^{-1}
Scission Reaction	Oxidation (first order)	130.5
	Non-oxidative (second order)	110.8
Crosslinking Reaction	Non-oxidative (second order)	95.7

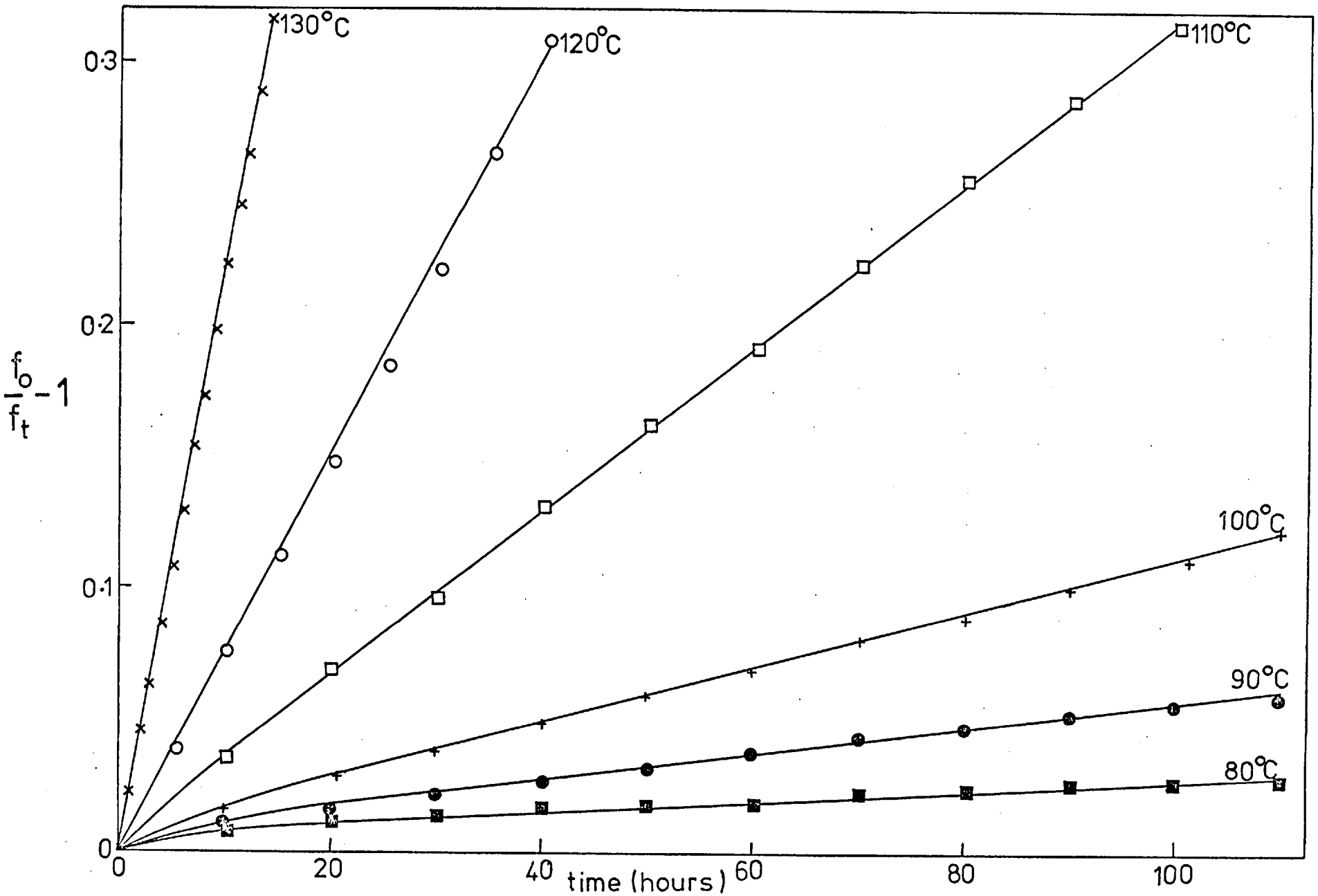


figure 7·38 : Adiprene CM- Second order analysis of continuous data for relaxation in nitrogen (C_1 = ×10^5 Nm^{-2})

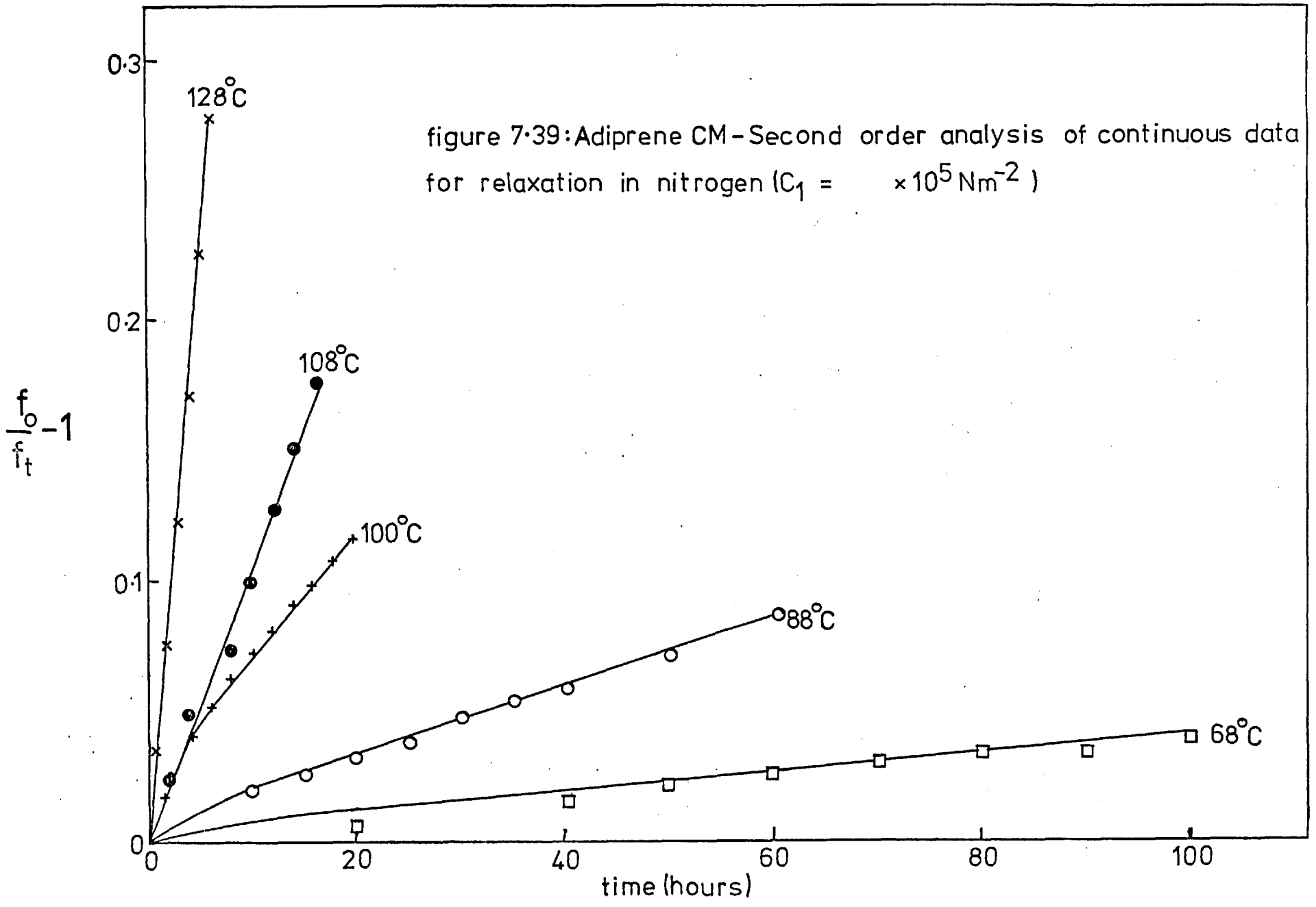


figure 7·39: Adiprene CM – Second order analysis of continuous data for relaxation in nitrogen (C_1 = $\times 10^5 Nm^{-2}$)

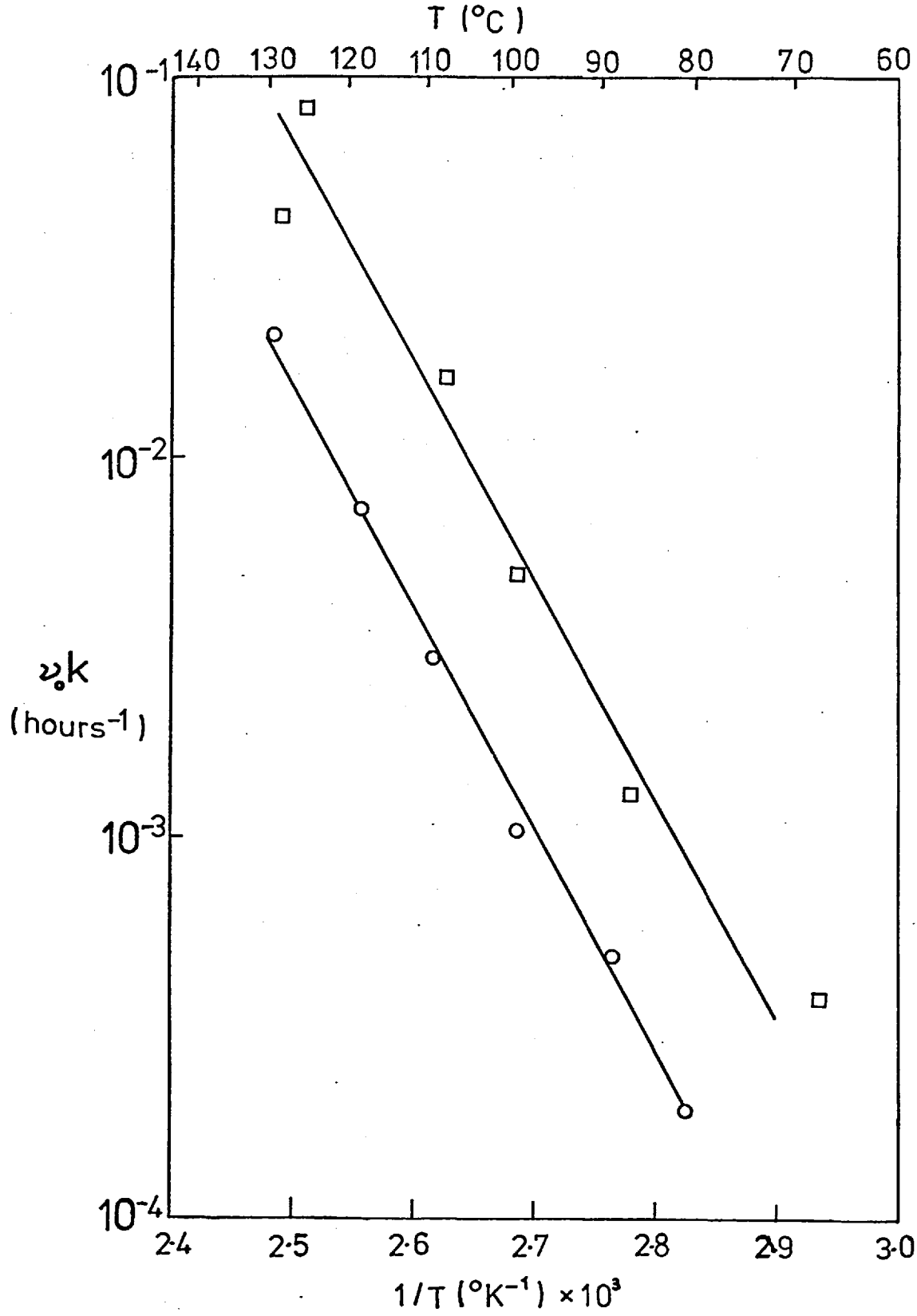
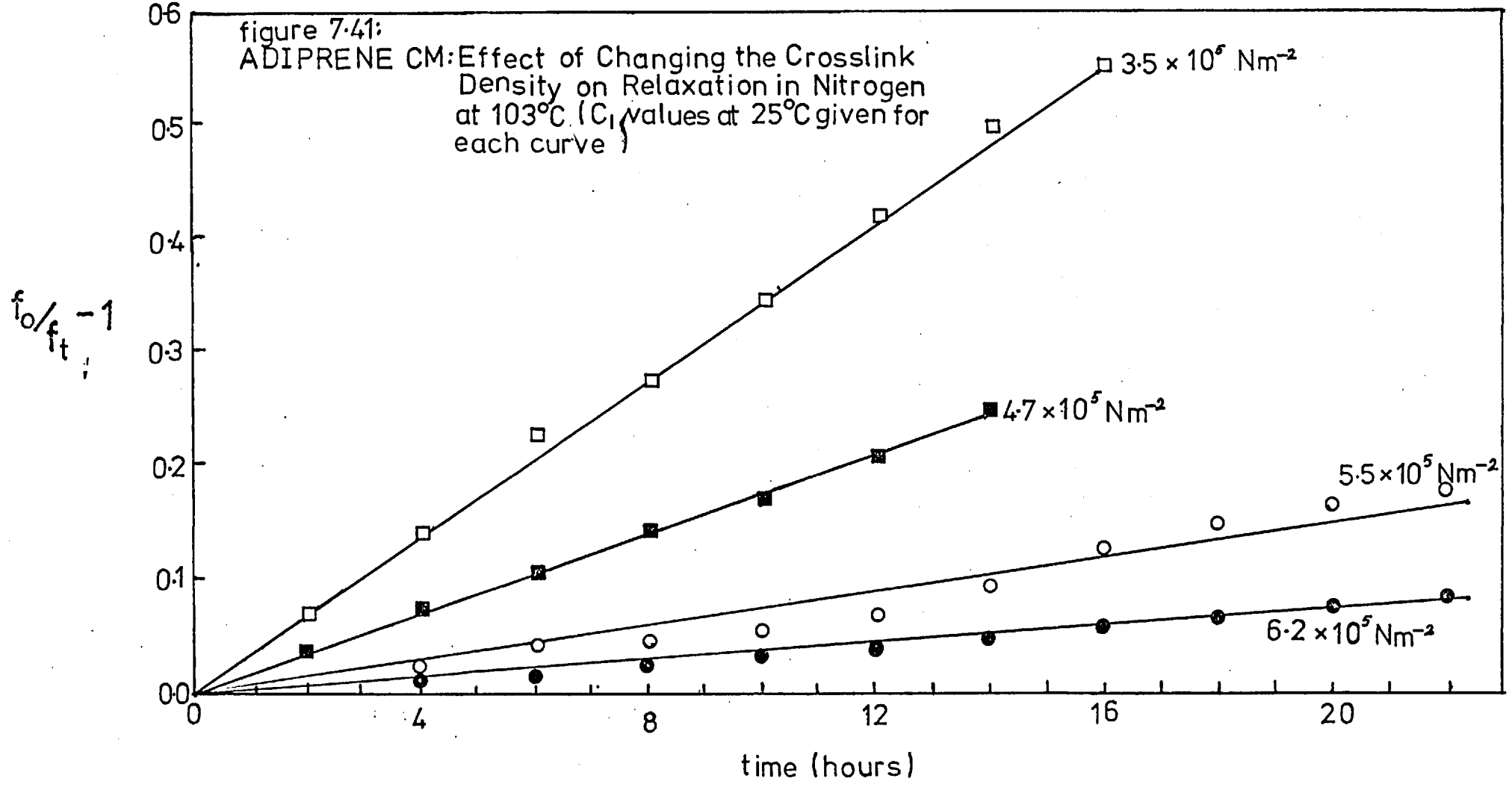


fig. 7·40: ADIPRENE CM: Arrhenius Correlation for Continuous Relaxation in Nitrogen (o - C_1= $\times 10^5$ Nm^{-2}, □ - C_1= $\times 10^5$ Nm^{-2})


figure 7·41:
ADIPRENE CM: Effect of Changing the Crosslink Density on Relaxation in Nitrogen at 103°C (C1 values at 25°C given for each curve)
3·5 × 10⁵ Nm⁻²
4·7 × 10⁵ Nm⁻²
5·5 × 10⁵ Nm⁻²
6·2 × 10⁵ Nm⁻²
f0/ft − 1
time (hours)
0·0
0·1
0·2
0·3
0·4
0·5
0·6
0
4
8
12
16
20

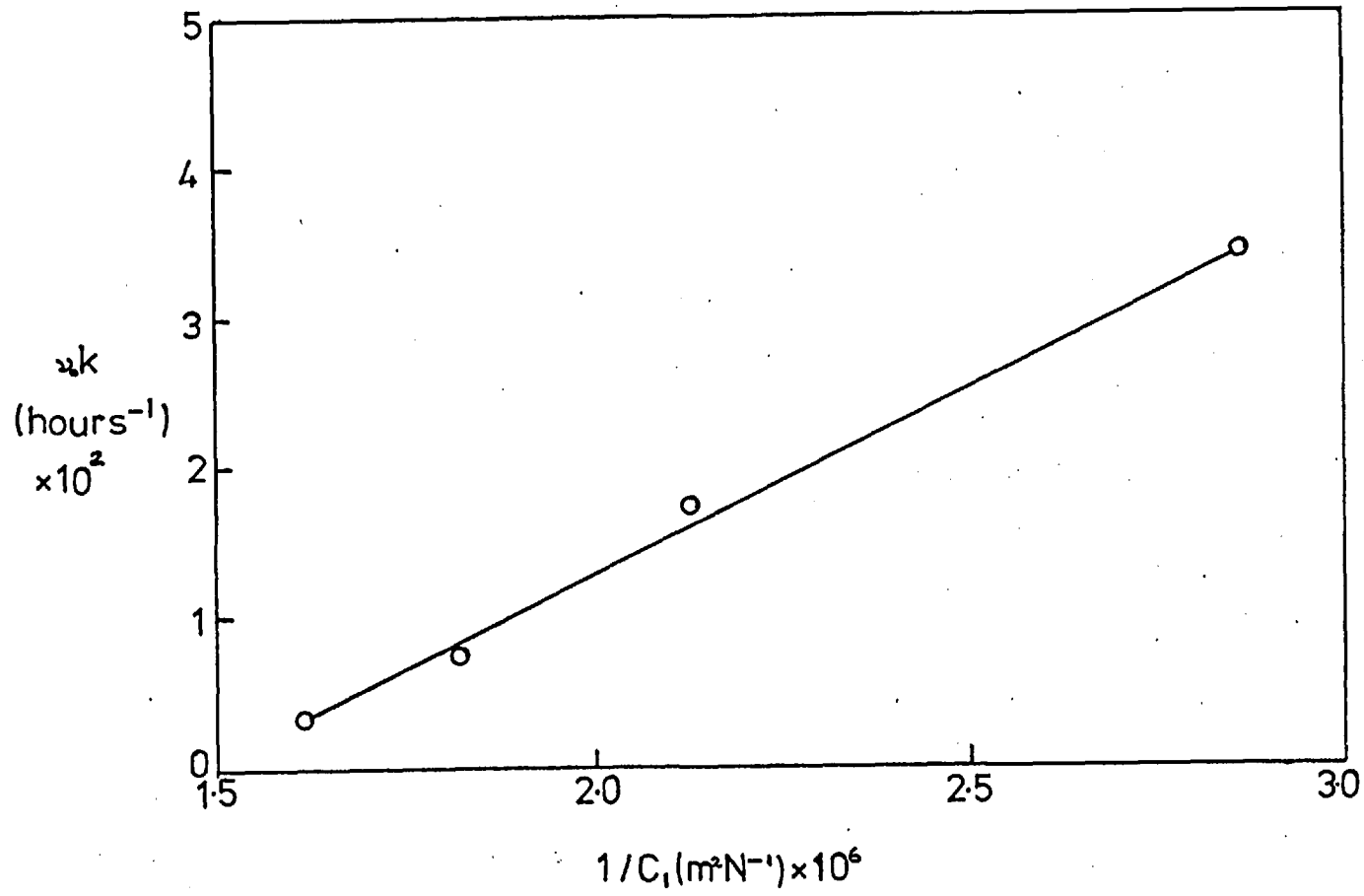
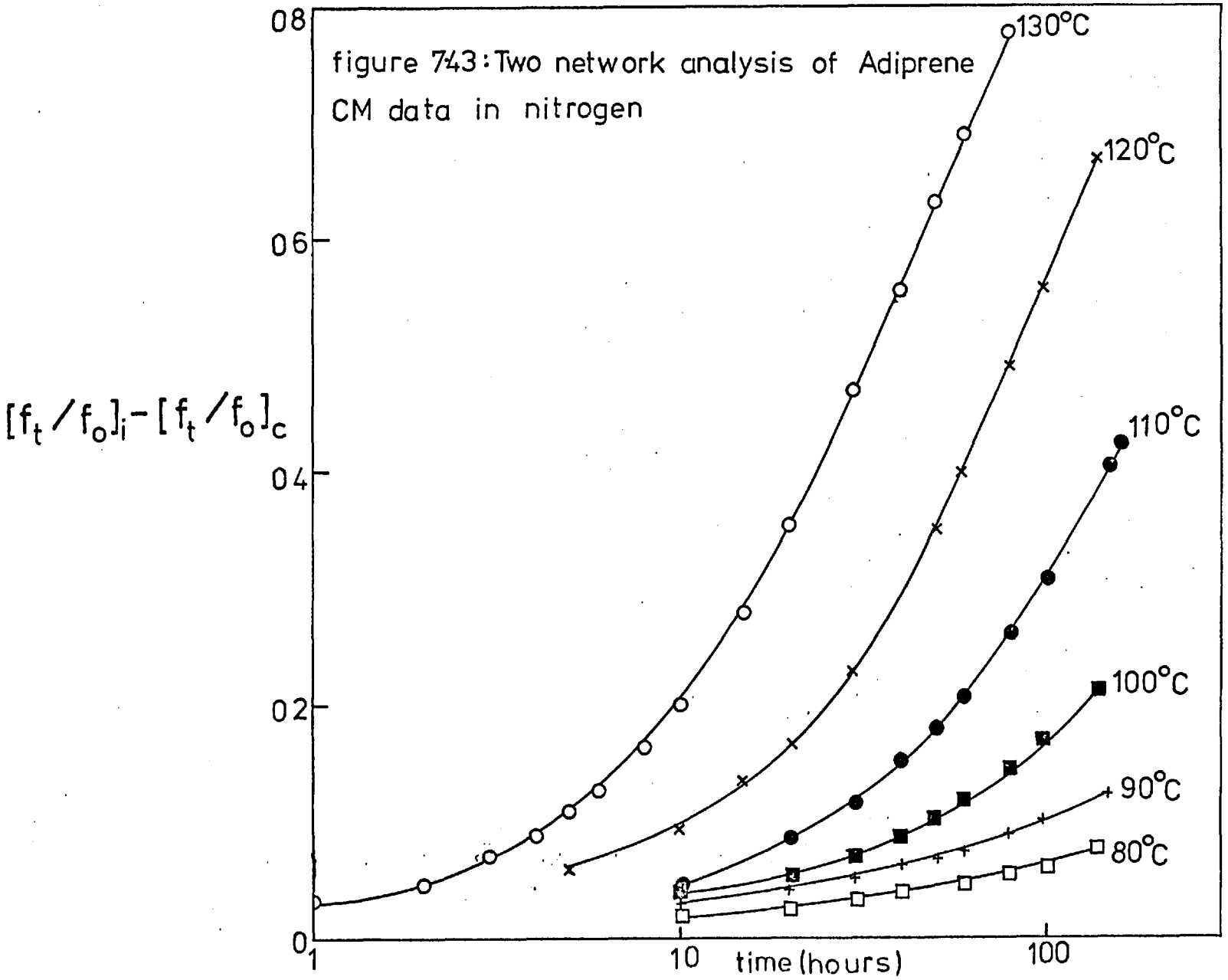


figure 7·42: ADIPRENE CM: Correlation of Relaxation Rate with Crosslink Density in Nitrogen at 103°C


figure 743: Two network analysis of Adiprene CM data in nitrogen
$[f_t/f_o]_i - [f_t/f_o]_c$
0·8
0·6
0·4
0·2
0
1
10
100
time (hours)
130°C
120°C
110°C
100°C
90°C
80°C

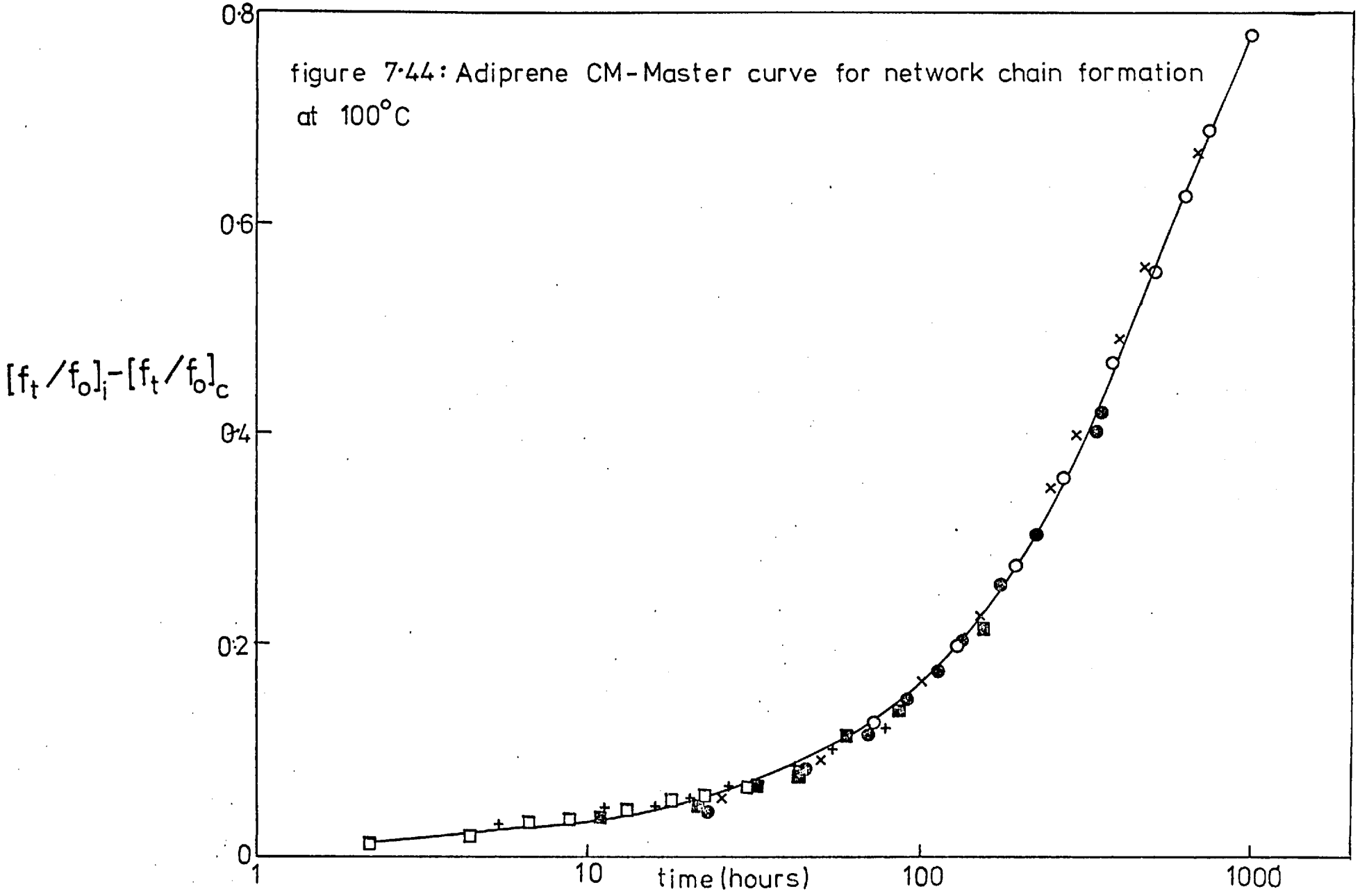


figure 7·44: Adiprene CM-Master curve for network chain formation at 100°C

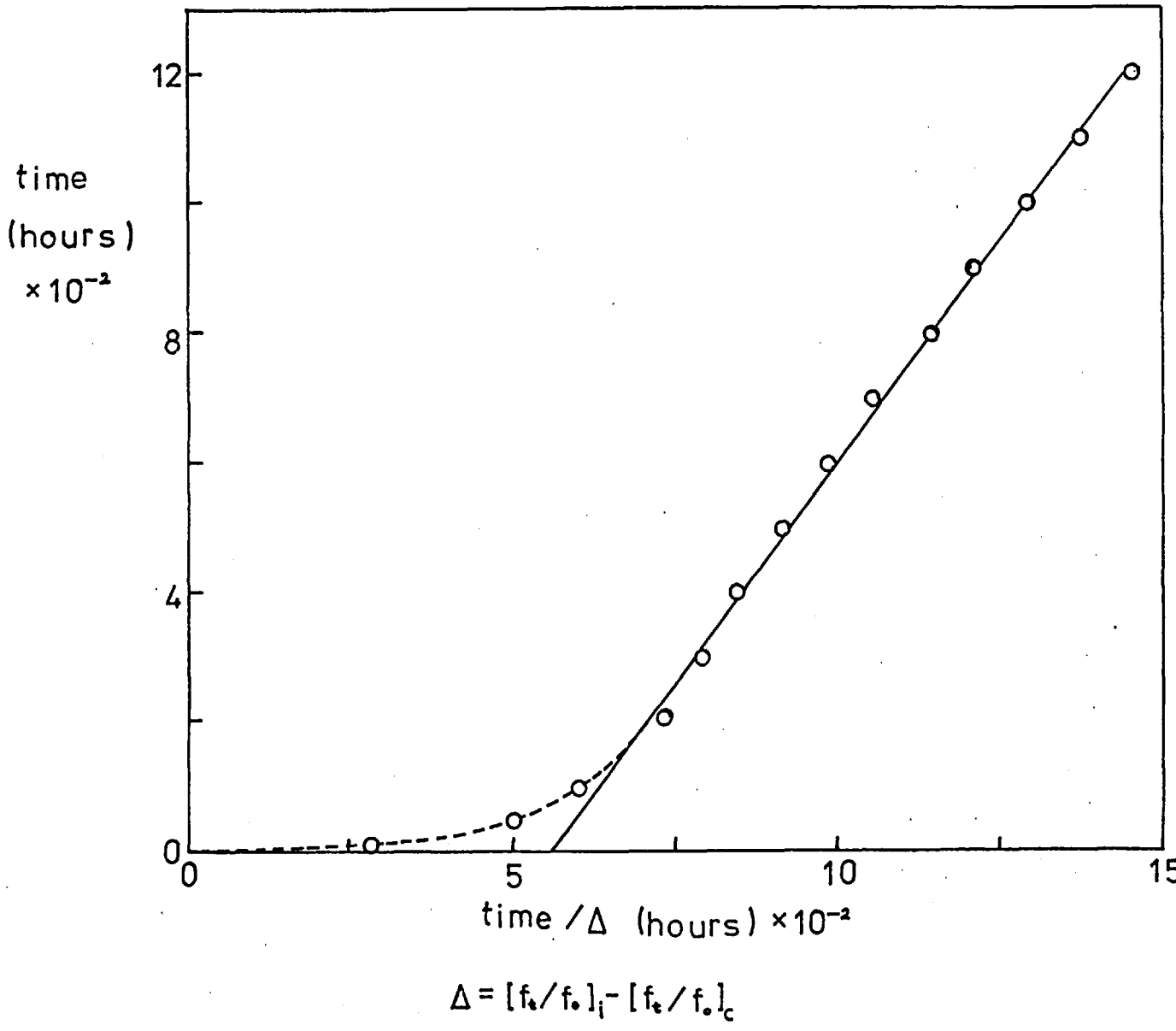


figure 7·45 :
ADIPRENE CM: Second Order Analysis of Two Network Data from Relaxation in Nitrogen Normalised to 100°C

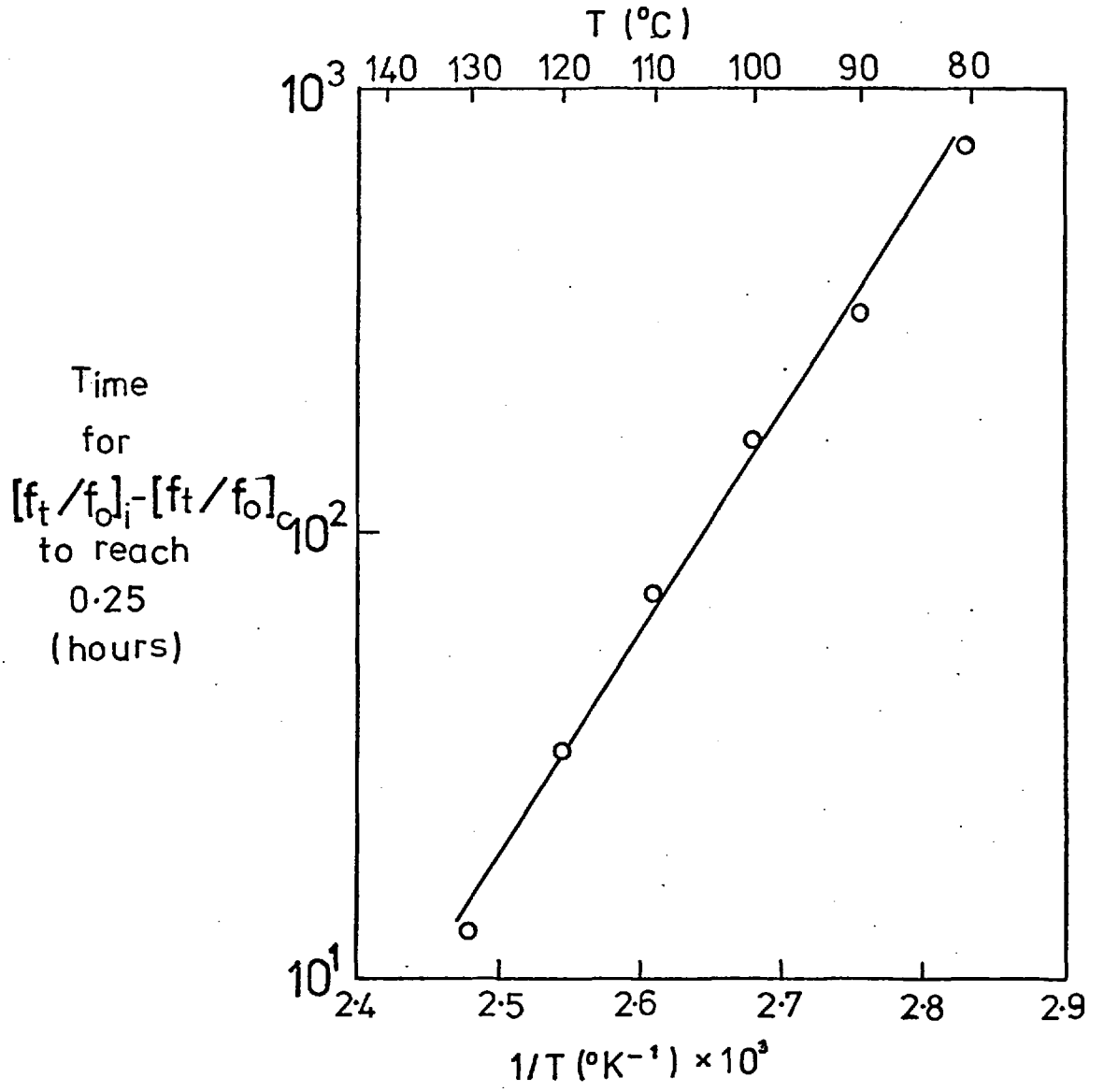


fig : 7·46: ADIPRENE CM : Arrhenius Correlation of Intermittent Data in Nitrogen

scission and network chain formation reactions compare favourably with those obtained for Genthane S.

(7.2.4) Further Experiments on Adiprene CM and the Effect of Additives

The effect of an antioxidant on the rate of continuous stress relaxation was mentioned in section 7.2.3; further experiments were conducted to investigate the effect of different concentrations of antioxidant (see fig. 7.47).

As for Genthane S, the rate of continuous relaxation was reduced by treatment with an isocyanate (fig. 7.48).

Thomas[243] showed (fig. 7.49) that the rate of continuous relaxation was unaffected by high humidity except for the high rate of relaxation just after the high humidity was introduced due to dimensional changes in the sample.

(7.3) DISCUSSION OF RESULTS

(7.3.1) Network Reactions in Genthane S

The continuous and intermittent stress relaxation data for Genthane S show that there are chemical reactions taking place that lead to both the removal of network chains and the formation of new ones. The reaction leading to the removal of network chains involves the cleavage of the main chain.

The rates of scission and network chain formation are inhibited when the samples have been heated with phenyl isocyanate or an isocyanate terminated carbodiimide. Since this inhibition is still observed after the samples have been extracted with benzene the additives must become attached to the polymer chains or must modify them, making them less susceptible to reaction.

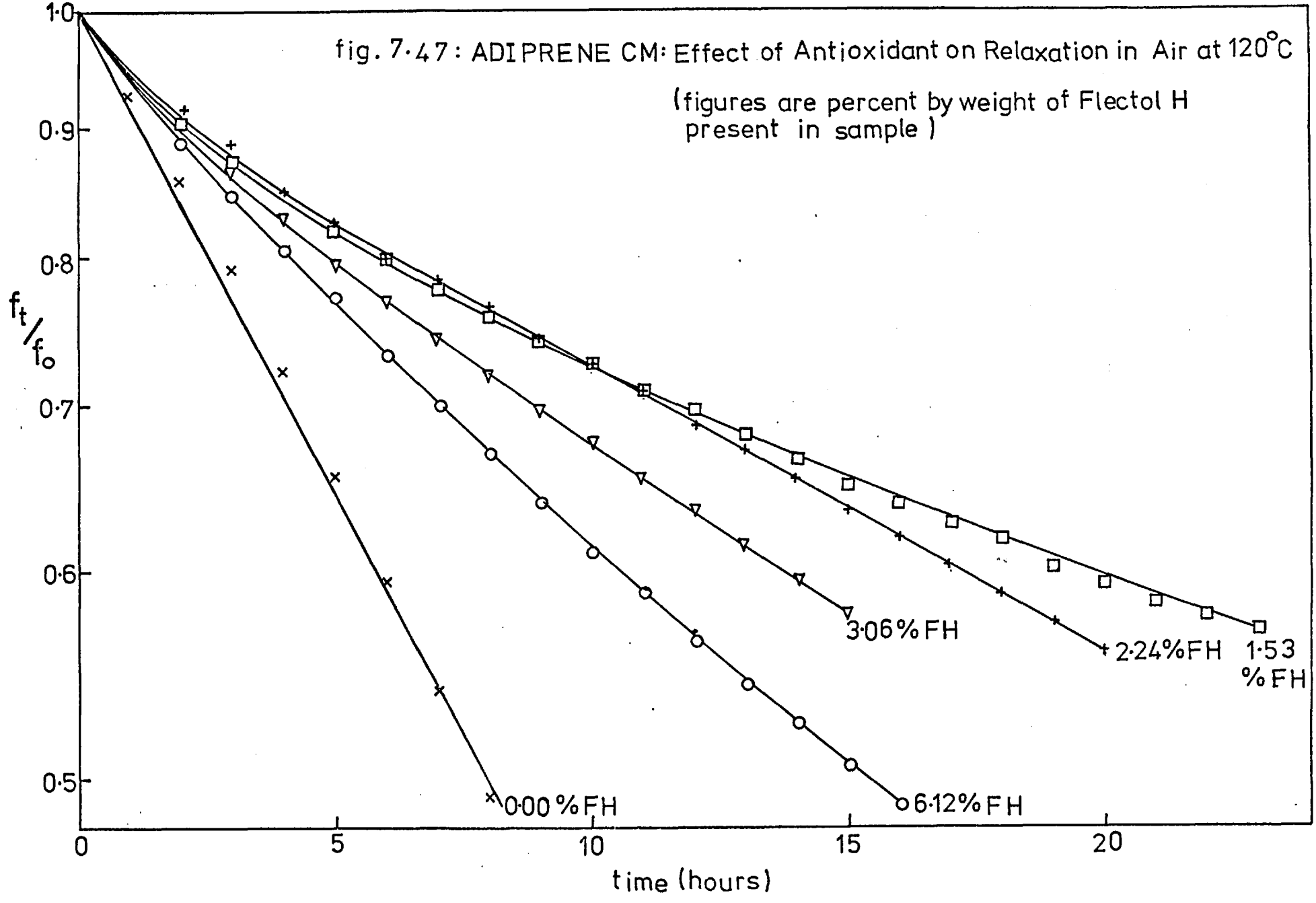
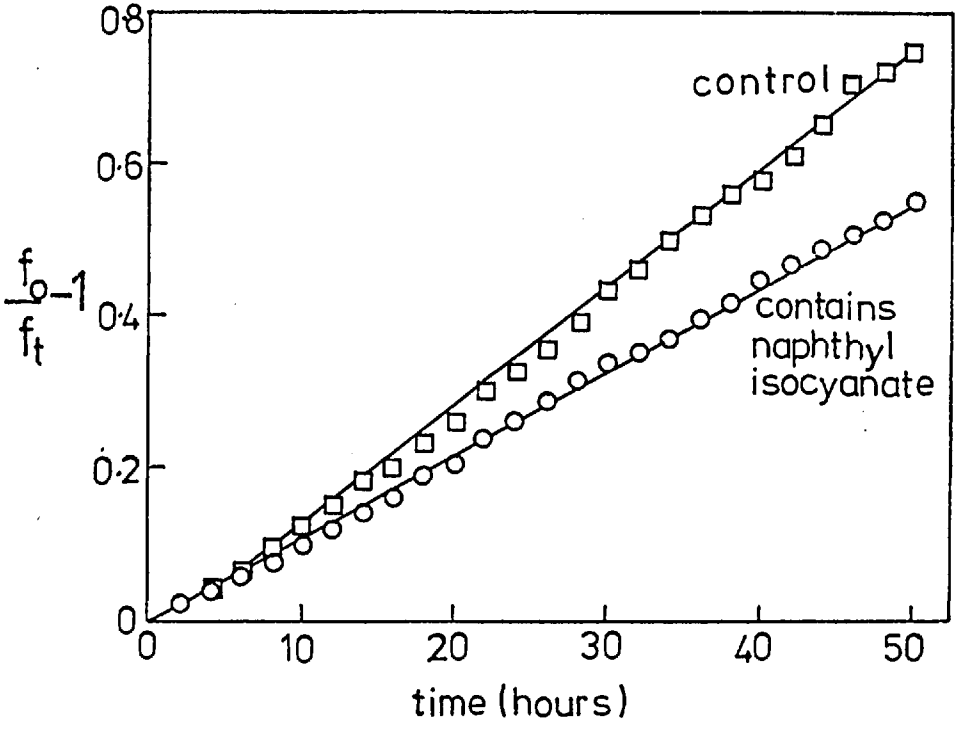


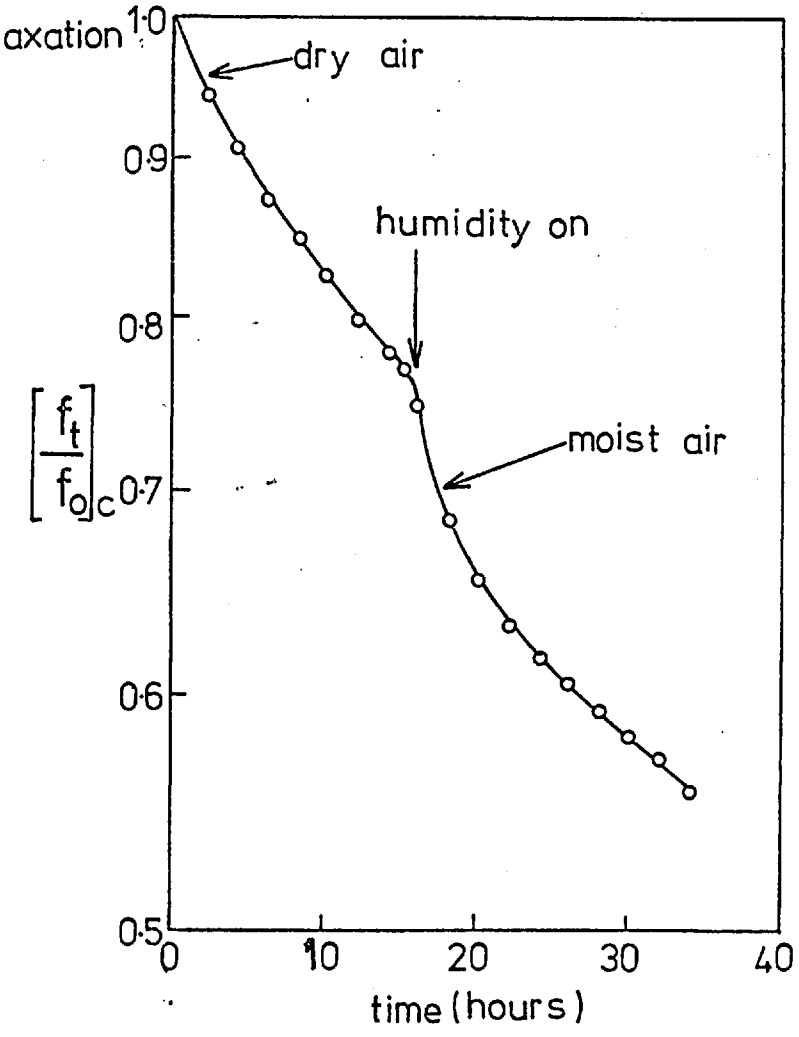
fig. 7·47 : ADIPRENE CM: Effect of Antioxidant on Relaxation in Air at 120°C

(figures are percent by weight of Flectol H present in sample)

figure 7·48 : (right) Effect of humidity on the relaxation of Adiprene CM in air (humidity = 95% at 100°C)

figure 7·49 : (below) Effect of isocyanate on the relaxation of Adiprene CM in nitrogen at 120°C





Fortunately the reactions of isocyanates are well-known,[1,2,3] and are limited to reactions with groups that contain active hydrogen. In Genthane S the only sources of active hydrogen are the hydroxl groups that terminate the primary polymer molecules and the urethane linkages; there are about 16 urethane links for every hydroxl group.

Reaction of the isocyanate with a hydroxl group will lead to a urethane

$$R'OH + RNCO \longrightarrow RNH - \overset{O}{\overset{\|}{C}} - OR' \qquad 7.1$$

whilst reaction with a urethane will lead to an allophanate.

$$R' - NH - \overset{O}{\overset{\|}{C}} - OR'' + RNCO \longrightarrow R - \underset{\underset{O = C - NH - R}{|}}{N} - \overset{C}{\overset{\|}{C}} - OR'' \qquad 7.2$$

Reaction according to equation 7.1 will only affect relaxation if the OH groups participate in the cleavage and network chain formation reactions; this is possible if a hydroxyl/urethane or a hydroxyl/ester interchange reaction occurs, in fact this type of reaction is known to occur between monomeric alcohols and esters.[244]

Reaction according to equation 7.2 will affect the relaxation if it involves the urethane linkage at all.

There are two reasons why reaction involving hydroxyl group participation is unlikely. First the stress relaxation of Adiprene CM under nitrogen indicates that this elastomer behaves in the same way as Genthane S, although some differences might be expected in Adiprene CM where ester/hydroxyl interchange is excluded. This suggests that if urethane/hydroxyl interchange does take place it is not

accompanied by ester/hydroxyl interchange. Secondly, it will be shown later that the kinetics of the cleavage reaction are indicative of a bimolecular reaction and urethane/hydroxyl interchange, though second order, will not be a bimolecular or a pseudo bimolecular reaction since the initial concentrations of hydroxyl and urethane groups are very different.

It can thus be concluded that the cleavage and network chain formation reactions are probably associated with the urethane group with the remote possibility of hydroxyl groups also being involved in the reaction.

The inhibition of urethane dissociation when the urethane hydrogen is removed (as in equation 7.2) is in agreement with published work.[20,210]

Having indicated that the reactions leading to network breakdown is associated with the urethane link, the kinetics of the reaction can be considered in more detail. Clearly the most satisfactory interpretation of the continuous stress relaxation data is that using equation (3.79), which states

$$f_o/f_t - 1 = \nu_1(o)\, kt \qquad 7.3$$

This type of equation could result from either a first or a second order reaction depending on which equation is selected to relate q(t), the number of cuts, to $\nu_1(o)$, the initial crosslink density (see section 3.5.2). Figure 7.20 shows that $\nu_1(o)\, k$ is inversely proportional to $\nu_1(o)$ at short times or small amounts of dissociation; unfortunately this type of dependence can be predicted by all the equations discussed in section 3.3.2, and cannot be used to determine

which equation relating q(t) to $\nu_1(o)$ is applicable here. This means that the dependence of relaxation rate on crosslink density cannot be used to distinguish between the first and second order kinetic equation.

If the equation is first order then according to equation 3.69

$$\nu_1(o)\ k = \bar{m}\ k_u t \qquad 7.4$$

where $\bar{m}$ is the number of urethane groups per network chain and k_u is the specific rate constant for cleavage of the urethane link. One of the assumptions required to derive equation 3.69 is that $\bar{m}$ is large, in this case $\bar{m}$ is never greater than about 10 (see table 6.19) and so this assumption will not be valid and the first order equation will not take on the form of equation 7.3.

The derivation based on second order kinetics makes no assumptions about the magnitude of $\bar{m}$ (see sections 3.3.2 and 3.5.2) and requires only that $\bar{m}\,\nu_1(o)\ kt$ is small. This assumption is perfectly valid under the conditions of the experiments described. It should be noted that the linearity of the plots was rather better than would be expected from equation 3.74; good straight lines were obtained up to $f_o/f_t - 1 = 3.0$ where the derivation of equation 3.74 suggests that a 25% deviation should be observed; this deviation reduces to 14% at $f_o/f_t - 1 = 2.0$ and to 8% at $f_o/f_t - 1 = 1.0$.

The fact that the activation energy obtained from the second order rate constants is in agreement with that obtained by the time-temperature superposition principle indicates that they are genuine rate constants and that the theoretically predicted deviations are not important.

The reaction leading to the formation of new network chains can also be described by a second order bimolecular reaction since excellent fits are obtained when equation 3.87 is used (see fig. 7.23).

It is interesting that the activation energies for both scission and network chain formation are very similar (i.e. 94.6 and 107.9 kJ $mole^{-1}$ respectively).

The experiments on postcured samples (figs. 7.26 and 7.27) and the fact that the infra red spectra of aged samples were the same as those of unaged samples indicate that the chemical structure is largely unaltered during ageing, except that the network chain density is reduced by about 40%. This means that the new network chains formed must be chemically identical to those cleaved and that the chemical bonds formed are the same as those that are broken. Assuming that these bonds are the urethane links, the network reactions could be explained by the regeneration of a proportion of the bonds broken, according to the following type of mechanism.

$$2\left[\text{RNH} - \overset{\overset{O}{\|}}{C} - O - R'\right] \underset{k_f}{\overset{k_u}{\rightleftharpoons}} \left[\text{Intermediate Products}\right] \xrightarrow{k_d} \text{Inert Products} \qquad 7.5$$

In a strained sample, urethane groups that dissociate in chains under stress reform to give chains that are not under stress, so that:

$$2\left[\text{RNH} - \overset{\overset{O}{\|}}{C} - O - R'\right]_{\text{strained}} \xrightarrow{k_u} \left[\text{Intermediate Products}\right] \downarrow \overset{k_f}{} \; 2\left[\text{RNH} - \overset{\overset{O}{\|}}{C} - O - R'\right]_{\text{unstrained}}$$

If k_f is much greater than k_u, that is the reformation reaction is much faster than the dissociation reaction, the dissociation reaction will be rate determining and would explain the almost identical activation energies.

The reaction leading to inert products is included to account for the fact that not all the chains broken are replaced by new chains.

The number of urethane links per network chain has been calculated from the n.m.r. data (section 6.5.1) and the network chain density has been calculated from the stress-strain data (section 6.5.2). It is then fairly easy to calculate the specific rate of urethane cleavage from the continuous stress relaxation data.

$$k_u = 2.65 \times 10^{13} \quad \exp(-94600/RT) \qquad 7.7$$

where k_u is in $cm^3\ mole^{-1}\ hours^{-1}$.

The rate of continuous stress relaxation is given by:

$$\nu_1(o)k = 2.66 \times 10^7\ \bar{M}c \exp(-94600/RT) \qquad 7.8$$

where $\nu_1(o)k$ is in $hours^{-1}$.

The reaction leading to network chains formation can now be considered in terms of a recombination reaction that is not 100% efficient. Let the fraction of the cut chains that regenerate be α, so that if $\left[\nu_1(o) - \nu_1(t)\right]$ chains are removed, $\alpha\left[\nu_1(o) - \nu_1(t)\right]$ new chains will be formed. Equation (3.79) states that:-

$$f_o/f_t - 1 = \nu_1(o)/\nu_1(t) - 1 = \nu_1(o)k \qquad 7.9$$

$$\text{so} \quad \nu_1(t) = \nu_1(o)\,(1 + \nu_1(o)kt)^{-1} \qquad 7.10$$

$$\therefore \quad \nu_1(o) - \nu_1(t) = \nu_1(o)\left[1 - (1 + \nu_1(o)kt)^{-1}\right] \qquad 7.11$$

So that the number of new chains formed is given by

$$\nu_2(t) = \alpha \nu_1(o) \left[1 - (1 + \nu_1(o)kt)^{-1}\right] \qquad 7.12$$

$$\therefore \quad \Delta/\alpha = \nu_2(t)/\alpha\nu_1(o) = 1 - (1 + \nu_1(o)kt)^{-1} \qquad 7.13$$

$$\therefore \quad t = \alpha(t/\Delta) - 1/\nu_1(o)k \qquad 7.14$$

This equation has the correct form to describe the experimental results (i.e. it has the same form as equation 3.87), α is found to be 0.59. However, $\nu_1(o)k$ calculated from this equation is larger than that obtained from the continuous stress relaxation data (i.e. 1.7×10^{-2} compared with 6.55×10^{-3} at $100^{o}C$). Since the activation energies for network chain formation and cleavage are almost the same, it is clear that these rate differences are due to different pre-exponential factors. If the rate constant obtained from the two network data is denoted k^c and the specific rate constant for urethane reaction is k_u^c then

$$k_u^c = 4.61 \times 10^{15} \exp(-107900/RT) \qquad 7.15$$

where k_u^c is in cm^3 $mole^{-1}$ $hours^{-1}$.

Applying the theory of absolute reaction rates (see section 3.5.1) leads to the interpretation of the pre-exponential factors in terms of activation entropies so that:

$$k_u = RT/Lh \exp(-57.8/R)\exp(-94600/RT) \qquad 7.16$$

and

$$k_u^c = RT/Lh \exp(-15.0/R) \exp(-107900/RT) \qquad 7.17$$

where the activation energies are -57.8 J $mole^{-1}$ for cleavage and -15.0 J $mole^{-1}$ for network chain formation

The reasons for the different pre-exponential factors for network chain formation and cleavage probably lie in the

fact that the back reaction characterised by k_f in equation 7.5 may play a part in the overall kinetic scheme. Whilst the rate of cleavage is probably far more important, the participation of the back reaction could lead to these different pre-exponential factors.

(7.3.2) Network Reactions in Adiprene CM

In nitrogen the behaviour of Adiprene is broadly the same as that of Genthane S, the scission reaction is second order and is inhibited by treatment with napthyl isocyanate indicating that scission takes place at the urethane link. The relaxation behaviour can be explained by equation 7.5 except that the "inert products" must be different since for every 100 chains removed by scission about 130 new chains are formed. This can be explained if some of the products are three functional branch points.

The continuous stress relaxation data can be used, as with Genthane S, to calculate the specific rate constant for urethane cleavage.

$$k_u = 3.16 \times 10^{14} \exp(-110800/RT)$$

so that the rate of relaxation is given by

$$\nu_1(o)k = 2.51 \times 10^8 \bar{M}c \exp(-110800/RT)$$

where k_u is in cm^3 $mole^{-1}$ $hours^{-1}$ and $\nu_1(o)k$ is in $hours^{-1}$.

As for Genthane S, the network chain formation reaction could be described by equation 7.14 where $\alpha = 1.36$ although here the $\nu_1(o)k$ value obtained for the formation reaction was approximately the same as that obtained for the cleavage reaction (1.31×10^{-3} compared with 1.25×10^{-3} at 100^oC) and the activation energies were again very similar (i.e. 110.8 kJ $mole^{-1}$ for cleavage and 95.7 kJ $mole^{-1}$ for formation).

The specific rate constant for urethane reaction was

$$k_u^c = 1.95 \times 10^{12} \exp(-95700/RT)$$

where k_u^c is in $cm^3\ mole^{-1}\ hours^{-1}$.

Interpreting the pre-exponential factors as activation entropies gives:

$$k_u = RT/Lh \exp(-37.2/R) \exp(-110800/RT)$$

$$k_u^c = RT/Lh \exp(-95.5/R) \exp(-95700/RT)$$

The main difference here is that in Genthane S the activation entropy for cleavage was smaller than that for formation whereas the opposite is true here. However, these differences should not obscure the similarities between Genthane S and Adiprene CM since pre-exponential factors are rather poorly understood and seem to be dependent on structural and stereochemical factors and a large number of other variables.

Apart from the non-oxidative reactions, Adiprene CM undergoes an oxidative reaction that results in the cleavage of the crosslinks. This reaction obeys first order kinetics, the rate constant being given by

$$k = 1.07 \times 10^{16} \exp(-130500/RT)$$

or

$$k = RT/Lh \exp(-8.0/R) \exp(-130.5/RT)$$

so that the entropy of activation is $-8.0\ J\ mole^{-1}$ and the activation energy is $130.5\ kJ\ mole^{-1}$.

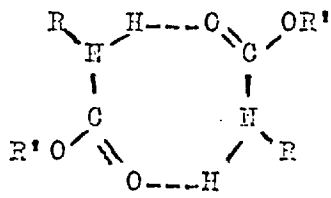
(7.3.3) The Mechanism of Urethane Degradation

The results show that there are marked similarities between the mechanisms of non-oxidative degradation operating in Adiprene CM and Genthane S. They both undergo a second order cleavage reaction involving the urethane group in

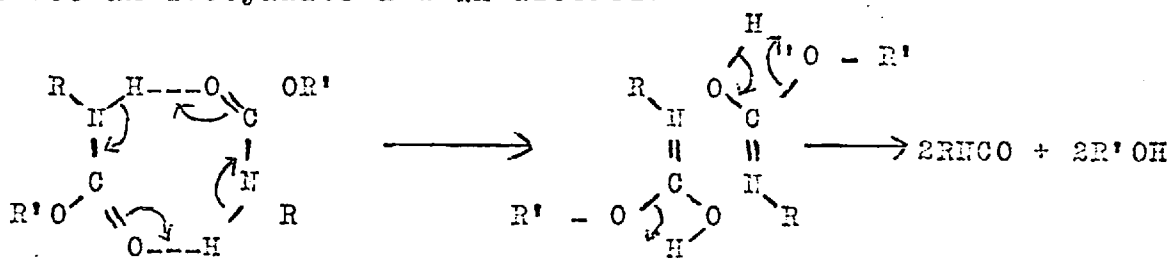
addition to a reaction leading to the regeneration of the urethane links that have undergone rupture. The results can be rationalised in terms of equation 7.5 which states:

$$2\,[\text{Urethane}] \underset{k_f}{\overset{k_u}{\rightleftharpoons}} [\text{Intermediate}] \xrightarrow{k_d} \text{Inert Products}$$

This mechanism proposes a bimolecular decomposition process involving two urethane links and it is interesting that a hydrogen bonded, dimeric structure is believed to exist in urethane systems (see section 5.3). It is proposed that this dimer has the following structure:



Assuming that this structure does exist, it is easy to see how a bimolecular dissociation could take place to produce an isocyanate and an alcohol.

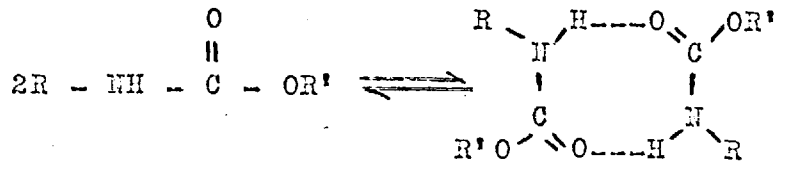


Since isocyanates and alcohols react together very readily these two residues can combine to regenerate urethane links.

$$\text{RNCO} + \text{R'OH} \longrightarrow \text{RNH} - \overset{\overset{\text{O}}{\|}}{\text{C}} - \text{OR'}$$

If this recombination reaction is fast compared with the cleavage reaction then the kinetics will be largely determined by the kinetics of cleavage.

Clearly the hydrogen bound dimer will be very unstable since the activation energy for dissociation is only 16 kJ mole^{-1} per bond and will be a transient species in dynamic equilibrium with the unbound urethane links, so that:



where the equilibrium lies on the left hand side. However, this is all that is required for the reaction to proceed by the bimolecular mechanism proposed.

Other mechanisms of the same type can be proposed but none of these utilise or exploit the phenomenon of hydrogen bonding as well as this one, which would seem to be the most likely candidate in view of the hydrogen bonding that is known to occur (see section 6.3.1.2). In addition, the products of decomposition are an isocyanate and an alcohol which are the most commonly observed products of urethane degradation under these conditions (see section 5.4.1.1).

The mechanism emphasises the role of the urethane hydrogen which must be transferred if dissociation is to occur and it also explains the production of the inert products which can result from the reaction of the isocyanate with groups other than the hydroxyl group. It could react with urethane groups, other isocyanate groups or water from the atmosphere to produce allophanate links, isocyanate dimers or trimers and amines.

This third possibility is particularly interesting; the reaction of an isocyanate with water produces an unstable

intermediate, carbamic acid, which decomposes to give an amine as follows:

$$RNCO + H_2O \rightarrow [RNHCOOH] \rightarrow RNH_2 + CO_2$$

This reaction explains some of the more unusual features of the observed behaviour.

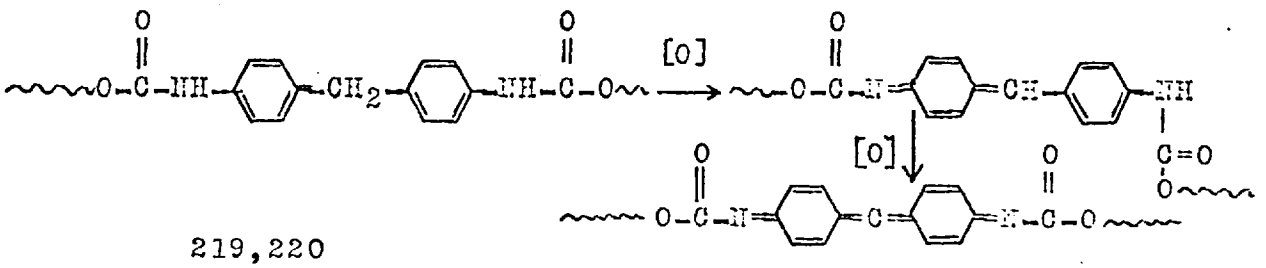
In Adiprene CM in air, degradation was largely the result of oxidative cleavage of the crosslinks; this occurred at a much faster rate than urethane cleavage and was responsible for the majority of the stress decay. However, the network chain formation reaction observed in nitrogen was reduced almost to zero in air. Thomas[245] has suggested that this occurs because water liberated, as a consequence of the crosslink oxidation, reacts with the isocyanate groups, resulting from the thermal dissociation of urethane groups, to produce amines and thus prevent the regeneration of urethane links. In Genthane S this does not occur although the percentage of chains cut that are replaced by new chains is greater in dry nitrogen than in ambient air; this could be due to the reaction of the isocyanates with atmospheric moisture. An attempt to simulate the behaviour of Adiprene CM in Genthane S by swelling cispolyisoprene into it was unsuccessful, but is not conclusive evidence against this mechanism since the oxidation mechanism tends to vary slightly from rubber to rubber and it is quite possible that the mechanisms of oxidation are different in polyisoprene and Adiprene CM.

The behaviour in the presence of antioxidants can also be explained; in Adiprene CM there is a substantial formation

reaction when samples containing Flectol H are relaxed in air; this probably occurs because the antioxidant reduces oxidative cleavage and, hence, the amount of water produced. If less water is produced then there is less available for reaction with isocyanate and so isocyanate groups are free to participate in reactions leading to the regeneration of urethane groups.

It is interesting that Flectol H has a similar, though much less significant effect on Genthane S and it is possible that this elastomer does contain a small number of groups that are susceptible to oxidation; typically these might be unsaturation introduced during cure.

In Genthane S another interesting observation was made; it was apparent that the rate of continuous stress relaxation was slightly faster in nitrogen or in air when Flectol H was present than in air when no additive was present. This type of behaviour can be described in terms of a free radical oxidative attack on the urethane group, as follows:



Schollenberger [219,220] has suggested that this quinone-imide structure is formed during the photochemical oxidation of urethanes containing MDI. Formation of this would lead to a reduced rate of urethane cleavage since this structure is devoid of urethane hydrogens and cannot undergo dissociation by the method suggested earlier.

It might have been expected that the increased free radical population brought about by the presence of cispolyisoprene would have caused an increase in the amount of this quinone-imide structure formed and a further decreased rate of oxidation. Unfortunately the presence of cispolyisoprene had no effect on the rate of continuous stress relaxation although again this is not a conclusive test of the postulated mechanism since the conditions for the formation of the above structure are not known.

This quinone-imide structure cannot be formed in TDI based polymers nor can any analogous type of structure; so that this type of oxidative interference cannot be expected in Adiprene CM.

To summarise the mechanics of urethane degradation as observed here there are considerable similarities between the behaviour observed for the two polymers. The broad agreement between the two polymers extends to the mechanism of degradation proposed which involves a hydrogen bonded intermediate which exploits the secondary bonding characteristics of the materials.

The mechanism explains most of the observed behaviour although it is necessary to include the production of quinone-imide structures to explain the inhibition of urethane dissociation in the presence of oxygen for Genthane S. It should be noted that the inhibitory effect of oxygen in Genthane S is a fairly minor one and the majority of the relaxation behaviour can be explained in terms of the mechanism proposed to explain the urethane dissociation.

(7.3.4) Conclusions and Suggestions for Further Work

The principal conclusion to be drawn from the results is that the non-oxidative network reactions observed in Genthane S and Adiprene CM are broadly similar and purely thermal in nature. A second order, bimolecular, thermal dissociation mechanism exploiting the phenomenon of hydrogen bonding in these urethane elastomers is capable of explaining most of the observations.

The proposal of Thomas, that urethane group regeneration might be inhibited by water, has interesting repercussions on the mechanism of hydrolytic degradation in urethane elastomers when combined with the fact that high humidity had little effect on the scission rate in either Genthane S or Adiprene CM. It is possible that the mechanism of hydrolysis involved the thermal dissociation of the urethane group followed by the reaction of water with the isocyanate group produced.

To investigate the effect of high humidity on the urethane regeneration reaction, further experiments should be done. These experiments could be either intermittent stress relaxation experiments or oven ageing followed by swelling in a suitable solvent; if the latter are done a calibration curve of ϕ_2 against C_1 or ν_1 must first be constructed. In the apparatus at Imperial College and the R.A.E., intermittent stress relaxation cannot be done at humidities higher than the saturated vapour pressure at room temperature, the continuous relaxation experiments in water and at high humidity reported here were done on the tensometer described in Chapter 6 and a small continuous relaxometer built at the R.A.E.[241]; neither of these instruments are suitable for doing intermittent stress relaxation experiments.

Experiments of the oven ageing type are being undertaken
245
at the R.A.E. using a humidity cabinet.

A feature of particular practical interest is the inhibition of the dissociation reactions; if hydrolysis does proceed via reaction with residues from the thermal decomposition, then inhibition of the thermal reaction will also improve the hydrolytic stability. It is evident from the results obtained that the thermal stability of the materials is enchanced when the urethane hydrogen is removed. Removal by an isocyanate leading to an allophanate, as used here, is clearly not the most satisfactory method of doing this, because of the limited stability of the allophanate link produced (see section 5.4.1.2). A more satisfactory procedure would probably be the production of N-alkyl urethanes but these are, unfortunately, difficult and expensive to produce. Clearly then, some work should be done both to assess the relative stabilities of different N-substituted urethanes and to develop practical ways of preparing them.

Apart from these studies on urethane elastomers, a study of the mechanism of urethane degradation using simple, monomeric urethanes would be interesting. It should be possible to heat two urethanes together, say one prepared from phenyl-isocyanate and ethanol and another prepared from naphthyl-isocyanate and another alcohol; samples could be withdrawn periodically and the yields of the various products separated chromatographically. Further studies along these lines might use tracers to look in more detail at aspects of the mechanism.

Clearly there are a number of further experiments that could be done; however, the experiments done and the results obtained in this study have led to a mechanism that is consistent with the majority of them.

REFERENCES

1. J.H. Saunders and K.C. Frisch, "Polyurethanes: Chemistry and Technology: Part I. Chemistry", High Polymers XVI, Interscience (1962)
2. J.H. Saunders and K.C. Krisch, "Polyurethanes: Chemistry and Technology: Part II. Technology", High Polymers XVI, Interscience (1964)
3. P. Wright and A.P.C. Cummings, "Solid Polyurethane Elastomers", Maclaren and Sons, London (1969)
4. P.F. Bruins, "Polyurethane Technology" Interscience (1969)
5. J.M. Buist and H. Gudgeon, "Advances in Polyurethane Technology", Maclaren and Sons, London (1969)
6. Kunstoff -Handbuch (Band VII): Polyurethane, Carl Hauser Verlag, Munich (1966)
7. B.A. Dombrow, "Polyurethanes", 2nd Edn., Reinhold, New York (1965)
8. Encyclopaedia of Polymer Science and Technology, Interscience 5, 416; 6, 573; 11, 506-563 (1969)
9. S.G. Starling and A.J. Woodall, "Physics", 2nd Edn., Longmans, London, Chapter 4 (1964)
10. L.R.G. Treloar, "The Physics of Rubber Elasticity", Oxford University Press (1958)
11. K. Dusek and W. Prins, Adv. Polymer Sci., 6, 1 (1969)
12. P.J. Flory, "Principles of Polymer Chemistry", Cornell University Press (1953)
13. G. Gee, Quart. Revs., 3,71 (1953)
14. A. Beerbower and J.R. Dickey, ASLE Transactions, 12, 1 (1969)
15. A.V. Tobolsky, "Properties and Structure of Polymers," John Wiley and Sons, New York, Chapter 5 (1960)
16. J.A. Offenbach and A.V. Tobolsky, J. Colloid Sci., 11, 39 (1956)
17. P.C. Colodny and A.V. Tobolsky, J. Amer. Chem. Soc., 79, 4320 (1957)
18. L. Weissbein and A. Singh, J. Polym. Sci., A,3,1675 (1965)
19. L. Weissbein and A. Singh, J. Polym. Sci., A1, 4, 2551 (1966)
20. A.V. Tobolsky, H. Yu and R. Thach, J. Appl. Polym. Sci., 6, S44 (1962)
21. J. Standen, Ph.D Thesis, University of London (1965)
22. P.J. Flory, "Statistical Mechanics of Chain Molecules", Interscience (1969)
23. M.V. Volkenstein, "Configurational Statistics of Polymer Chains", Interscience (1963)
24. T.M. Birshtein and O.B. Ptitsyn, "Conformations of Macromolecules", Interscience (1966)
25. W.R. Krigbaum and R-J Roe, Rubber Chem. Technol., 38, 1039 (1965)
26. E. Guth, J. Polym. Sci., C, 12, 89 (1966)
27. H.M. James and E. Guth, J. Polym. Sci, 4, 153 (1949)
28. F.T. Wall and P.J. Flory, J. Chem. Phys., 19, 1435 (1951)
29. J.J. Hermans, Trans. Faraday Soc., 43, 591 (1947)
30. H.M. James and E. Guth, J. Chem. Phys., 11, 455 (1943)
31. H.M. James, J. Chem. Phys., 15, 651 (1947)
32. H.M. James and E. Guth, J. Chem. Phys., 15, 669 (1947)

33. H.M. James and E. Guth, J. Chem. Phys., 21, 1039 (1953)
34. P.J. Flory and J. Rehner, J. Chem. Phys., 11, 512 (1943)
35. P.J. Flory and J. Rehner, J. Chem. Phys., 11, 521 (1943)
36. F.T. Wall, J. Chem. Phys., 11, 527 (1943)
37. G. Gee, Polymer, 7, 373 (1966)
38. P.J. Flory, J. Chem. Phys., 18, 108 (1950)
39. J.J. Hemans, J. Polym. Sci., 59, 191 (1962)
40. H.M. James and E. Guth, J. Appl. Phys., 15, 294 (1944)
41. E. Guth, J. Polym. Sci., C, 31, 267 (1970)
42. A.V. Tobolsky, D.W. Carlson and M. Indictor, J. Polym. Sci., 54, 175 (1961)
43. A.V. Tobolsky and L.H. Sperling, J. Phys. Chem., 72, 345 (1968)
44. A.V. Tobolsky and M. Shen, J. Appl. Phys., 37, 1952 (1966)
45. J.H. Hildebrand and R.L. Scott, "Regular Solutions", Prentice-Hall, New Jersey (1962)
46. P.A. Small, J. Appl. Chem., 3, 71 (1953)
47. G.M. Bristow and W.F. Watson, Trans. Faraday Soc., 54, 1731 (1958)
48. D. Mangaraj, Die Makromol. Chem., 65, 29 (1963)
49. D. Mangaraj, S. Patra and S. Rashid, Die Makromol. Chem., 65, 39 (1963)
50. J.D. Crowley, G.S. Teague and J.W. Lowe, J. Paint Tech., 38, 269 (1966)
51. J.D. Crowley, G.S. Teague and J.W. Lowe, J. Paint Tech., 39, 19 (1967)
52. C.M. Hansen, J. Paint Tech., 39, 105 (1967)
53. R.S. Rivlin, "Rheology, Theory and Applications", Academic Press, London, 1, 351 (1956)
54. Mooney, J. Appl. Phys., 11, 582 (1940)
55. A.G. Thomas, Trans. Faraday Soc., 51, 569 (1955)
56. Carmichael and Holdaway, J. Appl. Phys., 32, 159 (1961)
57. Carmichael and Holdaway, J. Appl. Phys., 32, 1724 (1961)
58. K.J. Smith, A. Ciferri and J.J. Hemans, J. Polym. Sci., A, 2, 1025 (1964)
59. M. Gordon, J.A. Love and D. Pugh, J. Chem. Phys., 49, 4680 (1969)
60. M. Gordon, J. Chem. Phys., 50, 3889 (1969)
61. A.R. Shultz, "Characterisation of Polymer Networks", G.E., R and D Center, Schenectady, New York, No. 67-C-291 (1967)
62. M.V. Volkenstein, Y.Y. Gotlib and O.B. Ptitsyn, Vysokonolskul Soedin 1, 1056 (1959)
63. H.M. James and E. Guth, Proc. Third Rubber Technol. Conf., Hetfner, London (1954)
64. R. Blokland and W. Prins, J. Polym. Sci., A 2, 7, 1595 (1969)
65. M. Yamamoto and J.L. White, J. Polym. Sci., A 2, 9, 1399 (1971)
66. M. Shen, W.F. Hall and R.E. De Wames, J. Macromol. Sci., C 2, 183 (1968)
67. S.F. Edwards, Proc. Phys. Soc., London, 85, 613 (1965)
68. D.A. McQuarrie and M. Shen, First Western Regional Meeting, A.C.S., Los Angeles (1965)
69. H. Reiss, J. Chem. Phys., 47, 186 (1967)
70. E.A.Di Marzio, J. Chem. Phys., 36, 1563 (1962)
71. L.S. Priss, Dokl. Akad. Nauk, SSSR, 116, 225 (1957)

72. J.L. Jackson, M. Shen and D.A. McQuarrie, J. Chem. Phys., 36, 1563 (1962)
73. G.R. Dobson and M. Gordon, Trans. I.R.I., 40, T 261 (1964)
74. P. Thirion and R. Chasset, Compt. Rend., 264, Série C, 958 (1967)
75. W.R. Krigbaum and M. Kaneko, J. Chem. Phys., 36, 99 (1962)
76. P.J. Flory, C.A.J. Hoeve and A. Ciferri, J. Polym. Sci., 34, 337 (1959)
77. P.J. Flory and A. Ciferri, J. Appl. Phys., 30, 1498 (1959)
78. S.M. Gumbrell, L. Mullins and R.S. Rivlin, Trans. Faraday Soc., 49, 1495 (1955)
79. A.V. Tobolsky, I.B. Prettyman and J.H.D. Dillon, J. Appl. Phys., 15, 324 (1944)
80. A.V. Tobolsky, J. Appl. Phys., 27, 673 (1956)
81. A.V. Tobolsky, R.D. Andrews and E.E. Hanson, J. Appl. Phys., 17, 352 (1946)
82. J.P. Berry, J. Scanlan and W.F. Watson, Trans. Faraday Soc., 52, 1137 (1956)
83. P.J. Flory, Trans. Faraday Soc., 56, 722 (1960)
84. D.K. Thomas, Polymer 7, 125 (1966)
85. J. Scanlan and W.F. Watson, Trans. Faraday Soc., 54, 740 (1958)
86. J.R. Dunn and J. Scanlan, "The Chemistry and Physics of Rubber-like Substances", ed. L. Bateman, Maclaren, London, Chapter 18 (1969)
87. J.P. Berry and W.F. Watson, J. Polym. Sci., 18, 201 (1955)
88. A.V. Tobolsky, J. Polym. Sci., B, 2, 637 (1964)
89. H. Yu, J. Polym. Sci., B, 2, 631 (1964)
90. J. Scanlan, J. Polym. Sci., 43, 501 (1960)
91. L. Mullins and A.G. Thomas, J. Polym. Sci., 43, 13 (1960)
92. G.R. Dobson, Ph.D Thesis, University of London (1965)
93. G.R. Dobson and M. Gordon, J. Chem. Phys., 43, 705 (1965)
94. J. Scanlan, Trans. Faraday Soc., 57, 839 (1961)
95. K.J. Laidler, "Reaction Kinetics, Volume I: Homogeneous Gas Reactions", Pergamon Press, London (1966)
96. S.H. Maron and C.F. Prutton, "Principles of Physical Chemistry", Macmillan, New York (1965)
97. A.V. Tobolsky and K. Murakami, J. Polym. Sci., 40, 443 (1959)
98. S. Baxter and H.A. Vodden, Polymer, 4, 145 (1963)
99. R.B. Beevers, J. Colloid Sci., 19, 40 (1964)
100. A.V. Tobolsky, V. Johnson and W.J. MacKnight, J. Phys. Chem., 69, 476 (1965)
101. A.V. Tobolsky, J. Polymer Sci., B, 2, 823 (1964)
102. A.V. Tobolsky and W.J. MacKnight, "Polymeric Sulphur and Related Polymers", Interscience, New York, Chapter 4 (1965)
103. M.T. Shaw, J. Chem. Phys., 54, 2172 (1971)
104. L. Bateman, C.G. Moore, M. Porter and B. Saville, "The Chemistry and Physics of Rubber-like Substances", ed. L. Bateman, Maclaren, London, Chapter 18 (1963)
105. J.R. Dunn, J. Macromol. Chem., 1, 739 (1966)
106. B. Saville and A.A. Watson, Rubber Chem. Technol. 40, 100 (1967)
107. L. Bateman, Quart. Revs., 8, 147 (1954)

108. J.L. Bolland, Quart. Revs., 3, 1 (1949)
109. J.I. Cunneen, Rubber Chem. Technol., 41, 182 (1968)
110. D. Barnard, L. Bateman, J.I. Cunneen and J.F. Smith, "The Chemistry and Physics of Rubber-like Substances", ed L. Bateman, Maclaren, London, Chapter 17 (1963)
111. P.M. Norling, T.C.P. Lee and A.V. Tobolsky, Rubber Chem. Technol., 38, 1198 (1965)
112. J.R. Dunn, J. Scanlan and W.F. Watson, Trans. Faraday Soc., 55, 667 (1959)
113. J.R. Dunn, J. Appl. Polym. Sci., 7, 1543 (1963)
114. P. Thirion and R. Chasset, Rubber Chem. Technol. 37, 617 (1964)
115. W. Scheele and K.H. Hillmer, Kolloid Zeitschrift 197, 80 (1964)
116. W. Scheele and K.H. Hillmer, Rubber Chem. Technol., 32, 759 (1964)
117. W. Scheele and K.H. Hillmer, Rubber Chem. Technol., 39, 1640 (1966)
118. J.R. Dunn, J. Scanlan and W.F. Watson, Trans. Faraday Soc., 54, 730 (1958)
119. J. Morand, Rubber Chem. Technol., 39, 537 (1966)
120. J.R. Dunn, Rubber Chem. Technol., 34, 910 (1961)
121. A.V. Tobolsky and H. Yu, J. Appl. Polymer Sci., 6, S 55 (1962)
122. W. Scheele and K.H. Hillmer, Rubber Chem. Technol., 43, 304 (1970)
123. J.R. Dunn, J. Appl. Polym. Sci., 4, 151 (1960)
124. J.R. Dunn, Rubber Chem. Technol., 34, 919 (1961)
125. J.R. Dunn and J. Scanlan, Trans. I.R.I., 34, 229 (1958)
126. J.R. Dunn and J. Scanlan, J. Polymer Sci., 35, 267 (1959)
127. C.L.M. Bell, M.E. Cain, D.J. Elliott and B. Saville, Rubber Chem. Technol., 39, 1565 (1966)
128. L.J. Maisey and J. Scanlan, J. Appl. Polymer Sci., 7, 1147 (1963)
129. A.V. Tobolsky, T. Yuzo and N. Shunji, Chem. Abs., 75, 89227y (1972)
130. A.V. Tobolsky, D.J. Metz and R.B. Mescrobian, J. Amer. Chem. Soc., 72, 1942 (1950)
131. D.K. Thomas, R.A.E. Technical Rept., 70008 (1970)
132. P.F. Lyons, T.C.P. Lee and A.V. Tobolsky, Rubber Chem. Technol., 39, 1634 (1966)
133. P.F. Lyons, T.C.P. Lee and A.V. Tobolsky, J. Macromol. Sci., Chem., 2, 1149 (1968)
134. M, Imoto, Y. Minowa, K. Goto, H. Harada, K. Nishihira, H. Fujita, K. Fujimoto, T. Izuta, K. Kono, K. Fujioka, A. Shiota, M. Oba, H. Oshita and T. Usamoto, Rubber Chem. Technol., 43, 451 (1970)
135. M. Markis and A.V. Tobolsky, J. Appl. Polym. Sci., 13, 2257 (1969)
136. M. Markis and A.V. Tobolsky, J. Appl. Polym. Sci., 14, 65 (1970)
137. A.V. Tobolsky, P.M. Norling, H.H. Frick and H. Yu, J. Amer. Chem. Soc., 86, 3925 (1964)
138. W. Scheele, K.H. Hillmer and C. Brudemann, Rubber Chem. Technol., 43, 788 (1970)
139. K. Murakami and S. Tamura, J. Polymer Sci., A 1, 9, 425 (1971)
140. K. Murakami and S. Tamura, Polymer J., 2, 528 (1971)
141. R.G. Bauman and J.M. Bon, J. Appl. Polym. Sci., 1, 351 (1959)

142. A.V. Tobolsky and A. Mercurio, J. Polymer Sci., 36, 467 (1959)
143. M. Kenkichi and T. Saburo, Chem. Abs., 75, 119055k (1972)
144. A.V. Tobolsky and P.M. Norling, J. Polymer Sci., A 3, 1435 (1965)
145. A. Singh and L. Weissbein, Rubber Age, 97, 72 (1965)
146. P.M. Norling and A.V. Tobolsky, Rubber Chem. Technol., 39, 278 (1966)
147. F. Haaf and P.R. Johnson, Rubber Chem. Technol., 44, 1410 (1971)
148. R.B. Mescrobian and A.V. Tobolsky, J. Polymer Sci., 2, 463 (1947)
149. M.T. Shaw and A.V. Tobolsky, J. Polymer Sci., A 1, 9, 1937 (1971)
150. M.T. Shaw and A.V. Tobolsky, Macromolecules, 3, 552 (1970)
151. T.C.P. Lee, L.H. Sperling and A.V. Tobolsky, J. Appl. Polym. Sci., 10, 1831 (1966)
152. H. Yu and L.A. Wall, 150th Meeting A.C.S., Atlantic City (1965)
153. Y. Takahashi and A.V. Tobolsky, Polymer J, 2, 457 (1971)
154. D. Evans, J.T. Morgan, R. Sheldon and G.B. Stapleton, J. Polymer Sci, A 2, 725 (1969)
155. H. Yu, A.C.S., Div. Polymer Chem. Preprints 5(2), 545 (1964)
156. H. Yu and L.A. Wall, J. Phys. Chem., 69, 2072 (1965)
157. T. Kusano, Y. Susuki and K. Murakami, J. Appl. Polym. Sci., 15, 2453 (1971)
158. E.R. Bertozzi, Rubber Chem. Technol., 41, 114 (1968)
159. M.D. Stern and A.V. Tobolsky, J. Chem. Phys., 14, 93 (1946)
160. M. Mochulsky and A.V. Tobolsky, Ind. Eng. Chem., 40, 2155 (1948)
161. G.D.T. Owen, W.J. MacKnight and A.V. Tobolsky, J. Phys. Chem., 68, 784 (1964)
162. A.V. Tobolsky, R.B. Beevers and G.D.T. Owen, J. Colloid Sci., 18, 359 (1963)
163. G. Gee, F. Fairbrother and G.T. Merrall, J. Polymer Sci., 16, 459 (1955)
164. A.V. Tobolsky, W.J. MacKnight and M. Takahashi, J. Phys. Chem., 68, 787 (1968)
165. P.C. Colodny and A.V. Tobolsky, J. Appl. Polym. Sci., 4, 39 (1959)
166. E.R. Bertozzi, F.O. Davis and E.M. Fettes, J. Polymer Sci., 19, 17 (1956)
167. P. Alexander and R.F. Hudson, "Wool: its Chemistry and Physics", Chapman and Hall Ltd., London (1954)
168. A. Robson, M.J. Williams and J.M. Woodhouse, J. Text. Inst., 60, 140 (1969)
169. S. Miyauchi, K. Kajiyama, M. Sakamoto and H. Tonami, Appl. Polym. Symposia, 18, 925 (1971)
170. I.B. Angliss, J.R. Cook, J. Delmenico, H.D. Feldtman, B.E. Fleischfresoer, F.W. Jones and M.A. White, Appl. Polym. Symposia, 18, 1027 (1971)
171. H.D. Weigmann, L. Rebenfield and C.J. Dansizer, Test. Res. J., 36, 535 (1966)
172. H.D. Weigmann and C.J. Dansizer, Appl. Polym. Symposia, 18, 795 (1971)
173. R.S. Asquith and J.B. Speakman, Nature, 170, 798 (1952)

174. J.M. Swan, Nature, 197, 965 (1965)
175. S. Miyanchi, M. Sakamoto and H. Tonami, J. Appl. Polym. Sci., 13, 2169 (1969)
176. W. Cooper, J. Polymer Sci., 28, 195 (1958)
177. Z.N. Tarasova and B.A. Dogadkin, Rubber Chem. Technol., 7, 1147 (1963)
178. T.C. Ward and A.V. Tobolsky, J. Appl. Polym. Sci., 11, 2403 (1967)
179. D.K. Thomas, R.A.E. (Farnborough), Tech. Note No. CPM. 82 (1964)
180. R.C. Osthoff, A.M. Bueche and W.T. Grubb, J. Amer. Chem. Soc., 76, 4659 (1954)
181. M.J. Turner and J.T. Lewis, Fourth Rubber Technol. Conf., London (1962)
182. D.H. Johnson, J.R. McLoughlin and A.V. Tobolsky, J. Phys. Chem., 58, 1073 (1954)
183. D.K. Thomas, Polymer, 7, 99 (1966)
184. D.K. Thomas, R.A.E. (Farnborough), Tech. Note No. CPM 27 (1963)
185. M.T. Shaw and A.V. Tobolsky, Polym. Engineering and Sci., 10, 225 (1970)
186. D.K. Thomas, R.A.E. (Farnborough), Tech. Rept., TR 68234 (1968)
187. E.J. Zaganiaris, L.H. Sperling and A.V. Tobolsky, J. Macromol Sci., Chem., A 1, 1111 (1967)
188. L.H. Sperling, S.L. Cooper and A.V. Tobolsky, J. Appl. Polym. Sci., 10, 1725 (1966)
189. D.K. Thomas, J. Appl. Polym. Sci., 8, 1415 (1964)
190. D.K. Thomas, R.A.E. (Farnborough), Report No., Chem. 533 (1962)
191. D.K. Thomas, R.A.E. (Farnborough), Tech. Note CPM. 3 (1963)
192. D.K. Thomas, R.A.E. (Farnborough), Tech. Note CPM. 24 (1963)
193. D.K. Thomas, L.N. Phillips, A.S. Atkinson and R. Sinnott, Rubber and Plastics Age, 46, 1020 (1965)
194. T. Yoshida, R.E. Florin and L.A. Wall, J. Polymer Sci., A, 3, 1685 (1965)
195. D.K. Thomas, R.A.E. (Farnborough), Tech. Rept. No. 65247 (1965)
196. A.V. Tobolsky and E. Peterson, J. Phys. Chem., 67, 930 (1963)
197. A.V. Tobolsky, V. Johnson and W.J. MacKnight, J. Phys. Chem., 69, 476 (1965)
198. D.J. David and H.B. Staley, "Analytical Chemistry of the Polyurethanes", High Polymers XVI, Part III, Interscience (1969)
199. D.J. Lyman, Rev. Macromol. Chem., 1, 191 (1966)
200. E.E. Gruber and O.C. Keplinger, Ind. Eng. Chem., 51, 151 (1959)
201. W. Cooper, Post Experience Course, "Elastomers", University of Bradford November (1970)

202. J. Bailey and S.M. Walker, European Polym. J., 8, 339 (1972)
203. T. Tanaka, T. Yokoyama and K. Kanji, Chem. Abs., 60: 10872C (1964)
204. Pimentel and McClellan, "The Hydrogen Bond", W.H. Freeman and Company, San Francisco (1960)
205. O.G. Tarakanov, V.A. Orlov and V.K. Beljokov, J. Polym. Sci., C, 23, 117 (1968)
206. H.C. Beachell and C.P. Ngoc Son, J. Polym. Sci., A 2, 4773 (1964)
207. H.C. Beachell and C.P. Ngoc Son, J. Appl. Polym. Sci., 7, 2217 (1963)
208. H.C. Beachell and I.L. Chang, J. Polym. Sci., A 1, 10, 503 (1972)
209. E. Dyer and R.E. Read, J. Org. Chem., 26, 4388 (1961)
210. H.C. Beachell and C.P. Ngoc Son, J. Appl. Polym. Sci., 8, 1089 (1964)
211. J.D. Ingham and N.S. Rapp, J. Polym. Sci, A 2, 4941 (1964)
212. E. Dyer and G.C. Wright, J. Amer. Chem. Soc., 81, 2138 (1959)
213. J.H. Engel, S.L. Reegan and P. Weiss, J. Appl. Polym. Sci., 7, 1679 (1963)
214. V.A. Orlov and O.G. Tarakanov, Chem. Abs., 63: 4463f (19[illegible])
215. W.D. Woolley, Brit. Polym. J., 4, 27 (1972)
216. B. Bott, J.G. Firth and T.A. Jones, Brit. Polym. J., 1, 203 (1969)
217. A. Davis and J.H. Golden, Makromol. Chem., 81, 38 (1965)
218. "Encyclopaedia of Polymer Science and Technology", 13, 685, Interscience (1969)
219. C.S. Schollenberger and K. Dinberg, S.P.E. Trans. 1, 31 (1961)
220. C.S. Schollenberger, H. Scott and G.R. Moore, Rubber World, 137, 549 (1958)
221. R.J. Athey, Rubber Age, 96, 705 (1965)
222. G. Magnus, R.A. Dunleavy and F.E. Critchfield, Rubber. Chem. Technol., 39, 1328 (1966)
223. D.O. Hummel, "Infra red Analysis of Polymers, Resins and Additives: An Atlas", Volume I: Plastics, Elastomers, Fibres and Resins, Spectra 1342, 1343, 1337 and 1338, Wiley-Interscience (1969)
224. L. Maisey, Personal Communication (1972)
225. J.H. Sexton, Personal Communication (1972)
226. J.C. Moore, J. Polym. Sci., A 2, 835 (1964)
227. J.C. Moore and J.G. Hendrickson, J. Polym. Sci., C, 233 (1965)
228. L.E. Maley, J. Polym. Sci., C 6, 253 (1965)
229. J. Cazes, J. Chem. Ed., 43, A 567 (1966)
230. J. Cazes, J. Chem. Ed., 43, A 625 (1966)
231. A.J. de Vries, I.U.P.A.C. International Symposium of Macromolecular Chemistry, preprint 139, Prague (1965)
232. K.H. Altgelt and J.C. Moore, "Polymer Fractionation", ed. M.J. Cantow, Chapter B4, Academic Press (1967)
233. J.C. Moore, "Characterisation of Macromolecular Structure", page, 273, National Academy of Sciences, Washington D.C. (1968)

234. J.C. Moore and J.G. Hendrickson, J. Polym. Sci., A 1, 4, 167 (1966)
235. J.D. Harmon, G.P.C. Seminar, Boston, Mass., September (1965)
236. L. Gamble, L. Westerman and K. Knipp, "The Molecular Weight Distribution of Elastomers - Comparison of Gel Permeation Chromatography with Other Techniques", Rubber Div. A.C.S. Miami Beach, Florida (1965)
237. "Interatomic Distances", Special publication, No. 11. The Chemical Society, London (1956)
238. L. Maisey, Personal Communication, March (1971)
239. E.F. Cluff, E.K. Gladding and R. Pariser, J. Polymer Sci., 45, 341 (1960)
240. E. Kay, B.B. Moore and D.K. Thomas, Polymer, 10, 55 (1969)
241. A.S. Atkinson, R.A.E. Tech. Note CPM 2, Chem. 1393 (1965)
242. A.S. Atkinson, R.A.E. Tech. Memo, MAT 109 (1971)
243. D.K. Thomas, Unpublished Results (1971)
244. P. Sykes, "A Guidebook to Mechanism in Organic Chemistry", Longmans (1966)
245. D.K. Thomas, Personal Communication (1972)

APPENDIX A: Stress-Strain Data

TABLE 1A: Tension of Dry Adiprene CM Samples (Continuous Loading)

1.0% Dicumyl Peroxide		1.5% Dicumyl Peroxide	
$f\phi_2^{1/3}/2(\lambda-\lambda^{-2})$ x 10^{-2} Nm	λ^{-1}	$f\phi_2^{1/3}/2(\lambda-\lambda^{-2})$ x 10^{-2} Nm	λ^{-1}
2.96	0.909	3.91	0.966
2.86	0.889	3.71	0.946
2.83	0.858	3.83	0.924
2.80	0.824	3.77	0.898
2.77	0.790	3.74	0.873
2.70	0.752	3.74	0.849
2.68	0.719	3.72	0.825
2.59	0.680	3.65	0.798
2.56	0.646	3.60	0.771
2.52	0.612	3.59	0.746
2.46	0.576	3.54	0.719
2,42	0.544	3.46	0.691
2.37	0.512	3.34	0.612
2.33	0.481	3.29	0.588
2.29	0.454	3.27	0.566
		3.23	0.541
		3.19	0.519
		3.18	0.499
		3.16	0.480
		3.14	0.462

2.0% Dicumyl Peroxide		2.5% Dicumyl Peroxide	
$f\phi_2^{1/3}/2(\lambda-\lambda^{-2})$ x 10^{-2} Nm	λ^{-1}	$f\phi_2^{1/3}/2(\lambda-\lambda^{-2})$ x 10^{-2} Nm	λ^{-1}
4.85	0.946	6.41	0.970
4.83	0.936	6.42	0.965
4.73	0.917	6.22	0.954
4.79	0.899	6.29	0.934
4.69	0.878	6.20	0.912
4.72	0.879	7.06	0.905
4.81	0.862	7.78	0.896
4.69	0.840	6.20	0.850
4.66	0.820	6.19	0.828
4.62	0.800	6.15	0.806
4.60	0.780	6.08	0.784
4.54	0.759	6.03	0.762
4.47	0.719	5.98	0.741
4.45	0.700	5.98	0.721
4.47	0.683	5.81	0.694
4.38	0.659	5.96	0.682
4.37	0.658	5.92	0.661
4.34	0.638	5.91	0.643
4.31	0.620		
4.27	0.600		
4.24	0.598		
4.22	0.581		
4.19	0.562		
4.14	0.530		
4.10	0.499		

TABLE 2A: Tension of Dry Adiprene CM Samples (Intermittent Loading)

1.0% Dicumyl Peroxide		1.5% Dicumyl Peroxide	
$f\phi^{1/3}/2(\lambda-\lambda^{-2})$ $\times 10^{-2}$ Nm	λ^{-1}	$f\phi^{1/3}/2(\lambda-\lambda^{-2})$ $\times 10^{-2}$ Nm	λ^{-1}
3.08	0.993	5.20	0.995
3.09	0.984	3.35	0.986
3.33	0.977	2.72	0.974
3.28	0.969	3.47	0.974
3.19	0.959	3.35	0.968
3.25	0.952	3.43	0.962
3.32	0.942	3.53	0.955
3.32	0.926	3.52	0.946
3.20	0.905	3.70	0.939
3.21	0.892	3.61	0.930
3.19	0.870	3.70	0.920
3.15	0.841	3.64	0.902
3.12	0.820	3.64	0.865
3.12	0.796	3.82	0.851
3.06	0.774	3.60	0.830
3.09	0.745	3.60	0.815
3.02	0.710	3.70	0.805
3.00	0.673	3.55	0.777
2.95	0.613	3.52	0.760
2.93	0.540	3.41	0.735
		3.47	0.711
		3.44	0.683

2.0% Dicumyl Peroxide		2.5% Dicumyl Peroxide	
$f\phi^{1/3}/2(\lambda-\lambda^{-2})$ $\times 10^{-2}$ Nm	λ^{-1}	$f\phi^{1/3}/2(\lambda-\lambda^{-2})$ $\times 10^{-2}$ Nm	λ^{-1}
4.30	0.995	5.69	0.996
4.23	0.979	6.23	0.991
4.32	0.967	7.28	0.990
4.33	0.955	5.01	0.974
4.53	0.943	6.69	0.971
4.59	0.945	6.00	0.958
4.59	0.931	4.99	0.939
4.61	0.918	5.83	0.932
4.48	0.905	6.84	0.920
4.50	0.888	5.62	0.900
4.18	0.872	5.66	0.889
4.40	0.859	5.89	0.879
4.40	0.824	5.78	0.863
4.40	0.808	5.66	0.846
4.41	0.791	5.86	0.870
4.30	0.770	5.82	0.857
4.58	0.750	5.78	0.843
		5.69	0.824
		5.69	0.811
		5.59	0.794
		5.53	0.775

TABLE 3A: Tension Experiments on Ethanol Swollen Adiprene CM Samples

1.0% Dicumyl Peroxide		1.5% Dicumyl Peroxide	
$f\phi^{1/3}/2(\lambda-\lambda^{-2})$ $\times 10^{-2}$ Nm	λ^{-1}	$f\phi^{1/3}/2(\lambda-\lambda^{-2})$ $\times 10^{-2}$ Nm	λ^{-1}
2.95	0.982	4.91	0.991
2.79	0.971	4.93	0.979
2.79	0.961	4.55	0.973
2.71	0.954	4.49	0.967
2.78	0.947	4.63	0.963
2.81	0.940	4.69	0.959
2.75	0.931	4.50	0.953
2.83	0.926	4.58	0.952
2.69	0.916	4.54	0.948
2.77	0.912	4.61	0.943
2.73	0.903	4.65	0.933
2.70	0.891	4.67	0.923
2.65	0.877	4.78	0.926
2.71	0.869	4.78	0.915
2.76	0.861	4.76	0.905
2.81	0.853	4.76	0.873
2.90	0.837	4.77	0.848
2.98	0.821	4.79	0.835
2.89	0.791	4.71	0.814
2.79	0.758	4.59	0.792
2.82	0.714	4.54	0.768
2.83	0.665	4.56	0.747

2.0% Dicumyl Peroxide		2.5% Dicumyl Peroxide	
$f\phi^{1/3}/2(\lambda-\lambda^{-2})$ $\times 10^{-2}$ Nm	λ^{-1}	$f\phi^{1/3}/2(\lambda-\lambda^{-2})$ $\times 10^{-2}$ Nm	λ^{-1}
5.44	0.979	5.84	0.983
4.75	0.971	5.84	0.980
4.72	0.963	6.12	0.978
5.37	0.962	5.63	0.974
5.57	0.959	5.92	0.970
5.14	0.950	5.98	0.966
5.22	0.947	6.19	0.965
5.36	0.944	5.76	0.961
5.45	0.939	5.88	0.960
5.52	0.933	5.97	0.957
5.38	0.926	5.94	0.952
5.33	0.918	5.92	0.948
5.31	0.911	6.35	0.944
5.57	0.910	6.01	0.937
5.57	0.903	6.13	0.936
5.52	0.897	5.99	0.930
5.63	0.893	5.90	0.924
5.62	0.886	6.05	0.920
5.58	0.880	6.25	0.917
5.74	0.864	6.05	0.907
5.64	0.837	6.12	0.901
5.67	0.763	6.32	0.896
5.24	0.697	6.15	0.877
		6.24	0.874
		6.06	0.864
		6.12	0.860
		6.11	0.852
		6.13	0.836

TABLE 4A: Tension of dry Genthane S. (Continuous Loading)

1.5% Dicumyl Peroxide		2.0% Dicumyl Peroxide	
$f\phi^{1/3}/2(\lambda-\lambda^{-2})$ $\times 10^{-2}$ Nm	λ^{-1}	$f\phi^{1/3}/2(\lambda-\lambda^{-2})$ $\times 10^{-2}$ Nm	λ^{-1}
1.80	0.913	2.70	0.893
1.79	0.886	2.25	0.826
1.74	0.855	2.28	0.781
1.69	0.824	2.25	0.736
1.73	0.801	2.31	0.699
1.70	0.772	2.16	0.637
1.69	0.744	2.02	0.541
1.61	0.713	1.90	0.452
1.60	0.678	1.75	0.385
1.62	0.655	1.77	0.333
1.59	0.625	1.75	0.295
1.49	0.579	1.74	0.267
1.46	0.551		
1.45	0.526		
1.42	0.501		
1.40	0.475		
1.35	0.443		
1.34	0.425		
1.32	0.403		
1.31	0.370		
1.25	0.330		
1.24	0.307		
1.23	0.286		
1.23	0.269		

2.5% Dicumyl Peroxide	
$f\phi^{1/3}/2(\lambda-\lambda^{-2})$ $\times 10^{-2}$ Nm	λ^{-1}
3.18	0.866
3.13	0.833
3.11	0.801
3.05	0.766
2.96	0.730
2.96	0.700
2.91	0.666
2.86	0.653
2.79	0.598
2.73	0.565
2.67	0.532
2.65	0.506
2.61	0.478
2.57	0.453
2.53	0.429
2.50	0.407
2.49	0.388

TABLE 5A: Tension of Genthane S Swollen to Equilibrium in Ethyl Acetate

1.0% Dicumyl Peroxide		1.5% Dicumyl Peroxide	
$f\phi^{1/3}/2(\lambda-\lambda^{-2})$ $\times 10^{-2}$ Nm	λ^{-1}	$f\phi^{1/3}/2(\lambda-\lambda^{-2})$ $\times 10^{-2}$ Nm	λ^{-1}
0.55	0.916	2.37	0.969
0.59	0.903	2.36	0.936
0.62	0.889	2.31	0.902
0.59	0.866	2.35	0.871
0.62	0.862	2.31	0.841
0.67	0.845	2.26	0.808
0.63	0.824	2.24	0.775
0.61	0.809	2.24	0.749
0.63	0.805	2.25	0.728
0.64	0.804	2.23	0.704
0.71	0.816	2.22	0.683
0.66	0.794	2.24	0.665
0.64	0.768	2.23	0.654
0.68	0.751	2.22	0.642
0.70	0.738	2.21	0.627
0.67	0.709	2.22	0.612
0.67	0.698	2.22	0.597
0.67	0.668	2.23	0.576
0.66	0.630	2.24	0.548
0.67	0.624		

2.0% Dicumyl Peroxide		2.5% Dicumyl Peroxide	
$f\phi^{1/3}/2(\lambda-\lambda^{-2})$ $\times 10^{-2}$ Nm	λ^{-1}	$f\phi^{1/3}/2(\lambda-\lambda^{-2})$ $\times 10^{-2}$ Nm	λ^{-1}
2.17	0.951	3.00	0.967
2.19	0.930	2.87	0.935
2.44	0.915	2.94	0.907
2.17	0.885	2.89	0.893
2.25	0.865	2.84	0.874
2.26	0.847	2.89	0.863
2.14	0.827	2.91	0.852
2.17	0.806	2.90	0.832
2.18	0.793	2.95	0.821
2.20	0.781	2.96	0.798
2.19	0.764	2.91	0.782
2.28	0.760	2.83	0.762
2.22	0.735	2.81	0.736
2.25	0.730	2.76	0.715
2.27	0.717	2.96	0.718
2.22	0.696	3.02	0.712
2.30	0.694	3.04	0.697
2.26	0.673	3.13	0.694
2.20	0.656	3.12	0.679
2.20	0.641	3.12	0.671
2.19	0.628	3.13	0.662
2.26	0.627	3.12	0.668
2.28	0.613	3.17	0.653
2.29	0.602	3.17	0.645
2.28	0.592	3.15	0.636
2.33	0.582	3.18	0.632
2.35	0.572	3.14	0.617
		3.23	0.613
		3.19	0.592
		3.18	0.576

TABLE 6A: Compression of Adiprene CM Swollen to Equilibrium in Cyclohexene

1.0% Dicumyl Peroxide		2.0% Dicumyl Peroxide	
$f\phi^{1/3}/2(\lambda-\lambda^{-2})$ $2 \quad 5 \quad -2$ $\times 10 \quad Nm$	λ^{-1}	$f\phi^{1/3}/2(\lambda-\lambda^{-2})$ $2 \quad 5 \quad -2$ $\times 10 \quad Nm$	λ^{-1}
3.07	1.0032	5.72	1.0032
3.13	1.0043	5.70	1.0033
3.04	1.0050	5.66	1.0039
2.98	1.0061	5.25	1.0047
3.20	1.0072	5.25	1.0052
3.34	1.0077	5.25	1.0058
3.30	1.0082	5.27	1.0063
3.27	1.0092	5.28	1.0069
3.42	1.0102	5.28	1.0080
5.43	1.0106	5.13	1.0094
3.43	1.0115	5.27	1.0102
3.46	1.0124	5.28	1.0113
3.54	1.0131	5.28	1.0124
3.57	1.0137	5.50	1.0132
3.40	1.0144	5.53	1.0142
3.46	1.0160	5.36	1.0167
3.48	1.0175	5.34	1.0190
3.48	1.0191	5.45	1.0201
3.56	1.0209	5.45	1.0231
3.50	1.0220	5.50	1.0251
3.57	1.0259	5.53	1.0271
3.60	1.0289	5.55	1.0291
3.60	1.0321	5.56	1.0312
3.59	1.0355	5.60	1.0331
3.63	1.0392	5.66	1.0352
		5.68	1.0368
		5.65	1.0391
		5.63	1.0413
		5.66	1.0432

2.0% Dicumyl Peroxide		2.5% Dicumyl Peroxide (contd)	
$f\phi^{1/3}/2(\lambda-\lambda^{-2})$ $2 \quad 5 \quad -2$ $\times 10 \quad Nm$	λ^{-1}	$f\phi^{1/3}/2(\lambda-\lambda^{-2})$ $2 \quad 5 \quad -2$ $\times 10 \quad Nm$	λ^{-1}
6.48	1.00.5	6.45	1.0131
5.77	1.0022	6.41	1.0141
5.85	1.0048	6.37	1.0152
5.95	1.0052	6.40	1.0162
6.20	1.0055	6.30	1.0181
6.41	1.0058	6.28	1.0202
6.50	1.0066	6.23	1.0222
6.45	1.0076	6.20	1.0242
6.38	1.0086	6.25	1.0260
6.40	1.0096	6.26	1.0277
6.47	1.0104	6.18	1.0300
6.43	1.0114	6.33	1.0313
6.50	1.0121		

TABLE 7A: Compression of Adiprene CH Swollen to Equilibrium in Benzene

1.0% Dicumyl Peroxide		1.5% Dicumyl Peroxide	
$f\phi^{1/3}/2(\lambda-\lambda^{-2})$ $\times 10^{5}$ Nm^{-2}	λ^{-1}	$f\phi^{1/3}/2(\lambda-\lambda^{-2})$ $\times 10^{5}$ Nm^{-2}	λ^{-1}
3.60	1.0037	4.84	1.0015
3.54	1.0042	4.90	1.0019
3.41	1.0051	5.12	1.0022
3.22	1.0060	4.60	1.0030
3.26	1.0067	4.81	1.0033
3.34	1.0070	4.71	1.0036
3.27	1.0079	4.74	1.0043
3.26	1.0085	4.77	1.0047
3.72	1.0091	4.80	1.0051
3.35	1.0114	4.73	1.0057
3.48	1.0122	4.84	1.0060
3.59	1.0131	4.69	1.0066
3.62	1.0140	4.64	1.0072
3.60	1.0152	4.80	1.0074
3.60	1.0175	4.62	1.0081
3.27	1.0199	4.53	1.0088
3.56	1.0224	4.52	1.0097
3.57	1.0247	4.66	1.0104
3.50	1.0275	4.73	1.0112
3.50	1.0300	4.79	1.0119
3.51	1.0322	4.69	1.0131
3.53	1.0344	4.74	1.0139
3.56	1.0362	4.79	1.0147
3.51	1.0394	4.60	1.0162
3.49	1.0417	4.69	1.0177
3.47	1.0446	4.82	1.0190
3.50	1.0465	4.63	1.0217
3.55	1.0482	4.70	1.0233
		4.71	1.0250
		4.57	1.0277
		4.78	1.0283
		4.70	1.0306
		4.79	1.0319

2.0% Dicumyl Peroxide		2.5% Dicumyl Peroxide	
$f\phi^{1/3}/2(\lambda-\lambda^{-2})$ $\times 10^{5}$ Nm^{-2}	λ^{-1}	$f\phi^{1/3}/2(\lambda-\lambda^{-2})$ $\times 10^{5}$ Nm^{-2}	λ^{-1}
6.78	1.0021	5.41	1.0017
7.46	1.0022	7.30	1.0022
6.52	1.0028	7.21	1.0026
5.93	1.0035	7.15	1.0029
5.84	1.0039	7.09	1.0032
5.76	1.0044	6.26	1.0040
5.83	1.0047	6.29	1.0043
5.64	1.0053	6.48	1.0049
5.82	1.0055	6.49	1.0056
5.62	1.0065	6.50	1.0062

TABLE 7A: (contd)

2.0% Dicumyl Peroxide		2.5% Dicumyl Peroxide	
$f\phi^{1/3}/2(\lambda-\lambda^{-2})$ $\times 10^{2}$ Nm	λ^{-1}	$f\phi^{1/3}/2(\lambda-\lambda^{-2})$ $\times 10^{2}$ Nm	λ^{-1}
5.72	1.0071	6.30	1.0071
5.42	1.0083	6.24	1.0079
5.44	1.0091	6.18	1.0087
5.41	1.0100	6.13	1.0095
5.54	1.0106	6.12	1.0109
5.50	1.0114	6.16	1.0123
5.57	1.0121	6.19	1.0137
5.48	1.0131	6.36	1.0147
5.62	1.0136	6.46	1.0158
5.55	1.0154	6.10	1.0182
5.52	1.0170	6.19	1.0194
5.63	1.0183	6.21	1.0208
5.41	1.0207	6.15	1.0224
5.57	1.0217	6.11	1.0240
5.63	1.0230	6.15	1.0253
5.57	1.0249	6.13	1.0268
5.52	1.0267	6.12	1.0283
5.50	1.0284	6.10	1.0298
5.50	1.0300	6.11	1.0312
5.48	1.0318	6.11	1.0327
5.48	1.0334	6.08	1.0343
		6.12	1.0355
		6.09	1.0372

TABLE 8A: Compression of Adiprene CM Swollen to Equilibrium in Chloroform

1.0% Dicumyl Peroxide		1.5% Dicumyl Peroxide	
$f\phi^{1/3}/2(\lambda-\lambda^{-2})$ $\times 10^{2}$ Nm^{-2}	λ^{-1}	$f\phi^{1/3}/2(\lambda-\lambda^{-2})$ $\times 10^{2}$ Nm^{-2}	λ^{-1}
3.53	1.0025	5.30	1.0021
3.64	1.0029	5.14	1.0029
3.11	1.0040	4.88	1.0046
3.16	1.0045	4.63	1.0065
3.15	1.0051	4.63	1.0081
3.38	1.0062	4.64	1.0098
3.01	1.0065	4.67	1.0113
3.09	1.0069	4.60	1.0131
3.09	1.0075	4.60	1.0148
2.91	1.0086	4.67	1.0161
3.06	1.0088	4.76	1.0174
3.00	1.0095	4.57	1.0198
3.08	1.0104	4.75	1.0206
3.01	1.0119	4.69	1.0225
3.03	1.0130	4.72	1.0240
2.98	1.0144	4.65	1.0259
3.08	1.0163		
3.04	1.0189		
3.07	1.0210		
3.14	1.0228		
3.03	1.0260		
3.11	1.0277		
3.18	1.0294		
3.23	1.0311		
3.18	1.0339		
3.16	1.0363		
3.22	1.0378		
3.09	1.0418		
3.16	1.0432		
3.18	1.0452		
3.17	1.0475		

2.0% Dicumyl Peroxide		2.5% Dicumyl Peroxide	
$f\phi^{1/3}/2(\lambda-\lambda^{-2})$ $\times 10^{2}$ Nm^{-2}	λ^{-1}	$f\phi^{1/3}/2(\lambda-\lambda^{-2})$ $\times 10^{2}$ Nm^{-2}	λ^{-1}
5.50	1.0049	5.28	1.0017
5.69	1.0061	5.04	1.0022
5.13	1.0076	5.40	1.0028
5.15	1.0091	5.53	1.0031
5.00	1.0109	5.97	1.0032
5.05	1.0123	5.88	1.0036
5.21	1.0134	5.67	1.0040
5.15	1.0150	5.81	1.0046
5.15	1.0166	5.81	1.0052
5.23	1.0193	5.81	1.0066
5.40	1.0312	5.96	1.0077
5.60	1.0236	5.87	1.0091
5.20	1.0284	5.97	1.0103
5.20	1.0314	5.99	1.0115
		5.84	1.0131
		5.87	1.0144
		6.08	1.0164

TABLE 9A: Compression of Adiprene CM Swollen to Equilibrium in Ethanol

1.0% Dicumyl Peroxide		1.5% Dicumyl Peroxide	
$f\phi^{1/3}/2(\lambda-\lambda^{-2})$ $\times 10^{5}$ Nm^{-2}	λ^{-1}	$f\phi^{1/3}/2(\lambda-\lambda^{-2})$ $\times 10^{5}$ Nm^{-2}	λ^{-1}
5.42	1.0016	5.63	1.0040
4.36	1.0026	4.80	1.0059
4.34	1.0033	4.77	1.0071
3.62	1.0047	4.60	1.0085
3.74	1.0059	4.60	1.0109
3.57	1.0077	4.73	1.0129
3.51	1.0094	4.70	1.0153
3.50	1.0109	4.61	1.0180
3.50	1.0124	4.62	1.0202
3.36	1.0145	4.81	1.0217
3.40	1.0159	4.72	1.0244
3.38	1.0176	4.92	1.0257
3.43	1.0204	5.05	1.0272
3.44	1.0234	4.81	1.0331
3.45	1.0265	4.80	1.0377
3.50	1.0291	4.81	1.0422
3.49	1.0323	4.72	1.0475
3.44	1.0358	4.82	1.0579
3.46	1.0387		
3.41	1.0424		
3.41	1.0455		
3.39	1.0488		
3.51	1.0502		

2.0% Dicumyl Peroxide		2.5% Dicumyl Peroxide	
$f\phi^{1/3}/2(\lambda-\lambda^{-2})$ $\times 10^{5}$ Nm^{-2}	λ^{-1}	$f\phi^{1/3}/2(\lambda-\lambda^{-2})$ $\times 10^{5}$ Nm^{-2}	λ^{-1}
5.40	1.0052	6.01	1.0019
5.36	1.0063	6.27	1.0027
5.15	1.0076	6.66	1.0033
5.15	1.0087	6.71	1.0041
4.89	1.0103	6.92	1.0047
4.97	1.0112	6.61	1.0057
4.93	1.0124	7.06	1.0061
5.01	1.0144	6.78	1.0071
5.23	1.0159	7.81	1.0069
4.92	1.0191	7.00	1.0084
5.19	1.0202	6.98	1.0099
5.38	1.0215	6.73	1.0119
5.47	1.0232	6.55	1.0138
5.52	1.0249	6.68	1.0151
5.50	1.0270	6.68	1.0167
5.52	1.0289	6.65	1.0184
5.46	1.0311	6.39	1.0207
5.53	1.0328	6.34	1.0226
5.39	1.0377	6.39	1.0240
5.40	1.0377	6.54	1.0251
		6.61	1.0264
		6.62	1.0280

TABLE 10A: Compression of Genthane S Swollen to Equilibrium in Cyclohexane

1.0% Dicumyl Peroxide		1.5% Dicumyl Peroxide	
$f\phi_2^{1/3}/2(\lambda-\lambda^{-2})$ x 10^5 Nm^{-2}	λ^{-1}	$f\phi_2^{1/3}/2(\lambda-\lambda^{-2})$ x 10^5 Nm^{-2}	λ^{-1}
1.53	1.0093	3.26	1.0042
1.36	1.0152	2.79	1.0071
1.29	1.0212	2.33	1.0112
1.21	1.0280	2.24	1.0145
1.31	1.0309	2.10	1.0184
1.27	1.0369	1.96	1.0229
1.25	1.0426	2.06	1.0279
1.23	1.0487	1.97	1.0356
1.25	1.0535	2.05	1.0402
1.28	1.0572	2.07	1.0459
1.26	1.0683	2.14	1.0502
1.29	1.0767	2.08	1.0577
1.29	1.0867	2.00	1.0664
1.31	1.0955	2.05	1.0708
1.29	1.1068	2.02	1.0778
1.28	1.1176	2.00	1.0848
1.30	1.1264	1.99	1.0916
1.27	1.1494	1.97	1.0989
1.31	1.1649	2.01	1.1032
		2.04	1.1075
		2.04	1.1139

2.0% Dicumyl Peroxide		2.5% Dicumyl Peroxide	
$f\phi_2^{1/3}/2(\lambda-\lambda^{-2})$ x 10^5 Nm^{-2}	λ^{-1}	$f\phi_2^{1/3}/2(\lambda-\lambda^{-2})$ x 10^5 Nm^{-2}	λ^{-1}
3.15	1.0044	3.63	1.0104
2.90	1.0070	3.58	1.0123
2.65	1.0101	3.62	1.0138
2.77	1.0119	3.58	1.0158
2.60	1.0152	3.61	1.0173
2.17	1.0172	3.54	1.0194
2.80	1.0210	3.62	1.0224
2.78	1.0258	3.56	1.0262
2.87	1.0294	3.55	1.0297
2.90	1.0336	3.63	1.0325
2.98	1.0370	3.47	1.0375
2.95	1.0418	3.64	1.0425
3.04	1.0447	3.60	1.0498
2.89	1.0514	3.50	1.0582
2.93	1.0551	3.48	1.0658
2.95	1.0591	3.58	1.0706
2.94	1.0636	3.52	1.0892
2.90	1.0689	3.64	1.1029
2.98	1.0757		
2.79	1.0852		

TABLE 11A: Compression of Genthane S Swollen to Equilibrium in Choloroform

1.0% Dicumyl Peroxide		1.5% Dicumyl Peroxide	
$f\phi_2^{1/3}/2(\lambda-\lambda^{-2})_5$ x 10^{-2} Nm	λ^{-1}	$f\phi_2^{1/3}/2(\lambda-\lambda^{-2})_5$ x 10^{-2} Nm	λ^{-1}
0.43	1.0162	0.96	1.0080
0.43	1.0195	0.91	1.0101
0.46	1.0215	0.88	1.0121
0.48	1.0235	0.90	1.0137
0.49	1.0259	0.92	1.0150
0.50	1.0281	0.93	1.0164
0.50	1.0311	0.93	1.0181
0.50	1.0336	0.95	1.0194
0.49	1.0402	0.95	1.0225
0.49	1.0454	0.96	1.0255
0.50	1.0510	0.96	1.0288
0.49	1.0576	0.97	1.0314
0.48	1.0644	0.94	1.0359
0.48	1.0699	0.96	1.0384
0.47	1.0783	0.95	1.0449
0.47	1.0827	1.01	1.0483
0.47	1.0896	0.98	1.0561
0.46	1.0911	0.99	1.0621
0.47	1.0955	1.06	1.0635
0.47	1.1014	1.00	1.0738
0.46	1.1333	1.00	1.0796
0.46	1.1443	1.01	1.0849
0.46	1.1591	1.01	1.0903
0.45	1.1720	0.97	1.1008
0.46	1.1822	0.89	1.1168
0.45	1.1978	0.90	1.1222
0.45	1.2087	0.90	1.1296
0.44	1.2249	0.90	1.1352
0.43	1.2453	0.91	1.1399

2.0% Dicumyl Peroxide		2.0% Dicumyl Peroxide (contd)	
$f\phi_2^{1/3}/2(\lambda-\lambda^{-2})_5$ x 10^{-2} Nm	λ^{-1}	$f\phi_2^{1/3}/2(\lambda-\lambda^{-2})_5$ x 10^{-2} Nm	λ^{-1}
2.01	1.0041	1.97	1.0199
1.83	1.0054	2.06	1.0223
2.02	1.0057	2.08	1.0253
2.01	L.0065	2.10	1.0281
2.14	1.0077	2.09	1.0315
2.32	1.0085	2.08	1.0347
2.31	1.0100	2.09	1.0376
2.15	1.0122	2.09	1.0409
2.19	1.0135	2.08	1.0441
2.23	1.0147	2.08	1.0474
2.19	1.0165	2.09	1.0502

TABLE 12A: Compression of Genthane S Swollen to Equilibrium in Ethyl Acetate

1.0% Dicumyl Peroxide		1.5% Dicumyl Peroxide	
$f\phi^{1/3}/2(\lambda-\lambda^{-2})$ x 10^{5} Nm^{-1}	λ^{-1}	$f\phi^{1/3}/2(\lambda-\lambda^{-2})$ x 10^{5} Nm^{-1}	λ^{-1}
0.33	1.023	1.22	1.007
0.36	1.027	1.29	1.008
0.36	1.032	1.29	1.010
0.35	1.038	1.29	1.012
0.36	1.042	1.21	1.014
0.35	1.050	1.20	1.016
0.37	1.052	1.31	1.019
0.37	1.058	1.34	1.023
0.35	1.066	1.29	1.027
0.37	1.074	1.24	1.028
0.34	1.090	1.38	1.032
0.35	1.099	1.34	1.039
0.36	1.108	1.30	1.048
0.38	1.112	1.24	1.052
0.37	1.123	1.30	1.061
0.38	1.143	1.24	1.066
0.35	1.176	1.28	1.073
0.37	1.188	1.28	1.080
0.35	1.218	1.27	1.089
0.34	1.243	1.24	1.092
0.34	1.268	1.28	1.098
0.35	1.278	1.29	1.108
0.35	1.304	1.25	1.114
0.37	1.309	1.26	1.121
0.37	1.328	1.33	1.126
0.35	1.361		
0.36	1.369		

2.0% Dicumyl Peroxide		2.5% Dicumyl Peroxide	
$f\phi^{1/3}/2(\lambda-\lambda^{-2})$ x 10^{5} Nm^{-2}	λ^{-1}	$f\phi^{1/3}/2(\lambda-\lambda^{-2})$ x 10^{5} Nm^{-2}	λ^{-1}
1.80	1.005	2.82	1.003
1.74	1.006	3.02	1.005
1.77	1.007	2.96	1.006
1.83	1.008	2.92	1.008
1.81	1.010	2.87	1.010
1.95	1.011	2.88	1.011
1.81	1.015	3.02	1.012
1.84	1.017	3.01	1.014
1.85	1.019	2.90	1.016
1.95	1.021	3.09	1.018
1.81	1.025	3.01	1.021
1.90	1.028	3.25	1.023
1.77	1.036	3.17	1.026
1.78	1.041	3.12	1.032
1.86	1.044	3.11	1.035
1.84	1.049	2.93	1.041

TABLE 12A: (contd)

2.0% Dicumyl Peroxide		2.5% Dicumyl Peroxide	
$f\phi^{1/3}/2(\lambda-\lambda_5^{-2})^{-2}$ $\times 10^{2}$ Nm	λ^{-1}	$f\phi^{1/3}/2(\lambda-\lambda_5^{-2})^{-2}$ $\times 10^{2}$ Nm	λ^{-1}
1.88	1.053	2.90	1.044
1.89	1.057	2.83	1.049
1.88	1.062	2.94	1.050
1.88	1.067	2.83	1.055
1.91	1.071	2.92	1.057
1.85	1.078	2.97	1.059
1.80	1.090	2.97	1.062
1.84	1.093	2.90	1.066
1.85	1.097	2.93	1.069
		2.97	1.071
		2.95	1.075
		2.96	1.078
		2.95	1.080

APPENDIX B: Chemical Stress Relaxation Results

(I) CHEMICAL STRESS RELAXATION OF GENTHANE S

TABLE 1B: Genthane S: Continuous Relaxation of Samples Cured with 2.5% Dicumyl Peroxide in Ambient Air

(C_1 = 3.03 x 10^5 Nm^{-2})

80°C		90°C		95.5°C		100°C	
t (hours)	f_t/f_o	t (hours)	f_t/f_o	t (hours)	f_t/f_o	t (hours)	f_t/f_o
		10	0.934	5	0.955	10	0.898
10	0.989	20	0.899	10	0.919	20	0.834
30	0.916	30	0.869	15	0.884	30	0.776
40	0.904	40	0.843	20	0.856	40	0.737
50	0.892	50	0.817	25	0.837	50	0.704
60	0.889	60	0.794	30	0.820	60	0.671
70	0.868	70	0.771	35	0.793	70	0.643
80	0.857	80	0.753	40	0.781	80	0.617
90	0.850	90	0.736	45	0.762	90	0.595
100	0.828	100	0.716	50	0.750	100	0.569
110	0.830	110	0.697	55	0.739	110	0.551
120	0.823			60	0.720		
130	0.813			65	0.707		
140	0.800						

110°C		130°C		150°C		151.5°C	
t (hours)	f_t/f_o	t (hours)	f_t/f_o	t (hours)	f_t/f_o	t (hours)	f_t/f_o
10	0.805	2	0.822	2	0.540	2	0.525
20	0.699	4	0.711	4	0.399	4	0.365
30	0.628	6	0.633	6	0.320	6	0.286
40	0.575	8	0.574	8	0.270	8	0.244
50	0.530	10	0.530	10	0.225	10	0.206
60	0.496	12	0.493	12	0.190	12	0.172
70	0.467	14	0.462	14	0.165	14	0.150
80	0.441	16	0.432	16	0.143	16	0.135
90	0.418	18	0.404	18	0.126	18	0.119
100	0.396	20	0.385	20	0.109	20	0.109
110	0.377	22	0.363				

140°C	
t (hours)	f_t/f_o
2	0.690
4	0.555
6	0.474
8	0.420
10	0.379
12	0.344
14	0.314
16	0.291

TABLE 2B: Genthane S: Intermittent Relaxation of Samples cured with 2.5% Dicumyl Peroxide in Ambient Air

($C_1 = 3.03 \times 10^{5}$ Nm^{-2})

80°C			100°C			110°C		
t (hours)	f_t/f_o	Δ	t (hours)	f_t/f_o	Δ	t (hours)	f_t/f_o	Δ
5	1.024	0.055	5	1.010	0.072	5	1.010	0.131
10	1.023	0.065	10	1.006	0.108	10	1.000	0.195
15	1.023	0.074	15	1.002	0.138	20	0.977	0.278
30	1.009	0.093	20	0.997	0.163	30	0.960	0.333
40	1.003	0.099	25	0.994	0.186	40	0.943	0.368
50	0.996	0.104	30	0.992	0.216	50	0.925	0.395
60	0.996	0.107	40	0.984	0.247	60	0.910	0.414
70	0.993	0.125	50	0.976	0.272	70	0.897	0.430
80	0.990	0.133	60	0.976	0.303	80	0.882	0.441
90	0.990	0.140	70	0.960	0.317	90	0.870	0.452
100	0.988	0.150	80	0.946	0.329	100	0.858	0.462
110	0.986	0.156	90	0.942	0.347	110	0.845	0.468
120	0.984	0.161	100	0.934	0.365			
130	0.979	0.166	110	0.928	0.377			

130°C			140°C			150°C		
t (hours)	f_t/f_o	Δ	t (hours)	f_t/f_o	Δ	t (hours)	f_t/f_o	Δ
1	1.000	0.105	1	0.993	0.186	1	0.989	0.307
2	1.000	0.179	2	0.973	0.283	2	0.947	0.407
3	0.990	0.230	3	0.952	0.339	3	0.905	0.448
4	0.976	0.265	4	0.937	0.382	4	0.881	0.482
5	0.961	0.295	5	0.921	0.410	5	0.852	0.495
6	0.952	0.319	6	0.912	0.438	6	0.835	0.515
7	0.945	0.343	7	0.897	0.451	7	0.811	0.519
8			8	0.886	0.468	8	0.792	0.522
9	0.928	0.375	9	0.875	0.478	9	0.776	0.513
10	0.922	0.392	10	0.867	0.488	10	0.763	0.538
11	0.917	0.402	11	0.858	0.500	11	0.752	0.546
12	0.910	0.417	12	0.849	0.505	12	0.736	0.548
13	0.903	0.426	13	0.839	0.510	13	0.727	0.549
14	0.898	0.436	14	0.834	0.520	14	0.721	0.556
15	0.896	0.450	15	0.828	0.526	15	0.713	0.559
16	0.884	0.452	16	0.822	0.531	16	0.700	0.557
17	0.884		17	0.813	0.535	17	0.692	0.558
18	0.876	0.472				18	0.681	0.555
19	0.870	0.472				19	0.673	0.556
20	0.865	0.480				20	0.667	0.558
21	0.860	0.485						

TABLE 3B: Stress Relaxation of Genthane S. Samples of Different Crosslink Densities

Continuous Relaxation in Air at 130°C

1.0% Dicumyl Peroxide		1.5% Dicumyl Peroxide		2.0% Dicumyl Peroxide		2.5% Dicumyl Peroxide	
t (hours)	f_t/f_o	t (hours)	f_t/f_o	t (hours)	f_t/f_o	t (hours)	f_t/f_o
2	0.641	2	0.737	2	0.820	2	0.843
4	0.493	4	0.594	4	0.694	4	0.740
6	0.386	6	0.502	6	0.610	6	0.669
8	0.314	8	0.442	8	0.546	8	0.614
10	0.263	10	0.393	10	0.494	10	0.569
12	0.223	12	0.353	12	0.452	12	0.530
14	0.193	14	0.323	14	0.416	14	0.498
16	0.170	16	0.298			16	0.468
18	0.149	18	0.274			18	0.444
		20	0.254			20	0.420

Continuous Relaxation in Air at 90°C

1.0% Dicumyl Peroxide		1.5% Dicumyl Peroxide		2.0% Dicumyl Peroxide		2.5% Dicumyl Peroxide	
t (hours)	f_t/f_o	t (hours)	f_t/f_o	t (hours)	f_t/f_o	t (hours)	f_t/f_o
5	0.870	5	0.936	5	0.959	10	0.955
10	0.820	10	0.905	10	0.935	20	0.920
15	0.786	15	0.881	15	0.916	30	0.900
20	0.752	20	0.859	20	0.897	40	0.876
25	0.720	25	0.837	25	0.881	50	0.854
30	0.695	30	0.820	30	0.867	60	0.831
35	0.668	35	0.803	35	0.854	70	0.812
40	0.647	40	0.785	40	0.840	80	0.796
		45	0.771	45	0.826	90	0.778
		50	0.758				
		55	0.742				
		60	0.730				
		65	0.718				

TABLE 4B: Intermittent Relaxation in Air at 130°C

2.5% Dicumyl Peroxide			1.5% Dicumyl Peroxide			2.0% Dicumyl Peroxide		
t (hours)	f_t/f_o	Δ	t (hours)	f_t/f_o	Δ	t (hours)	f_t/f_o	Δ
2	0.983	0.140	2	0.990	0.253	2	0.991	0.171
4	0.964	0.224	4	0.969	0.375	4	0.970	0.276
6	0.943	0.274	6	0.951	0.449	6	0.946	0.336
8	0.926	0.312	8	0.932	0.490	8	0.928	0.382
10	0.912	0.343	10	0.914	0.521	10	0.910	0.416
12	0.898	0.368	12	0.898	0.545	12	0.895	0.443
14	0.888	0.390	14	0.879	0.556	14	0.882	0.466
16	0.876	0.408	16	0.869	0.571			
18	0.864	0.420	18	0.852	0.576			
20	0.853	0.433	20	0.845	0.591			

% Dicumyl Peroxide	$C_1 \times 10^5$ Nm^{-2}
1.0	0.48
1.5	1.15
2.0	2.06
2.5	3.00

TABLE 5B: Stress Relaxation of Gonthane S cured with 2.5% Dicumyl Peroxide

($C_1 = 3.03 \times 10^{5}$ Nm^{-2})

Continuous Relaxation

Relaxation in Nitrogen				Sample Postcured for 25 hours at 150°C Relaxed in air at 130°C	
90°C		130°C			
t (hours)	f_t/f_o	t (hours)	f_t/f_o	t (hours)	f_t/f_o
5	0.962	2	0.792	2	0.774
10	0.941	4	0.664	4	0.635
15	0.925	6	0.572	6	0.572
20	0.910	8	0.498	8	0.511
30	0.884	10	0.438	10	0.445
40	0.857	12	0.389	12	0.418
50	0.835	14	0.350	14	0.384
		16	0.314	16	0.350
		18	0.283	18	0.331
		20	0.205	20	0.314

Intermittent Relaxation

Relaxation in Nitrogen at 130°C			Sample Postcured for 25 hours at 150°C Relaxed in air at 130°C		
t (hours)	f_t/f_o	Δ	t (hours)	f_t/f_o	Δ
2	1.034	0.242	2	1.000	0.226
4	1.028	0.364	4	0.998	0.363
6	1.030	0.458	6	0.994	0.422
8	1.022	0.524	8	0.992	0.481
10	1.007	0.569	10	0.992	0.547
12	1.000	0.611	12	0.986	0.568
14	0.996	0.614	14	0.984	0.600
16	0.989	0.635	16	0.973	0.619
18	0.983	0.700	18	0.968	0.637
20	0.979	0.774	20	0.963	0.649

TABLE 6B: Continuous and Intermittent Stress Relaxation of Genthane S Samples containing Flectol H in Air at 150°C

1.5% Dicumyl Peroxide (C_1 = 1.15 x 10^5 Nm^{-2})			
t (hours)	$(f_t/f_o)_c$	$(f_t/f_o)_i$	Δ
2	0.721	1.012	0.291
4	0.580	1.004	0.424
6	0.488	0.988	0.500
8	0.420	0.971	0.551
10	0.368	0.953	0.585
12	0.328	0.939	0.611
14	0.292	0.919	0.627
16	0.265	0.905	0.640
18	0.241	0.889	0.648
20	0.218	0.876	0.658

TABLE 7B: Continuous and Intermittent Stress Relaxation of Genthane S Samples containing Polyisoprene and Flectol H in Air at 150°C

Sample Containing Polyisoprene				Sample Containing Polyisoprene and Flectol H			
t (hours)	$(f_t/f_o)_c$	$(f_t/f_o)_i$	Δ	t (hours)	$(f_t/f_o)_c$	$(f_t/f_o)_i$	Δ
2	0.792	0.976	0.134	2	0.740	0.970	0.230
4	0.689	0.968	0.279	4	0.615	0.945	0.330
6	0.614	0.960	0.346	6	0.520	0.930	0.410
8	0.588	0.955	0.367	8	0.465	0.913	0.448
10	0.530	0.957	0.427	10	0.426	0.893	0.467
12	0.491	0.948	0.457	12	0.388	0.879	0.491
14	0.461	0.940	0.479	14	0.361	0.857	0.496
16	0.435	0.923	0.488	16	0.332	0.857	0.525
18	0.411	0.916	0.504	18	0.309	0.846	0.537
20	0.389	0.904	0.515	20	0.282	0.832	0.550

TABLE 8B: Continuous and Intermittent Stress Relaxation of Phenyl Isocyanate Treated Genthane S in Air at 130°C

(2.5% Dicumyl Peroxide; $C_1 = 2.63 \times 10^{5}$ Nm^{-2})

t (hours)	$(f_t/f_o)_c$	$(f_t/f_o)_i$	Δ
1	0.955	1.015	0.047
2	0.914	0.979	0.065
3	0.886	0.988	0.102
4	0.870	0.997	0.127
5	0.836	1.018	0.182
6	0.815	1.026	0.211
7	0.791	1.029	0.238
8	0.778	1.035	0.257
9	0.761	1.039	0.263
10	0.744	1.044	0.300
11	0.727	1.059	0.332
12	0.714	1.068	0.344
13	0.702	1.065	0.363
14	0.692	1.070	0.378
15	0.680	1.074	0.394

TABLE 9B: Continuous Stress Relaxation of Genthane S Samples Containing Stabaxol PCD and Cured with 2.5% Dicumyl Peroxide ($C_1 = 2.63 \times 10^{5}$ Nm^{-1}) Relaxed at 130°C

	% by weight of Stabaxol PCD in Sample							
	0.0	0.46	0.87	1.25	1.70	3.4	10.38	3.4*
t (hours)	f_t/f_o	f_t/f_o	f_t/f_o	f_t/f_o	f_t/f_o	f_t/f_o	f_t/f_o	f_t/f_o
2	0.763	0.769	0.320	0.862	0.885	0.870	0.820	0.882
4	0.629	0.641	0.699	0.769	0.806	0.800	0.725	0.812
6	0.546	0.549	0.621	0.709	0.756	0.763	0.676	0.758
8	0.485	0.431	0.562	0.680	0.699	0.725	0.641	0.722
10		0.418	0.510	0.654	0.667	0.685	0.610	0.695
12	0.397	0.373	0.461	0.637	0.657		0.581	0.675
14	0.356	0.341	0.442	0.614	0.610		0.559	0.661
16	0.319							
18	0.301							
20	0.282							

* Samples heated at 130°C for 1 hour then extracted for 48 hours with benzene

TABLE 10B: Intermittent Stress Relaxation of Genthane S Containing 3.4%* of Stabaxol PCD and cured with 2.5% Dicumyl Peroxide ($C_1 = 2.63 \times 10^{5}$ Nm^{-2})

Relaxed at 130°C

t (hours)	f_t/f_o	Δ
2	1.020	0.138
4	1.043	0.248
6	1.065	0.329
8	1.075	0.367
10	1.088	0.393
12	1.096	0.421
14	1.112	0.451

* Samples heated at 130°C for 1 hour then extracted for 48 hours with benzene

TABLE 11B: Continuous Stress Relaxation of Genthane S Cured with 2.5% Dicumyl Peroxide ($C_1 = 3.03 \times 10^{5}$ Nm^{-2})

Relaxed in water at 95.5°C

t (hours)	f_t/f_o
5	0.864
10	0.851
15	0.815
20	0.791
25	0.778
30	0.774
35	0.760
40	0.726
45	0.702

(II) CHEMICAL STRESS RELAXATION OF ADIPRENE CH

TABLE 12B: Continuous Relaxation of Adiprene CH cured with 2.0% Dicumyl Peroxide in Ambient Air

($C_1 = 5.1 \times 10^{5}$ Nm^{-2})

60°C		70°C		80°C		100°C	
t (hours)	f_t/f_o	t (hours)	f_t/f_o	t (hours)	f_t/f_o	t (hours)	f_t/f_o
10	0.963	10	0.955	10	0.942	5	0.921
20	0.953	20	0.943	20	0.920	10	0.867
30	0.949	30	0.934	30	0.906	15	0.822
40	0.942	40	0.923	40	0.890	20	0.776
50	0.937	50	0.918	50	0.873	25	0.722
60	0.934	60	0.910	60	0.859	30	0.678
70	0.927			70	0.845	35	0.638
80	0.926			80	0.832	40	0.601
90	0.920			90	0.818	45	0.563
100	0.917			100	0.804		
110	0.916			110	0.789		
120	0.914						
130	0.912						

105.5°C[x]		105.5°C		110°C		120°C	
t (hours)	f_t/f_o	t (hours)	f_t/f_o	t (hours)	f_t/f_o	t (hours)	f_t/f_o
2	0.961	2	0.927	2	0.914	2	0.856
4	0.903	4	0.876	4	0.840	4	0.723
6	0.860	6	0.820	6	0.768	6	0.599
8	0.833	8	0.778	8	0.699	8	0.492
10	0.765	10	0.734	10	0.634	10	0.409
12	0.738	12	0.687	12	0.575	12	0.337
14	0.700	14	0.643	14	0.522	14	0.281
16	0.664	16	0.604	16	0.477	16	0.234
18	0.630	18	0.566	18	0.435	18	0.195
20	0.598	20	0.532				

131°C		150°C	
t (hours)	f_t/f_o	t (hours)	f_t/f_o
0.33	0.842	1	0.153
0.67	0.708	2	0.020
1.0	0.578		
1.33	0.485		
1.67	0.402		

x Sample extracted in benzene for 24 hours

TABLE 13B: Continuous Relaxation of Adiprene CM Samples cured with Different Crosslink Densities in Ambient Air at 105.5°C

1.0% Dicumyl Peroxide				1.5% Dicumyl Peroxide		2.0% Dicumyl Peroxide	
t (hours)	f_t/f_o	t (hours)	f_t/f_o	t (hours)	f_t/f_o	t (hours)	f_t/f_o
2	0.912	2	0.925	2	0.973	2	0.944
4	0.826	4	0.862	4	0.916	4	0.899
6	0.744	6	0.807	6	0.892	6	0.860
8	0.662	8	0.749	8	0.855	8	0.825
10	0.584	10	0.696	10	0.820	10	0.782
12	0.508	12	0.638	12	0.783	12	0.744
14	0.439	14	0.583	14	0.748	14	0.706
16	0.376	16	0.529	16	0.712	16	0.669
18	0.320	18	0.489	18	0.677	18	0.629
20	0.269	20	0.442	20	0.643	20	0.592
		22	0.400	22	0.617		
		24	0.357				

2.0% Dicumyl Peroxide		2.5% Dicumyl Peroxide	
t (hours)	f_t/f_o	t (hours)	f_t/f_o
2	0.986	2	0.954
4	0.945	4	0.914
6	0.906	6	0.877
8	0.866	8	0.838
10	0.841	10	0.794
12	0.790	12	0.754
14	0.748	14	0.714
16	0.708	16	0.673
		18	0.637
		20	0.611

% Dicumyl Peroxide	$C_1 \times 10^5$ Nm^{-2}
1.0	3.41
1.5	4.65
2.0	5.35
2.5	6.25

TABLE 14B: Continuous Stress Relaxation of Adiprene CM cured with 2.0% Dicumyl Peroxide in Nitrogen

($C_1 = 5.1 \times 10^{5}$ Nm^{-2})

68°C		88°C		100°C		108°C	
t (hours)	f_t/f_o	t (hours)	f_t/f_o	t (hours)	f_t/f_o	t (hours)	f_t/f_o
10	1.000	5	0.998	2	0.976	2	0.983
20	0.995	10	0.980	4	0.961	4	0.954
30	0.991	15	0.975	6	0.950	6	0.949
40	0.984	20	0.969	8	0.939	8	0.933
50	0.979	25	0.963	10	0.932	10	0.910
60	0.975	30	0.954	12	0.924	12	0.887
70	0.970	35	0.949	14	0.916	14	0.869
80	0.967	40	0.945	16	0.910	16	0.850
90	0.967	50	0.934	18	0.902		
100	0.962	60	0.920	20	0.896		

128°C		126°C	
t (hours)	f_t/f_o	t (hours)	f_t/f_o
2	0.927	2	0.869
4	0.854	4	-
6	0.782	6	0.649
8	0.723	8	0.556
10	0.666	10	0.478
12	0.620	12	0.407
14	0.567	14	0.352
16	0.525		

TABLE 15B: Continuous Stress Relaxation of Adiprene CM cured with 2.5% Dicumyl Peroxide in Nitrogen

($C_1 = 6.3 \times 10^{5}$ Nm^{-2})

80°C		90°C		100°C		110°C	
t (hours)	f_t/f_o	t (hours)	f_t/f_o	t (hours)	f_t/f_o	t (hours)	f_t/f_o
10	0.994	10	0.989	10	0.986	10	0.967
20	0.990	20	0.983	20	0.974	20	0.935
30	0.987	30	0.977	30	0.965	30	0.912
40	0.985	40	0.974	40	0.953	40	0.884
50	0.984	50	0.969	50	0.945	50	0.861
60	0.982	60	0.964	60	0.935	60	0.839
70	0.979	70	0.958	70	0.926	70	0.818
80	0.977	80	0.954	80	0.918	80	0.796
90	0.975	90	0.950	90	0.910	90	0.778
100	0.975	100	0.946	100	0.901	100	0.761
110	0.973	110	0.944	110	0.892	110	0.742
120	0.972	120	0.941	120	0.884	120	0.723
130	0.971	130	0.937	130	0.878	130	0.708
140	0.969	140	0.933	140	0.870	140	0.694
150	0.969	150	0.925	150	0.862	150	0.677

120°C		130°C	
t (hours)	f_t/f_o	t (hours)	f_t/f_o
5	0.964	2	0.958
10	0.931	4	0.921
15	0.898	6	0.885
20	0.871	8	0.852
25	0.844	10	0.818
30	0.819	12	0.790
35	0.790	14	0.759
40	0.766	16	0.733
45	0.738	18	0.705
50	0.717	20	0.678

TABLE 16B: Intermittent Stress Relaxation of Adiprene CM cured with 2.0% Dicumyl Peroxide in Ambient Air

($C_1 = 5.1 \times 10^5$ Nm^{-2})

100°C			120°C		
t (hours)	f_t/f_o	△	t (hours)	f_t/f_o	△
5	0.996	0.075	2	0.899	0.043
10	0.958	0.091	4	0.758	0.035
15	0.921	0.099	6	0.630	0.031
20	0.883	0.107	8	0.527	0.035
25	0.847	0.125	10	0.440	0.031
30	0.811	0.133	12	0.372	0.035
35	0.775	0.137	14	0.318	0.037
40	0.740	0.139	16	0.287	0.053
45	0.713	0.150	18	0.241	0.046

TABLE 17B: Intermittent Stress Relaxation of Adiprene CM cured with 2.0% Dicumyl Peroxide in Nitrogen at 100°C

($C_1 = 5.1 \times 10^5$ Nm^{-2})

t (hours)	f_t/f_o	△
2	1.000	0.087
4	0.997	0.147
6	1.000	0.197
8	1.002	0.235
10	1.004	0.278
12	1.008	0.321
14	1.010	0.356
16	1.013	0.391
18	1.015	0.425
20	1.015	0.454

TABLE 18B: Intermittent Stress Relaxation of Adiprene CH cured with 2.5% Dicumyl Peroxide in Nitrogen

($C_1 = 6.3 \times 10^{5}$ Nm^{-2})

80°C			100°C			120°C		
t (hrs)	f_t/f_o	Δ	t (hrs)	f_t/f_o	Δ	t (hrs)	f_t/f_o	Δ
10	1.013	0.019	10	1.018	0.032	5	1.023	0.059
20	1.016	0.026	20	1.027	0.053	10	1.024	0.093
30	1.021	0.034	30	1.035	0.070	15	1.033	0.135
40	1.025	0.040	40	1.041	0.088	20	1.037	0.166
50	1.026	0.042	50	1.048	0.103	25	1.041	0.197
60	1.028	0.046	60	1.054	0.119	30	1.046	0.227
70	1.031	0.052	70	1.058	0.132	35	1.053	-
80	1.034	0.057	80	1.064	0.146	40	1.056	0.253
90	1.035	0.060	90	1.068	0.158	45	1.064	0.326
100	1.036	0.061	100	1.072	0.171	50	1.068	0.351
110	1.038	0.065	110	1.076	0.184	55	1.074	-
120	1.040	0.068	120	1.081	0.197	60	1.075	0.401
130	1.041	0.070	130	1.084	0.206	65	1.083	-
140	1.043	0.074	140	1.085	0.215	70	1.085	0.448

90°C			110°C			130°C		
t (hrs)	f_t/f_o	Δ	t (hrs)	f_t/f_o	Δ	t (hrs)	f_t/f_o	Δ
10	1.020	0.031	10	1.012	0.045	2	1.004	0.046
20	1.026	0.043	20	1.022	0.087	4	1.012	0.091
30	1.028	0.051	30	1.030	0.118	6	1.013	0.128
40	1.030	0.056	40	1.036	0.153	8	1.019	0.167
50	1.034	0.065	50	1.041	0.180	10	1.021	0.203
60	1.040	0.076	60	1.046	0.207	12	1.019	0.229
70	1.040	0.082	70	1.055	0.236	14	1.025	0.266
80	1.044	0.090	80	1.058	0.262	16	1.026	0.293
90	1.046	0.096	90	1.063	0.285	18	1.029	0.324
100	1.048	0.102	100	1.069	0.308	20	1.032	0.354
110	1.048	0.104	110	1.071	0.329			

TABLE 19B: Continuous Stress Relaxation of Adiprene CM Samples with Different Crosslink Densities in Nitrogen at 103°C

1.0% DCP		1.5% DCP		2.0% DCP		2.5% DCP	
t (hours)	f_t/f_o	t (hours)	f_t/f_o	t (hours)	f_t/f_o	t (hours)	f_t/f_o
2	0.935	2	0.965	2	-	2	-
4	0.877	4	0.936	4	0.980	4	0.990
6	0.823	6	0.901	6	0.962	6	0.985
8	0.787	8	0.877	8	0.956	8	0.975
10	0.746	10	0.855	10	0.947	10	0.971
12	0.704	12	0.826	12	0.938	12	0.962
14	0.669	14	0.800	14	0.917	14	0.952
16	0.645			16	0.889	16	0.943
				18	0.873	18	0.938
				20	0.858	20	0.935
				22	0.851	22	0.926

% DCP	$C_1 \times 10^5$ Nm^{-2}
1.0	3.41
1.5	4.65
2.0	5.35
2.5	6.25

TABLE 20B: Continuous Stress Relaxation of Adiprene CM cured with 2.0% Dicumyl Peroxide in Air at 120°C - Containing Antioxidant (Flectol H)

($C_1 = 5.35 \times 10^{5}$ Nm^{-2})

6.12% FH		3.06% FH		2.24% FH		1.53% FH	
t (hours)	f_t/f_o	t (hours)	f_t/f_o	t (hours)	f_t/f_o	t (hours)	f_t/f_o
2	0.888	2	0.897	2	0.913	2	0.904
4	0.806	4	0.827	4	0.850	4	0.849
6	0.733	6	0.769	6	0.803	6	0.800
8	0.670	8	0.719	8	0.765	8	0.759
10	0.614	10	0.676	10	0.726	10	0.727
12	0.566	12	0.637	12	0.687	12	0.696
14	0.525	14	0.599	14	0.654	14	0.667
16	0.487			16	0.622	16	0.641
18	0.454			18	0.590	18	0.621
20	0.430			20	0.561	20	0.596
						22	0.578
						24	0.562

TABLE 21B: Intermittent Stress Relaxation of Adiprene CM cured with 2.0% Dicumyl Peroxide in Air at 120°C - Containing Antioxidant (Flectol H)

($C_1 = 5.35 \times 10^{5}$ Nm^{-2})

	2.24% FH	
t (hours)	f_t/f_o	Δ
2	1.000	0.087
4	0.997	0.147
6	1.000	0.197
8	1.002	0.235
10	1.004	0.278
12	1.008	0.321
14	1.010	0.356
16	1.013	0.391
18	1.015	0.425
20	1.015	0.454

TABLE 22B: Continuous Relaxation of Adiprene CN cured with 2.5% Dicumyl Peroxide in Nitrogen at 120°C: Effect of Treatment with Naphthyl Isocyanate

($C_1 = 6.5 \times 10^{5}$ Nm^{-2})

	without isocyanate	with isocyanate
t (hours)	f_t/f_o	f_t/f_o
2	0.979	0.983
4	0.955	0.966
6	0.936	0.950
8	0.914	0.929
10	0.893	0.913
12	0.870	0.896
14	0.849	0.878
16	0.831	0.862
18	0.814	0.842
20	0.792	0.829
22	0.768	0.804
24	0.757	0.792
26	0.740	0.776
28	0.720	0.761
30	0.699	0.745
32	0.682	0.738
34	0.665	0.728
36	0.658	0.716
38	0.643	0.704
40	0.633	0.691
42	0.620	0.682
44	0.606	0.672
46	0.587	0.663
48	0.579	0.652
50	0.571	0.644

APPENDIX C:

(C 1) A Computer Programme to Analyse the Results of Stress-Strain Measurements

The programme enables the data to be fitted to the Mooney-Rivlin equation or to the Kinetic Theory equation. A weighted least squares fitting procedure is used, the weighting process used allows for the fact that an error in the undeformed dimensions of the sample has a disproportionate effect on the points with λ values that are close to unity.

The standard deviation of $f\phi_2^{1/3}/2(\lambda-\lambda^{-2})$ is given by:

$$\sigma_y^2 = (d_y/d_{l_0})^2 \sigma_{l_0}^2 + (d_y/d_1)\sigma_1^2$$

where $y = f\phi_2^{1/3}/2(\lambda-\lambda^{-2})$, l_0 is the undeformed length of the sample etc. The weighting factors for a particular point is the reciprocal of the square of its standard deviation.

Assuming that all the variables except l_0 are error free then

$$\sigma_y^2 = (d_y/d_{l_0})^2 \sigma_{l_0}^2$$

$\sigma_{l_0}^2$ is unknown but is constant for all the points for a particular experiment so that

$$1/\sigma_y^2 \quad \alpha \quad 1/(d_y/d_{l_0})^{-2} \text{ where:}$$

$$(d_y/d_{l_0}) = \frac{f\phi_2^{1/3} l^2 \; 1 + 3l_0^3(l^3 - l_0^3)^{-1}}{(l^3 - l_0^3)}$$

Accepting the fact that l_0 was in error the programme then allowed l_0 to vary slightly and determined the l_0 value that gave rise to be best fit to the required equation. In

tension experiments the l_0 was never less than 3 cm long, the maximum amount this was allowed to vary was 0.1 cm, that is 3% of the length.

In a compression experiment the undeformed height of the sample, l_0, was never less than 0.7 cm, the maximum amount this was allowed to vary was 0.01 cm, that is 1.3% of the height.

The best value of l_0 was, hence, always close to the extrapolated value.

Bad points were rejected in the calculation but this was only done when their residuals were more than 3.5 times the standard deviation, points whose residuals were between 2.0 and 3.5 times the standard deviation were marked £ and rejected points were marked x . Thus no points were rejected without informing the user and at most only two points were rejected in any block of data.

Checks were built into the programme that informed the user whenever points were rejected or trivial or indefinite results were obtained.

The programme is given on pages 327 to 337 inclusive; it is written in A.S.A. Fortran and was used on the University of London CDC 6600/6400 installation and the Imperial College CDC 6400 computer.

```
      PROGRAM STRECH(INPUT,OUTPUT,TAPE5=INPUT,TAPE6=OUTPUT)
C     PROGRAM EVALUATES STRESS-STRAIN DATA FOR SWOLLEN OR DRY RUBBER
C     SAMPLES IN UNIAXIAL TENSION OR COMPRESSION
      DIMENSION WT(500),ZL(500),IT(16),X(500)
      DIMENSION D(8)
      DATA COM,TEN,TEST/6HCOMPRS,6HTENSUN,1H /
C     THE FIRST TWO DATA CARDS CONTAIN ANY REQUIRED ALPHANUMERIC
C     INFORMATION THAT MAY BE REQUIRED...IT IS OUTPUTED AT THE HEAD
C     OF THE BLOCK OF DATA TO WHICH IT REFERS
  641 READ(5,2999)(IT(I),I=1,16)
      WRITE(6,2888)
      WRITE(6,2777)(IT(I),I=1,16)
 2999 FORMAT(8A10)
 2888 FORMAT(1H1)
 2777 FORMAT(1X,8A10)
C     THE SECOND DATA CARD CONTAIN WATSIT AND IWAT.........
C                   WATSIT = COMPRS IF THE DATA REFERS TO COMPRESSION
C                   WATSIT = TENSUN IF THE DATA REFERS TOTENSION
C                   IWAT = 1 IF A KINETIC THEORY FIT IS REQUIRED , LEFT BLANK
C                   IF A MOONEY RIVLIN FIT IS REQUIRED
      READ(5,5555)WATSIT,IWAT
      IF(IWAT.EQ.TEST)IWAT=0
      IF(WATSIT.EQ.COM)GO TO 994
 5555 FORMAT(A6,1X,I1)
C     READ ON TENSION DATA...W=SAMPLE WIDTH,T=SAMPLE THICKNESS,Z=ZERO LOAD
C          LENGTH,V=VOLUME FRACTION OF RUBBER,N=NUMBER OF DATA POINTS,
C           ZL=LENGTH OF SAMPLE,WT=APPLIED LOAD IN GRAMS
      READ(5,2000)W,T,Z,V,N
 2000 FORMAT(4(F5.3,2X),I2)
      IFLAG = 0
      DO 200 J=1,N
  200 READ(5,2001)ZL(J),WT(J)
 2001 FORMAT(F6.4,F5.1)
  671 CALL TENSUN(W,T,Z,V,ZL,WT,N,IFLAG,Q,IWAT,WATSIT,COM)
C     NOGO TELLES PROGRAM WHAT IS REQUIRED.....IF 1 READS AN AMMENDED Z AND
C      RECOMPUTES,IF 2 RECOMPUTES WITH VARIABLE Z AND FINDS BEST VALUE,
C      ANYTHING ELSE  EXCEPT 0 STARTS PROGRAM AGAIN WITH NEW DATA BLOCK....
C      .......0 ENDS PROGRAM
```

```
      PEAD(5,9641)NOGO
 9641 FORMAT(I1)
      GO TO 661
C       READ ON COMPRESSION DATA .....VARIABLES AS BEFORE BUT.......
C             WS=INITIAL STARTING LOAD TO BE ADDED TO APPLIED LOAD TO
C       GIVE TOTAL APPLIED LOAD...HS=ANALOGOUS HEIGHT QUANTITY
  994 READ(5,5001)WS,HS,Z,N,V
      Z = Z*10.0
C       D=DIAMETER OF SAMPLE ....GIVE 8 VALUES ....AVERAGE COMPUTED
      READ(5,5002)(D(I),I=1,8)
      READ(5,5003)(ZL(J),WT(J),J=1,N)
 5001 FORMAT(F4.1,2X,2(F6.4,2X),I3,2X,F6.4)
 5002 FORMAT(8(F6.4,4X))
 5003 FORMAT(4(F6.4,4X,F6.1,4X))
      SUM = 0.0
      DO 985 JI=1,N
C     ADJUST HEIGHT AND LOAD TO GIVE OVERALL VALUES AND MULTIPLY HEIGHT BY 10 TO
C     ALLOW USE OF SAME ITERATIVE PROCEDURE FOR TENSION AND COMPRESSION
      ZL(JI) = ZL(JI) + HS
      ZL(JI) = ZL(JI)*10.0
  985 WT(JI) = WT(JI) + WS
      DO 51 JK=1,8
C     COMPUTE AVERAGE DIAMETER
   51 SUM = SUM + (D(JK)/2.0)
      W = SUM/8.0
      W = W*W
      T = 3.14159
      GO TO 671
C     READ AMMENDED Z VALUE FOR FURTHER CALCULATION
  651 READ(5,9642)Z
 9642 FORMAT(F5.3)
      GO TO 671
C     IFLAG=1...SUPRESSES PRINTING DURING ITERATIVE BEST FIT PROCEDURE
  681 IFLAG = 1
C     BEGIN ITERATIVE BEST FIT PROCEDURE WITH VARYING Z
      Z = Z - 0.100
```

```
      DO 691 IX = 1,200
      CALL TENSUN(W,T,Z,V,ZL,WT,N,IFLAG,P,IWAT,WATSIT,COM)
      Z = Z + 0.001
C     X(IX) IS THE STANDARD DEVIATION FOR A PARTICULAR Z VALUE
      X(IX) = P
  691 CONTINUE
      ZPUT = X(1)+999.9
C     TEST STANCARD DEVIATIONS OF VARIOUS Z VALUES TO TEST WHICH IS
C            BEST VALUE
      DO 692 IY = 1,200
      IF(X(IY).LT.ZPUT)GO TO 993
      GO TO 692
  993 ZPUT = X(IY)
      NUMB = IY
  692 CONTINUE
C     RECOMPUTE WITH BEST Z VALUE
      Z = Z - 0.201 + (0.001*FLOAT(NUMB))
      IFLAG = 0
      GO TO 671
C     TEST VALUE OF NOGO
  661 IF(NOGO.EQ.1)GO TO 651
      IF(NOGO.EQ.2)GO TO 681
      IF(NOGO.NE.0)GO TO 641
      STOP
      END

      SUBROUTINE WT(H,F,WEIGHT,HO)
C     SUBROUTINE CALCULATES RELEVANT WEIGHTING FACTORS FOR STRESS-STRAIN
C      DATA
      SIG1 = (H**3)-(HO**3)
      SIG1=1.0/SIG1
      SIG2=F*(H**2)
      SIG3=1.0+(3.0*(HO**3)*SIG1)
      SIG=SIG1*SIG2*SIG3
      WEIGHT=SIG*SIG
      WEIGHT=1.0/WEIGHT
      RETURN
      END
```

```
      SUBROUTINE TENSUN(WIDE,THICK,ZLONG,VFRACT,ZONG,WAYT,NG,IFL,P,IWAT,
     1WATSIT,COM)
C     SUBROUTINE CALCULATES THE STRESS-STRAIN PARAMETERS OF THE DATA
      DIMENSION ZONG(50),WAYT(50),FORCE(50),ZLAMDA(50),FUNCTN(50)
      DIMENSION ENDVAL(50),ZLOMDA(50)
      DIMENSION FUDGE(100)
      DATA CHARGE/+1.0E-15/
      WETONE = 1.0 / 3.0
      ND=NG
      IF(IFL.EQ.1)GO TO 141
C     AVOID WRITING WRONG ZERO LENGTH VALUE IF COMPRESSION DATA
      IF(WATSIT.EQ.COM)GO TO 755
C     WRITE ZERO LENGTH OF SAMPLE
      WRITE(6,3524)ZLONG
 3524 FORMAT(1X/////1X,16HSAMPLE LENGTH = ,F5.3,3HCMS)
  756 WRITE(6,3523)
 3523 FORMAT(1X/////1X,5X5HFORCE,11X,17HLAMDA-LAMDA(**-2),9X,5HLAMDA,14X
     1,11HLAMDA(**-1),2X,25HFORCE/(LAMDA-LAMDA(**-2)))
C     COMPUTE  STRESS-STRAIN PARAMETERS
  141 I=0
      DO 140 J = 1,ND
C     CHECK TO SEE IF LAMDA IS EQUAL TO 1
      IF((ZONG(J)-ZLONG).GE.(-1.0E-10).AND.WATSIT.EQ.COM)GO TO 591
      IF((ZONG(J)-ZLONG).LE.(+1.0E-10).AND.WATSIT.NE.COM)GO TO 591
      I=I+1
      ZLAMDA(I) = ZONG(J)/ZLONG
      FORCE(I) = WAYT(J) * (VFRACT ** (WETONE ))/(WIDE*THICK)
      FORCE(I) = FORCE(I) * 981.0
      FUNCTN(I) = ZLAMDA(I) - (1.0/(ZLAMDA(I) *ZLAMDA(I)))
      ENDVAL(I) = FORCE(I)/FUNCTN(I)
      ZLOMDA(I) = 1.0/ZLAMDA(I)
C     CALL ROUTINE TO CALCULATE WEIGHTING FACTORS FOR LEAST SQUARES DATA FIT
      CALL WT(ZONG(I),FORCE(I),FUDGE(I),ZLONG)
      IF(IFL.EQ.1)GO TO 140
      WRITE(6,1400)FORCE(I),FUNCTN(I),ZLAMDA(I),ZLOMDA(I),ENDVAL(I)
 1400 FORMAT(1X,5(1PE16.6,5X))
      GO TO 140
```

```
  591 IF(IFL.EQ.1)GO TO 140
      WRITE(5,6631)
 6631 FORMAT(1X,*POINT REJECTED AS GIVES RISE TO INDEFINITE RESULT*)
  140 CONTINUE
      ND=I
      IF(IWAT.EQ.1)GO TO 753
C      FIT DATA TO MOONEY RIVLIN EQUATION
      CALL LEAST(ZLOMDA,ENDVAL,FUDGE,S,A,P,Y,Z,ND,6,IFL)
      GO TO 754
C     FIT DATA TO KINETIC THEORY EQUATION
  753 CALL KINET(ENDVAL,FUDGE,ND,ZLOMDA,IFL,SL,P,6)
  754 RETURN
  755 ZLX = ZLONG/10.0
C     WRITE ZERO LENGTH FOR COMPRESSION DATA
      WRITE(6,3522)ZLX
 3522 FORMAT(1X/////1X,*SAMPLE LENGTH = *,F6.4,*CMS*)
      GO TO 756
      END



      SUBROUTINE KINET(X,W,ND,Y,IFLG,AVX,ERP,MOUT)
C     SUBROUTINE FITS STRESS-STRAIN DATA TO KINETIC THEORY DATA
      DIMENSION X(ND),Y(ND),W(ND)
      DIMENSION XA(100),YA(100),WA(100),RES(100),INDEX(100)
      DATA IND1,IND2,IND3/1H ,1H*,1H£/
C     NUMBER OF DATA POINTS IS INITIALLY TOTAL NUMBER PRESENTED
      NA = ND
      DO 360 I=1,NA
C     COPY WORKING PARAMETERS TO AVOID OVERWRITING THEM IN MAIN PROGRAM
      XA(I)=X(I)
      YA(I)=Y(I)
  360 WA(I)=W(I)
C     SET SUMS TO ZERO
  380 SUMX=0.0
      SUMW=0.0
C     CALCULATE BEST FIT FOR PARAMETERS PRESENTED
      DO 361 J=1,NA
```

```
      SUMX=SUMX+(XA(J)*WA(J))
  361 SUMW=SUMW+WA(J)
      AVX=SUMX/SUMW
C     SET SUMS TO ZERO
      SUMR=0.0
C     CALCULATE STANDARD DEVIATION OF DATA
      DO 362 L=1,NA
      RES(L)=AVX-XA(L)
      RES(L)=RES(L)*RES(L)
      SUMR=SUMR+RES(L)
  362 RES(L)=SQRT(RES(L))
      ERP=SUMR/FLOAT(NA-1)
      ERP=SQRT(ERP)
C     CHECK DATA ....BAD POINT MARKED * AND REJECTED........POOR POINTS
C     POINTS MARKEDE BUT KEPT IN CALCULATION
      DO 363 M=1,NA
      INDEX(M)=IND1
      IF(RES(M).GE.(3.5*ERP))GO TO 371
      IF(RES(M).GE.(2.0*ERP))GO TO 372
      GO TO 363
  371 INDEX(M)=IND2
      GO TO 363
  372 INDEX(M)=IND3
  363 CONTINUE
C     UNLESS ITERATING PRINT OUT RESULTS
      IF(IFLG.EQ.1)GO TO 379
      WRITE(MOUT,3600)
      WRITE(MOUT,3700)(XA(M),YA(M),RES(M),INDEX(M),M=1,NA)
      WRITE(MOUT,3800)AVX,ERP
  379 NB=0
C     RESET ARRAYS FOR RECALCULATION WITHOUT REJECTED POINTS
      DO 364 N=1,NA
      IF(INDEX(N).EQ.IND2)GO TO 364
      NB=NB+1
      YA(NB)=YA(N)
      XA(NB)=XA(N)
      WA(NB)=WA(N)
  364 CONTINUE
```

```
C     IF ONLY ONE POINT LEFT INFORM USER ...RESULT TRIVIAL
      IF(NB.EQ.1)GO TO 365
C     CHECK NUMBER OF REJECTED POINTS IF 0 STOP RECALCULATIONS

      IF(NB.EQ.NA)GO TO 366
C     RESET NUMBER OF POINTS AFTER POINT REJECTION AND RECOMPUTE RESULTS
  367 NA=NB
      GO TO 380
  366 RETURN
  365 WRITE(MOUT,3900)
      RETURN
 3900 FORMAT(1X,*TRIVIAL RESULT BASED ON ONE POINT ONLY ...HENCE BLOCK R
     1EJECTED.............*)
 3600 FORMAT(1H1,*         X                    Y                  RES*)
 3700 FORMAT(1X,3(1PE16.6,4X),A1)
 3800 FORMAT(1X////1X,*SLOPE OF KINETIC THEORY PLOT = *,1PE16.6,1X///1X,
     1*STANDARD DEVIATION = *,1PE16.6)
      END



      SUBROUTINE LEAST(X,Y,W,A,B,ERP,ERA,ERB,ND,MOUT,IFLG)
C     SUBROUTINE FITS DATA TO MOONEY RIVLIN EQUATION
      DIMENSION X(ND),Y(ND),W(ND)
      DIMENSION XA(100),YA(100),WA(100),SMOOTH(100),RES(100),INDEX(100)
      DATA IND1,IND2,IND3/1H ,1H*,1HC/
C     INITIAL NUMBER OF POINTS IS TOTAL NUMBER PRESENTED
      NA=ND
      DO 200 I = 1,NA
C     COPY WORKING PARAMETERS TO PREVENT THEM BEING RESET IN MAIN PROGRAM
      XA(I) = X(I)
      YA(I) = Y(I)
  200 WA(I) = W(I)
C     SET SUMS TO ZERO
  245 SUMX = 0.0
      SUMY = 0.0
      SUMW = 0.0
      SUMXP = 0.0
```

```
C       COMPUTE LEAST SQUARES FIT PARAMETERS
        DO 210 J = 1,NA
        SUMXP = SUMXP + XA(J)
        SUMX = SUMX + (XA(J) * WA(J))
        SUMY = SUMY + (YA(J) * WA(J))
  210   SUMW = SUMW + WA(J)
        AVXA = SUMX/SUMW
        AVYA = SUMY / SUMW
        AVXAP = SUMXP/FLOAT(NA)
C       SET SUMS TO ZERO
        SUM1 = 0.0
        SUM2= 0.0
        SUM3 = 0.0
        DO 220 K = 1,NA
C       EVALUATE SLOPE AND INTERCEPT
        SUM1 = SUM1 + (WA(K) * (XA(K) - AVXA) * (YA(K) - AVYA))
        SUM2 = SUM2 +(WA(K) * (ABS(XA(K) - AVXA)**2))
  220   SUM3 = SUM3 + (WA(K) * (ABS(YA(K)- AVYA)**2))
        A = SUM1/SUM2
        B = AVYA - (A * AVXA)
C       SET SUMS TO ZERO
        SUMR = 0.0
        SUMXR = 0.0
C       COMPUTE STANDARD DEVIATIONS OF CALCULATED PARAMETERS
        DO 239 L = 1,NA
        SMOOTH(L) = (A*XA(L))+B
        RES(L) = YA(L) - SMOOTH(L)
        RES(L) = RES(L)*RES(L)
        SUMXR = SUMXR + ((XA(L)-AVXAP)*(XA(L)-AVXAP))
        SUMR = SUMR + RES(L)
  239   RES(L) = SORT(RES(L))
        ERP = SUMR/FLOAT(NA - 2)
        ERA = ERP/SUMXR
        ERB = ERP*((1.0/FLOAT(NA))+(AVXAP/SUMXR))
        ERP = SQRT(ERP)
        ERA = SQRT(ERA)
        ERB = SQRT(ERB)
C       COMPARE DATA WITH STANDARD DEVIATION....MARK BAD POINTS * AND REJECT.....
C       .....MARK POOR POINTS & BUT RETAIN
```

```
      DO 230 M = 1,NA
      INDEX(M) = IND1
      IF(RES(M).GE.(3.5*ERP))GO TO 231
      IF(RES(M).GE.(2.0*ERP))GO TO 232
      GO TO 230
  231 INDEX(M) = IND2
      GO TO 230
  232 INDEX(M) = IND3
  230 CONTINUE
      IF(IFLG.EQ.1)GO TO 221
C     UNLESS ITERATING PRINT OUT RESULTS
      WRITE(MOUT,2000)
      WRITE(MOUT,2001)(XA(M),YA(M),SMOOTH(M),RES(M),INDEX(M),M=1,NA)
      WRITE(MOUT,2002)A,B,ERP,ERA,ERB
  221 NB = 0
      DO 240 N = 1,NA
      IF(INDEX(N).EQ.IND2)GO TO 240
      NB = NB + 1
C     RESET ARRAYS OF WORKING PARAMETERS FOR RECOMPUTING WITHOUT REJECTED POINTS
      XA(NB)= XA(N)
      YA(NB)= YA(N)
      WA(NB) = WA(N)
  240 CONTINUE
C     CHECK IF NUMBER OF POINTS 1 GIVE UP AND INFORM USER
      IF(NB.EQ.1)GO TO 241
C     CHECK IF NUMBER OF POINTS 2 INFORM USER RESULT TRIVIAL
      IF(NB.EQ.2)GO TO 242
C     CHECK...IF 0 POINTS REJECTED FINISH ITERATION
      IF(NB.EQ.NA)GO TO 243
  244 NA = NB
      GO TO 245
```

```
 243 RETURN
 242 WRITE(MOUT,2003)
     GO TO 244
 241 WRITE(MOUT,2004)
     RETURN
2000 FORMAT(1H1,8X,1HX,19X,1HY,16X,6HSMOOTH,16X,3HRES)
2001 FORMAT(1X,4(1PE16.6,4X),A1)
2002 FORMAT(1X////1X,4HA = ,1PE16.6,1X//1X,4HB = ,1PE16.6,1X//1X,7HERP
    1= ,1PE16.6,1X//1X,7HERA = ,1PE16.6,1X//1X,7HERB = ,1PE16.6)
2003 FORMAT(1X,*TRIVIAL RESULT BASED ON TWO POINTS ONLY*)
2004 FORMAT(1X,*INDEFINATE RESULT BASED ON ONE POINT .... HENCE JOB ABO
    1RTED*)
     END
```

(C 2) A Computer Programme to Calculate the Best Arrhenius Plot and Calculate Activation Energies and Pre-exponential Factors

This programme was a standard least squares programme adapted so that the input parameters were rate constants and the temperatures, in degrees centigrade, at which they were obtained.

After obtaining the slope and intercept, the activation energy and pre-exponential factor were calculated.

The programme is given on pages 339 to 341 inclusive; it is written in A.S.A. Fortran and was used on the Imperial College CDC 6400 computer and the University of London CDC 6600/6400 installation.

```
      PROGRAM LSTSQT(INPUT,OUTPUT,TAPE5=INPUT,TAPE6=OUTPUT)
      DIMENSION Y(100),X(100),Z(100),V(100),NAMEIT(16)
  999 READ(5,6325)(NAMEIT(I),I = 1,16)
 6325 FORMAT(8A10)
      WRITE(6,8998)(NAMEIT(I),I = 1,16)
 8998 FORMAT(1X,20X,8A10,1X//1X,20X,8A10,1X////1X)
      READ(5,2110)INDEX,NUMBER
      READ(5,2000)(Y(I),X(I),I=1,NUMBER)
 2110 FORMAT(2I3)
 2000 FORMAT(2(E8.0,1X))
      IF(INDEX.EQ.0)GO TO 90
      WRITE(6,2111)
 2111 FORMAT(1X,4X,1HK,11X,5HLN(K),8X,4HT(C),9X,6H1/T(K))
      DO 91 NO = 1,NUMBER
      Z(NO) = ALOG(Y(NO))
      V(NO) = 1.0/(273.2 + X(NO))
   91 WRITE(6,2002)Y(NO),Z(NO),X(NO),V(NO)
 2002 FORMAT(1X,4(1PE9.2,5X))
      GO TO 99
   90 WRITE(6,3000)
 3000 FORMAT(1X,4X,1HY,13X,1HX)
      DO 92 MO = 1,NUMBER
      Z(MO) = Y(MO)
      V(MO) = X(MO)
   92 WRITE(6,2003)Z(MO),V(MO)
 2003 FORMAT(1X,2(1PE9.2,5X))
   99 WRITE(6,3100)
 3100 FORMAT(1X,1X//////////1X)
      CALL LSQ(Z,V,D,C,NUMBER,STDC,STDD)
      IF(INDEX.EQ.0)GO TO 93
      DELH = C * 8.314/1000.0
      PREX = D*8.314
      ERD = STDC * 8.314/1000.0
      ERP = STDD*8.314
      DELH = -DELH
      ERD = -ERD
```

```
      WRITE(6,2008)DELH,ERD,PREX,ERP
 2008 FORMAT(1X,20HACTIVATION ENERGY = ,F9.4,8H + OR - ,F9.4,1X,19HKILOJ
     1OULES PER MOLE,1X///1X,21HACTIVATION ENTROPY = ,F10.4,8H + OR - ,F
     210.4,1X,15HJOULES PER MOLE)
   93 IF(INDEX.EQ.1)GO TO 999
      STOP
      END

      SUBROUTINE LSQ(Y,X,D,C,N,STDC,STDD)
      DIMENSION Y(100),X(100)
C     2222222222222222222222222222222222222222222222222222222222222222
C     SUBROUTINE PERFORMS A LEAST SQUARES FIT GIVING D AS INTERCEPT AND
C     SLOPE
C     2222222222222222222222222222222222222222222222222222222222222222
      SUM1 = 0.0
      SUM2 = 0.0
      SUM3 = 0.0
      SUM4 = 0.0
      DO 86 IQ = 1,N
      SUM1 = SUM1 + Y(IQ)
      SUM2 = SUM2 + (X(IQ)*Y(IQ))
      SUM3 = SUM3 + X(IQ)
   86 SUM4 = SUM4 + (X(IQ)**2.0)
      D = ((SUM3*SUM2) - (SUM1*SUM4))/((SUM3**2.0) - (N*SUM4))
      C = ((N * SUM2) - ( SUM1*SUM3))/((N*SUM4) - (SUM3**2.0))
      XMN = SUM3/FLOAT(N)
      XMNS = 0.0
      ERS = 0.0
      DO 87 IP = 1,N
      DIFF = X(IP) - XMN
      EST = (C*X(IP)) + D
      ERR = EST - Y(IP)
      XMNS = (DIFF * DIFF) + XMN
   87 ERS = (ERR * ERR) + ERS
      VAR = ERS/FLOAT(N-2)
      VARC = VAR/XMNS
```

```
      VARD = VAR*((1.0/FLOAT(N)) + ((XMN * XMN)/XMNS))
      STDC = SQRT(VARC)
      STDD = SQRT(VARD)
      NU = N-2
      WRITE(6,1000)C,D,STDC,STDD,NU
 1000 FORMAT(1X,8HSLOPE = ,1PE16.6,1X///1X,12HINTERCEPT = ,1PE16.6,1X///
     11X,36HSTANDARD DEVIATION IN SLOPE = ,1PE16.6,1X///1X,34HSTANDARD D
     2EVIATION IN INTERCEPT = ,1PE16.6,1X///1X,11HNU = N-2 = ,I3)
C     2222222222222222222222222222222222222222222222222222222222
      RETURN
      END
```